UNIVERSITÀ DEGLI STUDI DI
CASSINO E DEL LAZIO MERIDIONALE

Corso di Dottorato in
Metodi, Modelli e Tecnologie per L'Ingegneria
curriculum Ingegneria Civile e Meccanica

Ciclo XXXVI

Development of an integrated platform for the biological valorization of syngas and biochar produced through pyrolysis of municipal sewage sludge

SSD: ICAR/03

Coordinatore del Corso
Chiar.mo Prof. Fabrizio Marignetti

Dottorando
Vincenzo Pelagalli

Supervisore
Prof. Marco Race
Dr. Michela Langone
Prof. Piet N. L. Lens

ACKNOWLEDGEMENTS

Vincenzo Pelagalli was supported through a doctoral research project funded on the PO FSE 2014-2020 of the Lazio region (Italy) (approval n.: G15074, date: 10/12/2020), which was co-funded by the Italian National Agency for New Technologies, Energy and Sustainable Economic Development (ENEA) and ACEA ELABORI S.p.A.

ABSTRACT

Municipal sewage sludge (MSS) management represents one of the most critical challenges related to wastewater management and environmental protection due to the high volumes produced globally every year (45 Mton of dry matter), the presence of hazardous organic and inorganic pollutants, high management costs, and environmental impacts. Interestingly, precious resources such as organic matter and nutrients are still present in MSS and should be recovered for multiple uses. Traditional treatment and disposal methods often fall short in fully addressing these issues, while innovative thermochemical processes (*e.g.* pyrolysis) are gaining interest in this field for their high versatility. Pyrolysis converts MSS into valuable products such as biochar, bio-oil, and pyrolysis gas, enabling simultaneous matter and energy recovery when these products are valorized in innovative biorefinery pathways. The main objective of this doctoral thesis is to investigate the potential of an integrated platform for the biological valorization of the products of MSS pyrolysis, with a particular focus on biochar and pyrolysis gas. To assess the influence of the pyrolysis process on the yields and composition of the products, the study of the MSS pyrolysis process was conducted experimentally by testing variable temperatures and the addition of variable zeolitic catalysts. The study demonstrated a significant influence of temperature on product yields and compositions, and an interesting capability of H-Mordenite and H-ZSM5 zeolites to influence product yields and sulfur migration in pyrolysis gas, reducing H_2S concentration in pyrolysis gas of up to 47 % by volume. The thesis further investigates the valorization of MSS-derived pyrolysis gas through biological processes. The production of microbial protein (MP) from pyrolysis gas mixtures using hydrogen-oxidizing bacteria (HOB) was investigated. Results indicate the feasibility of producing MP with up to 74 % protein content, leveraging the mixed culture's resistance to high H_2S and CO concentrations. This finding opens new avenues for synthesizing alternative protein sources, biopolymers, and fertilizers from MSS. Further experimental activities were conducted on the valorization of pyrolysis gas and its conversion to biomethane in a pilot-scale reactor. The biomethanation process effectively converts H_2 and CO into CH_4, achieving up to 90 % methane concentration by employing a Venturi-type ejector as a gas-solubilization method, and

by optimizing gas retention time and H_2/CO_2 ratios. This method enhances energy recovery from MSS and supports the transition to renewable energy sources. The thesis also evaluates the potential of biochar produced from MSS pyrolysis. Despite the limited CO_2 adsorption capabilities observed in the study, the role of biochar in the *in-situ* upgrading of biogas to biomethane is examined. Future research should focus on biochar activation to improve its CO_2 adsorption capabilities and effectiveness in anaerobic digestion processes. The construction of this innovative valorization platform for MSS through pyrolysis could represent a strategic and game-changing approach to advancing resource recovery from MSS, mitigating environmental pollution, and contrasting climate change.

TABLE OF CONTENTS

ABSTRACT I
List of Figures VI
List of Tables X
INTRODUCTION 1
CHAPTER 1. Pyrolysis of municipal sewage sludge: challenges, opportunities, and new valorization routes for biochar, bio-oil, and pyrolysis gas 5
1.1 Introduction 6
1.1.1 Main characteristics of municipal sewage sludge 8
1.1.2 Conventional management of municipal sewage sludge 13
1.2 Pyrolysis of municipal sewage sludge 14
1.2.1 Conventional reactor configurations and full-scale prototypes 18
1.2.2 Distribution of products from pyrolysis of municipal sewage sludge 21
1.3 Pyrolysis products: main characteristics and potential valorization pathways 27
1.3.1 Biochar 27
1.3.2 Bio-oil 40
1.3.3 Pyrolysis gas 45
1.3.4 Improvement of biochar, bio-oils, and pyrolysis gas characteristics through catalytic pyrolysis 53
1.4 Economic considerations 55
1.5 Integrated biorefinery platform for the pyrolysis of municipal sewage sludge: two possible scenarios 56
1.6 Conclusions 59
CHAPTER 2. In-situ catalytic pyrolysis of municipal sewage sludge for the reduction of H_2S content in pyrolysis gas 61
2.1 Introduction 62
2.2 Materials and methods 64
2.2.1 Municipal sewage sludge 64
2.2.2 Thermal and catalytic pyrolysis tests 65

2.2.3 Analytical methods 68
2.2.4 Calculations 68
2.2.5 Statistical analysis 71
2.3 Results and discussion 71
2.3.1 Product yields 71
2.3.2 Pyrogas composition 73
2.3.3 H_2S concentration in pyrogas 77
2.3.4 Sulfur migration to the pyrolysis products 81
2.4 Conclusions 84
CHAPTER 3. Syngas-driven sewage sludge conversion to microbial protein through H_2S- and CO-tolerant hydrogen-oxidizing bacteria 87
3.1 Introduction 88
3.2 Materials and methods 90
3.2.1 Experimental setup of the aerobic syngas bioconversion batch tests 90
3.2.2 Short-term batch tests 91
3.2.3 Long-term batch tests 94
3.2.4 Effect of CO on biomass productivity, concentration and yield 95
3.2.5 Analytical methods 96
3.2.6 Calculations 96
3.2.7 Balanced stoichiometric equation for HOB 97
3.2.8 Statistical analysis 97
3.2.9 Microbial community analysis 98
3.3 Results and discussion 98
3.3.1 Effect of varying syngas composition and presence of inhibitory compounds 98
3.3.2 Long-term batch tests 105
3.3.3 Effect of CO on maximum biomass productivity, concentration and yield 108
3.3.4 Microbiological analysis 109
3.4 Conclusions 112
CHAPTER 4. Biomethanation of pyrolysis gas in a pilot-scale bioreactor 115
4.1 Introduction 116
4.2 Materials and methods 120
4.2.1 Set up, inlet gas, and inoculum 120
4.2.2 Experimental phases 123
4.2.3 Analytical methods 124

4.2.4 Calculations 125
4.2.5 Statistical analysis 127
4.3 Results and discussion 127
4.3.1 Start-up phase 127
4.3.2 The effect of inlet gas and liquid recirculation flow rates on the biomethanation performance and stability 130
4.3.3 The effect of H_2/CO_2 ratio on the biomethanation performance and stability 132
4.4 Conclusions and future perspectives 134
CHAPTER 5. Biochar valorization in the anaerobic digestion of municipal sewage sludge 137
5.1 Introduction 138
5.2 Materials and methods 140
5.2.1 Municipal sewage sludge 140
5.2.2 Pyrolysis set-up 140
5.2.3 Characterization of biochar 140
5.2.4 Determination of CO_2 adsorption capability of biochar 141
5.2.5 Biomethanation potential tests 142
5.3 Results and discussion 143
5.3.1 Municipal sewage sludge and biochar characterization 143
5.3.2 Adsorption capability of biochar 146
5.3.3 Biochar addition in the anaerobic digestion process 149
5.4 Conclusions 151
CONCLUSIONS 153
Appendix A 156
Appendix B 159
Appendix C 161
References 168
Biography 209
Publications & relevant work 210

LIST OF FIGURES

Figure 1. 1. Integrated platform for the valorization of the products obtained by the pyrolysis of municipal sewage sludge (MSS). Challenges and opportunities for MSS management are schematized together with innovative valorization routes for biochar, bio-oil, and pyrolysis gas. 7

Figure 1. 2. Main disposal methods for municipal sewage sludge (MSS) in the EU-27 Countries. Advantages and drawbacks of landfilling, agricultural spreading, composting, incineration, and other methods, are reported. The disposal rate for each method in the EU-27 is indicated as well. [a]: expressed as tons of MSS disposed per tons of MSS produced. Data source: https://ec.europa.eu/eurostat/databrowser/product/page/ten00030..... 13

Figure 1. 3. Pyrolysis reactors. The main configurations for pyrolysis reactors are reported: A) vertical and B) horizontal fixed bed reactor, C) fluidized bed reactor, D) conical spouted bed reactor, E) rotary kiln reactor, and F) auger/screw reactor. Adapted from Babler et al. (2017), Campuzano et al. (2019), and Gao et al. (2022). 19

Figure 2. 1. Experimental set-up of the pyrolysis tests. The set-up was opportunely adapted in order to allow the condensation of the liquid products at temperatures of: A) 350 and 500 °C, B) 650 °C, and C) 800 °C. 67

Figure 2. 2. Yields of the products of pyrolysis of municipal sewage sludge (MSS). The yields were calculated for A) thermal pyrolysis at each tested temperature (350, 500, 650, and 800 °C), and B) catalytic pyrolysis at 500 °C, for each tested zeolite. Letters a, b, and c, result from the Tukey's comparison analysis: statistically similar means share the same letters. 72

Figure 2. 3. Composition and lower heating value of syngas produced by thermal pyrolysis at variable temperatures. The results of gas-chromatographic analyses of

pyrogas produced at 350, 500, 650, and 800 °C, are reported in terms of concentration of A) H_2, CO, and CO_2, and B) CH_4, C_2- C_3-, and C_4-, and C) lower heating value. 75

Figure 2. 4. H_2S in pyrolysis gas from thermal pyrolysis. The production of H_2S during thermal pyrolysis of municipal sewage sludge (MSS) at temperatures of 350, 500, 650, and 800 °C, was evaluated in terms of A) H_2S concentration in pyrogas, and B) H_2S formation ratio (HFR). Letters a, b, and c result from the Tukey's comparison analysis: statistically similar means share the same letters. 78

Figure 2. 5. H_2S concentration and formation ratio (HFR) in catalytic pyrolysis. The production of H_2S during catalytic pyrolysis of municipal sewage sludge (MSS) at 500 °C was evaluated in terms of A) H_2S concentration in pyrogas, and B) H_2S formation ratio (HFR), for each tested zeolite. Letters a, b, and c result from the Tukey's comparison analysis: statistically similar means share the same letters. 80

Figure 2. 6. Sulfur migration from municipal sewage sludge to biochar, bio-oil, and pyrogas. The amount of S migrated from MSS to the pyrolysis products is reported for A) thermal pyrolysis at 350, 500, 650, and 800 °C, and B) catalytic pyrolysis tests performed with different zeolites: H-Mordenite (Si/Al Ratio (SAR) = 220), H-ZSM5 (SAR = 250), and H-ZSM5 (SAR = 1880). 82

Figure 3. 1. Results of the H_2/CO_2 ratio short-term batch tests. The influence of the variable H_2/CO_2 ratio on the growth of the HOB enrichment is expressed in terms of: A) Pressure variation over time; B) Final biomass concentration and yield on hydrogen; C) H_2 and CO_2 consumption, and D) Biomass protein content. Initial biomass concentration: 0.088 g VSS/L. *: Statistically different value (p-value <0.05). Error bars refer to the standard deviation calculated from the triplicates of each test. 99

Figure 3. 2. Results of the H_2S concentration short-term batch test. The influence of increasing H_2S concentrations on the growth of the HOB enrichment is expressed in terms of: A) Pressure variation over time; B) Final biomass concentration and yield on hydrogen; C) H_2 and CO_2 consumption, and D) Biomass protein content. Initial biomass concentration: 0.087 g VSS/L. *: Statistically different value (p-value <0.05). Error bars refer to the standard deviation calculated from the triplicates of each test. 101

Figure 3. 3. Results of the CO concentration short-term batch test. The influence of increasing CO concentrations on the growth of the HOB enrichment is expressed in terms of: A) Pressure variation over time; B) Final biomass concentration and yield on hydrogen; C) H_2 and CO_2 consumption, and D) Biomass protein content. Initial biomass concentration: 0.129 g VSS/L. *: Statistically different value (p-value <0.05). Error bars refer to the standard deviation calculated from the triplicates of each test. 104

Figure 3. 4. Results of the long-term batch test. The performance of the HOB enrichment during long-term batch test is expressed in terms of: A) Average final biomass concentration and average biomass yield on hydrogen; B) Average volumetric biomass productivity, and C) Biomass protein content. Initial biomass concentration: 0.115 g VSS/L. *: Statistically different value (p-value <0.05). Error bars refer to the standard deviation calculated from the triplicates of each test. 105

Figure 3. 5. Results on the effects of CO on maximum biomass productivity, concentration and yield. A) Biomass concentration and yield on hydrogen; B) Volumetric biomass productivity, and C) Biomass protein content. Initial biomass concentration: 0.042 g VSS/L. Error bars refer to the standard deviation calculated from the triplicates of each test. 108

Figure 3. 6. Evolution of the mixed microbial HOB culture across the long-term batch tests. The relative abundances of the bacterial genera and species in the HOB enrichment at the start (T0) and at the end of the 30 days long-term batch test (Control, CO10, CO10+H_2S, and CO40) are reported. 110

Figure 4. 1. Pilot-scale biomethanation set-up. The experimental set-up employed for the pilot-scale biomethanation of pyrolysis gas with H_2 addition is schematized. MFM: mass flow meter; VTE: Venturi-type ejector; BPV: back-pressure valve; GC: gas cromatograph; Q_{IN}: inlet gas flow rate; Q_R: liquid recirculation flow rate; Qout: outlet gas flow rate; T: temperature probe; P: pressure probe. 121

Figure 4. 2. Bioreactor performance in the start-up phase. The performance of the biomethanation process is evaluated for variable inlet gas flow rates (Qgas,in) in terms of A) outlet gas composition, B) H_2 and CO solubilization efficiency, and C) CH_4 yield on H_2, outlet gas flow rate, and methane production rate (MPR). 128

Figure 4. 3. Stability parameters in the start-up phase. The stability of the biomethanation process is evaluated in terms of A) total VFAs concentration, total alkalinity (TA), partial alkalinity (PA), and the difference between TA and PA, and B) pH. 129

Figure 4. 4. Bioreactor performance in the experimental phases. The performance of the biomethanation process in the experimental periods A1, A2, and B, is evaluated in terms of a) outlet gas composition, b) H_2 and CO solubilization efficiency, and c) CH_4 yield on H_2, outlet gas flow rate, and methane production rate (MPR). 131

Figure 4. 5. Stability parameters in the experimental phases. The stability of the biomethanation process in the experimental periods A1, A2, and B, is evaluated in terms of a) total VFAs concentration, total alkalinity (TA), partial alkalinity (PA), and the difference between TA and PA, and b) pH. 133

Figure 5. 1. Results of thermo-gravimetric analysis for the determination of CO_2 adsorption capability of biochar. The different biochars tested were produced through conventional pyrolysis at temperatures of 350, 500, 650 and 800 °C (namely BC350, BC500, BC650, and BC800, respectively). A) Percentages of mass variation, and B) TG curves, are reported for every biochar. 147

Figure 5. 2. CO_2 adsorption tests with variable CO_2 inlet temperatures. The adsorption of CO_2 on A) biochar produced at 350 °C (BC350), and B) biochar produced at 800 °C (BC800), was tested in TGA with CO_2 inlet temperature of 25, 70, and 100 °C. The influence on the initial mass loss (IML), N_2 adsorption ($AdsN_2$), and CO_2 adsorption ($AdsCO_2$), was evaluated. 148

Figure 5. 3. Biochar addition in the biomethanation potential tests of municipal sewage sludge. The results of biomethanation potential test of municipal sewage sludge (MSS) with and without biochar addition were reported in terms of A) cumulative CH_4 production, and B) final composition of biogas. MSS-derived biochar produced at 350, 500, 650, and 800 °C (namely, BC350, BC500, BC650, and BC800) was employed. 150

Figure C1. 1. Gas consumption, pressure variation over time and biomass concentration observed in the preliminary enrichment phase. 163

Figure C5. 1. Trend of the final NH_4^+-N concentration in each condition during the long-term batch tests. 166

LIST OF TABLES

Table 1. 1. Composition and main characteristics of different municipal sewage sludge streams. % wt: percentage on weight; db: on a dry basis; MSS: municipal sewage sludge; MC: moisture content; VM: volatile matter; AC: ash content; FC: fixed carbon; HHV: higher heating value; n.r.: not reported. 12

Table 1. 2. Dry and hydrothermal technologies for the thermochemical conversion of municipal sewage sludge. Adapted from Chen et al. (2020), Djandja et al. (2021), Gao et al. (2020), Jiang et al. (2021), Langone and Basso (2020), and Xiao et al. (2022). HTC: hydrothermal carbonization; HTL: hydrothermal liquefaction; WO: wet oxidation; SCWO: supercritical water oxidation; SCWG: supercritical water gasification; VFAs: volatile fatty acids. 17

Table 1. 3. Influence of municipal sewage sludge characteristics and pyrolysis operating parameters on products yield and distribution. [a] dry basis; [b] dry ash free basis; [c] deducted from graphics ; MSS: municipal sewage sludge; MC: moisture content; VM: volatile matter; FC: fixed carbon; T: temperature; SRT: solid retention time; VRT: vapour retention time; HR: heating rate; n.r.: not reported; wt: on a weight basis 25

Table 1. 4. Composition and surface properties of sewage sludge-derived biochar. T: temperature; SSA: specific surface area; PV: pore volume; EC: electric

conductivity; CEC: cation exchange capacity; n.r.: not reported; wt: on a weight basis 29

Table 1. 5. Biochar employment in nutrient recovery and contaminant removal from water. [a]: deducted from graphics; b: higher initial concentration (50 mg U/L); c: lower initial concentration (1 mg U/L); MSS: municipal sewage sludge; PTEs: potentially toxic elements; PFAS: per- and poly-fluoroalkyl substances; wt: on a weight basis; n.r.: not reported..... 37

Table 1. 6. Composition and fuel properties of municipal sewage sludge- and lignocellulosic materials-derived bio-oils (SDBO and LDBO, respectively), and petroleum fuels. [a] evaluated at 40 °C; [b] evaluated at 20 °C; [c] evaluated at 50 °C; SDBO: sludge-derived bio-oils; LDBO: lignocellulosic-derived bio-oils; T: temperature; HHV: higher heating value; LHV: lower heating value; MC: moisture content; n.r.: not reported; wt: on a weight basis. 41

Table 1. 7. Evolution of pyrolysis gas composition based on the moisture content of the municipal sewage sludge (MSS) feedstock, as well as the heating rate of MSS, and the pyrolysis temperature. [a] deducted from graphics; MC: moisture content; MSS: municipal sewage sludge; HR: heating rate; T: temperature; LHV: lower heating value; n.r.: not reported; v/v: on volume. 46

Table 1. 8. Metabolic pathways involved in syngas biomethanation, stoichiometric reactions, and favourable temperature conditions. 51

Table 2. 1. Ultimate and proximate analysis of the municipal sewage sludge employed for thermal and catalytic pyrolysis tests. [a]: calculated as difference; wt: on a weight basis; db: on a dry basis; MC: moisture content; VM: volatile matter; FC: fixed carbon; AC: ash content..... 65

Table 2. 2. Experimental conditions of the thermal and catalytic pyrolysis tests. The main operative parameters are reported for each tested condition. MSS: municipal sewage sludge; SAR: Si/Al ratio; T: temperature; SRT: solid retention time; wt: on a weight basis..... 66

Table 2. 3. Composition of syngas produced by catalytic pyrolysis of municipal sewage sludge (MSS). The catalytic process was conducted at 500 °C, by employing different types of zeolites (H-Mordenite and H-ZSM5), with variable Si/Al ratio (SAR). Composition of syngas from thermal pyrolysis of the sole MSS is reported for comparison. v/v: by volume; * Statistically different value (p-value < 0.05). 76

Table 2. 4. Influence of feedstock composition and pyrolysis parameters on H_2S concentration in syngas. A comparison between this and other studies from the literature is reported. [a]: the heating rate was not calculable, as the MSS feedstock was introduced in the oven only after reaching the operative temperature; [b]: deducted from graphics; wt: on a weight basis; db: on a dry basis; MSS: municipal sewage sludge; HR: heating rate; SRT: solid retention time; MC: moisture content; AC: ash content; VM: volatile matter; FC: fixed carbon; v/v: by volume; n.r.: not reported. 79

Table 3. 1. Experimental conditions tested in the short-term batch tests to assess the effects of variable H_2/CO_2 ratios, H_2S equivalent concentrations and CO concentrations on the performance of HOB. Although the percentages of H_2, O_2 and CO_2 in each condition of the CO concentration test could vary, the H_2/CO_2 and H_2/O_2 ratios were maintained constant. 93

Table 3. 2. Experimental conditions tested in the long-term batch tests in order to assess the effect on HOB of variable CO concentrations with and without the presence of H_2S for a duration of 30 days. 94

Table 3. 3. Experimental conditions used to test the effect of CO on biomass concentration and volumetric productivity. 95

Table 4. 1. Metabolic pathways involved in syngas-like mixtures biomethanation, stoichiometric reactions, and favourable temperature conditions. 118

Table 4. 2. Experimental set-up and properties of the inoculum. The characteristics of the reactor set-up, the feed-gas mixture, and the gas supply system are reported, together with the chemical characterization of the inoculum. Q_R: recirculation flow

rate; Q_{IN}: inlet gas flow rate; GRT: gas retention time; TS: total solids; VS: volatile solids; VFAs: volatile fatty acids 122

Table 4. 3. Experimental periods and tested variables. The different experimental conditions tested in the dedicated experimental periods of the study are reported. Q_R: recirculation flow rate; $Q^{gas,IN}$: inlet gas flow rate; GRT: gas retention time; TS: total solids; 124

Table 5. 1. Characterization of substrate and inoculum employed in the biomethanation potential test. PS: primary sludge; SS*: concentrated secondary sludge; ADS: anaerobically digested sludge; TS: total solids; VS: volatile solids; tCOD: total COD; sCOD: soluble COD; 142

Table 5. 2. Proximate and ultimate analysis of municipal sewage sludge and biochar produced with variable pyrolysis temperature. BC350, BC500, BC650 and BC800 refer to biochar produced at 350, 500, 650, and 800 °C, respectively, with solid retention time of 15 min. [a]: calculated as difference; db: on a dry basis; MSS: municipal sewage sludge; MC: moisture content; VM: volatile matter; FC: fixed carbon; AC: ash content. 144

Table B. 1. Elemental composition of biochar. The results of the elemental analysis conducted on biochar produced from thermal and catalytic pyrolysis of municipal sewage sludge (MSS) are reported. Thermal pyrolysis of MSS was conducted at 350, 500, 650, and 800 °C. The catalytic process was conducted at 500 °C, by employing different types of zeolites (H-Mordenite and HZSM-5), with variable Si/Al ratio (SAR). wt: on a weight basis; db: on a dry basis; 159

Table B. 2. Elemental composition of bio-oil. The results of the elemental analysis conducted on bio-oil produced from thermal and catalytic pyrolysis of municipal sewage sludge (MSS) are reported. Thermal pyrolysis of MSS was conducted at 350, 500, 650, and 800 °C. The catalytic process was conducted at 500 °C, by employing different types of zeolites (H-Mordenite and HZSM-5), with variable Si/Al ratio (SAR). wt: on a weight basis; db: on a dry basis; 160

Table C1. 1.. Composition of the mineral medium used for the HOB enrichment, prepared accordingly to Yu et al., (2013). 161

Table C2. 1. Concentration of $Na_2S \cdot 9H_2O$ used in each tested condition and equivalent H_2S concentration in the gas headspace. The calculated H_2S concentrations were dependent upon the pH, temperature and pressure conditions set in each test. 164

INTRODUCTION

Effective urban wastewater treatment is vital for sustainable human-environment interactions, yet the overproduction of excess municipal sewage sludge (MSS) presents significant health, environmental, and economic challenges. Amounts as high as 45 Mton of dry MSS per year are produced globally, with MSS management accounting for 50 % of the overall WWTP costs [1,2]. In addition, MSS is characterized by the presence of hazardous organic and inorganic components such as polycyclic-aromatic hydrocarbons (PAHs), per- and poly-fluoroalkyl substances (PFAS), pathogens, and potentially toxic elements (PTEs), posing high risks for MSS treatment and disposal [3–7]. Nevertheless, valuable organic matter and nutrients are still present in MSS, suggesting the opportunity for innovative circular approaches towards MSS valorization, overcoming the conventional methods employed for MSS management. Thermochemical processes, such as pyrolysis, gasification, and hydrothermal treatments, especially when combined with anaerobic digestion, are promising for MSS management and valorization, allowing simultaneous energy recovery, pathogens neutralization, pollutants degradation, and the obtainment of a wide range of valuable products [8,9]. Pyrolysis, in particular, offers a high versatility for the conversion of MSS into biochar, bio-oil, and syngas (or pyrolysis gas), which could be involved in biorefinery approaches towards the synthesis of numerous value-added materials [2]. Biochar could be employed as adsorbent material thanks to its specific surface area and pore structure, resulting in positive effects as a soil conditioner, or for the removal of contaminants from water and soils, as well as for CO_2-capture in many applications [10–13]. On the other hand, bio-oil is generally employed to produce biofuels, to correct and adapt its composition [14,15]. Finally, apart from energy recovery through direct combustion or thermochemical conversion into chemicals and biofuels via the Fischer-Tropsch process [16,17], syngas produced from MSS pyrolysis could be employed as gas substrate for aerobic and anaerobic

fermentation processes, towards the obtainment of microbial protein (employable for the production of feed and food, biopolymers, and slow-release fertilizers) [18], liquid biofuels (*e.g.* ethanol) [19], or biomethane [20].

The aim of the research presented in this thesis was that of evaluating the potential of an integrated biorefinery platform for the biological valorization of biochar and syngas produced from MSS-pyrolysis, by experimentally investigating methods for the optimization of their characteristics and the enhancement of their innovative valorization potential.

The research activities were conducted in the framework of an industrial PhD project, hosted by the Department of Civil and Mechanical Engineering of the University of Cassino and Southern Lazio as the main institution, and co-funded by Regione Lazio, ENEA and Acea Elabori SpA. The experiments conducted at the University of Cassino and Southern Lazio were focused on: *a)* the aerobic fermentation of gas mixtures simulating realistic MSS-derived pyrolysis gas with variable composition towards microbial protein production, and *b)* biomethanation potential tests for the anaerobic digestion of MSS with the addition of MSS-derived biochar. Point *b)* was then further investigated during a 3-months secondment period conducted at the University of Galway, Ireland. ENEA hosted parts of the research activities as well: experiments on the optimization of thermal and catalytic pyrolysis processes towards the improvements of product yields and pyrolysis gas composition were conducted at the ENEA Casaccia Research Center (Rome, Italy), for a period of about 6 months (15 January 2023 – 30 July 2023). A following research period of 7 months was conducted at the ENEA Bologna/Brasimone Research Center (Bologna, Italy), during which the investigation of the syngas biomethanation process was performed by means of a pilot-scale bioreactor. Acea Elabori SpA provided continued support and supervision along the doctoral research project, including the supply of the MSS necessary for the pyrolysis tests and biochar production.

This thesis is composed of five chapters, including a first literature review and four experimental chapters, followed by a conclusion section. The overall description of the structure of the thesis is reported below:

Chapter 1 results from a critical literature review on the challenges and opportunities related to MSS management and valorization, focused on the description of MSS characteristics, classic management methods, potentials of the thermochemical treatments in general, and of pyrolysis in particular. The description of the influence of MSS composition and pyrolysis operative parameters on the characteristics of the products is reported. A deep overview of the innovative valorization solutions for biochar, bio-oil, and pyrolysis gas, is provided. Economic considerations over the pyrolysis of MSS are included as well.

Chapter 2 focuses on studying the thermal and catalytic MSS-pyrolysis process. A first series of thermal pyrolysis tests were conducted by varying pyrolysis temperature, in order to assess variations on the product yields and compositions. Then, catalytic MSS-pyrolysis with the addition of H-Mordenite and H-ZSM5 zeolites was conducted, by focusing on their effects on product yields, gas composition, H_2S production and concentration, and sulfur migration from MSS.

Chapter 3 investigates the syngas-driven bioconversion of MSS into microbial protein through H_2S- and CO-tolerant hydrogen-oxidizing bacteria (HOB). A mixed culture of HOB was enriched and employed for the fermentation of synthetic $H_2/CO/CO_2/H_2S$ mixtures simulating realistic MSS-derived pyrolysis gas. Batch aerobic fermentation tests were performed, and the influence of gas composition on the fermentation process was assessed.

Syngas valorization is the main object of **Chapter 4** as well, where the research activity on the pilot-scale syngas biomethanation is presented. A pilot-scale tubular bioreactor was employed for the conversion of synthetic $H_2/CO/CO_2$ mixtures, simulating realistic cleaned MSS-derived syngas, into biomethane. A Venturi-type ejector was employed as a gas solubilization system to maximize the gas-liquid mass transfer.

Chapter 5 focuses on adding MSS-derived biochar in the anaerobic digestion of MSS, as a method for the *in-situ* upgrading of biogas to biomethane. A characterization of the biochar produced through the pyrolysis tests reported in Chapter 2 was conducted, in terms of composition and CO_2 adsorption capability ($AdsCO_2$). The influence of temperature, and therefore of the different $AdsCO_2$, on the CO_2 capture

on biochar during biomethanation potential tests was investigated, as well as the overall effect of biochar on biogas/biomethane production in the anaerobic digestion of MSS.

Finally, a conclusion section is reported to highlight the main outcomes of this PhD thesis and to propose further approaches in view of the future development of the related research activities.

CHAPTER 1. PYROLYSIS OF MUNICIPAL SEWAGE SLUDGE: CHALLENGES, OPPORTUNITIES, AND NEW VALORIZATION ROUTES FOR BIOCHAR, BIO-OIL, AND PYROLYSIS GAS

This chapter was based on:

Pelagalli V., Langone M., Matassa S., Race M., Tuffi R., Papirio S., Lens P.N.L., Lazzazzara M., Frugis A., Petta L., Esposito G., 2024. Pyrolysis of municipal sewage sludge: challenges, opportunities and new valorization routes for biochar, bio-oil, and pyrolysis gas. *Environmental Science: Water Research & Technology*, https://doi.org/10.1039/D4EW00278D.

1.1 Introduction

Although the efficient treatment of urban wastewater is crucial for the sustainability of human-environment interactions, the generation of large amounts of municipal sewage sludge (MSS) imposes health and environmental safety concerns as well as high management costs. In the last two decades, the production of MSS across the EU-27 member states can be estimated at about 8.2 - 8.3 million tons per year on a dry basis (db), resulting in a per capita MSS production that varies between 5 and 26 kg db per inhabitant per year, depending on the wastewater composition, sewage system and level of treatment [21]. Germany, Spain, France and Italy are the greatest producers in the EU-27, responsible for 60 % on a weight basis (wt) of the total MSS production [21]. At the global level, a production of 45 million tons db of MSS in 2017 has been reported [22].

Issues such as the shortage of landfills, the environmental cost of improper disposal, the high costs of the actual management of such massive MSS quantities, which accounts for as much as 50% of the total operational expenses of wastewater treatment plants (WWTPs) [1], and the stricter environmental regulations, indicate the need for improving the current MSS disposal practices. Dried MSS can be regarded as a potential source of energy, having a higher-heating value (HHV) that varies between 5 and 29 MJ/kg db, which is comparable to other low-rank fuels including lignite and most of the biomass types [23]. Moreover, by following emerging circular economy practices, MSS can also be considered a renewable source of carbon (C) and nutrients (*i.e.* N and P) [24]. Thus, the proper management of MSS, besides ensuring environmental protection, must simultaneously employ resource recovery and valorization strategies to promote novel circular practices with both environmental and economic benefits. In order to achieve this, modern thermochemical processes (*i.e.* pyrolysis, gasification, and hydrothermal treatments) are attracting interest [25], especially in combination with anaerobic digestion (AD) of MSS [26].

Thermochemical MSS treatment leads to the synthesis of a wide array of products, allowing the efficient and simultaneous recovery of energy and other resources from

MSS, together with the partial/total neutralization of pathogens as well as the degradation of organic and inorganic pollutants [27]. Among thermochemical processes, pyrolysis of MSS has been receiving increasing attention as a potential route for sludge management because of its potential to simultaneously target energy recovery [28,29], nutrient recycling, potentially toxic elements (PTEs) immobilization, and environmental protection [30], as well as its product selectivity, process scalability and versatility potential [31].

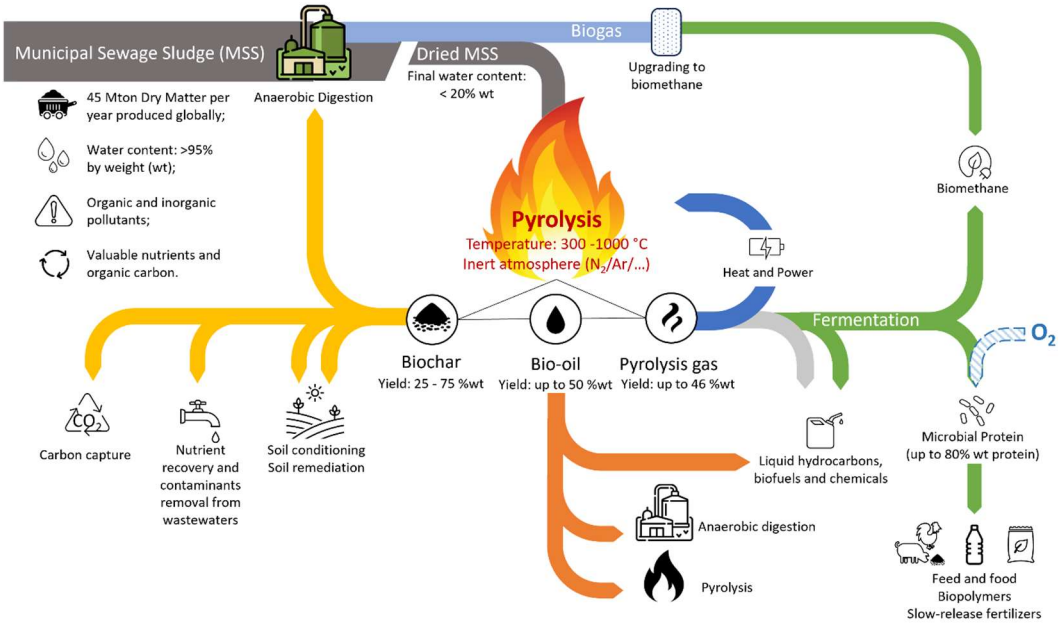


Figure 1. 1. Integrated platform for the valorization of the products obtained by the pyrolysis of municipal sewage sludge (MSS). Challenges and opportunities for MSS management are schematized together with innovative valorization routes for biochar, bio-oil, and pyrolysis gas.

With the aim to critically evaluate the potential of pyrolysis in the context of more sustainable and circular MSS management practices, this work combines an overview of the state-of-the-art of MSS pyrolysis with the analysis of possible valorization routes for its products. After reviewing the main characteristics, current management practices, and European legislation concerning MSS, the review focuses on the multiple recovery and valorization potentials offered by pyrolysis products moving beyond bioenergy generation. Particular attention is placed on innovative and

emerging routes involving bioconversion of MSS pyrolysis products into biofuels and value-added bioproducts (**Figure 1.1**).

1.1.1 Main characteristics of municipal sewage sludge

MSS represents the main residual product of WWTPs and takes the form of a semiliquid material with a high water content (80 − 99 % wt) [32], produced in huge volumes, and characterized by offensive odours and the presence of pathogens. It is a complex mixture of organic and inorganic substances as well as microorganisms removed or generated during wastewater treatment. The treatment lines of WWTPs are organized in order to obtain different levels of contaminants removal from wastewaters (primary, secondary, and tertiary treatment), implementing a combination of physical, chemical and biological processes [33,34].

Further, specific treatments are required to reduce the total weight, volume, and volatile matter (VM) content in MSS, as well as to decrease the load of pathogenic microorganisms [35]. Generally, raw MSS is treated following the sequence of thickening, stabilization and dewatering [23]. Among the main stabilization methods, AD is certainly the most established one, allowing a decrease of VM in MSS of up to 30 – 67 % wt [29] while recovering biogas. After dewatering, the volume of MSS can be reduced by 90 %, with an increase in total solids (TS) concentration up to 20 - 40 % wt [36,37].

MSS composition (**Table 1.1**) highly affects its employment in thermochemical conversion processes since the different compounds generally contained in MSS, with their respective thermal behaviour, can vary widely [23]. The moisture content (MC) obviously greatly affects the thermal degradation of MSS. Raw (MC up to 97 % wt) or even dewatered (MC of 69 – 89 % wt) MSS is generally not directly subjected to pyrolysis due to the negative effects given by the excessive MC on the overall energy balance of the process [38]. This implies the necessity to invest additional energy to dry MSS to a MC not higher than 20 % wt prior to pyrolysis [39,40], which can account for a large part of the MSS management costs [41] . The content of VM in MSS gives a first indication of the production potential of bio-oil and pyrolysis gas through

pyrolysis, since it represents the portion of MSS which partially or completely leaves the solid state in the form of vapours (condensable or non-condensable) during the thermochemical conversion. On the other hand, the fixed carbon (FC) and ash content (AC) of MSS are generally lower and higher, respectively, than those of other biomasses conventionally subjected to pyrolysis, which turns out to be unfavourable in view of the mere energetic valorization of MSS (*e.g.* through incineration), as this leads to a lower energy content of the products and a lower energy conversion efficiency [23]. Finally, the HHV of MSS assumes values comparable with those of biomasses such as lignite, walnut shell, hazelnut husk, and wheat straw, and is variable with MSS composition [23].

Traces of toxic pollutants such as polycyclic aromatic hydrocarbons (PAHs), polychlorinated biphenyls (PCBs), polybrominated diphenyl ethers (PBDEs), di(2-ethylhexyl) phthalate (DEHP), pharmaceuticals, synthetic steroids, polychlorinated dibenzo-p-dioxins and dibenzo-p-furans (PCDD/Fs), microplastics, and per- and poly-fluoroalkyl substances (PFAS) can be found in MSS [3–7]. In particular, PFAS-derived contamination has been recently gaining utmost attention because of the strong persistence of these contaminants in the environment, especially because currently established technologies for wastewaters and MSS treatment are not able to completely remove them [42,43]. Further, compared to conventional biomasses, MSS is characterized by higher concentrations of some inorganic elements which contribute to ash formation [23], depending on the inorganic matter of the raw wastewater and the WWTP processes. The major ash-forming elements in MSS are PTEs such as Al, Ca, Cl, Fe, K, Mg, Mn, Na, P, Si and Ti, but Ag, Cd, Co, Cr, Cu, Ni, Pb and Zn can also be present in high concentrations, being variable consistently with the typology of MSS [23].

The remarkable content of nutrients such as N and P in MSS (up to 7.2 and 9.2 % wt db, respectively, in dewatered MSS) [38] motivates their recovery and valorization pursued in many applications (*i.e.* agricultural usage). On the other hand, this high N content coming from proteins and peptides is responsible for the formation of NO_x precursors (*e.g.* NH_3, HCN) when MSS is subjected to thermochemical treatments (*i.e.*

in the presence of O_2), while the S concentration (0.7 – 2.7 % wt db) [38] is responsible for the formation of H_2S and other gaseous S-compounds [44].

Characteristics	Primary Sludge	Secondary Sludge	Mixed Sludge	Anaerobically Digested MSS	Dewatered MSS	References
Carbon (% wt db)	19.4 – 45.2	41.5 – 47.2	33.3 – 43.4	25.6 – 49.3	24.9 – 39.9	Alvarez et al. (2016); Djandja et al. (2021); Ruiz-Gómez et al. (2017)
	n.r.	n.r.	n.r.	n.r.	32.1 – 69.3	Syed-Hassan et al. (2017)
Hydrogen (% wt db)	3.2 – 7.3	6.0 – 7.2	4.7 – 6.5	4.0 – 7.0	4.2 – 6.4	Djandja et al. (2021); Ruiz-Gómez et al. (2017)
	n.r.	n.r.	n.r.	n.r.	4.4 – 8.5	Alvarez et al. (2016); Syed-Hassan et al. (2017)
Oxygen (% wt db)	17.4 – 52.3	31.3 – 35.8	26.4	15.2 – 34.0	15.3 – 35.9	Djandja et al. (2021); Ruiz-Gómez et al. (2017)
	n.r.	n.r.	n.r.	n.r.	22.3 – 56.3	Alvarez et al. (2016); Syed-Hassan et al. (2017)
Sulfur (% wt db)	0.5 – 0.6	0.7 – 3.2	0.8	<0.1 – 1.7	0.7 – 2.7	Djandja et al. (2021); Ruiz-Gómez et al. (2017)
	n.r.	n.r.	n.r.	n.r.	0.6 – 2.1	Alvarez et al. (2016); Syed-Hassan et al. (2017)
Nitrogen (% wt db)	4.0 – 9.3	6.7 – 6.8	5.0 – 5.2	3.6 – 8.4	3.9 – 7.2	Djandja et al. (2021); Ruiz-Gómez et al. (2017)
	n.r.	n.r.	n.r.	n.r.	5.7 – 9.1	Alvarez et al. (2016); Syed-Hassan et al. (2017)
Phosphorus (% wt db)	2.0	2.0	n.r.	0.6 – 3.1	1.3 – 9.2	Djandja et al. (2021)
MC (% wt)	85.0 – 97.0	85	n.r.	75.7 – 80.0	69.3 – 89.4	Djandja et al. (2021)

VM (% wt db)	37.7 – 77.5	73.6	68.0	50.0 – 51.5	39.9 – 71.5	Alvarez et al. (2016); Djandja et al. (2021); Ruiz-Gómez et al. (2017)
	n.r.	n.r.	n.r.	n.r.	21.7 – 60.1	Syed-Hassan et al. (2017)
AC (% wt db)	20.9 – 55.6	13.7 – 76.6	30.5	40.0 – 46.5	20.9 – 54.7	Alvarez et al. (2016); Djandja et al. (2021); Ruiz-Gómez et al. (2017)
	n.r.	n.r.	n.r.	n.r.	10.9 – 76.5	Syed-Hassan et al. (2017)
FC (% wt db)	1.6 – 6.7	12.7	1.6	3.5 – 8.6	2.7 – 9.2	Alvarez et al. (2016); Djandja et al. (2021); Ruiz-Gómez et al. (2017)
	n.r.	n.r.	n.r.	n.r.	1.8 – 21.8	Syed-Hassan et al. (2017)
Protein (% wt db)	20.0 – 30.0	32.0 – 41.0	30.0	15.0 – 20.0	n.r.	Gururani et al. (2022); Suárez-Iglesias et al. (2017)
	n.r.	n.r.	n.r.	n.r.	26 – 28	Ruiz-Gómez et al. (2017); Xiong et al. (2013)
HHV (MJ/kg TS)	20.0	20.0	20.0	5.0 – 10.0	11.1 – 15.2	Alvarez et al. (2016); Gao et al. (2020); Gururani et al. (2022)
pH	5.0 – 8.0	6.5 – 8.0	6.5	6.5	7.0	Manara and Zabaniotou (2012); Suárez-Iglesias et al. (2017)

Table 1. 1. Composition and main characteristics of different municipal sewage sludge streams. % wt: percentage on weight; db: on a dry basis; MSS: municipal sewage sludge; MC: moisture content; VM: volatile matter; AC: ash content; FC: fixed carbon; HHV: higher heating value; n.r.: not reported.

1.1.2 Conventional management of municipal sewage sludge

In **Figure 1.2**, conventional methods for MSS management, their characteristics, and their percentages of disposal at the EU-27 level are reported. Although landfilling of MSS has been restricted at the EU level [50], 12 % of the MSS produced among the EU-27 member states is still disposed in landfills [21], implying several drawbacks such as the lack of energy, nutrient and material recovery from MSS, as well as the risk of leaching of harmful compounds into soil and water, resulting in potentially

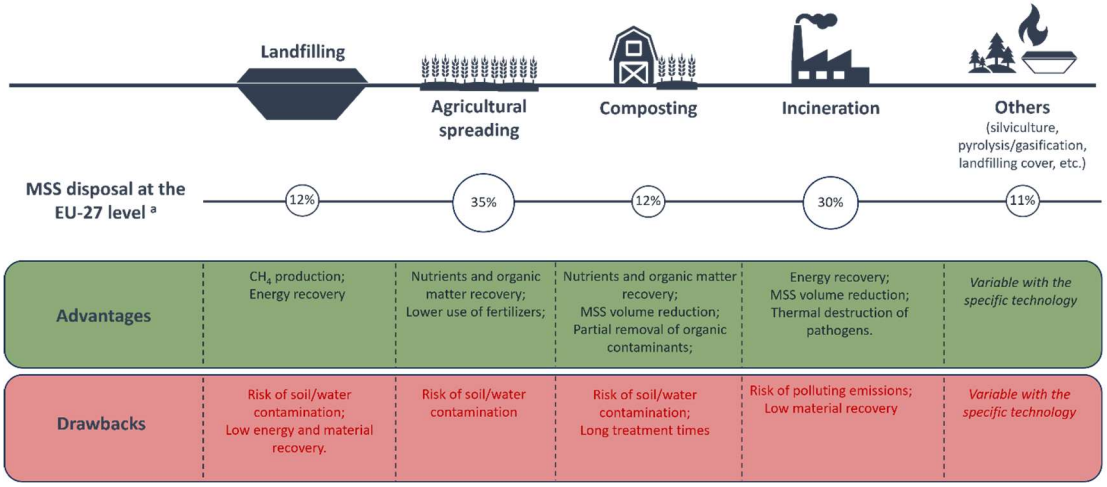


Figure 1. 2. Main disposal methods for municipal sewage sludge (MSS) in the EU-27 Countries. Advantages and drawbacks of landfilling, agricultural spreading, composting, incineration, and other methods, are reported. The disposal rate for each method in the EU-27 is indicated as well. [a]: expressed as tons of MSS disposed per tons of MSS produced. Data source: https://ec.europa.eu/eurostat/databrowser/product/page/ten00030

heavy environmental impacts [51,52]. On the other hand, 35 % wt of the MSS produced at the EU level is managed through direct application on agricultural soils [21], since it allows the agricultural reuse of the nutrients and organic matter embedded in MSS, thereby decreasing the need for chemical fertilizers, especially phosphorus-based ones [53,54].

Composting of MSS (applied to 12 % wt of the produced MSS [21]) offers advantages similar to the direct application on soil in terms of organic matter and nutrients recycling, and can also lead to the reduction of volume (up to 60 % on volume (v/v)), and the partial removal of organic pollutants and pathogens, thereby mitigating

the risks connected to their spreading [55,56]. Compared with raw MSS, composted MSS is characterized by better soil conditioning performances but requires further processing in dedicated facilities, with longer treatment times and higher costs [57].

MSS is also used outside agriculture in the EU-27 (applied to 11 % of the produced MSS [21]), including use in silviculture, forests and green areas, land reclamation, pyrolysis/gasification, and landfill cover.

Finally, due to advantages such as volume reduction, thermal destruction of pathogens, and energy recovery [58], incineration (either mono- or co-incineration) is also widely adopted in the EU-27 (applied to 30 % of the produced MSS [21]). A pre-treatment of MSS before incineration is usually necessary (mainly dewatering and drying) to achieve a MC of less than 25 - 30 % wt. During the incineration process, organic matter is thermally oxidized to form mainly CO_2 and water, with the production of ashes, generally around 30 % wt db [24,59]. Ashes can be landfilled or diverted to different uses, from building materials [60] to fertilizers [61]. Recently, an increasing interest in incineration has occurred in relation to phosphorus (P) recovery from ashes. White phosphorus and phosphate rock are included among the 30 critical raw materials for the EU [62], and MSS ashes are highly rich in P [63], in concentrations from 1 up to 14 % wt total P [64]. Nevertheless, incineration is still affected by many economic and environmental issues [65] and its application is meant to decrease in a context where high-value resource recovery is hierarchically preferred to energy recovery by environmental policies [66,67].

Nowadays, innovative thermochemical technologies (*e.g.* pyrolysis, wet oxidation, hydrothermal carbonization, gasification and combined processes) offer clear advantages over incineration in terms of flue gas and ash treatment costs [8], as well as for the multiple valorization opportunities associated with the obtainable products [9].

European legislation on MSS management and its evolution are described in detail in the **Appendix A**.

1.2 Pyrolysis of municipal sewage sludge

Different thermochemical processes can be applied to MSS management (**Table 1.2).** Pyrolysis is the dry thermochemical treatment [40] in which the thermal destruction of organic matter occurs in an inert atmosphere (*i.e.* in the absence of O_2), generally at atmospheric pressure [23,25]. Pyrolysis of MSS is conducted at temperatures spanning from 300 °C to a maximum of 900 – 1000 °C [33,40], but temperatures as high as 1400 °C have also been tested [68]. Pyrolysis of MSS allows to achieve three different end-products: biochar (solid carbonaceous product), bio-oil (liquid product), and pyrolysis gas. The pyrolysis process usually evolves with increasing temperatures through three different steps (drying, below 180 - 200 °C; active pyrolysis, from 180 - 200 to 540 - 600 °C; char decomposition, beyond 540 - 600 °C) [31], with the main decomposition occurring during the second step (up to 60 - 70 % wt loss), when most of the organic compounds are converted into the final products [69–71].

Depending on the operating conditions such as solid residence time (SRT) of the feedstock, heating rate (HR), and temperature, pyrolysis can be classified into: *slow* pyrolysis (HR: 0.1 – 1 °C/s; SRTs: 5 – 30 min; temperature: 300 - 700 °C), *fast* pyrolysis (HR: 10 - 200 °C/s; SRTs: 0.1 – 0.3 s; temperature: 400 - 600 °C), and *flash* pyrolysis (HR > 200 °C/s; SRTs <1 s; temperature: 750 – 1000 °C) [40], where fast and flash pyrolysis are generally used to maximize the liquid and gaseous yields, while slow pyrolysis is generally applied towards solid yield maximization [71]. Further, the distribution and properties of the resulting products are also influenced by other operative conditions (*e.g.* pressure, fluid dynamics, and reactor design), and MSS characteristics [72]. Combined control and steering of these parameters allow maximizing the yield and optimize the quality of the product(s).

When comparing pyrolysis to other thermochemical treatments such as gasification or hydrothermal conversion technologies, some critical considerations can be made. Both pyrolysis and gasification are affected by the necessity of strongly reducing the initial MC of the MSS (below 20 and 30 % wt, respectively), resulting in high energy consumption [40]. On the other hand, despite the opportunity of dealing with wet MSS (MC as high as 70 – 90 % wt), high pressures (2 – 10 and 4 – 25 MPa, respectively) are necessary for treatments such as hydrothermal carbonization (HTC) and

liquefaction (HTL) [2]. Additionally, the absence of an energetically valuable gaseous fraction produced by HTC, besides the technological issues related to the valorization of the liquid fraction [26], limits the recovery of energy in this process mostly to hydrochar combustion. Nonetheless, hydrochar yield can reach values up to 80 % wt, and about 50 % of the energy produced through hydrochar combustion can cover the whole energy required by the HTC process [73]. In a recent study [74], three different scenarios of AD coupled with gasification, pyrolysis, and HTC were analysed and compared. What emerged is that the solid fraction (*e.g.* bio- or hydrochar) produced from the different treatments is differently suitable for variable applications (*e.g.* additive in AD, soil conditioner, and fuel) because of the variability in its characteristics. Thus, it appears clear how a best-performing treatment among those mentioned for MSS cannot be univocally identified, since the final product applications largely determine the suitability of each treatment. Interestingly, as reported in **Table 1.2**, pyrolysis is characterized by a wider operative range for key parameters such as temperature and HR, with respect to other thermochemical treatments. Although MSS pyrolysis has been generally optimized towards the production of liquid bio-fuels, this versatile process can be tuned towards the maximization of the most desired products (biochar, bio-oil or pyrolysis gas), thereby allowing multiple valorisation routes.

Technologies	Acceptable Moisture (% wt)	Temperature (°C)	Pressure (MPa)	Heating Rate	Retention Time	Atmosphere	Products
Slow Pyrolysis		300-700		0.1 - 1 °C/s	5-30 min		
Fast Pyrolysis	< 20	400-600	0.1	10-200 °C/s	0.1 – 0.3 s	Ar / N_2 / He	Syngas/pyrolysis gas (H_2, CO, CO_2, CH_4, ...), bio-oils, biochar
Flash Pyrolysis		750-1000		>200 °C/s	< 1 s		
Gasification	< 30	700-1000		> 0.1 °C/s	< 30 min	Air / O_2 / CO_2 / Steam / Mix	
HTC		150-250	2-10	≈ 10 °C/min	5 min – 24 h	Ar / N_2	Hydrochar (main), liquid, CO_2
HTL		250-450	4-25			N_2 / O_2-free	Bio-oils (main), biochar, gas
WO	70-90	120-370	1.5-16	-	15-120 min	Air / O_2	VFAs (main), alcohols, ketones, NH_3, CO_2, H_2O
SCWO		500-600	30-40	-	< 1 min	Air / O_2 / H_2O_2	CO_2, H_2O
SCWG		600-700	>22	-	< 20-30 min	-	H_2, CH_4, (CO, CO_2)

Table 1. 2. Dry and hydrothermal technologies for the thermochemical conversion of municipal sewage sludge. Adapted from Chen et al. (2020), Djandja et al. (2021), Gao et al. (2020), Jiang et al. (2021), Langone and Basso (2020), and Xiao et al. (2022). *HTC: hydrothermal carbonization; HTL: hydrothermal liquefaction; WO: wet oxidation; SCWO: supercritical water oxidation; SCWG: supercritical water gasification; VFAs: volatile fatty acids.*

1.2.1 Conventional reactor configurations and full-scale prototypes

Pyrolysis has been conducted for decades on different feedstocks (*e.g.* plastics and lignocellulosic materials), resulting in the conceptualization and evolution of many reactor configurations. According to the literature, pyrolysis reactors are mainly classified based on vapours residence time (VRT) and HR in fast, intermediate, and slow pyrolysis reactors, yet additional classifications can be done based on other process variables (*e.g.* targeted final product, reactor operation mode, heating system and source, feedstock loading process, and operative pressure) [76,77]. Among the numerous possible reactor configurations, fixed bed, bubbling and circulating fluidized bed (FBR), conical spouted bed (CSBR), rotary kiln (RKR), and auger/screw reactors represent established and widely employed technologies, also owing to their scalability potential [2].

Fixed bed reactors are represented by classic batch reactors where the solid feedstock is heated and put in contact with the inert gas flow in a stationary process. This is the simplest configuration, affected by limited heat transfer rates, and generally employed at lab scale, in its vertical or horizontal configurations (**Figure 1.3A** and **1.3B**, respectively). In order to improve heat and mass transfer rates during the process, the FBR was designed [78].

In the FBR (or bubbling FBR) (**Figure 1.3C**), a pressurized gas flows from the bottom through the solid feedstock and the inorganic particles (*i.e.* sand or catalysts) composing the bed [79,80]. The gas flow causes the solid phase to act as a fluid (*i.e.* fluidization), allowing improved heat transfer between the different phases, with short residence times, and isothermal behaviour within the reactor [78]. Biochar is then moved outside of the reactor by the vapours, and collected through a cyclone, while bio-oil and pyrolysis gas are separated through a condensation step [80]. FBR can be operated in continuous mode, making this configuration more efficient than fixed bed reactors, and suitable both for lab- and full-scale applications [80]. Besides high energy consumption, long times for cooling and condensation, and important investment

costs, the main bottleneck of FBR is represented by the phenomenon of defluidization, consisting in the agglomeration of the solid particles inside the reactor, preventing biochar from being collected [79,81].

The conical spouted bed reactor (CSBR) was introduced to overcome these limitations of the FBR, since its design (**Figure 1.3D**) allows strong collision between the solid particles, resulting in a lower risk of agglomeration and consequent defluidization [78,81].

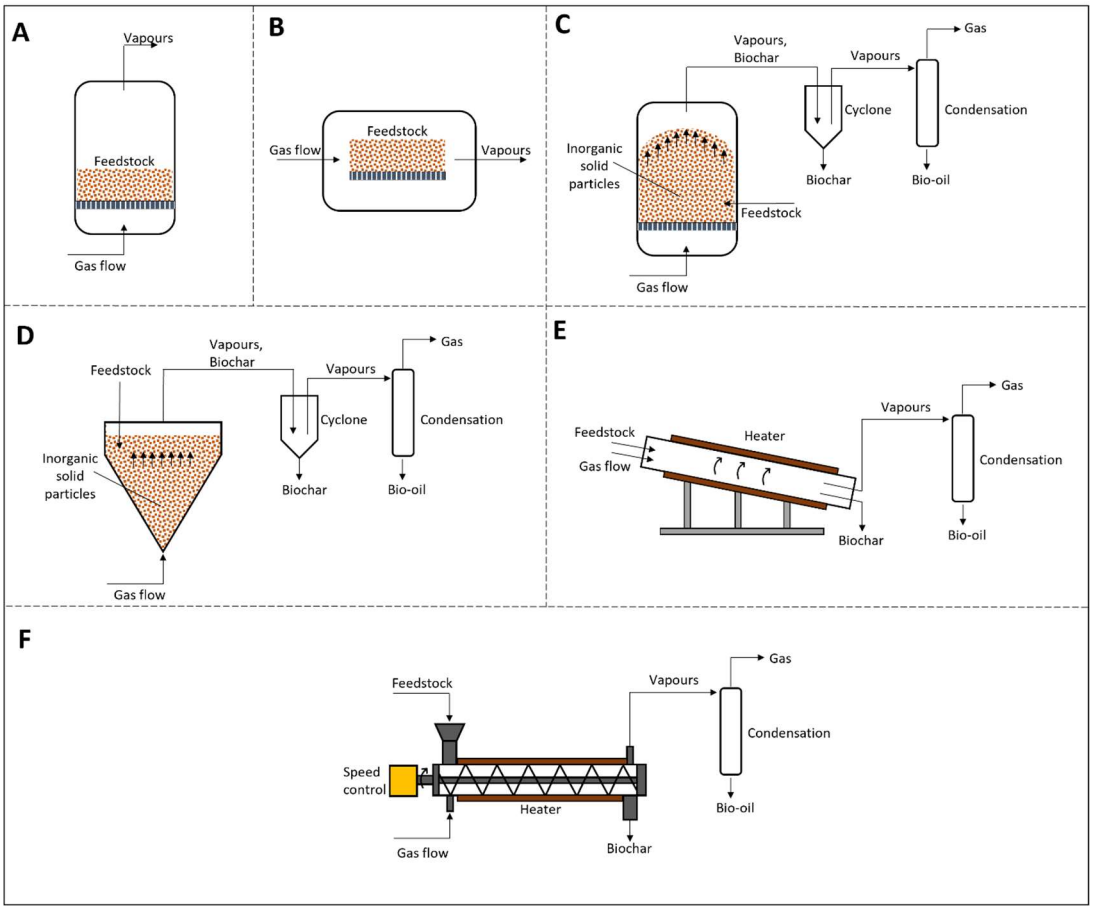


Figure 1. 3. Pyrolysis reactors. The main configurations for pyrolysis reactors are reported: A) vertical and B) horizontal fixed bed reactor, C) fluidized bed reactor, D) conical spouted bed reactor, E) rotary kiln reactor, and F) auger/screw reactor. Adapted from Babler et al. (2017), Campuzano et al. (2019), and Gao et al. (2022).

In the RKR, the feedstock moves through the reactor owing to its rotation speed and its slightly angled position (**Figure 1.3E**), resulting in the uniform heating of the feedstock [82,83]. Biochar is collected from the bottom, while vapours reach a

condensation step for bio-oil separation from the gas fraction. The RKR can be operated continuously using feedstocks with variable particle size, resulting in high efficiency and versatility for industrial applications, although low bio-oil yields are generally obtained with respect to those achieved with other configurations [2].

Finally, auger/screw reactors consist of an endless screw moving biomass through a heated tube, with biochar collected at the end, and volatiles conveyed to a condenser for bio-oil and pyrolysis gas separation (**Figure 1.3F**). These reactors can be easily moved to the desired location, including the production site of the biomass, therefore avoiding biomass transportation costs [81,84] . When compared to FBRs and SBRs, they are the most competitive on the market [2]. These reactors are generally widely employed in full-scale plants by industrial companies.

From the application of these and other reactor configurations, multiple full-scale prototypes and plants have been designed by private companies for the pyrolysis of different feedstocks, including MSS. The *Kore* (California, USA) company has recently realized a full-scale plant for the conversion of 800-900 t MSS/y into renewable diesel fuel [85], while a 70,000 t/y-capacity circulating FBR has been realized by *Dall Energy ApS* (Denmark) for the conversion of agricultural waste products into up to 20,000 t of biochar, and an amount of pyrolysis gas equivalent to an energy production of up to 90,000 MWh [86]. Interestingly, the Australian *Pyrotech Energy* company has placed a series of mobile screw-reactors on the market, with the possibility of installing a pyrolysis gas-fed generator at the end of the treatment train to fulfil the plant energy demand [87]. *AquaGreen* (Denmark) developed the module HECLA® Setores 1.000/1500 which integrates drying and pyrolysis in one system, able to treat 1000/1500 t MSS/y (5 installation in the Scandinavian Peninsula) [88]. Finally, Luo *et al.* [89] have thoroughly described the design and economic aspects related to a full-scale MSS pyrolysis plant operated in China, capable of treating about 100 t of wet MSS (MC of 80 % wt) per year at 450 °C, employing a screw-type configuration. Data from this latter work have been used as reference for the economic considerations reported in section 1.4.

1.2.2 Distribution of products from pyrolysis of municipal sewage sludge

The present section provides an overview of the most relevant experiences from literature on MSS pyrolysis. **Table 1.3** summarises the main results obtained in the literature about the effect of the MSS feedstock composition in terms of MC, VM, AC, and FC, as well as that of the main pyrolysis operating parameters (temperature, SRT, and HR), on pyrolysis products yield. This aspect is thoroughly discussed in the sections below.

1.2.2.1 Influence of municipal sewage sludge composition

A high VM generally leads to lower biochar yields since the organic volatile compounds tend to volatilize with high temperatures, which means higher bio-oil and/or pyrolysis gas production [71,90]. However, such a reduction of the biochar yields linked to a high VM content is limited by the content of FC, which represents the combustible organic C remaining solid after the complete degradation of VM, and is therefore considered as the minimum achievable biochar yield [91,92].

A positive correlation between MC and pyrolysis gas yield can also be observed. This is explainable by the fact that an atmosphere rich in vapour within the pyrolysis reactor promotes secondary cracking reactions (SCRs) of bio-oil [23]. In fact, in continuous pyrolysis systems, some of the organic compounds in the vapour phase can be further degraded and diverted to the gaseous phase, resulting in reduced bio-oil yields and higher pyrolysis gas yields. The role of MC in this phenomenon was highlighted by Xiong *et al.*, who studied the pyrolysis of the same MSS at 1000 °C, with and without drying (MC of 0 and 80 % wt) and obtained an increase of 25 % of the pyrolysis gas yield using an MSS with MC of 80 % wt [49].

Finally, as observed by Hossain *et al.*, two different dried MSS with AC as high as 30.9 and 42.5 % wt led to a biochar yield of 51.6 and 64.0 % wt, respectively [93]. AC, indeed, is representative of the amount of solid inorganic matter not susceptible to volatilization towards liquids and/or gases production, which is retained in the solid

phase instead. Thus, a higher AC leads to higher solid yields, with a high resulting AC in the obtained biochar [94].

1.2.2.2 Influence of pyrolysis parameters

Biochar yield is reported to constantly decrease with temperature increase, achieving its optimum in the 300 - 500 °C range and reaching values from 25 up to over 75 % wt [71,90], while pyrolysis gas yield increases slowly at lower temperatures and generally starts to become relevant only after 600 °C [95,96], reaching up to 46 % wt over 1000 °C [68]. A different behaviour characterizes bio-oil formation: the highest yields are obtainable between 450 and 550 °C [28], while above this range, the onset of SCRs leads to a decrease of the bio-oil fraction in pyrolysis products [97]. Huang *et al.* efficiently showed the simultaneous effect of SCRs on liquid and gaseous yields. Starting from 400 °C, bio-oil and pyrolysis gas yields grew to the detriment of biochar due to the decomposition and volatilization of the solid organic matter, with bio-oil reaching a maximum yield of 44.5 % wt on a dry ash-free basis (daf) at 500 °C and then decreasing to 32 % wt daf at 700 °C [98]. At the same time, pyrolysis gas yield kept increasing at a higher rate between 500 and 700 °C, confirming the further decomposition of VM and its migration from bio-oil to pyrolysis gas [98].

Gao *et al.* studied the effect of different SRTs (6, 23, and 46 minutes) during the pyrolysis of a dried MSS at 700 °C in a spiral continuous reactor [99] . The increase of SRT from 6 min up to 23 min enhanced VM degradation at the same temperature, resulting in a 51 and 23 % higher pyrolysis gas and bio-oil yield, respectively, with a 13 % reduction of the biochar yield. On the other hand, higher SRTs (46 minutes) had a negligible influence on the achieved product yields, indicating how higher SRT do not lead to further improvements. Nevertheless, the open configuration of the reactor in the mentioned study probably prevented vapours from remaining in contact with the solid phase for the entire SRT, therefore avoiding the onset of further SCRs for SRTs between 23 and 46 min.

MSS characteristics				Pyrolysis operating conditions						Pyrolysis products			References
MC % wt	Ash [a] % wt	VM [a] % wt	FC [a] % wt	T (°C)	HR (°C/min)	SRT (min)	VRT (s)	Inert	Reactor	Pyrolysis gas % wt	Bio-oils % wt	Biochar % wt	
5.60 11.10	30.90 42.50	53.20 45.90	10.30 0.50	550	10	n.r.	n.r.	Ar	Fixed bed	5.7 5.6	42.7 30.4	51.6 64.0	Hossain et al. (2009)
6.70 5.30 7.10	39.90 52.00 41.00	47.00 38.30 46.60	6.40 4.40 5.30	550	n.r.	n.r.	n.r.	N_2	Fluidized bed	25.0 20.0 25.0 - 30.0 [c]	50.0 45.0 50.0	25.0 35.0 25.0	Fonts et al. (2009)
80.40 0.00	47.60 47.60	45.50 45.50	6.90 6.90	1000	-	60	n.r.	N_2	Horizontal; quartz	36.2 29.0	16.2 17.9	47.6 53.1	Xiong et al. (2013)
4.49- 7.39	22.45- 38.01	51.01- 63.05	5.98- 7.11	300 500 700	10	5	2.7	Ar	Fixed bed	2.0 - 6.0 n.r. 17.5 - 27.4	26.0 37.0 - 47.0 37.0 - 42.0	62.0 - 65.0 35.0 - 45.0 30.0 - 42.0	Fan et al. (2014)
7.50	24.08	59.06	9.36	450-650	8 100	n.r.	n.r.	N_2	Horizontal tubular furnace	14.2 - 28.6 10.0 – 30.0	32.2 - 38.3 43.0 – 40.0	53.6 - 33.2 47.1 - 30.0	Gao et al. (2014)
5.60	56.80	40.10	3.10	400 500 600 700	-	10	n.r.	Ar	Drop tube; quartz	14.7 [b] 17.7 [b] 27.3 [b] 40.7 [b]	38.0 [b] 44.5 [b] 37.0 [b,c] 32.0 [b]	30.0 [b] 22.0 [b,c] 18.0 [b,c] 16.0 [b]	Huang et al. (2014)

Table 1.3. (continued)

12.70	27.70	50.90	9.10	250 500 700	10	n.r.		N_2	Cylindrical quartz glass vessel	11.8 18.9 22.6	17.2 22.4 19.0	71.0 58.7 58.4	Ghodke et al. (2021)
19.50	60.80	31.30	7.90	1000 1400	n.r.	n.r.	n.r.	n.r.	Free-fall	37.0 46.0	9.0 0.0	53.0 51.0	Zhang et al. (2014)
6.30	31.84	54.06	7.80	400 700 700 700 800	n.r.	23 6 23 46 23	n.r.	N_2	Spiral continuous	10.0 [c] 16.5 25.0 [c] 25.7 29.3	12.0 13.6 16.7 15.8 11.8	75.0 [c] 65.2 57.0 [c] 55.6 57.0	Gao et al. (2017)
5.60	37.20	54.20	8.60	450 500 600	-	2	< 1	N_2	Conical spouted bed	3.0 5.2 11.4	44.8 48.5 45.4	52.2 46.3 43.2	Alvarez et al. (2016)
5.0	35.00	60.00	n.r.	500 600 750	10	60 120 180 60 120 180 60 120 180	n.r.	N_2	Tubular packed-bed	14 [c] 20.0-21.0 [c] n.r. 22.0 32.0	26-28 [c] 23.0 [c] 23.0 [c] 18.0 [c] 18.0 [c]	58-60 [c] 55.0-57.0 [c] 50.0 [c]	Halalsheh et al. (2024)

Table 1.3. (continued)

5.0	35.00	60.00	n.r.	850	10	60	n.r.	N_2	Tubular packed-bed	28.0	24.0 [c]	48.0 [c]	Halalsheh et al. (2024)
						120				33.0	14.0 [c]	52.0 [c]	
						180				30.0 [c]	15.0 [c]	51.0 [c]	

Table 1. 3. Influence of municipal sewage sludge characteristics and pyrolysis operating parameters on products yield and distribution. [a] dry basis; [b] dry ash free basis; [c] deducted from graphics ; MSS: municipal sewage sludge; MC: moisture content; VM: volatile matter; FC: fixed carbon; T: temperature; SRT: solid retention time; VRT: vapour retention time; HR: heating rate; n.r.: not reported; wt: on a weight basis

Interestingly, after a 12 % reduction of biochar yield registered when moving from 600 to 750 °C, Halalsheh *et al*. [100] observed a further increase in biochar yield when temperature increased up to 850 °C, for SRTs as long as 2 and 3 hours. The authors associated this phenomenon to gas condensation and consequent repolymerization, due to prolonged VRT. Slow pyrolysis processes with excessively long SRTs could therefore affect pyrolysis gas yield. The extent of SRTs can also influence the effect of SCRs: Halalsheh *et al*. [100] reported a decreasing trend for bio-oil yield at increasing temperature for high SRTs (2 and 3 hours). On the other hand, for a lower SRT (1 hour), the increasing temperature had no effect on the bio-oil yield.

Gao *et al.* investigated the role of HR during the pyrolysis process [97]. An interesting behaviour can be observed by considering the HRs variable at constant pyrolysis maximum temperatures (450 – 650 °C). At 450 °C, thus in the optimal temperature range for biochar formation, the two different HRs (8 and 100 °C/min) led to biochar yields of 53.6 and 47.1 % wt, respectively. The yield of bio-oil benefitted from the faster pyrolysis, moving from 32.2 to 43.0 % wt, while pyrolysis gas yield decreased from 14.2 to 10.0 % wt. This result indicates that at low temperatures, high HRs (thus faster pyrolysis) cause a more complete degradation of the MSS solid matrix towards the liquid bio-oil fraction. It is worth noting that increasing HR from 8 to 100 °C/min is less influent when the process is operated at higher temperatures (650 °C) since no important variations in the products yields can be observed. As a matter of fact, when moving to higher temperatures, the effect of SCRs in reducing bio-oil yield acts predominantly, and the role of HR is less important [101].

In fact, in fast pyrolysis, moderate temperatures as well as short SRTs and VRTs are employed, resulting in the avoidance of SCRs, therefore leading to the maximization of bio-oil yield [102]. This is consistent with what Alvarez *et al.* [46] observed, who reported pyrolysis gas yields as low as 3.0 and 5.2 % wt at 450 and 500 °C, respectively, with a maximum bio-oil yield of 48.5 % wt at 500 °C, and a SRT of 2 min. As discussed for HR, even for SRT, the effect of SCRs becomes predominant at higher temperatures, resulting in the decrease of the bio-oil yield to 45.4 % wt at 600 °C.

1.3 Pyrolysis products: main characteristics and potential valorization pathways

Maximizing the recovery and valorization potential of the resources embedded within MSS through pyrolysis requires a holistic approach, considering how the MSS matrix composition as well as the operating conditions can steer product distribution in support of innovative biorefinery strategies. For instance, improving pyrolysis gas yields could enable the application of gas fermentation processes towards the synthesis of value-added products, while optimal biochar production could be targeted in view of agronomic applications. On the other hand, bio-oil has already been applied as a possible alternative to fossil fuels. Nevertheless, the application of these valorization routes needs to be evaluated in relation with the specific composition and properties of pyrolysis gas, bio-oil and biochar. In this section, the characteristics and the valorization potential of each of the pyrolysis products are reviewed by considering both established and innovative solutions.

1.3.1 Biochar

Biochar is a solid, stable carbonaceous material [103], characterized by interesting physical-chemical properties and a strong multi-application potential, including soil conditioning and nutrients supply [10,11], carbon capture [12], pollutant removal from both soils and wastewaters [13], as well as more innovative applications.

The valorization potential of biochar, including MSS-derived biochar (SDBC), is highly influenced by its surface properties such as the specific surface area (SSA), pore volume (PV), pH, alkalinity, electric conductivity (EC), cation exchange capacity (CEC), and surface functional groups [104–106]. All these characteristics are directly influenced by pyrolysis parameters, especially temperature (see **Table 1.4**), but also by the composition of the feedstock.

During pyrolysis, dehydration and depolymerization reactions occur, leading to a reduction of H and O concentration [104] and, thus, a decrease of the H/C and O/C ratios in biochar, which is directly proportional to rising temperatures [107]. The H/C is indicative of the level of aromatization of biochar, and is further related to its

stability: lower H/C ratios ensure biochar resistance to degradation in soils [103]. On the other hand, higher O/C ratios provide higher polarity, which is strictly connected

Pyrolysis T (°C)	Ash (% wt)	H/C	O/C	SSA (m^2/g)	PV (cm^3/g)	pH	EC (dS/m)	CEC (cmol/kg)	References
400	72.02	n.r.	n.r.	33.44	n.r.	7.76	3.04	29.90	Méndez et al. (2013)
600	78.53			37.18		8.72	1.46	11.67	
300	65.80	n.r.	n.r.	14.37	0.1080	6.66	7.75	n.r.	Yuan et al. (2015)
500	80.60			24.53	0.1390	7.50	2.55		
700	86.80			26.70	0.1590	8.40	1.56		
400	52.00	n.r.	n.r.	0.10	0.0014	7.70 - 7.80	n.r.	n.r.	Song et al. (2014)
450	55.60			2.90	0.0036	8.20 - 8.30			
500	57.60			3.20	0.0017	9.00 - 9.10			
550	58.50			13.30	0.0066	9.90 - 10.00			
300	83.25	0.10	0.95	5.11	n.r.	6.43	n.r.	n.r.	Zhang et al. (2022)
500	87.93	0.09	0.82	15.23		6.96			
700	91.93	0.07	0.85	13.57		10.50			
500	74.21	0.48	0.45	25.45	0.0560	8.81	n.r.	76.75	Chen et al. (2014)
700	81.53	0.15	0.30	32.17	0.0680	11.11		50.34	
900	88.07	0.09	0.12	67.60	0.0990	12.15		247.51	
300	n.r.	0.18	n.r.	14.28	n.r.	n.r.	n.r.	n.r.	Yuan et al. (2013)
500		0.22		24.36					
700		0.19		26.87					

Table 1. 4. Composition and surface properties of sewage sludge-derived biochar. T: temperature; SSA: specific surface area; PV: pore volume; EC: electric conductivity; CEC: cation exchange capacity; n.r.: not reported; wt: on a weight basis

to the hydrophilicity of biochar [111]. Thus, biochar with a high O/C ratio has a higher adsorption capacity of polar substances such as water, meaning that a positive effect on water retention in soils may be achieved by adding biochar characterized by an elevated O/C ratio.

The pH of SDBC is generally alkaline and increases with pyrolysis temperature [108], with values ranging between 6.5 and 12.0. This characteristic allows a good retention of PTEs when SDBC is applied on soils [103]. SSA and PV are shown to increase with pyrolysis temperatures from 300 to 500 - 600 °C [110,113], while beyond 700 - 750 °C the collapsing of biochar pore structure and the subsequent reduction of SSA and PV may take place [111,114]. Nevertheless, Chen *et al.* reported a continue increase of the Brunauer-Emmett-Teller (BET) surface area and PV with higher temperatures, even in the range of 700 - 900 °C, up to 67.60 m^2/g and 0.099 cm^3/g, respectively, which were respectively 110.1 and 45.6 % higher than the values obtained at 700 °C [103]. These different trends could be attributed to the variable composition (especially AC) of SDBCs and, therefore, that of the original MSS feedstock. Higher ACs in MSS are indeed known to inhibit the proper development of SSA and pore structure of SDBC [115]. Biochars derived from other feedstocks (*e.g.* wood, wheat straw, pig manure, and peanut shell) can generally be characterized by higher SSAs and PVs than those of SDBC [116], up to 132 m^2/g and 0.083 cm^3/g, respectively, but values as high as 490.8 m^2/g and 0.25 cm^3/g can be reached when proper pyrolysis conditions are designed [117]. Lignocellulosic materials are indeed characterized by lower AC and higher C content with respect to MSS [118].

According to Leng *et al.*, biochars with high SSA and PV could be generally obtained by conducting pyrolysis of various feedstocks at mild temperatures (400 - 700°C) and HR (5 - 30 °C/min), with elevated SRT (30 - 120 min), gas flow rates in the range of 50 - 150 mL/min, and atmospheric pressure [117]. These ranges are merely indicative, and the effect of MSS characteristics needs to be taken into account for the efficient optimization of SDBC properties.

Besides trying to optimize SDBC properties through *in-situ* variation of temperature, HR, and/or SRT during pyrolysis, surface properties amelioration can be performed through pre- or post-treatments on raw MSS or directly on SDBC, respectively [13,40]. Physical modifications of biochar generally consist in biochar exposure to an oxidizing atmosphere (typically CO_2, air or steam) at elevated temperatures (over 700 °C) in order to induce further development of SSA, and pore structure and distribution [119]. According to Leng *et al*. [117], a 13-times higher SSA can be achieved in biochar after CO_2 post-activation. The same authors also indicated the pyrolysis in a CO_2-atmopshere as a possible method for the amelioration of biochar properties, since it can result in a 2-times higher SSA with respect to what was obtained in a N_2 atmosphere. Interestingly, in order to induce formation of N-containing functional groups on biochar, pyrolysis in a NH_3-atmosphere was investigated as well [120].

Chemical modification of biochar is instead pursued through the addition of acid or basic compounds (KOH, K_2CO_3, H_3PO_4, $ZnCl_2$, H_2SO_4, or others) during pyrolysis of the feedstock or during a second thermal activation conducted on biochar [121–124]. The employment of such chemicals was reported to improve SDBC surface properties by enhancing the presence of oxygen-, phosphate-, and carbonyl-containing functional groups [40]. A SSA up to 3263 m^2/g was achieved by Liu *et al.* [125] in rice husk-derived biochar through biomass impregnation with KOH in a 4:1 KOH to rice husk mass ratio.

1.3.1.1 Soil conditioning

SDBC application on soils can contribute to P, N and organic C supply [126], with positive effects on soil characteristics. Additionally, over 90 % of the initial P content of MSS is retained within SDBC [127], P represents the preponderant nutrient in SDBC, which could therefore be used as an efficient soil conditioner for P-deficient soils [128]. In fact, SDBC was observed to increase nutrient circulation and to avoid nutrient leaching in acidic soils [10], owing to its capability of retaining P within the solid matrix, with better effects observed when SDBC was produced at higher temperatures [129]. On the other hand, according to Marcińczyk and Oleszczuk,

biochar with low nutrient content and high porosity can be harmful for nutrient bioavailability within soils [130]. Nevertheless, SDBC is generally characterized by a higher N and P content when compared with biochar obtained from nutrient-poor lignocellulosic feedstocks such as rice husk and corn cobs [116]. Therefore, the use of SDBC may avoid this possibility. The commercialization of biochar as soil conditioner is gaining momentum: companies such as *Black Owl Biochar*/*Biochar Supreme*, *Swiss Biochar*, *Carbon Gold*, and *Bioforcetech Corporation*, are marketing biochar produced from different types of biomass for the amelioration of soil properties. Nevertheless, according to European legislation, MSS-derived biochar is nowadays still considered as a mere waste, with no possibility of commercialization [131].

The risk of PTEs leaching connected to the direct use of MSS on soils is strongly reduced through its conversion to SDBC. Although PTEs concentrations in SDBC reported by Alipour *et al.* were several times higher than those of the initial MSS, less than 20% of the PTEs content was in a bioavailable form, with this fraction decreasing with pyrolysis temperature increasing [132]. This data is consistent with what Xing *et al.* observed: a reduction of the concentration of bioavailable Cu from 92 to 9 % of the total Cu concentration when SDBC was produced at 900 °C instead of 300 °C, from the same feedstock [133].

Finally, according to the literature, SDBC application as conditioner might induce groundwater and soil contamination from PAHs [134]. A total concentration of the 16 United States Environmental Protection Agency (USEPA) PAHs in SDBC as high as 1942 µg/kg db was reported by De la Rosa *et al*.[135] , although it was lower than those observed in biochar derived from other biomass types (*i.e.* vineyard wood, wood chips, rice husk, and wheat husk) produced under the same conditions. Although the total PAHs concentration in biochar is reported to decrease with pyrolysis temperature, the PAHs migration rate from SDBC is reported to increase with higher pyrolysis temperatures, resulting in the mobilization of up to 16 % of the initial PAHs content [135]. Further investigations on this aspect are required.

1.3.1.2 Soil remediation

Although SDBC under some conditions could be responsible of PAHs leakage to the soil, its physical-chemical characteristics make it a suitable material for the removal of emerging contaminants, such as PAHs, PFAS, PTEs, and other pollutants from soils. A decrease of 56 – 67 % in the bioaccumulation of PAHs in plant biomass was reported for plants grown within contaminated soils after the addition of SDBC with application rates as high as 10 % wt db [136]. Interestingly, Zhang *et al.* reported a few possible adverse effects of biochar application for PAHs remediation, which may also involve SDBC application, that are mostly connected to the different nature and/or molecular weight of different PAHs [137]. These effects included the possibility of reducing the biodegradability of PAHs while adsorbing them on the biochar surface, together with the alteration of the soil microbial community after biochar addition. Additional dedicated studies investigating these dynamics are required.

PFAS removal from contaminated soils can be efficiently performed by SDBC with performances comparable with or higher than those of activated carbons, although lower efficiencies were reported for the removal of short-chain PFAS [138].

PTEs adsorption on SDBC can strongly reduce the Al^{3+} and Pb content in soils [139], but SDBC can also favour the indirect stabilization. According to Li *et al.*, SDBC can stimulate proliferation of N-fixing bacteria when applied in combination with crops dedicated to phytoremediation processes, resulting in the efficient stabilization of PTEs [140].

Finally, SDBC obtained from pyrolysis at 850 °C showed promising adsorption performances in the removal of organic recalcitrant compounds in landfill leachate, suggesting the possibility of employing SDBC for remediation of contaminated dismissed landfill sites [141].

1.3.1.3 Carbon capture

Among the main technologies for gas capture and sequestration (*i.e.* absorption, adsorption and membranes), adsorption is generally the least expensive and the most efficient solution [142]. Nevertheless, finding a suitable sorbent to separate CO_2 from

the gas stream can be challenging [143]. High SSA, elevated porosity, and recalcitrance to biodegradation are some advantageous characteristics that allow to recognize SDBC (and biochars in general) as a promising and cost-effective material for carbon capture and storage [12]. Xu *et al.* underlined the double role played by SDBC in this field, given its capability of carbon sequestration during the pyrolysis process, and that of adsorbing CO_2 from the environment [144].

Brassard *et al.* studied the effects of the addition of different biochars on CO_2 and N_2O emissions from soils and indicated that biochars may impact positively or negatively these emissions according to their characteristics and those of the soil [145]. More specifically, a correlation between pyrolysis temperature during biochar production and CO_2 emissions was observed. Low temperatures (350 °C) limit the degradation of VM during pyrolysis, stimulating the C mineralization of biochar within soils by microbial activity, and resulting in higher CO_2 and N_2O emissions independently from the pyrolysis feedstocks [146]. On the other hand, as already reported for biochars from different feedstocks [147–149], SDBC can capture CO_2 from the environment through both physical and chemical sorption, by means of its porous structure and chemical surface characteristics (*e.g.* functional groups), respectively [139,144].

A CO_2 adsorption capability of 28.36 mg/g was achieved at 30 °C by using a SDBC produced at 800 °C [150]. In the latter study, the employment of cationic polyacrylamide as a dewatering agent for MSS prior to pyrolysis at 600 °C allowed to achieve the highest CO_2 adsorption capability at 90 °C by SDBC up to 48.54 mg/g, owing to a more efficient development of microporosity in the biochar structure. CO_2 adsorbed by SDBC can eventually be desorbed and recovered for multiple industrial applications as well as being converted into value-added products [139].

Although biochar has a lower environmental impact than other adsorbent materials [151], modification pretreatments are often required in practical applications for CO_2 capture to improve its physicochemical properties [148]. Apart from the treatments mentioned in section 1.3.1 (*i.e.* CO_2-, air, and steam-activation, and chemical modification), innovative methods including, metal-impregnation, and plasma

treatment have recently been studied specifically for CO_2 capture by biochar: Mg-impregnation resulted in a higher CO_2 adsorption capability when compared to other metals, while plasma treatment allowed a better development of O- and N-based functional groups, with positive influence on CO_2 adsorption [152,153].

1.3.1.4 Nutrient recovery and contaminants removal from wastewater

Table 1.5 overviews examples from the literature regarding biochar and SDBC employment for nutrients recovery and contaminants removal from wastewater.

Tang *et al.* reported the capability of a SDBC produced at 450 °C to recover ammonium-N from municipal wastewaters, with a removal capacity of 1.2 mg NH_4^+-N/g SDBC, similar to that of activated carbons [154]. According to Yin *et al.*, co-pyrolysis of MSS and walnut shell resulted in a biochar which was more capable of adsorbing ammonium when compared with a biochar derived from the pure MSS, the latter having higher affinity with phosphate instead [155]. The possibility of using SDBC as an adsorbent material for P recovery may represent a valid and economic alternative to other expensive solutions, such as chemical precipitation or the utilization of adsorbents derived from virgin materials [156]. Yang *et al.* achieved more than 96 % efficiency in terms of phosphate removal from aqueous solution using a Ca-modified biochar obtained by co-pyrolysis of MSS and eggshell [157]. The obtained P-loaded biochar was then successfully used as an adsorbent for PTEs removal from aqueous solutions (efficiency over 99 %). Further, after the efficient P removal from an aqueous solution, Liu *et al.* observed how SDBC released the adsorbed P with slow rates [158], thus suggesting the possibility of using P-loaded SDBC as a fertilizer in an integrated valorization scheme.

Many examples are reported in the literature for SDBC as an adsorbent material for the removal of phenolic compounds, antibiotics, textile dyes, and PTEs from wastewaters by leveraging surface polymerization and physisorption mechanisms, polar and electrostatic interactions, and the presence of specific functional groups (*i.e.* phenolic, hydroxyl and carboxyl) [105,159]. Interestingly, SDBC can be used to remove more than 80 % of the long-chain PFAS from water, although the efficiency of the adsorption process is directly proportional to SDBC's porosity and SSA, and

therefore biochar produced from lignocellulosic materials generally offers higher performances. On the other hand, lower efficiencies for short-chain PFAS were reported [160].

Biochar		Matrix	Removed substance	Removal efficiency		References
Feedstock	Modification			% wt	mg/g biochar	
MSS	-	Municipal wastewaters	NH_4^+-N	n.r.	1.2	Tang et al. (2019)
MSS			NH_4^+ PO_4^{3-}	2 % 65 %	0.62 49.95	
MSS + Walnut shell	-	Aqueous solution	NH_4^+ PO_4^{3-}	7 % 52 %	2.31 40 [a]	Yin et al. (2019)
Walnut shell			NH_4^+ PO_4^{3-}	5 % 1 %	1.58 0.65	
MSS + Eggshell	Ca-addition Ca-addition; P-adsorption	Aqueous solution	PO_4^{3-} PTEs (Cd^{2+}, Pb^{2+}, Cu^{2+}, Zn^{2+})	> 96 % > 99 %	> 24 2.5 – 5.0	Yang et al. (2021)
MSS	-	Contaminated water	Long-chain PFAS Short-chain PFAS	> 80 % 19 – 27 %	n.r. n.r.	Kundu et al. (2021)
MSS	Air-roasting oxidation	Aqueous solution	U(VI)	73 % [b]	282.4	Sun et al. (2022)

Table 1. 5. Biochar employment in nutrient recovery and contaminant removal from water. [a]: deducted from graphics; b: higher initial concentration (50 mg U/L); c: lower initial concentration (1 mg U/L); MSS: municipal sewage sludge; PTEs: potentially toxic elements; PFAS: per- and poly-fluoroalkyl substances; wt: on a weight basis; n.r.: not reported.

1.3.1.5 Improvement of anaerobic digestion performance

Biochar addition has been recently investigated as a possible solution for multiple critical issues affecting the AD process, *i.e.* acidic stress, inhibitory compounds, microbial strains vulnerability, CH_4 upgrading efficiency and costs [164]. In an AD process, biochar is capable of improving CO_2 adsorption, thereby reducing the cost of biogas upgrading. At the same time, its buffering properties and specific functional groups can enhance CH_4 production by decreasing the formation of microbial inhibitors such as NH_3/NH_4^+ and H_2S [165,166], while its remarkable electron transfer ability is determinant for enhancing biogas production and VFAs degradation. Nevertheless, the limited SSA and porosity typical of SDBCs suggest the necessity of physical/chemical modifications prior to its employment in such a process [167].

Chiappero *et al.* conducted batch tests of mesophilic AD of MSS with and without the addition of SDBC [168]. Almost no effect on biogas production was detected, while a significant increase of the final biomethane content was observed (37 % v/v vs 29 % v/v of the control). The latter values were still lower than those observed for biochar obtained from rice husk in the same study (67 % v/v), because of the lower SSA and PV in the former, and thus its lower CO_2 physical adsorption capacity. Interestingly, Wu *et al.* reported negligible or negative effects of SDBC on the final yield in the AD of MSS [169]. According to the authors, these effects were probably due to the inhibition of the short-chain fatty acids production during the process because of the limited SSA and porosity, which resulted in unfavourable conditions for acid-producing microorganisms. On the other hand, Liu *et al.* observed an improvement in biogas production up to 54.5 % when SDBC produced at 400 °C was added in the AD of MSS, with an MSS to biochar ratio of 5:1 [170]. Finally, Zhang *et al.* reported a 77 % higher cumulative biomethane yield in the AD of MSS upon the addition of SDBC produced at 400 °C compared to the control without SDBC [171]. The authors indicated a dosage of 26 g SDBC/L as optimal for maximization of cumulative biomethane yield and avoidance of excessive dosages, which would result in inhibition of the AD process.

SDBCs are generally characterized by a higher pH (up to 12) with respect to other types of biochars. Thus, their addition in AD can help mitigating the acidic stress caused by acids accumulation, resulting in the improvement of the overall volatile fatty acids (VFAs) biodegradation capacity of methanogens [172]. Additionally, acidification is often induced by ammonia inhibition of methanogens occurring in the AD of feedstocks with low C/N ratios (*i.e.* below 15) such as manure or even MSS [165]. In fact, the conversion of large amounts of organic-N into free ammonia-N results in the inhibition of methanogenic activity, with the consequential accumulation of VFAs [165,173]. Among the multiple strategies developed for mitigating this phenomenon, the addition of adsorbent materials can represent a promising alternative. Zeolites, activated carbon, and biochar can help mitigate the effects of ammonia inhibition by retaining ammonia-N, owing to their physicochemical properties [174]. The SDBC capability of retaining total ammonia-N (TAN) during AD of MSS, with resulting positive effects on the biomethane yield, was reported by Zhang *et al.*, who observed a removal of 91.3 - 110 mg TAN/g SDBC with a dosage of 8 g SDBC/L [171].

Conductive materials such as graphene, activated carbon, and biochar (including SDBC), were reported to positively influence AD, due to their capability of improving direct interspecies electron transfer (DIET), justifying their employment for the production of bioelectrodes in microbial electrolysis cell systems combined with AD (MEC-AD) [175–177] . DIET represents the transmission of electrons among different microorganisms involved in the AD process (*i.e.* acetogens and methanogens), therefore it regulates the efficiency of the biochemical reactions occurring during AD, with direct influence on biogas production and VFAs degradation [178]. Yin *et al.* [179] reported a 25 % higher biomethane production and a 43 % shorter lag phase in the MEC-AD of waste activated sludge, by dosing 1 g SDBC/g dry matter. Interestingly, the improvement of DIET induced by biochar was reported to simultaneously enhance initial VFAs formation and their subsequent degradation [178,179]. Furthermore, it was reported that depending on the mode and extent of biochar dosage, excessive accumulation of VFAs can occur in the initial phases of the

process [178]. The mechanisms responsible for biochar-induced enhancement of MEC-AD processes are yet to be fully clarified, while the upscaling of such systems is still technically challenging.

1.3.2 Bio-oil

MSS-derived bio-oil (SDBO) is a dark viscous liquid composed by an aqueous phase and a mixture of organic compounds such as alcohols, phenols, carboxylic acids and aromatics, which is produced by the depolymerization and fragmentation of the organic matter during the pyrolysis process [71,180]. The main characteristics of SDBO are reported in **Table 1.6**, where they are compared with those of bio-oil produced from the pyrolysis of other feedstocks. A particular focus is given to SDBO fuel properties since its application as biofuel is the most commonly reported in the literature.

1.3.2.1 Pyrolysis-derived biofuels: properties and applications

Research on bio-oil has mainly focused on biofuel applications of lignocellulosic materials-derived bio-oil (LDBO) and SDBO as alternatives to petroleum fuels. Since raw materials may account for 80 % of the costs of bio-oil production, employing MSS as feedstock would reduce these costs while representing a competitive alternative to fossil fuels usage [14].

The C and H content in SDBO can vary in the ranges of 42.3 - 65.2 % wt and 7.3 - 9.3 % wt (**Table 1.6**), respectively, which are substantially higher than those observed for LDBO (32 - 58 % wt and 5.5 - 8.5 % wt) [15,46,181]. According to Alvarez *et al.*, the C and H content decreases when the pyrolysis temperature rises over 500 °C due to SCRs [46]. However, Huang *et al.* observed an increase in C content (from 57.1 to 60.6 % wt) when the temperature rose from 400 to 700 °C [98], which is probably due to a decrease in O concentration. The decrease of C and H content with temperature reasonably results in the decrease of the bio-oil heating value. A maximum HHV of 36.4 MJ/kg was observed in SDBO by Arazo *et al.*, which is higher than the maximum HHV reported for LDBO (16 - 19 MJ/kg) [182], and lower but comparable with that of 44 MJ/kg reported for petroleum fuels [183].

	Pyrolysis T (°C)	C (%wt)	H (%wt)	N (%wt)	O (%wt)	S (%wt)	HHV (MJ/kg)	LHV (MJ/kg)	pH	Density (kg/m^3)	Viscosity (cSt)	MC (%wt)	References
SDBO	450	58.9	9.3	5.9	12.3	1.5	31	n.r.	8.2	1040	64.9 - 66.8 [a]	n.r.	Kuan et al. (2020)
	400	44.4	8.8	5.8	40.5	0.5		18.4					
	500	45	8.8	6.6	39	0.7	n.r.	18.8	8.5	1050	28 [a]	23	Alvarez et al. (2016)
	600	42.3	8.6	7.6	41	0.4		17.6					
	n.r.	44.6	9	7.5	38.2	0.7	n.r.	20	7.9	1100	17 [b]	24	Fonts et al. (2009)
	400	57.1	8.3	9.5	23.4	1.7							
	500	58.8	7.8	10.5	21.5	1.4	n.r.	n.r.	n.r.	n.r.	n.r.	n.r.	Huang et al. (2014)
	600	60.4	7.3	12.3	17.8	2.2							
	700	60.6	6.8	12.6	18.4	1.6							
	n.r.	65.2	8.6	8.4	17.4	0.4	36.4	n.r.	6.8	1100	n.r.	11	Arazo et al. (2017)
LDBO	n.r.	32 - 48	7 - 8.5	<0.4	40 - 55	<0.05	n.r.	13 - 18	2.0 - 4.0	1050 - 1300	n.r.	20 - 40	Alvarez et al. (2016)
	n.r.	n.r.	n.r.	<0.4	35 - 40	<0.05	n.r.	13 - 18	2.0 - 3.0	1100 - 1300	n.r.	20 - 30	Lehto et al. (2014)
	n.r.	54 - 58	5.5 - 7	0 - 0.2	35 - 40	n.r.	16 - 19	n.r.	2.5	n.r.	40 - 100 [c]	15 - 30	Xiu and Shahbazi (2012)
Petroleum fuels	-	85	11	0.3	1	0.15	n.r.	40	n.r.	940	15 - 1000 [a]	0.1	Alvarez et al. (2016)
		86.7	11.56	0.46	0.49	0.46	44	n.r.	n.r.	930	321 [a]	0.3	Kuan et al. (2020)

Table 1. 6. Composition and fuel properties of municipal sewage sludge- and lignocellulosic materials-derived bio-oils (SDBO and LDBO, respectively), and petroleum fuels. [a] evaluated at 40 °C; [b] evaluated at 20 °C; [c] evaluated at 50 °C; SDBO: sludge-derived bio-oils; LDBO: lignocellulosic-derived bio-oils; T: temperature; HHV: higher heating value; LHV: lower heating value; MC: moisture content; n.r.: not reported; wt: on a weight basis.

The increased HHV of SDBO, as compared with LDBO, is due to a substantially lower O content in the former (minimum 12.3 % wt in SDBO and 35 % wt in LDBO) [15,181], which leads to a higher C and H content. However, the O content in SDBO is still excessively high if compared with that of petroleum fuels, leading to higher viscosities and tar formation, and worse fuel qualities [46]. Further, it is worth noting that the relatively low HHV of SDBO and LDBO is generally due to their higher MCs compared to those of petroleum fuels. This high MC results from the O-bonds broken through dehydration reactions during pyrolysis [184], as well as from the original moisture of the MSS feedstock. The excessive concentrations of both water and oxygenated compounds represent serious issues. A high MC results in low energy density and compromised stability of the ignition and combustion phases, while an excessive oxygen content additionally results in instability of the fuel, the necessity of adjusting the air/fuel ratio during combustion, and a poor compatibility of bio-oil with conventional hydrocarbon-based fuels [181,185].

Interestingly, the pH of bio-oil can influence its employment as biofuel since acidic bio-oil is responsible for corrosion and wearing of the engines [181]. One of the main issues related to LDBO employment as fuel is indeed its generally acidic pH (2.0 – 4.0), which therefore requires preliminary adjustments. On the other hand, SDBO is generally characterized by a basic pH (6.8 – 8.5) (**Table 1.6**), due to its high concentration of N-containing compounds [72,186]. The high N content in SDBO is shown to increase with temperature, with a maximum value of 12.6 % wt reported by Huang *et al.* at 700 °C [98], whereas substantially lower values below 0.5 % wt were reported for LDBO and petroleum fuels [15,181]. SDBO is indeed rich in N in the form of ammonia, nitriles, amines, and amides [23], deriving from the degradation of proteins in MSS [182], which can cause harmful NOx and N_2O emissions during combustion [98]. Since the necessity of N removal is not common in the oil refining industry, differently from what concerns oxygenated compounds, reports about this topic are scarce. However, N removal from biomass-derived bio-oil is fundamental for

its employment as fuel, and can generally be pursued through adsorption processes on zeolites or activated carbon [187], as well as hydrodenitrogenation treatments [188].

Similarly, the much higher S content reported for SDBO (up to 2.2 % wt)[98] with respect to LDBO (<0.05 % wt) [46,181] (**Table 1.6**) could be extremely challenging as well, due to the potential harmful development of S-containing compounds such as SO_x during combustion, resulting in technological and safety issues for SDBO handling facilities.

Thus, to substitute petroleum fuels, SDBO needs to be subjected to dedicated treatments aimed at achieving a suitable composition in order to reduce its acidity and viscosity, MC, instability, O, N and S content, as well as to increase its high-value hydrocarbons content [15]. Besides dedicated physical/chemical upgrading treatments, these improvements can be achieved by pre-treatments on MSS [189]. Desired variations in SDBO characteristics can also be achieved by purposely driving the conventional pyrolysis process under specifically optimized conditions, as well as by catalytic pyrolysis (see section 1.3.4.) [190–193], resulting into higher-value bio-oils, although often with lower yields [47,194]. Good results were achieved through wet transesterification of MSS and subsequent distillation of the obtained SDBO [195,196], while Liu *et al.* obtained a low N and O content in SDBO by coupling hydrothermal pre-treatment and pyrolysis of MSS [197]. According to Zhao *et al*. [198], an effective upgrading of bio-oil can be obtained through biomass washing (*e.g.* with water, alkali or acids) and the employment of catalysts, both during pyrolysis or for the catalytic reforming of vapours. It is worth noting that cleaning operations required by SDBO to be suitable for applications as fuel might be not economically sustainable by small-size WWTPs. Therefore, the centralization of the bio-oil cleaning process in dedicated facilities could be a valid alternative, as already reported in the literature for the pyrolysis of different biomass sources [199].

Additional drawbacks are related to PTEs and PAHs concentration in SDBO. Elements such as Cu, Cr, Cd, Zn, Pb, and Ni are partially diverted from the MSS to the SDBO, especially during high-temperature pyrolysis [200]. A high PTEs content in SDBO employed as biofuel might result in environmental pollution issues related

to leakages occurring during the storage phase, emissions during the combustion phase, and corrosion of the engines[201]. On the other hand, PAHs concentrations in SDBO ranging between 13.7 and 48.9 mg/kg were reported [202], resulting in serious environmental and health safety concerns related to SDBO handling and usage, but with the possibility of reducing the PAHs content through the addition of catalysts at elevated temperatures [203]. When bio-oil characteristics limit or obstacle its employment as fuel, fine chemicals can be obtained through extraction and fractionation techniques, such as the employment of organic or inorganic solvents, chromatography, and distillation [204]. The obtainable chemicals vary accordingly to the composition of bio-oil, and therefore depend on the pyrolysis feedstock and conditions. Alternative applications for bio-oil are reported in the sections below.

1.3.2.2 Pyrolysis of bio-oil

Performing a second pyrolysis on bio-oil can be advantageous when aiming to increase the overall efficiency of a pyrolysis process dedicated to gas production. The hydrocarbons present in bio-oil can indeed be further degraded into high-energy gaseous products. On the other hand, a second pyrolysis could be helpful to achieve a cleaner and higher-quality bio-oil by removing O-, N-, and S-containing compounds, and pollutants. Improvements in the characteristics of biochar can also be obtained from bio-oil pyrolysis. According to Chen *et al.*, a co-pyrolysis of bamboo-derived heavy bio-oil with bamboo resulted in higher biochar yield and C content with respect to the pyrolysis of solely bamboo [205]. Similar applications of such a post-pyrolysis step employing SDBO are yet to be reported in the literature.

1.3.2.3 Anaerobic digestion of bio-oil and its aqueous phase

The employment of bio-oil from wood as AD feedstock was investigated in recent years, as well as that of the aqueous phase (AP) of bio-oil produced from corn stalks or cow manure [206]. The AP can be separated from bio-oil in different ways, including fractionated condensation, solvent or water extraction, and spontaneous separation [207–209]. Although the AP can contain up to 60 % wt of the C present in the pyrolyzed biomass [210], this is generally treated in WWTPs since it is too diluted

for cost-efficient resource recovery, and it has low heating values and high corrosiveness [211]. Thus, the AD of biomass-derived AP is gaining interest as an alternative valorization route. As a matter of fact, AD might represent a cheaper alternative to other treatments including pure cultures-mediated AP fermentation, and AP catalytic conversion into fuels [211–213]. On the other hand, when not specifically pretreated, the AP may inhibit the AD process [214]. Interestingly, this inhibition effect seems to increase when AP is produced at higher temperatures [74]. According to Pecchi *et al.* [74], however, low a AP/inoculum ratio (< 0.1 wt) can mitigate inhibition, resulting in the best AD performance.

To the authors' best knowledges, examples of such applications of SDBO are yet to be reported in the literature, yet due to its complex composition, the risk of AD inhibition could be even higher. Further investigations in this field are required. However, the AD-pyrolysis combination might trigger innovative process integrations, spanning across different scenarios involving complete or partial application of SDBO as biofuel and/or AD feedstock towards biomethane production.

1.3.3 Pyrolysis gas

Valuable gases such as H_2, CO, and CH_4, together with CO_2, are the main components of MSS-derived pyrolysis gas. Light hydrocarbons (C_2-C_3), such as ethane, ethylene or propylene, are also produced in small concentrations, while minor components such as H_2S, NH_3, and HCN can be generated as well, depending on with the composition of the feedstock [96,215,216]. In **Table 1.7**, the H_2 concentration in pyrolysis gas is clearly shown to increase with temperature, reaching maximum values as high as 35 - 45 % v/v in the range 800 – 1400 °C, whereas concentrations as low as 5 - 10 % v/v are reported below 550 °C [49,68,95,217]. At such low temperatures, CO_2 is the main component, reaching 70 – 74 % v/v [95,97]. Nevertheless, when temperature increases, the CO_2 concentration rapidly decreases, reaching for instance values below 9 % v/v at 900 °C [217]. The concomitant evolution of CO_2, H_2, and CO is due to the occurrence of multiple reactions related to temperature and MC.

MC of MSS (% wt)	HR (°C/min)	Pyrolysis T (°C)	H_2 (% v/v)	CO (% v/v)	CO_2 (% v/v)	CH_4 (% v/v)	C_2-C_3 (% v/v)	H_2S (% v/v)	H_2/CO	H_2/CO_2	LHV (MJ/Nm^3)	References
12.7	10	n.p.	20.8	8.74	36.53	7.36	4.26	n.r.	2.38	0.57	n.r.	Ghodke et al. (2021)
n.r.	n.r.	400	10	18	70	5	0	0	0.56	0.14	n.r.	Jaramillo-Arango et al. (2016)
		800	45	20	20	5	3	0.2	2.25	2.25		
6.7	n.r.	550	5 [a]	32 [a]	42 [a]	11 [a]	3 [a]	2 [a]	0.16 [a]	0.12 [a]	11.39	Fonts et al. (2009)
5.3			27 [a]	15 [a]	41 [a]	10 [a]	3 [a]	2 [a]	1.80 [a]	0.66 [a]	10.98	
7.1			10 [a]	17 [a]	60 [a]	5 [a]	2 [a]	4 [a]	0.59 [a]	0.17 [a]	8.10	
19.5	n.r.	1000	30	25	23	17	5	n.r.	1.20	1.30	15.68	Zhang et al. (2014)
		1400	40	33	25	2	0		1.21	1.60	9.10	
7.5	8	450-650	10.41-26.9	6.89-9.8	74.17-31.95	3.25-19.87	5.29-11.48	n.r.	1.51-2.74	0.14-0.84	n.r.	Gao et al. (2014)
	100	450-650	8.96-22.29	6.16-17.29	70.55-19.81	5.97-20.66	8.35-19.94		1.45-1.29	0.12-1.12		
n.r.	n.r.	500	7.44	6.85	25.86	13.19	46.66	n.r.	1.09	0.29	39.98	Han et al. (2015)
		700	15.46	13.26	14.42	26.04	30.71		1.17	1.07	32.35	
		900	39.98	24.32	8.88	22.83	2.83		1.64	4.50	17.41	
0	10-25	1000	24.1	45 [a]	11.3	15 [a]	3 [a]	n.r.	0.5 [a]	2.1	n.r.	Xiong et al. (2013)
47			34 [a]	35 [a]	12 [a]	11 [a]	4 [a]		1 [a]	2.8 [a]		
80			34.9	32 [a]	15	11 [a]	4 [a]		1 [a]	2.3 [a]		

Table 1. 7. Evolution of pyrolysis gas composition based on the moisture content of the municipal sewage sludge (MSS) feedstock, as well as the heating rate of MSS, and the pyrolysis temperature. [a] deducted from graphics; MC: moisture content; MSS: municipal sewage sludge; HR: heating rate; T: temperature; LHV: lower heating value; n.r.: not reported; v/v: on volume.

According to Domínguez *et al.*, the vapor-rich atmosphere produced by the effect of high MC in MSS leads to steam reforming and steam gasification reactions (Eq. 1.1 and 1.2, respectively) involving water, hydrocarbons, organic matter and carbonaceous residues, towards the formation of new H_2 and CO [218].

$$C_xH_{y_{(g)}} + H_2O_{(g)} \overset{\square}{\leftrightarrow} CO + H_2 \quad (1.1)$$

$$Organic\ matter_{(g)} + H_2O_{(g)} \overset{\square}{\leftrightarrow} CO + H_2 \quad (1.2)$$

A higher MC is thus directly correlated to a higher final H_2 concentration, as well as to a higher gaseous yield [68]. However, Xiong *et al.* demonstrated that, although an increase from 24 to 35 % v/v in the H_2 concentration was observed when moving from an MC of 0 to 47 % wt, when the MC is further increased to 80 % wt a saturation point of the steam is achieved [49]. Thus, increasing the initial MC above 47 % wt would not result into a higher H_2 concentration.

Gao *et al.* observed that higher pyrolysis temperatures led to CO_2 reactions with atomic C towards the formation of more CO (Eq. 1.3) [97].

$$CO_2 + C \overset{\square}{\rightarrow} 2CO \quad (1.3)$$

Interestingly, after high-temperature pyrolysis at 1000 and 1400 °C of MSS with a MC of 19.4 % wt, Zhang *et al.* observed an increase of the H_2 content (from 30 to 40 % v/v), while the CO concentration increased only slightly (from 25 to 33 % v/v) and the CO_2 concentration was almost stable (from 23 to 25 % v/v) [68]. This behaviour could be justified by the occurrence of the water-gas shift (WGS) reaction and methane gasification reactions induced by high temperatures and MC (Eq. 1.4 and 1.5, respectively) [218].

$$CO + H_2O_{(g)} \leftrightarrow CO_2 + H_2 \quad (1.4)$$

$$CH_4 + H_2O_{(g)} \leftrightarrow CO + 3H_2 \quad (1.5)$$

The reaction expressed in Eq. 1.5 can also involve other light hydrocarbons. This would explain the parallel CH_4 and C_2-C_3 reduction, also observed by Han *et al.* at temperatures higher than 900 - 1000 °C [217], which led to a decrease in the lower heating value of pyrolysis gas in both cases, decreasing from a maximum of 40 MJ/Nm^3 to a minimum of 9 MJ/Nm^3.

Pyrolysis gas is commonly diverted to internal combustion engines towards energy recovery for the partial or complete sustainment of the pyrolysis process [16]. This application, as well as more innovative solutions reported in the following sections, generally requires pyrolysis gas cleaning, since some gaseous compounds, such as H_2S and CO, can easily harm combustion systems and result in pollutant emissions, as well as affect biological and/or chemical conversion of the pyrolysis gas [17,219]. Dedicated treatments, such as deacidification/desulfurization and WGS reaction, can be conducted towards H_2S removal, and CO conversion into H_2 and CO_2, respectively, with increased costs for pyrolysis gas production and valorization [220].

1.3.3.1 Pyrolysis gas fermentation towards liquid hydrocarbons and chemicals

During the last decades, the Fischer-Tropsch process has been widely applied for the catalytic production of liquid hydrocarbons and chemicals from gas mixtures derived from industrial off-gases or biomass gasification (*i.e.* syngas), mainly composed by H_2 and CO, with CO_2 and minor impurities [17,19], therefore quite similar to MSS-derived pyrolysis gas.

This high-performance process requires high temperature and pressure (200 - 350 °C and 1 - 5 MPa, respectively) and strict process conditions for the catalysts in terms of H_2/CO ratios (0.7 – 4.0 mol/mol) and gas impurities (HCl, alkali metals, and sulfonate compounds) [17]. Alternatively, syngas fermentation processes for the conversion of H_2, CO, and CO_2, into ethanol, methanol, butanol, acetic and butyric acid have been explored by leveraging the ability of acetogenic microorganisms [221–223].

The fermentation of such gas mixtures is affected by the low solubility of CO and H_2 within the liquid medium [224], which leads to low gas-liquid mass transfer rates and, therefore, relatively low product yields [225]. Hollow-fiber membranes biofilm reactors have thus been studied and applied as an alternative to most established configurations (*i.e.* continuous stirred tank reactor and bubble column reactor) [226,227] since they are capable of promoting higher mass transfer rates, H_2 utilization efficiency, and product yields, against lower operating costs [228,229]. Further, the effect of impurities and inhibitors present within MSS-derived pyrolysis gas (H_2S, NH_3, and CO) on liquid hydrocarbons production should be further investigated in the future.

For what concerns industrial applications, *Coskata Inc.*, *INEOS Bio*, and *LanzaTech* have been the main companies dealing with syngas fermentation since the beginning of the 2000s. Despite their role as pioneers of the syngas conversion to ethanol, both *Coskata Inc.* and *INEOS Bio* are not active anymore, while *LanzaTech* is today the biggest company in this field, with the upcoming realization of large-scale facilities in Asia, Europe, and Africa [230]. Interestingly, loop and bubble-column reactors are employed in *LanzaTech* facilities, while biofilm reactors are not yet commonly employed in full-scale plants, since technical issues related to their upscaling are still present [231]. Bioethanol produced from syngas fermentation can be employed as additive in fuels. In 2020, in partnership with the U.S. Department of Energy, *LanzaTech* founded *LanzaJet*, a new company dedicated to the conversion of the obtained bioethanol into sustainable aviation fuel (SAF) for the substitution of fossil fuels in the aviation sector.

1.3.3.2 Pyrolysis gas biomethanation

Besides liquid hydrocarbons, pyrolysis gas fermentation can also target biomethane production through biomethanation as advantageous alternative to catalytic methanation: as a matter of fact, thermochemical syngas conversion to biomethane through the Sabatier reaction (Eq. 1.6) [232] is substantially affected by issues related to H_2/CO ratios and the presence of impurities in the gas (*e.g.* S compounds), toxicity induced by high CO concentrations on catalysts, and the necessity of high temperature

and pressure [20,233]. Additionally, the WGS reaction prior to catalytic methanation is often required to convert CO in H_2 and CO_2 [20].

$$4\,H_2 + CO_2 \rightarrow CH_4 + 2\,H_2O \quad (1.6)$$

On the other hand, biomethanation of $H_2/CO/CO_2$ gas mixtures can occur more easily through H_2/CO_2-, CO-, and acetate-based metabolic pathways of many methanogenic microorganisms [234,235], resulting in CH_4 yields as high as 0.24 L_{CH4}/L_{mix} [236]. Issues related to CO inhibition on several methanogenic species have been highlighted [237], but the synergistic growth of the different microbial species involved in a mixed culture can result in the avoidance of CO-inhibition and a more efficient biomethanation process [235]. However, these metabolic pathways are differently favoured by operative temperatures (*i.e.* mesophilic or thermophilic conditions), as reported in **Table 1.8**. Methanogenic pathways (both hydrogenotrophic and carboxidotrophic) are generally dominant under thermophilic conditions, while competition between homoacetogens and hydrogenotrophic methanogens can take place under mesophilic conditions [235,238].

The presence of CO can result in the inhibition of acetoclastic methanogens, with consequent accumulation of VFAs. This phenomenon is generally more important under mesophilic conditions, in which the homoacetogenic/syntrophic metabolism is usually favoured [235]. Kuipers and Kofoed performed the enrichment of a mixed microbial culture for the biomethanation of a $H_2/CO/CO_2/CH_4$ mixture simulating biomass-derived syngas, in continuous mode and thermophilic conditions [239]. Inhibition tests with the employment of antibiotics and 2-bromoethanesulfonate (specific inhibitors of bacteria and archaea (*i.e.* methanogens), respectively) allowed to identify the methanogenic pathway as the dominant one in the process. Further, in the same study CO was observed to be mainly consumed for H_2 production through the biological WGS reaction, instead of being directly converted into acetate or biomethane.

As reported for syngas fermentation for liquid hydrocarbons and chemicals production, challenges can come from the low solubility of CO and H_2 within the

Metabolic pathway	Stoichiometric reaction	Influence of temperature	References
Carboxydotrophic hydrogenogenesis (Biological water-gas shift reaction)	$CO + H_2O \rightarrow CO_2 + H_2$	Mostly thermophilic microorganisms	Alfano and Cavazza (2018); Andreides et al. (2022)
Carboxydotrophic acetogenesis	$4\ CO + 2\ H_2O \rightarrow CH_3COOH + 2\ CO_2$	Mostly mesophilic microorganisms	Figueras et al. (2023)
Carboxydotrophic methanogenesis	$4\ CO + 2\ H_2O \rightarrow CH_4 + 3\ CO_2$	Higher growing rate of microorganisms in thermophilic conditions	Andreides et al. (2022)
Homoacetogenesis/Syntrophic acetate oxidation	$4\ H_2 + 2\ CO_2 \leftrightarrow CH_3COOH + 2\ H_2O$	Favoured by mesophilic conditions	Figueras et al. (2023)
Hydrogenotrophic methanogenesis	$4\ H_2 + CO_2 \rightarrow CH_4 + 2\ H_2O$	Favoured by thermophilic conditions	Figueras et al. (2023)
Acetoclastic methanogenesis	$CH_3COOH \rightarrow CH_4 + CO_2$	Favoured by mesophilic conditions	Grimalt-Alemany et al. (2020)

Table 1. 8. Metabolic pathways involved in syngas biomethanation, stoichiometric reactions, and favourable temperature conditions.

liquid medium during biomethanation. Increasing the pressure of the gaseous substrate represents a low-effort approach to enhance H_2 and CO solubilization [242]. Kuipers and Kofoed reported a 49 and 41 % higher conversion efficiency for H_2 and CO to CH_4, respectively, through a pressure increase of 58 % [239]. On the other hand, an excessive CO partial pressure can inhibit methanogenic activity, although it is somehow dependent on the growth conditions and the acclimation of the culture [238]. Interestingly, higher mass transfer rates can favour homoacetogenic activity, due to the resulting high H_2 concentrations in the liquid phase [235]. Although higher gas flow rates result in higher substrate concentrations, and therefore higher mass transfer rates, the consequently lower gas retention time in the reactor can lead to an incomplete conversion of the substrate, making the process less efficient [243,244].

More sophisticated strategies for enhancing gas-liquid mass transfer in bioreactors include the employment of hydrodynamic cavitation systems [245,246]. Giuliano *et al*. obtained final biomethane concentrations higher than 99 % v/v during the biomethanation of H_2/CO_2 in a 50 L tubular reactor in continuous mode, by employing a rotative hydrodynamic cavitation system [247]. After a first inhibition effect in the adaptation phase, the continuous biomethanation of syngas with CO concentration as high as 40 % v/v conducted by Li *et al*. [236] led to a final CH_4 concentration of 43.2 – 49.7 % v/v, with the main limitation being recognized in the gas-liquid mass transfer rate.

1.3.3.3 Pyrolysis gas fermentation for single cell protein production

Pyrolysis gas may also be potentially used in microbial fermentation processes to produce value-added products in the form of single cell protein (SCP). This protein-rich material, which can be produced by cultivating yeasts, bacteria, algae or fungi, capable of accumulating high-quality protein up to more than 80 % of their mass [248], can be used as slow-release fertilizers or as protein additive for feed and food [249]. After decades during which SCP production mainly relied on primary feedstocks such as natural gas and dedicated crops, secondary feedstocks such as C-rich biowastes, agro-industrial wastewaters, MSS, and CO_2 off-streams are now being studied for SCP production [250–253].

The biological exploitation of CO_2, CO and H_2 from syngas/pyrolysis gas produced from biowastes, including MSS, to SCP within a so-called “gas route” could result in highly positive economic and environmental impacts [254]. The aerobic fermentation of H_2/CO_2 mixtures by hydrogen-oxidizing bacteria (HOB) towards SCP production was studied by several authors [255–257], revealing how these particular bacteria offer advantages in terms of biomass productivity, yield, and final protein content. Pure/axenic cultures of HOB (*i.e. Cupriavidus necator* and *Ideonella*) were employed in the aerobic fermentation of H_2/CO_2 in the presence of variable CO concentrations, revealing severe inhibition of the cultures for CO concentrations above 30 % v/v [258,259]. On the other hand, Pelagalli *et al*. reported no inhibition of a mixed HOB culture in the batch aerobic fermentation of $H_2/CO_2/CO/H_2S$ mixtures simulating

realistic MSS-derived pyrolysis gas, with CO and H_2S concentrations up to 40 and 0.4 % v/v, respectively, and the achievement of a biomass protein content up to 74 % wt [18]. In the same study, theoretical considerations suggested the utilization of NH_3 from MSS-derived pyrolysis gas as N-source for the microbial culture.

1.3.4 Improvement of biochar, bio-oils, and pyrolysis gas characteristics through catalytic pyrolysis

Catalytic pyrolysis of MSS can lead to the enhancement of end-products properties and yields, often at lower pyrolysis temperatures [2]. The application of catalysts can be conducted with three different approaches: as *conditioners*, by pre-treating wet MSS with solutions of metal oxides (*e.g.* CaO, γ-Al_2O_3, and Fenton reagent) for accelerating the MSS decomposition [260]; *in-situ*, by adding solid catalysts such as acid or basic zeolites (*e.g.* Zeolite Socony Mobil-5 (ZSM-5), Y, Ultrastable Y (USY), and Mordenite) or other types of porous materials such as activated carbon/biochar, directly to the MSS feedstock within the pyrolysis reactor; as well as *ex-situ*, through reforming of the pyrolysis vapours by solid catalysts (typically zeolites or metal oxides) [2].

The choice of the zeolites for *in-situ* and ex-situ applications has to be made accordingly to the targeted characteristics of the products. Pore size and volume (shape selectivity), and acidity (expressed in terms of Si/Al ratio (SAR)) of zeolites determine their capability of reacting with the components of pyrolysis vapours in terms of selectivity and number/strength of active acidic sites, respectively [261,262]. Coke formation during catalytic pyrolysis and its deposition on the zeolites' surface leads to the deactivation of acidic sites, the modality and extent of which is strictly dependent on the structure of the zeolite [263]. A positive correlation between higher SARs and coke-formation resistance was reported in the literature [263,264].

As discussed in section 1.*3.2.1*, catalytic pyrolysis can substantially enhance the bio-oil fuel properties, especially in terms of stability and presence of O-, N-, and S-based compounds. Interestingly, the employment of catalysts can result in the

retainment of these compounds in biochar, while achieving cleaner and more stable bio-oil and pyrolysis gas [185].

HZSM-5 (obtained from calcination of ZSM-5) can be used *in-situ* to increase the H_2 and CO_2 content in pyrolysis gas, as well as the content of aromatic hydrocarbons in bio-oil, with lower concentrations of O- and N-containing compounds [2]. Similarly, enhancement in bio-oil and pyrolysis gas yields was obtained by employing USY zeolites [2]. The employment of Fenton reagent as conditioner was reported in the literature [265], showing its contribution in the retention of up to 97 % of raw MSS-sulfur in the obtained SDBC, therefore preventing it from accumulating in bio-oil and pyrolysis gas. Interestingly, the resulting S-rich SDBC could be useful for soil applications, as already reported elsewhere for different types of biochar [266].

While the catalytic reforming of different industrial off-gases (including syngas) by zeolites and biochar for the reduction of the H_2S concentration was reported in the literature [267,268], the *in-situ* catalytic pyrolysis towards H_2S removal from pyrolysis gas is yet to be reported. These catalytic treatments would be particularly useful to avoid S-related issues in thermochemical and biological facilities for pyrolysis gas and bio-oil valorization (see sections 1.3.2 and 3.3). Comparable effects of HZSM-5 and SDBC on the evolution of pyrolysis gas composition were reported in the catalytic pyrolysis of MSS [269]. Further evaluations of SDBC as potential *in-situ* or ex-situ catalyst should be conducted.

Catalytic reforming has gained much interest as efficient method for the upgrading of bio-oil, especially through hydrotreatment (HDT), including several H_2-based treatments generally conducted to remove N and/or S from bio-oil, and for the enhancement of its hydrocarbon content [198,270,271]. Complete N removal and increased hydrocarbons yield was achieved by Izhar *et al.* [188] through the hydrodenitrogenation (HDN) of SDBO, by employing $NiMo/Al_2O_3$ as catalyst.

In order to meet the objectives set by recent decarbonization policies, oil petroleum companies such as *Neste Oil, UOP-Eni*, and *CoconoPhilips* have developed the catalytic upgrading of vegetable oil and/or biomass-derived bio-oil towards biofuel production by means of HDT [272,273].

1.4 Economic considerations

The economic evaluation of MSS pyrolysis involves assessing the costs, benefits, and potential returns associated with implementing it as a waste treatment and resource recovery technology, considering market dynamics and regulatory conditions. Energy and material recovery, as well as volume reduction and resulting lower disposal expenses, need to be considered.

Capital costs, which include the initial investment required to set up an MSS-pyrolysis facility, may encompass the construction of the pyrolysis reactor, storage tanks, processing equipment (*e.g.* dryer and boiler), and infrastructure for handling feedstock and products. According to data reported for the PyroChar® project [274], and by Luo *et al.* [89], the capital costs for an MSS-pyrolysis plant can span between 350 - 450 $/ton per year. Regarding operative costs, the PyroChar® project estimated a cost of 0.11 $/kg TS, when considering a plant capacity of 1 tons of MSS db per hour, including electricity, inert gas (*i.e.* N_2), maintenance, and labour [274]. Consistently, a lower cost of 0.02 $/kg TS has been assumed by Luo *et al*. considering plants with a higher size [89].

Nevertheless, these evaluations do not take into account costs related to the handling of the obtainable products and by-products, such as those related to pyrolysis gas cleaning, process water treatment, and pollution control systems. Furthermore, the production of biochar, bio-oil, and pyrolysis gas with characteristics which do not meet commercialization standards would require higher costs for refining and amelioration processes.

Economic revenues can be generated by the heat and power recovered during the process. Evaluating the potential for energy recovery and considering how it can offset operational costs or generate revenue through electricity sales is crucial. Studies in the literature report a positive energy balance of the pyrolysis process. Indeed, Zhou *et al.* reported that the pyrolysis of MSS is a self-sustaining process [41]. Part of the energy produced from oil and pyrolysis gas combustion is indeed recovered for sustaining the pyrolysis and MSS drying processes. The study also highlighted that the most significant impact on the energy consumption of the system is given by the thermal

dryer unit, particularly by the initial MC of MSS, which significantly influences the consumption of the thermal drying stage. Economic profits can also be produced by the sale of pyrolysis products. Assessing the market demand and potential selling prices for the pyrolysis products, such as biochar, bio-oil, and pyrolysis gas, is a challenge point, as market prices can vary significantly based on regional factors and product quality. Conducting market research to understand the demand and competition for the pyrolysis products will help estimating potential revenue and market penetration. Furthermore, additional revenue streams, such as carbon credits or incentives for using renewable energy sources, should be considered, together with financing options, grants, subsidies, or incentives that may be available to support the implementation of MSS pyrolysis projects.

The economic evaluation should also consider financial modelling and risk assessment. The calculation of the net present value, internal rate of return, payback period, and sensitivity analysis, together with the identification and assessment of potential risks, such as variations in feedstock quality, market price fluctuations, and regulatory changes may be helpful to develop a strong business plan under different scenarios and risk factors.

Some studies consider the environmental and economic impacts over the entire life cycle of the MSS pyrolysis process, including resource extraction, production, operation, and end-of-life. Luo *et al.* performed a life cycle assessment and a cost-benefit analysis, considering different scenarios in China for MSS transportation distance, system size, product utilization and carbon tax [89]. They found that the global warming potential and minimum sludge handling price of MSS pyrolysis could be as low as -32.5 kg CO_2-Eq/ton TS and 188.8 $/ton TS, respectively.

1.5 Integrated biorefinery platform for the pyrolysis of municipal sewage sludge: two possible scenarios

An integrated platform for the valorization of MSS through pyrolysis would combine some of the possible solutions presented in the previous sections for biochar, bio-oil and pyrolysis gas. The choice of one valorization pathway with respect to another will

therefore depend not only on the characteristics of the specific product, but also on the overall target of the integrated platform. In **Figure 1.4** two possible scenarios are evaluated and compared, by reporting their main advantages and drawbacks from an environmental point of view.

Scenario A (*Resource recovery*) is devoted to the maximization of nutrient and organic matter recovery from MSS and their valorization into value-added materials. With this aim, SDBC is employed as soil conditioner or for nutrient recovery from soils/wastewaters (sections 1.3.1.1 and 1.3.1.4), while pyrolysis gas is converted to MP through aerobic fermentation (section 1.3.3.3).

On the other hand, Scenario B (*Energy recovery*) is finalized to the maximization of biomethane production for energetic purposes. In this scenario, biomethane yield in the AD of MSS is enhanced by means of SDBC addition for the *in-situ* upgrading of biogas (section 1.3.1.5), while pyrolysis gas is anaerobically fermented towards further biomethane production (section 1.3.3.2).

Bio-oil was not considered, since the solutions available for their valorization (section 1.3.2) could fit in both the evaluated scenarios for resource and/or energy recovery.

From an environmental point of view, the employment of SDBC as soil conditioner or for nutrient removal from soils/wastewaters (Scenario A) comes with the main advantages of avoiding the utilization of adsorbent materials derived from virgin resources, as well as lowering the demand of chemical fertilizers. Nevertheless, the risk of soil contamination with PTEs or PAHs needs to be evaluated. Similarly, the aerobic fermentation of pyrolysis gas allows the direct utilization of reactive nitrogen (*i.e.* under the form of NH_3) recovered from waste and its conversion into a value-added product such as MP. This comes with positive effects on the nitrogen biogeochemical cycle , and with the capture and utilization of the CO_2 produced during MSS pyrolysis.

In the configuration designed for the Scenario B, one of the main advantages is related to the production of biomethane as substitute for fossil fuels, with positive effects on the reduction of GHGs emissions. This is also valid for the CO_2 capture occurring through biochar addition in AD, as well as the CO_2 capture and utilization occurring

during the anaerobic fermentation of pyrolysis gas towards biomethane. Nevertheless, this Scenario is characterized by a lack of recovery of material resources, and usually requires external H_2 supply to fix the H_2/CO_2 ratio in the biomethanation process (section 1.3.3.2).

Additionally, the "*biochar loop*" taking place in the Scenario B configuration should be object of further studies. When biochar is produced through digested MSS pyrolysis, it is then employed back in the AD process conducted on MSS, and this digested MSS is then pyrolyzed again to produce SDBC. In this loop, MSS and SDBC characteristics can vary after each AD/Pyrolysis step. This variation should be analysed, in order to assess the feasibility and the outcomes of this cyclic treatment.

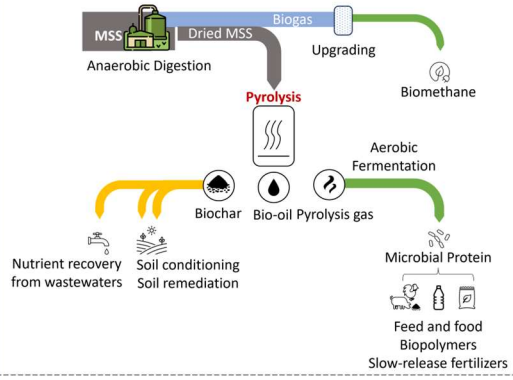
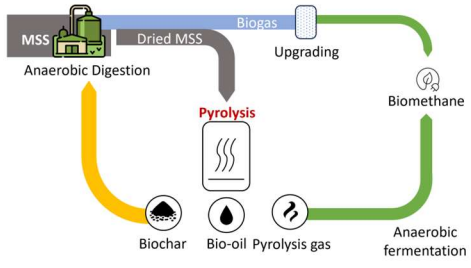
Scenario	Advantages	Drawbacks
A) Resource recovery 	• Reactive nitrogen recovery in the form of microbial protein; • CO_2 capture and utilization from pyrolysis gas towards microbial protein production. • Nutrients, metals and hydrocarbons removal from soils/wastewaters by means of waste-derived adsorbents; • Lower demand of chemical fertilizers;	• Risk of contamination derived from biochar employment in soils.
B) Energy recovery 	• Improved MSS conversion to biomethane towards fossil fuels substitution; • CO_2 capture from biogas on biochar; • CO_2 capture from pyrolysis gas and conversion to biomethane.	• Lack of material recovery; • Necessity of extra H_2 supply for the biomethanation process.

Figure 1. 4. Analysis of two possible scenarios for an integrated biorefinery platform for the pyrolysis of municipal sewage sludge (MSS). The considered scenarios are oriented to A) resource recovery, and B) energy recovery.

These configurations represent just two of the possible scenarios available for the design of an integrated biorefinery platform for MSS valorization through pyrolysis. However, a detailed analysis of the mass and energy flows characterizing the platform could be useful to design hybrid configurations in which resource recovery- and energy recovery-oriented solutions can be combined in order to compensate costs and revenues of the platform.

1.6 Conclusions

Multiple issues affecting MSS management require innovative solutions aimed to the valorization of residual organic matter and nutrients in an integrated biorefinery scheme. In order to overcome the limits of established MSS treatment/disposal methods (*i.e*. landfilling, agricultural spreading, composting, incineration), pyrolysis can represent a valid solution for the conversion of MSS into a wide range of valuable products, potentially allowing the simultaneous recovery of matter and energy.

MSS-derived biochar, bio-oil and pyrolysis gas composition and yields are substantially affected by MSS properties and pyrolysis conditions. The influence of main operative parameters such as temperature, solid retention time, and heating rate on the characteristics of the products has been analysed here starting from a wide review of the literature. Biochar yield exhibits a decreasing trend with increasing temperature, peaking between 300 °C and 500 °C with yields ranging from 25 % to over 75 % wt. In contrast, pyrolysis gas production increases gradually with temperature, becoming more significant from 600 °C, with yields up to 46 % wt beyond 1000°C. Bio-oil yields increase with temperature increase, up to 50 % wt between 450 and 550 °C. MSS characteristics such as MC, AC, FC and VM, can affect products yields as well. High MCs (up to 47 % wt) were reported to significantly enhance pyrolysis gas production, while high FC contents and ACs lead to maximization of the solid yield.

The combination of MSS pyrolysis and biological valorization processes in integrated biorefinery platforms can represent a successful strategy for the maximization of resource recovery from MSS. Innovative valorization routes for

biochar, bio-oil and pyrolysis gas from MSS were reported in the present study, as well as the influence of the process on the main characteristics of these products (SSA for biochar, fuel properties for bio-oil, and composition of pyrolysis gas). Future studies focusing on SDBC applications in soils and contaminated water should aim to assess its ability to remove emerging contaminants (*e.g.* PFAS). Innovative applications for SDBC as an additive in the AD of MSS and its potential for mitigating ammonia inhibition in protein-rich wastes should be explored. The co-digestion of MSS with such wastes using SDBC could prove to be a strategic combination. SDBO has potential to be involved in more than just energetic applications. An assessment of the influence of its composition on product quality and potential inhibitory effects during AD is necessary. Research on MSS-derived pyrolysis gas fermentation to biofuels should prioritize enhancing gas solubilization, scalability, and adaptability to various compositions. For the "pyrolysis gas-to-SCP" route, considering synergistic approaches involving HOB and photosynthetic microorganisms could help enhancing process efficiency. Furthermore, understanding the impact of pyrolysis gas composition on SCP characteristics for different applications is crucial. Safety evaluations concerning feed and food applications of SCP and biofuels from pyrolysis gas should be a priority. Exploring the feasibility of pyrolysis gas biomethanation on a larger scale might help understanding process limitations and performance capabilities. Investigating different $H_2/CO/CO_2$ ratios and using hydrodynamic cavitation systems to improve gas-liquid mass transfer rates are potential areas of interest in this field. Additionally, understanding the relationship between various biomethanation metabolic pathways and operational parameters is essential.

Economic considerations regarding the overall MSS pyrolysis process were conducted, basing on data coming from real large-scale applications of this technology at the European and global level. The capital and operative costs for an MSS-pyrolysis plant were considered to be as high as 350 – 450 $/ton per year, and 0.11 $/kg TS, respectively, when referring to a plant capacity of 1 to 4 tons of MSS db per hour. Finally, the overall MSS pyrolysis global warming potential can be estimated at -32.5 kg CO_2-Eq/ton TS.

CHAPTER 2. IN-SITU CATALYTIC PYROLYSIS OF MUNICIPAL SEWAGE SLUDGE FOR THE REDUCTION OF H_2S CONTENT IN PYROLYSIS GAS

This chapter was based on:

Pelagalli V., Tuffi R., Sabatino M.E., Langone M., De Angelis D., Matassa S., Race M., Papirio S., Lens P.N.L., Lazzazzara M., Frugis A., Petta L., Scarsella M., Esposito G., 2024. In-situ catalytic pyrolysis of municipal sewage sludge for the reduction of H_2S content in pyrolysis gas. (Submitted)

2.1 Introduction

The constant increase in global population, together with the desirable improvement in wastewater management and treatment, are inevitably leading to a growing production of municipal sewage sludge, recently estimated at an average of 45 Mton of dry solids generated globally every year [275]. MSS usually contains harmful contaminants such as polycyclic aromatic hydrocarbons (PAHs), per- and poly-fluoroalkyl substances (PFAS), and potentially toxic elements (PTEs), which represent serious threats to the preservation of the environmental matrices (*i.e.* soil, water, and atmosphere) [276,277]. Besides the huge costs for MSS management and the environmental risks coming from MSS-derived pollution, this problematic as widespread waste might disclose a broad spectrum of valuable resources, such as organic matter and nutrients: C is present in stabilized and dewatered MSS in concentrations up to 70 % by weight (wt) on a dry basis (db), while N and P can be found in concentrations as high as 9.1 and 9.2 % wt db, respectively [23,38,278]. In order to overcome the limitations in carbon, nutrients, and energy recovery affecting classic methods for MSS management, innovative thermochemical processes such as pyrolysis are gaining widespread interest [2]. MSS conversion into biochar, bio-oil, and gas via pyrolysis can lead to the production of a broad range of value-added materials when innovative biorefinery approaches are applied [9].

As for syngas produced from MSS gasification, MSS-derived pyrolysis gas (*pyrogas*), which is mainly composed by H_2, CO, CH_4 and CO_2, together with other minor components (*e.g.* C_2-C_3 hydrocarbons, H_2S, and NH_3), is generally employed as energy vector in co-heating and power (CHP) generations units, often for the sustainment of the pyrolysis process itself. At the same time the thermochemical production of biofuels and chemicals through the Fischer-Tropsch (FT) process is also widely applied [17]. However, the occurrence of H_2S and CO and related corrosion and toxicity issues [219], and the interest in new possibilities of broadening the range of recoverable products have triggered the exploration of alternatives for pyrogas

valorization: aerobic and anaerobic fermentation process for the conversion of H_2, CO, and CO_2 into value-added products (*e.g.* ethanol, methanol, acetate, biomethane, and microbial protein) have recently been investigated [18,19].

Pyrogas composition reasonably plays a crucial role in identifying the most suitable valorization pathways. As a matter of fact, pyrogas composition is directly influenced by the characteristics of MSS and the operative conditions of the pyrolysis process, such as temperature, solid retention time (SRT), and heating rate (HR) [2]. According to the literature, higher pyrolysis temperatures result in higher gaseous yields, with higher H_2 and CO concentrations, both up to 40 % by volume (v/v), respectively, to the detriment of CO_2 (minimum 9 % v/v) [68,217]. H_2/CO and H_2/CO_2 ratios represent important parameters for pyrogas employment in thermochemical and/or biological processes: for instance, H_2/CO ratios in the range of 0.7 – 4.0 mol/mol are required by catalysts commonly employed in the FT process [17], while a minimum stoichiometric H_2/CO_2 ratio of 2 – 4 is necessary for biomethanation [20] and a range of 2 – 10 was employed in the aerobic fermentation of synthetic pyrogas to microbial protein [18]. Little information on H_2S in MSS-derived pyrogas is reported in the literature: a maximum H_2S content of 2 – 4 % v/v was reported by Fonts *et al.* [90], while a value as low as 0.2 % v/v was indicated by Jaramillo-Arango *et al.* [95], for MSS-derived pyrogas produced at 500 and 800 °C, respectively. To avoid poisoning of catalysts employed in the FT process, H_2S concentration in syngas/pyrogas should be reduced below 1 ppmv (0.0001 % v/v) [219,279]. On the other hand, acetogenic microorganisms involved in gas fermentation might benefit from low concentrations of H_2S in pyrogas [280], while tolerance to H_2S up to 4000 ppmv (0.4 % v/v) was recently observed in the aerobic fermentation of pyrogas to microbial protein [18]. Thus, preliminary deacidification/desulfurization treatments such as acidic water scrubbing and physical adsorption on metal oxides are generally performed prior to pyrogas employment [281]. Nevertheless, these treatments often require high temperatures and/or pressures, resulting in increased operative costs [220].

Pyrogas composition can be influenced by the effects of catalysts (*e.g.* metal oxides, zeolites, and activated carbons) employed in the pyrolysis process [2]. Zeolites are 3D crystalline aluminosilicates composed by AlO_4 and SiO_4 tetrahedra, and their catalytic

activity is influenced by the number/strength of active acidic sites (*i.e.* Brönsted acidity) and by their microporous structure, affecting concentration, localization, accessibility, and selectivity of the acidic sites [282]. The strength of the acidic sites depends on the concentration and localization of the AlO_4 tetrahedra and therefore, on the Al distribution and the SiO_4/AlO_4 ratio (SAR) of the zeolite [283]. Thus, SAR is one of the main parameters influencing the hydrothermal stability of the zeolites, therefore regulating their reaction mechanisms during catalytic pyrolysis. Zeolites such as H-ZSM5, Mordenite, Y, and USY have often been used as *in-situ* and *ex-situ* catalysts towards the increase of bio-oil and syngas/pyrogas yields, as well as H_2 and CO_2 concentrations in pyrogas, and aromatic compounds in bio-oil [2]. The reduction of H_2S concentration in off-gases via *ex-situ* catalytic reforming was already reported in the literature [267,268], while no information on the *in-situ* application of zeolites for this aim is available. The same mechanisms already described in the literature for H_2S removal by means of zeolites might determine a variation in S migration from MSS during pyrolysis to the products, resulting in a lower concentration of gaseous S-compounds (*e.g.* H_2S). Such a result would limit the necessity of expensive desulfurization treatments to improve the quality of pyrogas, while potentially enhancing S content in biochar, resulting in positive effects on its agronomic application.

In the present study, a first observation of the effect of temperature in the range of 350 – 800 °C on the yields and composition of the products of MSS thermal pyrolysis was conducted, focusing on the pyrogas. Different zeolites (*i.e.* Mordenite and H-ZSM5) with variable SAR were then employed for *in-situ* catalytic pyrolysis tests at 500 °C. Their effect on product yields and pyrogas composition was investigated, especially focusing on the induced reduction of the H_2S concentration in pyrogas and the modification of S migration from MSS to the pyrolysis products.

2.2 Materials and methods

2.2.1 Municipal sewage sludge

MSS used for pyrolysis tests was collected at the end of the sludge line of a wastewater treatment plant located in Rome after thickening, anaerobic digestion, and dewatering through centrifugation. The MSS was then oven-dried at 105 °C for 24 h and sieved to a particle size below 0.5 mm through a cutting mill (SM 2000, Retsch GmbH, Haan, Germany). Proximate and ultimate analysis of MSS were conducted by mean of a TGA/DSC analyser (Star^e System, Mettler Toledo, Columbus, Ohio) and an elemental analyser (Vario Macro Cube, Elementar Italia Srl, Lomazzo, Italy), respectively. MSS composition is shown in **Table 2.1.**

	Municipal sewage sludge
Ultimate analysis	
C (% wt db)	35.94
H (% wt db)	5.18
N (% wt db)	5.76
S (% wt db)	1.12
O (% wt db) [a]	22.98
Proximate analysis	
MC (% wt)	2.35
VM (% wt db)	57.79
FC (% wt db)	10.66
AC (% wt db) [a]	29.02

Table 2. 1. Ultimate and proximate analysis of the municipal sewage sludge employed for thermal and catalytic pyrolysis tests. [a]: calculated as difference; wt: on a weight basis; db: on a dry basis; MC: moisture content; VM: volatile matter; FC: fixed carbon; AC: ash content.

2.2.2 Thermal and catalytic pyrolysis tests

Thermal and catalytic pyrolysis of dried MSS were performed in two different series of tests. Thermal pyrolysis was performed at four different temperatures (350, 500, 650, and 800 °C) and a constant SRT of 15 min. *In-situ* catalytic pyrolysis of the same MSS was studied at 500 °C under the same conditions applied for thermal pyrolysis, with the addition of zeolites in a 1:1 wt ratio. Different types of Mordenite and H-ZSM5 zeolites were employed as catalysts. All the catalysts were stored at room

temperature until use. The elemental composition of the zeolites was assessed (elemental analyser reported in section 2.2.1), and it was confirmed that no S was present. The effects of Mordenite and H-ZSM5 with variable chemical structure and SAR were investigated. All the tested conditions and the operative parameters of the pyrolysis process are reported in **Table 2.2**.

	Sample	Zeolite			T (°C)	SRT (min)
		Type	SAR	Producer		
Thermal Pyrolysis	MSS	-	-	-	350	15
		-	-	-	500	
		-	-	-	650	
		-	-	-	800	
Catalytic Pyrolysis	MSS + Zeolite (1:1 wt)	H-Mordenite	220	*Tosoh*, Japan	500	
		H-ZSM5	250	*Tricat Zeolites, G*ermany		
		H-ZSM5	1880	*Tosoh*, Japan		

Table 2. 2. Experimental conditions of the thermal and catalytic pyrolysis tests. The main operative parameters are reported for each tested condition. MSS: municipal sewage sludge; SAR: Si/Al ratio; T: temperature; SRT: solid retention time; wt: on a weight basis.

2.2.2.1 Pyrolysis set-up

In a vertical quartz tubular reactor (45 cm x 1.5 cm^2), a thermally controlled volume (8 cm x 1.5 cm^2) was filled with about 9 – 10 g of sample (*i.e.* MSS for thermal pyrolysis, and MSS + Zeolite for catalytic pyrolysis). The reactor was inserted in an electrically heated furnace as soon as the stable desired temperature was reached. The pyrolysis was therefore conducted iso-thermically, without an initial heating step. This choice was made in order to set pyrolysis conditions more similar to those occurring in continuous pyrolysis systems.

The bottom side of the reactor was connected outside the furnace to a first condensation system for the collection of pyrolysis liquids, made of a tightly closed conical flask submerged in an ice bath (**Figure 2.1A**). Within the reactor, a metallic net was used to sustain the sample and, therefore, to hold the remaining biochar after

the pyrolysis process. A hollow metal tube (3 mm diameter) connected the parts of the reactor located above and below the sample, in order to allow a proper gas flow through the reactor. From the conical flask, the non-condensable fraction of the vapours was then free to move through a plastic tube towards a dedicated gas bag.

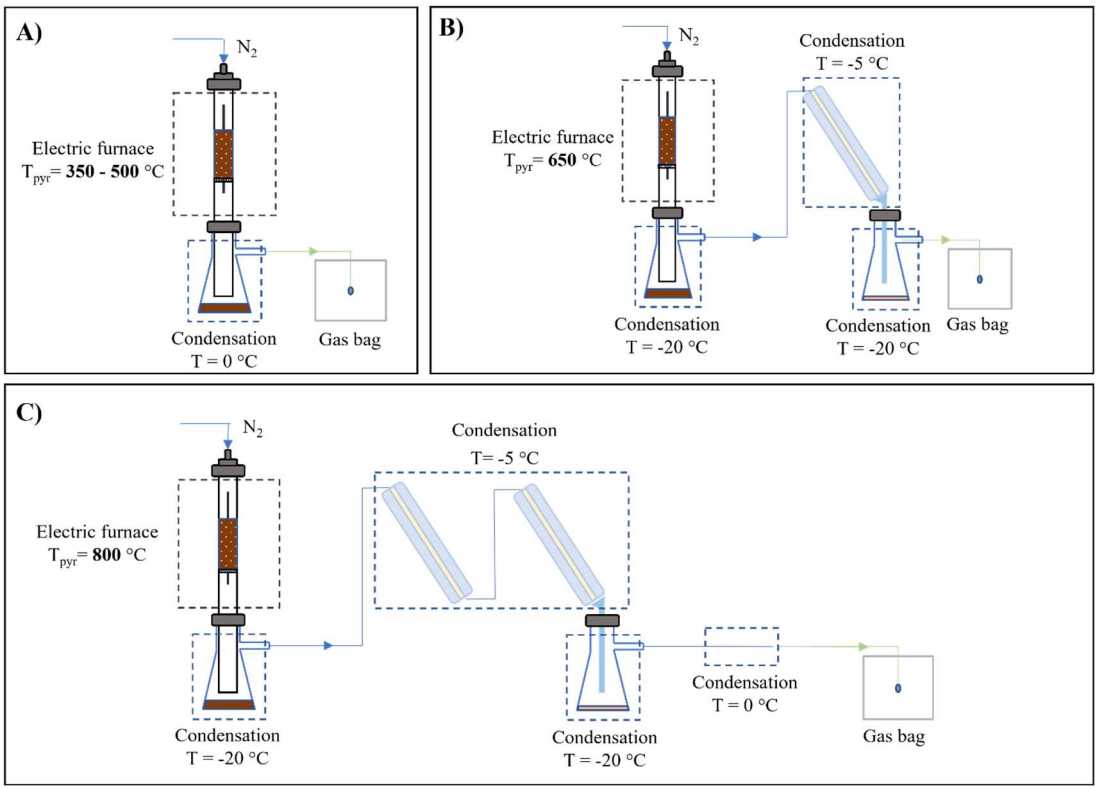


Figure 2. 1. Experimental set-up of the pyrolysis tests. The set-up was opportunely adapted in order to allow the condensation of the liquid products at temperatures of: A) 350 and 500 °C, B) 650 °C, and C) 800 °C.

This basic set-up was used for pyrolysis conducted at 350 and 500 °C, while higher temperatures required an improved condensation step for the complete collection of the liquids. At 650 °C (**Figure 2.1B**), the conical flask was followed by a glass condenser, cooled by a chiller (Alpha RA 8, Lauda, Lauda-Königshofen, Germany) (T = - 5 °C), followed by a second conical flask. For both the flasks, the cooling bath was realized with a frozen saturated aqueous solution of NaCl (about 400 g/L). A similar set-up was used for the pyrolysis at 800 °C (**Figure 2.1C**), with the addition of another glass condenser in series immediately after the first one and an ice bath between the

second flask and the gas bag. In each set-up, an N_2 flow of 10 mL/min was used as an inert carrier during the pyrolysis process. Before starting the process, the sample-loaded reactor was flushed with a higher N_2 flow of 200 mL/min for 15 min to ensure anoxic conditions. At the end of the pyrolysis process, the electric furnace was turned off, and the reactor was cooled while still kept in the N_2 atmosphere in order to avoid the combustion of the biochar. The gas bag was then closed and used for pyrogas characterization through gas chromatography analysis.

2.2.3 Analytical methods

The composition of pyrogas was measured by employing three different gas-chromatographs (GCs): a first GC (Trace GC Ultra, Thermo Fisher Scientific, MA, USA) equipped with a thermal-conductivity detector (TCD) for the analysis of H_2, CO, CO_2, and N_2 concentrations; a second GC (GC Trace 1300, Thermo Fisher Scientific, MA, USA) equipped with a flame ionization detector (FID) for the analysis of hydrocarbons (CH_4, C_2-, C_3-, and C_4-) concentrations; a last GC (Trace GC Ultra, Thermo Fisher Scientific, MA, USA) equipped with a flame photometric detector (FPD) for the analysis of H_2S concentration. These analyses were immediately performed at the end of the pyrolysis process (SRT of 15 minutes) by sampling pyrogas directly from the collection gas bag.

Biochar left within the quartz tube reactor was collected, weighted, sieved in a crucible to a particle size below 0.5 mm, and stored at room temperature in a plastic container. The mass of the liquid phase produced was determined by weighting the reactor and all the equipment which came in contact with the vapours before and after the process, as further described in section 2.2.4.

The same elemental analyser mentioned in section 2.2.1 was employed to determine the concentration of C, H, N, and S in biochar and the liquid phase produced during the thermal and catalytic pyrolysis tests. For the elemental analysis of the liquid, the samples were prepared by loading 15 – 20 mg of liquid on 20 – 25 mg of a solid adsorbent support (Chemosorb, Elementar Italia Srl, Italy).

2.2.4 Calculations

The products yields were calculated as the ratio between the mass of the product and the mass of the initial MSS sample. Biochar mass (M_{BC}) was determined by collecting biochar from the reactor and weighting it in a plastic container. Biochar yield (Y_{Bioch}) was then calculated as follows (Eq. 2.1):

$$Y_{Biochar}\left(\%\, wt, \frac{g}{g\ MSS}\right) = \frac{M_{BC}}{M_{MSS}} \quad (2.1)$$

Where M_{MSS} represents the initial mass of the dried MSS sample.

To determine the bio-oil mass (M_{BO}), all the equipment which came in contact with vapours (*i.e.* quartz reactor and its accessories, flasks, condensers, tubes) was weighted before and after the process. Bio-oil yield was therefore determined as follows (Eq. 2.2):

$$Y_{Bio-oil}\left(\%\, wt, \frac{g}{g\ MSS}\right) = \frac{M_{BO}}{M_{MSS}} = \frac{M_{eq,f} - M_{eq,i}}{M_{MSS}} \quad (2.2)$$

Where $M_{eq,i}$ and $M_{eq,f}$ represent the initial and final mass of the equipment.

Finally, pyrogas yield ($Y_{Pyrogas}$) was calculated as difference (Eq. 2.3).

$$Y_{Pyrogas}\left(\%\, wt, \frac{g}{g\ MSS}\right) = 1 - Y_{Biochar} - Y_{Bio-oil} \quad (2.3)$$

The final pyrogas net composition was calculated by excluding the exogenous N_2 used as inert gas in the pyrolysis process and all the components not detected through the gas chromatography analysis. The net concentration of the generic component of pyrogas (X_i^{net}) was calculated as follows (Eq. 2.4):

$$X_i^{net}(\%\, v/v) = \frac{X_i}{\sum_i X_i - X_{N_2}} * 100 \quad (2.4)$$

where X_i represents the volumetric fraction of the generic component of pyrogas as measured through the GC analysis, and X_{N_2} is the volumetric fraction of the exogenous N_2 as measured through the GC analysis.

The lower heating value (LHV) of pyrogas produced in thermal and catalytic pyrolysis tests, expressed in MJ/Nm^3, was calculated by considering the heating value (reported in the literature) and the volumetric concentration (X_i^{net}, % v/v) of each combustible component [284], as expressed in Eq. 2.5. H_2S was excluded from the calculation in this study since it would be removed from pyrogas prior to energy recovery due to corrosiveness issues.

$$LHV_{pyrogas} = 10.8\, X_{H_2}^{net} + 12.6\, X_{CO}^{net} + 35.9\, X_{CH_4}^{net} + 60.5\, X_{C_2-}^{net} + 88.0\, X_{C_3-}^{net} + 123.0\, X_{C_4-}^{net} \quad (2.5)$$

The portion of S migrating from MSS to the pyrolysis products was calculated for each tested condition. Biochar-S fraction (namely, BC-S) was calculated as the ratio between the S mass in biochar and the total S mass in the MSS sample (Eq. 2.6). The same criterium was used to calculate bio-oil-S fraction (namely, BO-S) (Eq. 2.7), while pyrogas-S fraction was calculated as difference.

$$BC - S\ \left(\%\, wt, \frac{g\ S}{g\ MSS-S}\right) = \frac{S_{BC} * M_{BC}}{S_{MSS} * M_{MSS}} \quad (2.6)$$

$$BO - S\ \left(\%\, wt, \frac{g\ S}{g\ MSS}\right) = \frac{S_{BO} * M_{BO}}{S_{MSS} * M_{MSS}} \quad (2.7)$$

Where S_{BC}, S_{BO}, and S_{MSS}, represent S concentration in biochar, bio-oil, and MSS, respectively, which were determined through elemental analysis (see section 2.2.3). For the determination of the composition of biochar produced in catalytic pyrolysis, the elemental analysis was conducted on the mix of biochar + zeolite collected at the end of the catalytic pyrolysis tests, and the mass of the zeolites was assumed constant during the pyrolysis process.

The H_2S formation ratio (HFR) was defined and calculated to express the amount of H_2S produced per mol of S initially contained in MSS (Eq. 2.8).

$$HFR\ \left(\frac{mol\ H_2S}{mol\ MSS-S}\right) = \frac{n_{pyrogas} * X_{H_2S}^{net}}{S_{MSS} * M_{MSS} * 32} \quad (2.8)$$

Where 32 (g/mol) is S atomic mass, and $n_{pyrogas}$ represents the mol of pyrogas produced, which were calculated as follows (Eq. 2.9):

$$n_{pyrogas}\ (mol) = \frac{M_{MSS} * Y_{pyrogas}}{\sum_i (X_i^{net} * MM_i)} \quad (2.9)$$

Where MM_i is the molar mass of the generic component of pyrogas, and $\sum_i (X_i^{net} * MM_i)$ is the overall molar mass of pyrogas.

2.2.5 Statistical analysis

All the experimental results are expressed as means calculated on triplicates. One-way ANOVA tests were performed to determine statistically significant (*p-value* < 0.05) differences among the calculated means. Tukey's method for multiple comparisons was applied. All the statistical analysis were performed by using Minitab Statistical Software v18.1 (Minitab Inc., State College, PA, USA).

2.3 Results and discussion

2.3.1 Product yields

2.3.1.1 The effect of pyrolysis temperature

The collection and weight of the different products in the thermal pyrolysis tests allowed the calculation of the respective yields for each tested temperature (**Figure 2.2A**). A maximum biochar yield of 58.4 % wt was observed at 350 °C, where liquid and pyrogas were produced with lower yields (34.0 and 7.6 % wt, respectively). Increasing temperatures to 500 – 650 °C induced an improved degradation of VM in MSS pyrolysis, leading to higher yields of liquid and pyrogas, up to 44.7 – 46.0 % wt and 11.4 – 12.7 % wt, respectively. The highest tested temperature (800 °C) resulted in a further increase in pyrogas yield (18.2 % wt) and a significant decrease in liquid yield to 43.2 % wt. On the other hand, the biochar yield progressively decreased,

reaching a minimum yield of 38.6 % wt at 800 °C. Thus, consistently with what is reported in the literature, the liquid and gaseous fractions increase at higher temperatures, to the detriment of the solid fraction, due to the progressive degradation of the VM content in the MSS sample [2,71]. As observed in this study, liquid yields are often reported to achieve their maximum around temperatures of 600 – 650 °C and to decrease significantly at higher temperatures, resulting in higher pyrogas yields, probably due to the occurrence of secondary cracking reactions (SCRs), responsible for the further degradation of organic compounds in the vapours [23].

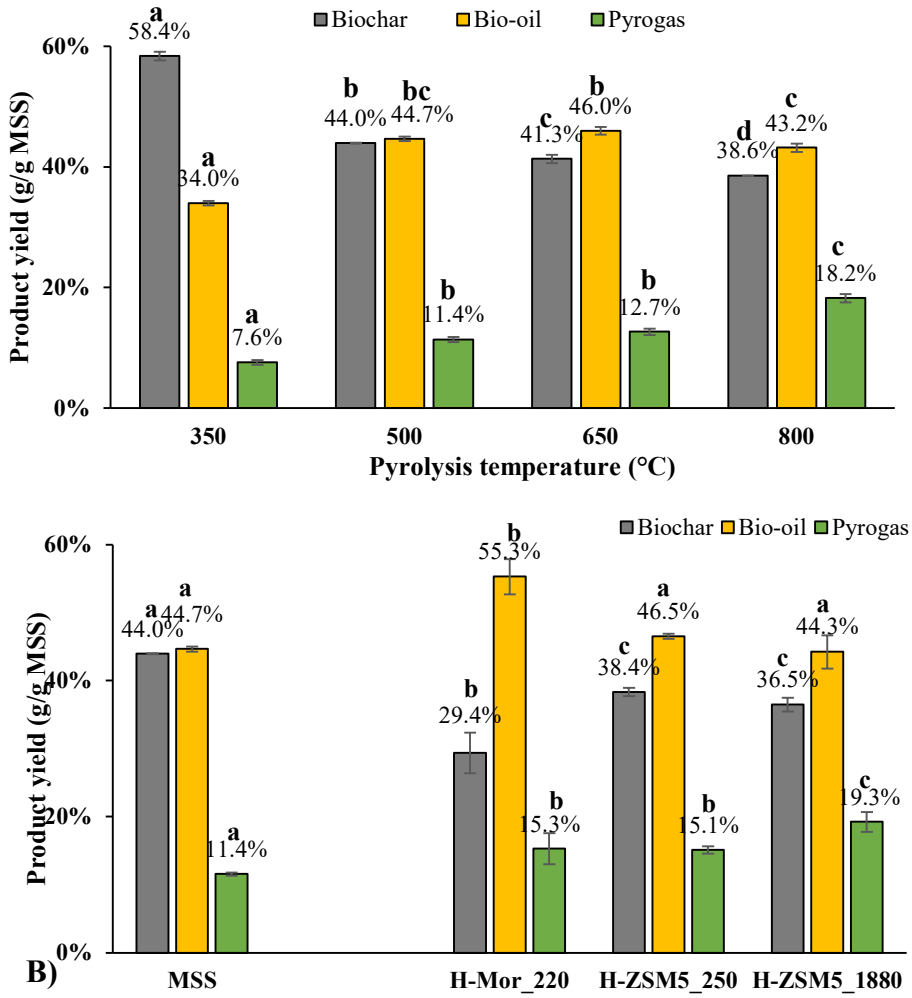


Figure 2. 2. Yields of the products of pyrolysis of municipal sewage sludge (MSS). The yields were calculated for A) thermal pyrolysis at each tested temperature (350, 500, 650, and 800 °C), and B) catalytic pyrolysis at 500 °C, for each tested zeolite. Letters a, b, and c, result from the Tukey's comparison analysis: statistically similar means share the same letters.

2.3.1.2 2.3.1.2 The effect of zeolites

The employment at 500 °C of the different zeolites used as a catalyst in the catalytic pyrolysis tests led to a significant decrease in biochar yield, with consequently higher pyrogas yield, in each condition, due to a stronger degradation of the organic matter in the solid phase (**Figure 2.2B**). The addition of H-Mordenite_220 caused the most important decrease in biochar yield (down to 29.4 % wt), resulting in the highest bio-oil yield (55.3 % wt), which was the only one significantly higher than that obtained from the pyrolysis of the sole MSS (44.6 % wt). Interestingly, despite the comparable SARs (220 and 250), H-Mordenite resulted in a 26 % reduction of biochar yield towards the enhancement of bio-oil yield, when compared to H-ZSM5. However, the pyrogas yields (15.3 and 15.1 % wt, respectively) were both significantly higher than that obtained by the sole MSS (11.6 % wt). Unlike other studies in which Mordenite has been used as a catalyst in the pyrolysis of different feedstocks (*i.e.* plastics) and where no effects on product yields had been detected due to its low mesopore content [285], in this study H-Mordenite was capable of substantially reducing biochar yield towards the enhancement of both liquid and pyrogas yields. On the contrary, the reduction of biochar yield obtained by H-ZSM5 (with both the tested SARs) had a positive influence only on the pyrogas yield, without affecting the liquid yield.

The reason for the observed difference between H-Mordenite and H-ZSM5 observed in this study has to be found in the variability of the inner structure of these two different zeolites, their porosity, and the system of inner channels which influence their catalytic activity [285]. H-ZSM5 is reportedly capable of increasing pyrogas yield, owing to its remarkable thermal cracking ability [78,286], and it showed a higher tendency to favouring SCRs and enhancing the formation of volatile components [287,288]. Interestingly, the employment of H-ZSM5_1880 resulted in a higher pyrogas yield (19.2 % wt) with respect to that obtained by H-ZSM5_250. Higher SARs indicate a lower number of acidic sites on the zeolites, yet characterized by higher strength, and generally resulting in lower cracking activity [288]. Nevertheless, the low MSS:catalyst ratio (1:1 wt) may compensate this low overall acidity.

2.3.2 Pyrogas composition

2.3.2.1 The effect of pyrolysis temperature

In the thermal pyrolysis tests, pyrogas composition varied with temperature, following the trend shown in **Figure 2.3**. CO_2 was the main component of pyrogas at almost all the tested temperatures, although its concentration progressively decreased with temperature increase (from 80.4 % v/v at 350 °C to 24.0 % v/v at 800 °C). On the other hand, CO and H_2 concentrations increased when temperature varied from 350 to 800 °C, reaching values between 8.4 and 25.1 % v/v for CO and from 0.5 to 19.8 % v/v for H_2 (**Figure 2.3A**).

The GC-FID analysis revealed a high presence of light hydrocarbons (**Figure 2.3B**), with CH_4 concentrations rapidly increasing from 1.7 to 18.2 % v/v in the 350 – 650 °C temperature range with a slight and not significant decrease to 17.3 % v/v at 800 °C. A similar trend was observed for C_2-, C_3-, and C_4- hydrocarbons, rapidly increasing in the 350 – 650 °C temperature range, and with a slight (and not significant) decrease at 800 °C. According to what has been reported by other authors in the literature [217,218], the trend followed by CH_4 and C_2-C_3 can be justified by the occurrence of reactions of degradation (*i.e.* steam gasification and reforming) of hydrocarbons with the production of new H_2 and CO. The water needed by these reactions came from the MSS sample itself. The slightly higher slope visible for H_2 and CO trends in the 650 – 800 °C temperature range might confirm this correlation. Additionally, the reduction of CO_2 concentration could also be favoured by the onset of WGS and Boudouard reactions, resulting in CO_2 conversion into more CO [218].

In pyrogas produced at 350 °C, the high CO_2 content and the low tenor of combustible gases resulted in an LHV as low as 2.09 MJ/Nm^3 (**Figure 2.3C**). By increasing pyrolysis temperature to 500 °C, the LHV significantly increased (16.92 MJ/Nm^3), consistently with the progressive reduction of CO_2 concentration, and a final substantial increase was achieved by raising pyrolysis temperature to 650 and 800 °C (LHV as high as 20.44 and 20.19 MJ/Nm^3, respectively). This stable trend observed in the 650 – 800 °C temperature range despite a continuous reduction of CO_2 concentration was a direct consequence of the decreasing concentration of C_2-, C_3-, and C_4- hydrocarbons.

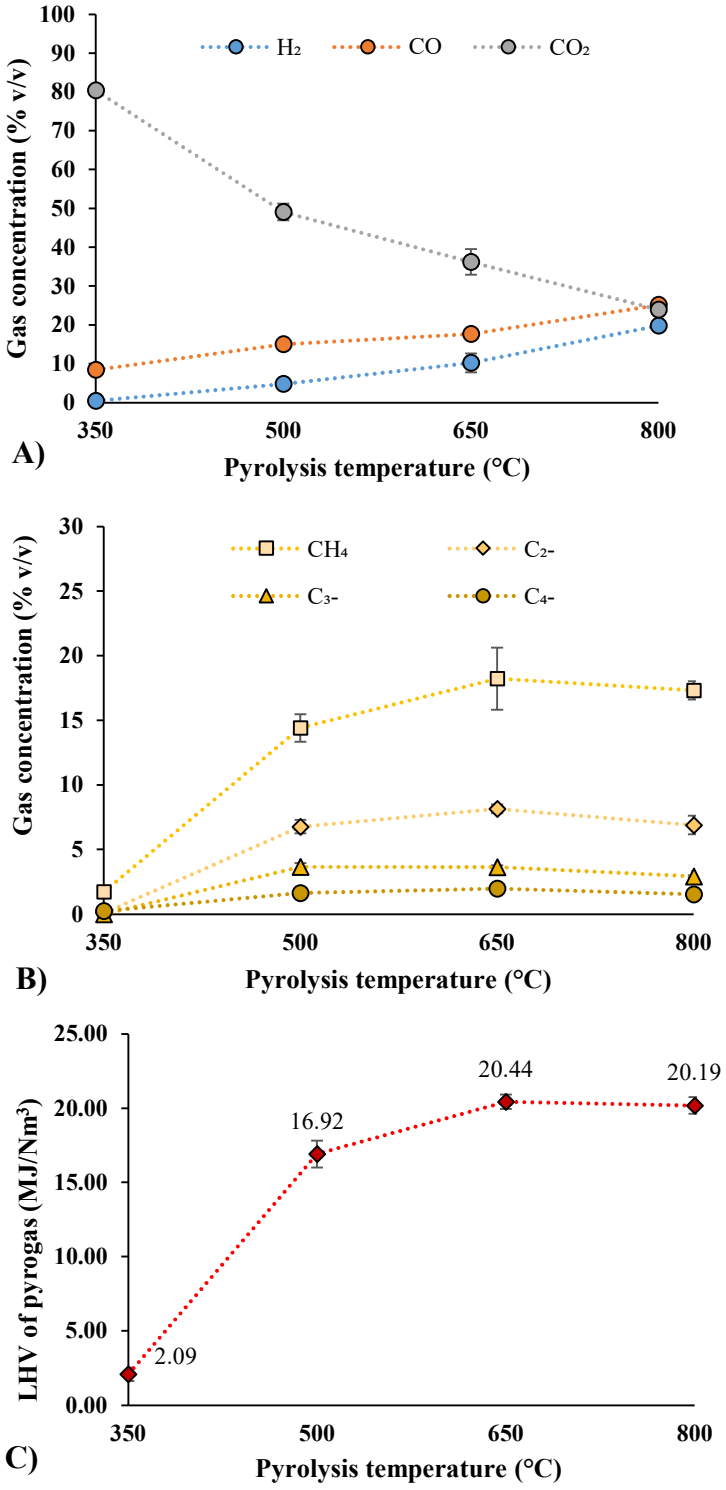


Figure 2. 3. Composition and lower heating value of syngas produced by thermal pyrolysis at variable temperatures. The results of gas-chromatographic analyses of pyrogas produced at 350, 500, 650, and 800 °C, are reported in terms of concentration of A) H_2, CO, and CO_2, and B) CH_4, C_2- C_3-, and C_4-, and C) lower heating value.

2.3.2.2 The effects of zeolites

Apart from an important effect on H_2S (thoroughly described in the following sections), the only significant effect of zeolite addition on pyrogas composition was that observed on CO concentration (**Table 2.3**). A substantial increase in CO concentration was observed with the addition of H-Mordenite_220 and H-ZSM5_250 (19.78 and 19.34 % v/v, respectively). The increase in CO concentration is consistent with other studies reporting the effects of ZSM-5-type zeolites [288].

	Thermal Pyrolysis	**Catalytic pyrolysis (MSS + Zeolite)**		
	MSS	**H-Mor_220**	**H-ZSM5_250**	**H-ZSM5_1880**
H_2 (% v/v)	4.82	3.84	3.36	5.33
CO (% v/v)	15.03	19.78*	19.34*	18.87
CO_2 (% v/v)	49.10	50.62	48.40	49.31
CH_4 (% v/v)	14.41	12.39	12.05	13.89
C_2- (% v/v)	6.78	6.05	6.68	6.89
C_3- (% v/v)	3.66	2.45	3.56	1.47
C_4- (% v/v)	1.63	2.45	2.32	1.84
H_2S (% v/v)	4.45	2.41*	4.27	2.60*
LHV (MJ/Nm^3)	16.92	16.19	17.16	15.67

*Table 2. 3. Composition of syngas produced by catalytic pyrolysis of municipal sewage sludge (MSS). The catalytic process was conducted at 500 °C, by employing different types of zeolites (H-Mordenite and H-ZSM5), with variable Si/Al ratio (SAR). Composition of syngas from thermal pyrolysis of the sole MSS is reported for comparison. v/v: by volume; * Statistically different value (p-value < 0.05).*

On the other hand, H-ZSM5 with the highest SAR (1880), had no influence on CO concentration. This could be motivated by the lower cracking activity resulting from the fewer (but stronger) acidic sites due to the higher SAR [288]. On the other hand, zeolites are generally capable of enhancing deoxygenation and denitrogenation reactions in biochar and vapours, favouring CO_2 formation. This usually happens to

the detriment of CO, which is more easily converted into CO_2 due to the higher availability of O radicals [289]. The observed increase in CO, together with a not significant variation of the CO_2 content, might indicate a partial deactivation of the zeolites due to coke deposition on their surface, which counteracted cracking and deoxygenation reactions and which could be favoured by the *in-situ* modality of catalysts addition [289]. This phenomenon commonly happens in acidic zeolites such as H-ZSM5 and H-Mordenite [290–292]. According to the literature, Si in zeolites is responsible for inhibition of coke formation, therefore higher SARs should result in lower risk of deactivation [288,293].

On the other hand, this high SAR of the zeolites would result in low cracking activity [288], therefore justifying the lack of evident effects on the main components of pyrogas, such as H_2 and CO_2. The neglectable effects of zeolite addition observed on almost all the pyrogas components (**Table 2.3**) resulted in similar LHVs for each tested condition (15.17 – 17.16 MJ/Nm^3).

2.3.3 H_2S concentration in pyrogas

2.3.3.1 The effect of temperature

H_2S concentration in pyrogas was measured for every tested temperature. As shown in **Figure 2.4A**, an H_2S concentration as high as 8.67 % v/v was observed in pyrogas produced at 350 °C. This value rapidly decreased with increasing temperatures, down to 2.4 % v/v at 800 °C, which is about 10 times higher than that reported by Jaramillo-Arango *et al.* [95] (2000 ppmv, equal to 0.2 % v/v) for pyrogas derived from MSS pyrolysis at the same temperature in a continuous pyrolizer. Interestingly, the initial S content in the MSS employed by Jaramillo-Arango *et al.* [95] was about 2 times lower than that of the MSS employed in the present study (0.55 vs 1.12 % wt db, respectively). This, combined with a 3 times lower H content (1.74 % wt db vs 5.18 % wt db, respectively), may justify the lower H_2S concentration reported in their study (see **Table 2.4**). Further, the higher SRT (90 min vs 15 min of this study) can result in an increase of the concentration of pyrogas main components: according to Gao *et al.* [99], H_2, CO_2, and CO concentrations in MSS-derived pyrogas produced at 700 °C in

a continuous system with an increasing SRT from 6 to 46 min experienced a 24, 111, and 70 % increase, respectively.

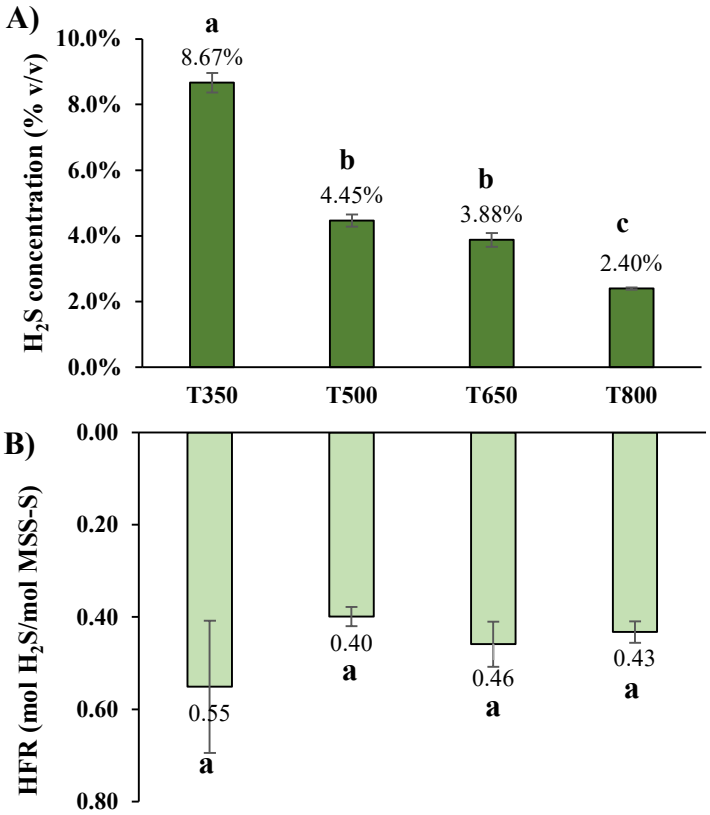


Figure 2. 4. H_2S in pyrolysis gas from thermal pyrolysis. The production of H_2S during thermal pyrolysis of municipal sewage sludge (MSS) at temperatures of 350, 500, 650, and 800 °C, was evaluated in terms of A) H_2S concentration in pyrogas, and B) H_2S formation ratio (HFR). Letters a, b, and c result from the Tukey's comparison analysis: statistically similar means share the same letters.

Although the influence of SRT on H_2S production is yet to be reported in the literature, lower final H_2S concentrations could be reasonably expected at higher SRTs, due to the dilution effect resulting from the increase of the main pyrogas components. However, Fonts *et al.* [90] reported a H_2S concentration around 2 - 4 % v/v in pyrogas produced from continuous pyrolysis of digested and dewatered MSS at 550 °C (comparable with the 4.52 % wt db observed in this study at 500 °C), with initial S and H content in MSS (0.8 – 0.9 and 3.1 – 4.4 % wt db, respectively) which were lower but comparable with those reported in this study (see **Table 2.4**).

	This study		[95]	[90]
Carbon (% wt db)	35.94		12.79	23.1 – 28.5
Hydrogen (% wt db)	5.18		1.74	3.1 – 4.4
Oxygen (% wt db)	22.98		16.22	17.7 – 22.4
Nitrogen (% wt db)	5.76		1.20	3.2 – 4.1
Sulfur (% wt db)	1.12		0.55	0.8 – 0.9
MC (% wt)	2.35		-	5.3 – 7.1
AC (% wt db)	29.02		67.50	39.9 – 52.0
VM (% wt db)	57.79		29.01	38.3 – 47.0
FC (% wt db)	10.66		3.49	4.4 – 6.4
Pyrolysis temperature (°C)	800	500	800	550
SRT (min)	15	15	90	n.r.
H_2S in syngas (% v/v)	2.40	4.45	0.20	2 – 4 [b]

Table 2. 4. Influence of feedstock composition and pyrolysis parameters on H_2S concentration in syngas. A comparison between this and other studies from the literature is reported. [a]: the heating rate was not calculable, as the MSS feedstock was introduced in the oven only after reaching the operative temperature; [b]: deducted from graphics; wt: on a weight basis; db: on a dry basis; MSS: municipal sewage sludge; HR: heating rate; SRT: solid retention time; MC: moisture content; AC: ash content; VM: volatile matter; FC: fixed carbon; v/v: by volume; n.r.: not reported.

The decreasing trend shown in **Figure 2.4A** for H_2S concentration with increasing temperatures seems to be in contrast with what is reported in the literature: H_2S concentration should decrease at higher temperatures due to the progressive degradation of organic S-compounds in MSS and in the produced vapours [294,295]. Nevertheless, as reported in **Figure 2.4B**, the HFR obtained from thermal pyrolysis was similar for each tested temperature (0.40 – 0.55 mol H_2S/mol MSS-S). Thus, the decreasing trend observed in H_2S concentration in pyrogas for increasing temperatures was only due to a dilution effect caused by the increasing pyrogas yield.

2.3.3.2 The effect of zeolites

During MSS catalytic pyrolysis tests, an interesting result was achieved concerning H_2S concentration in pyrogas (**Figure 2.5A**). The employment of H-Mordenite_220 and H-ZSM5_1880 resulted in final H_2S concentrations as low as 2.41 and 2.60 % v/v, respectively, which were 45.8 and 41.6 % lower than that obtained in the thermal pyrolysis of the sole MSS (4.45 % v/v) at the same temperature. On the other hand, the addition of H-ZSM5_250 caused no significant decrease in H_2S concentration (4.27 % v/v) when compared to the sole MSS.

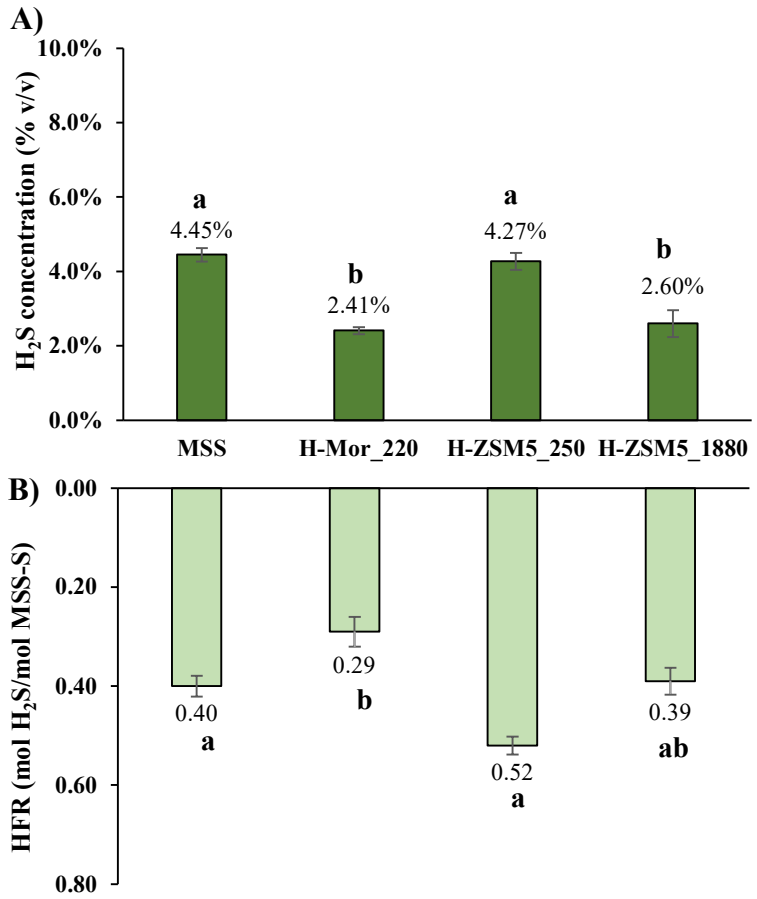


Figure 2. 5. H_2S concentration and formation ratio (HFR) in catalytic pyrolysis. The production of H_2S during catalytic pyrolysis of municipal sewage sludge (MSS) at 500 °C was evaluated in terms of A) H_2S concentration in pyrogas, and B) H_2S formation ratio (HFR), for each tested zeolite. Letters a, b, and c result from the Tukey's comparison analysis: statistically similar means share the same letters.

By calculating the HFR for catalytic pyrolysis (**Figure 2.5B**), it can be observed that pyrogas produced with the addition of H-ZSM5 with both SARs (220 and 1880) was

characterized by HFRs (0.52 and 0.39 mol H_2S/mol MSS-S, respectively) statistically similar to that related to the thermal pyrolysis of the sole MSS (0.40 mol H_2S/mol MSS-S). The 66 % wt increase in pyrogas yield determined by H-ZSM5_1880 with respect to the sole MSS was able to induce a significantly lower H_2S concentration. Furthermore, a significantly lower H_2S concentration in pyrogas derived from the addition of H-Mor_220 has been observed, caused not only by the observed increase in pyrogas yield, but also by a 28 % reduction of the HFR (0.29 mol H_2S/mol MSS-S). On the contrary, the 30 % wt higher pyrogas yield resulting from the addition of H-ZSM5_250 was not enough to significantly dilute H_2S concentration in pyrogas. According to the literature, the employment of zeolitic catalysts for the removal of H_2S from gas streams can occur through an adsorption-repolymerization mechanism [267]. H_2S can therefore be adsorbed on the surface of the zeolites, before repolymerizing in the solid/liquid phase. This can happen through physisorption (generally for higher SARs) and/or chemisorption (generally for lower SARs) [296]. This same mechanism might be at the basis of the *in-situ* catalytic activity of the zeolites as well.

It is worthwhile mentioning the effects arising from the addition of H-Mordenite and H-ZSM5 with comparable SARs (220 and 250), and the addition of the same zeolite type (H-ZSM5) with variable SAR (250 and 1880). The chemical structure of the H-Mordenite might have interacted with H_2S in a higher extent with respect to H-ZSM5_250. This effect has to be related to the chemical structure, since changing SAR in H-ZSM5 had no effect in this sense. On the other hand, the SAR increase from 250 to 1880 in H-ZSM5 indirectly affected H_2S concentration by stimulating a higher pyrogas yield.

2.3.4 Sulfur migration to the pyrolysis products

2.3.4.1 The effect of temperature

The results of the elemental analyses performed on biochar and bio-oil (reported in **Table B1** and **Table B2,** in **Appendix B**) were employed for the determination of S migration from MSS to the pyrolysis products. In thermal pyrolysis (**Figure 2.6A**), Biochar-S decreased from 37.0 to 19.5 % wt when temperature increased from 350 to 500 °C, reaching similar values at higher temperatures (17.0 and 18.3 % wt at 650 and

800 °C, respectively). This strong S migration from the solid fraction resulted in a high increase of pyrogas-S portion from 44.7 % wt at 350 °C to 60.1 % wt at 500 °C, while a slight increase in bio-oil-S (up to 27.5 % wt) was observed only at 650 °C.

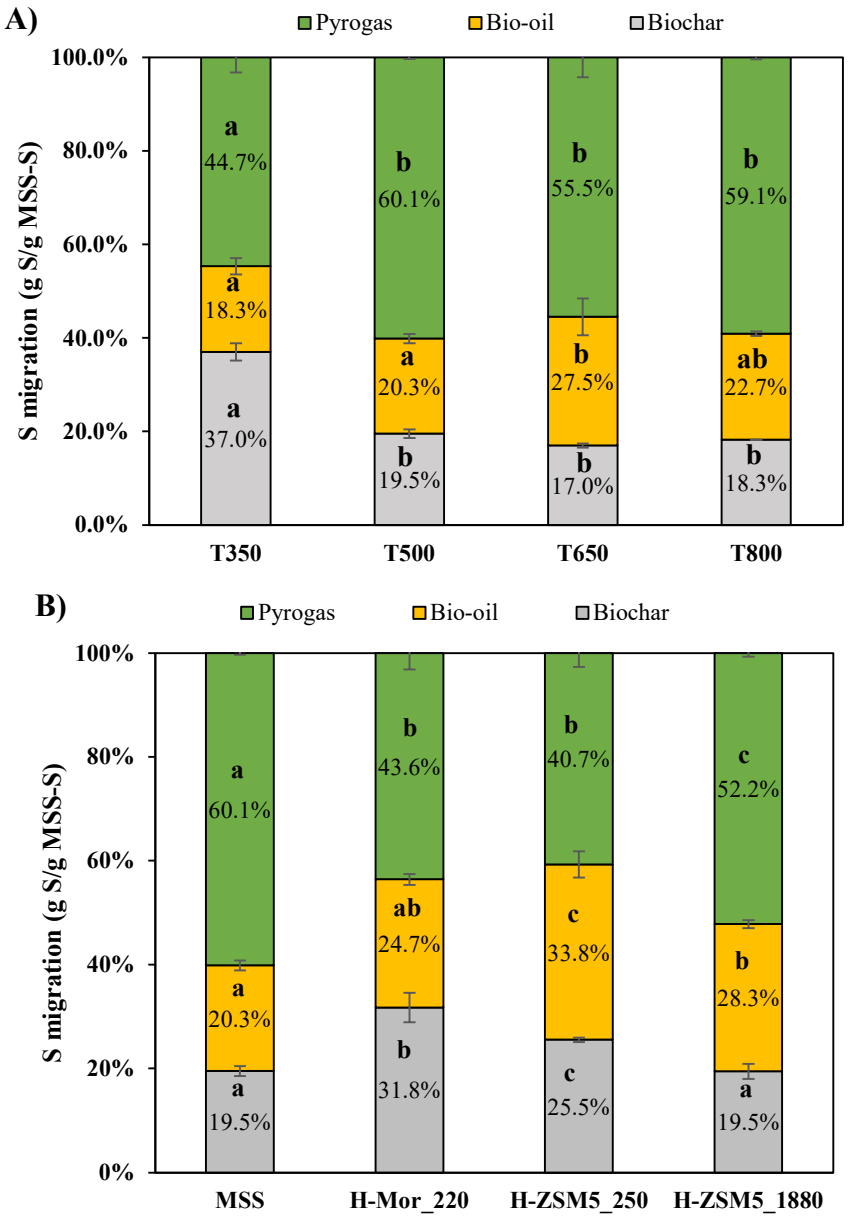


Figure 2. 6. Sulfur migration from municipal sewage sludge to biochar, bio-oil, and pyrogas. The amount of S migrated from MSS to the pyrolysis products is reported for A) thermal pyrolysis at 350, 500, 650, and 800 °C, and B) catalytic pyrolysis tests performed with different zeolites: H-Mordenite (Si/Al Ratio (SAR) = 220), H-ZSM5 (SAR = 250), and H-ZSM5 (SAR = 1880).

Pyrogas-S values were substantially higher than those reported by Liu *et al.* [265], who observed that almost 35 % wt of the initial MSS-S was present in gaseous form after pyrolysis at 450 °C. Such differences can reasonably be due to different speciation of organic S-compounds in MSS. According to what has been reported by Zhang *et al.* [297], the degradation of unstable mercaptans might be the main cause of S migration to pyrogas at temperatures of 350 – 500 °C. Then, increasing temperatures over 500 °C in this study probably led to the further degradation of more complex S-compounds (*e.g*. thiophene and more stable mercaptans), resulting in a higher pyrogas-S portion. Finally, pyrogas-S remained stable in the 500 – 800 °C temperature range, suggesting no further degradation of S-compounds could be obtained at those temperatures. Although the investigation of the degradation mechanisms and the fate of organic S-compounds possibly contained within MSS was beyond the scope of the present study, a complete characterization of the S-compounds in MSS could be helpful in the future.

2.3.4.2 The effect of zeolites

From the elemental analysis of biochar and bio-oil produced in the catalytic pyrolysis tests, the S-fractions migrated from MSS to the pyrolysis products were calculated (**Figure 2.6B**). Interestingly, all the tested zeolites could reduce S migration to pyrogas, by increasing the amount of S retained in biochar and bio-oils. This observation is consistent with the adsorption-repolymerization mechanisms assumed for S retention [267].

what is reported in the literature: in the application of zeolites for the removal of H_2S from off-gas streams, H_2S can be adsorbed on their surface before being subjected to repolymerization process, with the re-formation of solid/liquid S-compounds [267]. In the present study, a similar mechanism could have occurred with the addition of H-Mordenite and H-ZSM5 during pyrogas formation.

Biochar-S after H-ZSM5_1880 addition (19.5 % wt) remained equal to that obtained in the pyrolysis of the sole MSS (19.5 % wt), while the bio-oil-S fraction significantly increased from 20.3 to 28.3 % wt, resulting in a pyrogas-S fraction of 52.2 % wt, about 19.7 % higher than that obtained by H-Mor_220, despite the similar

H_2S concentration in pyrogas. This result confirms that the H_2S concentration reduction obtained with H-ZSM5_1880 was predominantly due to a dilution effect.

Interestingly, H-Mor_220 and H-ZSM5_250 led to similar S migration to pyrogas (43.6 and 40.7 % wt, respectively), which were 27.5 % and 32.3 % lower than that observed with the sole MSS (60.1 % wt). As already reported in sections 2.3.2.2 and 3.3.2, their addition resulted in similar pyrogas yields, while H-ZSM5_250 determined an HFR similar to that coming from the employment of the sole MSS, significantly higher than that obtained with H-Mor_220. Thus, it can be stated that H-Mor_220 and H-ZSM_5 had different effects on the speciation of S-compounds in pyrogas. Indeed, other gaseous S-compounds could be produced during MSS pyrolysis (*e.g.* SO_2, COS, CS_2 and CH_3SH) [295], although they were not monitored in the present study.

The fact that the H-ZSM5_250 addition resulted in the same H_2S concentration but with a significantly lower S migration to pyrogas, with respect to the condition with the sole MSS, suggests an effect of retention of other S-compounds different from H_2S. On the other hand, the fact that H-Mor_220 showed a reduction in H_2S concentration with respect to H-ZSM5_250, with similar S-migration, can be translated in a higher selectivity of the H-Mor_220 zeolite towards H_2S adsorption. H-ZSM5_250 could instead have a higher selectivity with other gaseous S-compounds, reducing their content in MSS-derived pyrogas. According to Pudi *et al.* [296], the selectivity towards H_2S adsorption depends on the available surface area and the pore diameter of the zeolite. Optimal ranges of 800 – 1600 m^2/g and 0.7 – 0.9 nm, respectively, were reported by Song *et al.* [298]. This difference in the selectivity towards H_2S between H-Mor_220 and H-ZSM5_250 could therefore be due to the different pore dimensions and surface area of the two zeolites.

2.4 Conclusions

In the present study, after observing the influence of temperature in the thermal pyrolysis of MSS, the *in-situ* catalytic pyrolysis of MSS at 500 °C was conducted with the addition of H-Mordenite and H-ZSM5 zeolites as catalysts with variable SARs. Their effect on product yields, syngas composition, H_2S production and S migration from MSS to pyrolysis products was evaluated and compared with the performance

obtained in the thermal pyrolysis of the sole MSS at the same temperature (500 °C). Here are the main conclusions of the study:

- Increasing temperatures induced an improved degradation of VM in MSS pyrolysis, leading to higher yields of liquid and pyrogas as compared to biochar yield. In the pyrogas, CO_2 was the main component at almost all the tested temperatures, and its concentration progressively decreased with temperature increase. Similarly, H_2S concentration rapidly decreased in the pyrogas with increasing temperatures.

- The addition of H-Mordenite and H-ZSM5 zeolites in MSS catalytic pyrolysis can substantially affect products yields. H-Mordenite had an increasing effect on liquid yield and pyrogas yield, while H-ZSM5 (with both SARs) favoured pyrogas yield increase. A higher SAR in H-ZSM5 resulted in a significantly higher pyrogas yield.

- Besides a slight increase effect in CO concentration, the addition of each zeolite had no significant effect on H_2 and CO_2 concentration, probably due to the occurrence of coke formation and catalysts deactivation. Further studies may be focused on the onset of practises aimed at contrasting this phenomenon.

- H-Mordenite (SAR 220) and H-ZSM5 (SAR 1880) reduced H_2S concentration in pyrogas with different mechanisms: H-Mor_220 induced dilution of the H_2S and partially prevented S conversion into H_2S, while H-ZSM5_1880 predominantly induced a dilution effect caused by the higher pyrogas yield obtained. H-ZSM5_250 had no effect on H_2S production and concentration.

- All the tested zeolites reduced S migration from MSS to pyrogas, resulting in higher S fractions retained in biochar and bio-oil. S retention probably occurred through adsorption-repolymerization mechanisms reported in the literature for H_2S removal from gas by means of zeolites.

- Other gaseous S compounds (*e.g.* SO_2, COS, CS_2 and CH_3SH) were probably produced during MSS pyrolysis. H-Mor_220 and H-ZSM5_250 had higher adsorption affinity with H_2S and not monitored S-compounds, respectively. In

future tests, an in-depth characterization of S speciation in MSS, biochar, bio-oil, and pyrolysis gas could be useful, as well as an in-depth characterization of the inner structure of the zeolites.

- The results obtained in the present study suggest new possibilities for employing H-Mordenite and H-ZSM5 in the catalytic pyrolysis of MSS for the retainment of different S-compounds, including H_2S. Future studies might focus on the individuation of optimal conditions for the removal of S-compounds in terms of pyrolysis conditions, zeolites SAR and dosage, and MSS pre-treatments. Additionally, the potential of MSS-derived biochar to be employed as an ex-situ catalyst should be assessed and compared with the performance of these and other catalysts.

CHAPTER 3. SYNGAS-DRIVEN SEWAGE SLUDGE CONVERSION TO MICROBIAL PROTEIN THROUGH H_2S- AND CO-TOLERANT HYDROGEN-OXIDIZING BACTERIA

This chapter was based on:

Pelagalli, V., Matassa, S., Race, M., Langone, M., Papirio, S., Lens, P.N.L., Lazzazzara, M., Frugis, A., Petta, L., Esposito, G., 2023. Syngas-driven sewage sludge conversion to microbial protein through H_2S- and CO-tolerant hydrogen-oxidizing bacteria. Water Research, 120698. https://doi.org/10.1016/j.watres.2023.120698

3.1 Introduction

Every year, about 45 Mton of dry municipal sewage sludge (MSS) are generated globally during wastewater treatment [1]. The treatment and disposal of this MSS accounts for as much as 50% of the total operational expenses of wastewater treatment plants (WWTPs) [2]. In view of the ongoing circular bioeconomy transition, MSS treatment is more and more regarded not only as a mere waste management issue, but rather as an opportunity to recover and valorise its energy, carbon, and nutrient content [25,299]. Following this approach, thermochemical processes such as pyrolysis are gaining momentum as they combine MSS treatment with the recovery of valuable products [39]. Pyrolysis consists in the thermal degradation of organic matter in inert atmosphere [23], resulting in MSS conversion into a solid (biochar), a liquid (bio-oils), and a gaseous (syngas) fraction, retaining precious resources such as hydrocarbons and nutrients in multiple forms, and employable in multiple applications [2,9].

Pyrolysis of MSS could thus enable novel and advanced biorefinery perspectives, particularly through the conversion of the MSS matrix into a clean gas feedstock, *i.e.* syngas, potentially suitable for the synthesis of high-value products such as microbial protein (MP) [254]. MP represents a protein-rich material (up to 80% on a dry weight basis) obtainable from different microbial sources and with applications spanning from animal feed and food production to agronomic additives (*e.g.* slow-release fertilizers) and biopolymer synthesis [251,252].

Being mainly composed by H_2, CO and CO_2, together with trace gases such as NH_3 and H_2S [96], the syngas from MSS pyrolysis could support autotrophic MP production through microorganisms such as hydrogen-oxidizing bacteria (HOB). As a matter of fact, HOB are capable of fixing CO_2 by using H_2 as electron donor and O_2 as electron acceptor, while NH_3 can serve as source of nitrogen for the production of the protein-rich biomass [256]. Thanks to the availability of all the main required substrates for autotrophic MP production on-site a WWTP, HOB have been proposed

as an upcycling platform to reassemble the energy, carbon and nutrient content of MSS under the form of a high-quality product such as MP [300].

Despite the promising application potential of HOB within WWTPs, biological syngas conversion faces severe challenges linked to the variable composition of the gaseous substrate, as well as to the high concentrations of inhibitory compounds such as CO and H_2S. In fact, the composition of MSS-derived syngas is highly affected by the characteristics of the pyrolyzed feedstock as well as by the operating conditions of the thermochemical process [2]. The H_2/CO_2 volumetric (v/v) ratios, for instance, can highly fluctuate within a range as broad as 0.1-10.0 [97,217], while HOB are usually grown by using gaseous mixtures with optimal H_2/CO_2 ratios around 7.0 [300], or at least falling within the 4.0-10.0 range [301]. Additionally, CO and H_2S concentrations in MSS-derived syngas can reach values up to 40 and 0.2% v/v, respectively [49,95]. A few studies investigated the effect of CO on HOB growth, reporting a complete inhibition of pure cultures of *Cupriavidus necator* and *Ideonella sp.* O-1 for CO concentrations of 30% v/v [258,259]. On the other hand, no information is yet available about the bioconversion by HOB of H_2S-containing syngas.

Owing to the synergistic interactions occurring within microbial consortia, mixed microbial cultures are characterized by a potentially higher degree of flexibility and resistance to varying substrate composition and presence of inhibitory compounds, as compared to pure/axenic cultures [252]. Therefore, while the employment of pure/axenic cultures would require an extensive pretreatment of syngas to continuously balance its composition (*e.g.* in terms of H_2/CO_2 ratio) and to avoid the presence of inhibitory substances, mixed cultures might enable the direct use and conversion of raw and untreated syngas, thereby lowering both operational and capital expenses. Moreover, being ubiquitous by nature, many HOB are capable of thriving within extreme environments such as deep-sea hydrothermal vents, thus getting adapted to the high presence of CO and H_2S in volcanic gases [302,303]. Therefore, the probability of finding HOB capable of resisting to high and variable concentrations of inhibitory gases is higher in mixed cultures with respect to pure/axenic cultures.

The present study aimed at establishing the potential of an enriched HOB mixed culture to directly upcycle MSS-derived syngas into MP. In this study, a HOB mixed culture was tested to perform syngas bioconversion, by simulating realistic MSS-derived syngas mixtures [49,95]. Synthetic syngas mixtures were prepared by varying the H_2/CO_2 ratio and the concentration of potential inhibitors such as H_2S and CO according to real values reported in literature for MSS pyrolysis. Aerobic syngas bioconversion was evaluated both through short-term (48-96 h) and long-term (30 days) batch tests by monitoring H_2 and CO_2 consumption, biomass concentration, biomass yield on H_2, volumetric biomass productivity and biomass protein content. The long-term tests were further used to monitor the evolution of the mixed HOB microbial community under the most relevant process conditions. The experimental results here presented and discussed are further complemented by a series of technical considerations and implications, including the potential of the envisioned process to directly upcycle other relevant MSS-derived syngas constituents such as ammonia into MP.

3.2 Materials and methods

3.2.1 Experimental setup of the aerobic syngas bioconversion batch tests

The HOB enrichment employed throughout the whole experimentation was prepared by using active compost as inoculum and a mineral medium prepared accordingly to Yu *et al.* [304]. The enrichment procedure was performed according to the description provided in **Appendix C1**. Short- and long-term batch tests of aerobic syngas bioconversion were conducted by exposing the HOB enrichment to different synthetic gas mixtures, simulating various potential syngas compositions. Each experimental condition was tested in triplicate within 280 mL serum bottles, with a liquid volume of 40 mL and an inoculum size between 10 and 25% v/v. Upon inoculation, the bottles were sealed with 20 mm diameter butyl septa and crimped through a metal ring. A total of 370 mL of feed gas was supplied within each serum

bottle. Each bottle was initially flushed with H_2 for 5-10 min in order to exchange the headspace with H_2. Subsequently, O_2 and CO_2 were added by means of a syringe in each bottle to achieve the desired $H_2/O_2/CO_2$ ratio and an initial pressure of 1.5 bar to allow to monitor gas consumption. The composition of the feed gas mixture was adapted according to each experimental condition by modifying the H_2/CO_2 ratio, supplying CO, and by dissolving Na_2S in the medium as source of H_2S, as further detailed in the following sections.

In this study, the CO_2 was supplied through gas bottles (Nippon Gases, Milan, Italy), while the required H_2 and O_2 gases were produced on-site through a lab-scale alkaline electrolysis cell (Hydrobullet, Athens, Greece) [305,306]. CO gas was also produced on-site through the dehydration of formic acid (85% v/v concentration) with sulfuric acid (96% v/v concentration) (both provided by Sigma Aldrich, St. Louis, MO, USA) [307], and then stored in a gas bag until further use. Prior to the start of each test, the bottles were covered to avoid the influence of light, incubated at 30 °C and agitated at 360 rpm. The pressure decrease within the bottles was monitored by means of manometric measurements once every 24 h. The headspace gas composition was sampled from each serum bottle and analysed periodically to evaluate H_2 and CO_2 consumption (section 3.2.4). Once the batch tests were completed, the liquid fraction of each replicate was analysed to determine the final ammonium and biomass concentration, as well as the total protein content of the biomass.

3.2.2 Short-term batch tests

The direct and immediate effect of variable simulated syngas compositions in terms of H_2/CO_2 ratios, as well as H_2S and CO concentrations on the HOB enrichment were evaluated in a series of short-term batch tests of the duration of 48 h. This duration was chosen based on the preliminary enrichment phase, which was performed through cycles of headspace and liquid medium refreshment of about 48 h. This time interval was indeed sufficient to achieve over 80% H_2 consumption and enable consistent biomass growth in the enrichment phase. The mineral medium was inoculated with the enriched HOB culture by using an inoculum size of 10% v/v. This dilution ensured a

starting optical density, measured at 605 nm (OD_{605}), between 0.2-0.3 in each test. The main characteristics of each experimental condition are summarized in **Table 3.1**.

3.2.2.1 H_2/CO_2 ratio test

H_2/CO_2 ratios of 2.0, 4.3 and 10.0 were tested in conditions R2, R4.3 and R10, respectively. The 2.0 to 10.0 H_2/CO_2 ratio was chosen to test a sufficiently wide range of values, which could realistically characterize most of the different syngas compositions potentially obtainable from MSS (section 3.3.1). The intermediate H_2/CO_2 ratio of 4.3 was selected in order to match the $H_2/O_2/CO_2$ ratio of 65/20/15 (v/v) used for the HOB enrichment phase (**Appendix C1**).

3.2.2.2 H_2S concentration test

Jaramillo-Arango *et al.* reported a H_2S concentration of 0.2% v/v, equivalent to 2000 ppmv, for syngas derived from MSS [95]. In order to evaluate the resistance of the HOB enrichment at this and at higher potential concentrations, H_2S equivalent gas concentrations of 2000, 3000, 4000, 6000 and 8000 ppmv were simulated and tested in five experimental conditions (namely, H_2S-2, H_2S-3, H_2S-4, H_2S-6, H_2S-8, respectively). The presence of H_2S in the syngas was simulated by means of $Na_2S \cdot 9H_2O$ addition in the liquid medium, according to the procedure and calculations reported by Xu *et al.* [308]. In brief, small volumes (1 to 2 mL) of a concentrated stock solution of $Na_2S \cdot 9H_2O$ (Sigma Aldrich, St. Louis, MO, USA) were added to each bottle to simulate the desired H_2S equilibrium concentration that would establish in the gas phase according to the specific physico-chemical conditions (see **Appendix C2** for further details). It is worth noting that the actual H_2S concentration present in the liquid phase in each condition was variable during the test due to the influence of pressure and pH on its gas-liquid equilibrium. A control condition (C) without $Na_2S \cdot 9H_2O$ addition was also performed. Every other experimental parameter (feed gas composition, starting pressure, temperature, and agitation) was maintained equal to the enrichment condition.

	Condition	H_2/O_2	H_2/CO_2	H_2		O_2		CO_2		CO		Equivalent H_2S
				%	mL	%	mL	%	mL	%	mL	ppmv
H_2/CO_2 ratio test	R2	3.3	2.0	55	205	17	63	28	102	-		-
	R4.3		4.3	65	240	20	74	15	55	-		-
	R10		10.0	71	263	22	81	7	26	-		-
H_2S concentration test	C	3.3	4.3	65	240	20	74	15	55	-		0
	H_2S-2											2,000
	H_2S-3											3,000
	H_2S-4											4,000
	H_2S-6											6,000
	H_2S-8											8,000
CO concentration test	C	3.3	4.3	65	240	20	74	15	55	0	0	-
	CO10			59	216	18	67	14	50	10	37	-
	CO20			52	192	16	59	12	44	20	74	-
	CO30			46	168	14	52	11	39	30	111	-
	CO40			39	144	12	44	9	33	40	148	-

Table 3. 1. Experimental conditions tested in the short-term batch tests to assess the effects of variable H_2/CO_2 ratios, H_2S equivalent concentrations and CO concentrations on the performance of HOB. Although the percentages of H_2, O_2 and CO_2 in each condition of the CO concentration test could vary, the H_2/CO_2 and H_2/O_2 ratios were maintained constant.

3.2.2.3 CO concentration test

Carbon monoxide is one of the main components of syngas, and that derived from MSS pyrolysis has been reported to have concentrations variable between 10 and 40% v/v [49,97]. In order to assess the influence of CO on the HOB mixed culture, a volume of CO corresponding to concentrations of 10, 20, 30 and 40 % v/v of the feed gas

mixture was added to each bottle (namely CO10, CO20, CO30 and CO40, respectively), together with H_2, O_2 and CO_2. A control condition (C) without CO was also performed, with a feed gas volumetric composition of $H_2/O_2/CO_2$ = 65/20/15.

3.2.3 Long-term batch tests

Three different test conditions were prepared to investigate the long-term (30 days) aerobic bioconversion of realistic syngas mixtures containing CO and H_2S (**Table 3.2**). The latter were compared with a control condition without CO and H_2S, prepared with a feed gas volumetric composition of $H_2/O_2/CO_2$ = 65/20/15. CO10 and CO40 conditions were characterized by CO concentrations of 10 and 40% v/v, respectively, thereby representing typical low and high CO concentrations in syngas. A mixed condition with CO and equivalent H_2S concentrations of 10% v/v and 2000 ppmv, respectively (CO10+H_2S), was also prepared to evaluate the combined effect of these two potential inhibitors. For the choice of CO and H_2S concentrations for this mixed condition, one of the highest H_2S concentrations in MSS-derived syngas was used (2000 ppmv) in the presence of a typical yet low CO concentration (10% v/v) in order to minimize the potential inhibitory effect while still evaluating the potential combined effect.

Condition	H_2/O_2	H_2/CO_2	H_2		O_2		CO_2		CO		Equivalent H_2S
			%	mL	%	mL	%	mL	%	mL	ppmv
Control	3.3	4.3	65	240	20	74	15	56	0	0	0
CO10			59	216	18	67	14	50	10	37	0
CO40			39	144	12	44	9	33	40	148	0
CO10+H_2S			59	216	18	67	14	50	10	37	2,000

Table 3. 2. Experimental conditions tested in the long-term batch tests in order to assess the effect on HOB of variable CO concentrations with and without the presence of H_2S for a duration of 30 days.

The supply of CO and H_2S to each bottle was performed as already described in sections 3.2.2.2 and 3.2.2.3.

Each bottle was sampled and opened every 48 – 96 h to exchange 75% of its volume with fresh medium and provide a fresh feed gas mixture. The quantification of the protein content of the biomass was conducted regularly on samples taken on days 2, 11, 19, 26 and 30, while samples taken at the beginning (day 0) and the end of the test (day 30) were used for microbial community analysis (section 3.2.8).

3.2.4 Effect of CO on biomass productivity, concentration and yield

An additional series of batch tests was conducted to further assess the effect of CO on biomass volumetric productivity and concentration achievable by the HOB enrichment. These batch tests were operated through a daily gas feeding, aiming at minimizing gas substrate limitation. Differently from short-term and long-term batch tests, the concentrations and volumes of H_2, O_2 and CO_2 in the feed gas were set as constant in each condition in order to exclude the potential influence of H_2 limitation and extra dosage, and evaluate the sole effect of CO concentrations of 10 and 40% v/v [258]. To this end, inert N_2 gas was used to achieve the same amount of feed gas (370 mL) and initial pressure (1.5 bar) in all conditions (**Table 3.3).** The tests lasted 96 h and were performed by daily refreshing the gas headspace. Prior to each supply of fresh gas, the headspace was sampled and a volume of 3 mL of the liquid culture was withdrawn and replaced with mineral medium.

Condition	H_2/O_2	H_2/CO_2	H_2		O_2		CO_2		CO		N_2	
			%	mL	%	mL	%	mL	%	mL	%	mL
Control									0	0	40	148
CO10	3.3	4.3	39	144	12	44	9	33	10	37	30	111
CO40									40	148	0	0

Table 3. 3. Experimental conditions used to test the effect of CO on biomass concentration and volumetric productivity.

3.2.5 Analytical methods

Gas samples were analysed by a gas-chromatograph (Varian 3400 GC, Varian Inc., Palo Alto, CA, USA), equipped with a thermal conductivity detector (TCD). Prior to analysis, liquid samples were centrifuged at 10,000 rpm for 5 min and filtered with 0.45 µm cellulose syringe filters (Alwsci, Hangzhou City, Zhejiang P.R., China). Biomass growth was monitored by measuring spectrophotometrically the optical density at 605 nm (OD_{605}) (PhotoLab S5, WTW-Xylem, Germany). The OD_{605} values were correlated to the volatile suspended solids (VSS) concentration by means of a calibration curve. The VSS concentration was measured according to the standard methods [309]. The concentration of ammonium nitrogen (NH_4^+-N) was analysed spectrophotometrically following the indophenol blue method [310], while the biomass protein content was assessed through the Lowry method on the frozen liquid biomass samples thawed at 50 °C to promote cell lysis [311].

3.2.6 Calculations

The volumetric biomass productivity was calculated as grams of biomass produced per litre per day (Eq. 3.1).

$$Volumetric\ biomass\ productivity\left(\frac{g\ VSS}{L\cdot d}\right) = \frac{Biomass\ concentration\ increase\ (g\ VSS/L)}{Time\ (d)} \quad (3.1)$$

Where *biomass concentration increase* is here referred to the net biomass generated during the aerobic bioconversion process, calculated as the difference between final and initial biomass concentration; *time* represents the time interval running between two consecutive sampling phases, expressed in days.

Biomass yield on hydrogen (Y_{H2}) was calculated as grams of biomass per grams of chemical oxygen demand (COD) hydrogen gas equivalent (H_2-COD) (3.2).

$$Y_{H_2}\left(\frac{g\ VSS}{g\ H_2-COD}\right) = \frac{Biomass\ concentration\ increase\ (g\ VSS/L)}{H_2\ gas\ uptake\ (mol)*16\ (g\ COD/mol)} * Liquid\ volume\ (L) \quad (3.2)$$

Where *H_2 gas uptake* was calculated as the difference between the initial H_2 supply and the residual amount of H_2 in the headspace. 16 g COD per mol of H_2 were considered for the conversion of H_2 uptake (mol) into H_2-COD (g H_2-COD) [255].

H_2 consumption by HOB was calculated by expressing the H_2 gas uptake as percentage of the H_2 initial supply (Eq. 3.3). The same was done to evaluate CO_2 consumption (Eq. 3.4).

$$H_2\ consumption\ (\%) = \frac{H_2\ gas\ uptake\ (mol)}{H_2\ initial\ supply\ (mol)} \quad (3.3)$$

$$CO_2\ consumption\ (\%) = \frac{CO_2\ gas\ uptake\ (mol)}{CO_2\ initial\ supply\ (mol)} \quad (3.4)$$

Biomass protein content was calculated as percentage of total protein in biomass expressed as VSS (Eq. 3.5).

$$Biomass\ protein\ content\ (\%) = \frac{Protein\ concentration\ (g\ Protein/L)}{Biomass\ concentration\ (g\ VSS/L)} \quad (3.5)$$

3.2.7 Balanced stoichiometric equation for HOB

In order to better evaluate the obtained results and compare them with stoichiometric reactions, a balanced equation for HOB growth (Eq. 3.6) was calculated from the general equation provided by Yu and Lu (2019) for the autotrophic growth of *Cupriavidus necator* using H_2 as electron donor. The stoichiometric equation was calculated by taking as reference the range of biomass yield on H_2 of 0.07 - 0.28 g VSS/g H_2-COD during HOB growth under batch conditions, as reported by Matassa *et al.*, therefore assuming an average biomass yield of 0.18 g VSS/g H_2-COD [255].

$$CO_2 + 8.47\ H_2 + 3.22\ O_2 + 0.24\ NH_3 \rightarrow CH_{1.68}O_{0.46}N_{0.24} + 8.23\ H_2O \quad (3.6)$$

The detailed calculations are reported in **Appendix C3**.

3.2.8 Statistical analysis

The obtained results were expressed through mean values and associated standard deviations as calculated from the experimental triplicates. Minitab Statistical

Software v18.1 (Minitab Inc., State College, PA, USA) was used to perform one-way ANOVA tests to evaluate the statistical significance of the experimental results. A 95% confidence level was applied, and the means were considered significantly different when a *p-value* <0.05 was obtained. The differences between the supposed equal means were compared through Tukey's method for multiple comparisons.

3.2.9 Microbial community analysis

The necessary operations for DNA extraction and quantification, PCR amplification, library quantification and sequencing were performed according to the methods described by Bianco *et al.* [312]. The protocol followed for sequence filtering and taxonomy assignation is described in detail **Appendix C4**.

3.3 Results and discussion

3.3.1 Effect of varying syngas composition and presence of inhibitory compounds

3.3.1.1 The role of the H_2/CO_2 ratio

Figure 3.1 shows that the pressure decrease (panel **A**) and the corresponding gas consumption (panel **C**) were similar for all tested conditions, eventually resulting in a comparable biomass growth (**Figure 3.1B**). More in detail, the H_2 consumption was similar among all tests, ranging between 83 and 87%, while CO_2 consumption in the R10 condition was significantly higher (*p-value* < 0.05) with respect to the R2 and R4.3 conditions (90% vs. 38% and 53%, respectively) (**Figure 3.1C**). The latter is consistent with the fact that the R10 condition was the one characterized by the lowest initial CO_2 content, which resulted in a more complete carbon capture and assimilation process.

This result can be better understood by calculating the H_2/CO_2 uptake ratios for each condition, given the measured H_2 and CO_2 consumptions. The calculated H_2/CO_2 uptake ratios were equal to 4.6, 7.1, and 9.2, for R2, R4.3 and R10, respectively. The H_2/CO_2 uptake ratio in the R10 condition (9.2) was slightly higher than the

stoichiometric H_2/CO_2 ratio estimated for HOB (8.5) through the balanced stoichiometric equation (Eq. 3.6), meaning that the amount of available CO_2 was lower than the stoichiometric demand, and probably imposing carbon-limited growth conditions. On the contrary, for R2 and R4.3 the H_2/CO_2 uptake ratios (4.6 and 7.1, respectively) were sensibly lower than the stoichiometric one, therefore meaning that CO_2 was present in excess.

Biomass yields on H_2 as high as 0.16, 0.15 and 0.14 g VSS/g H_2-COD were

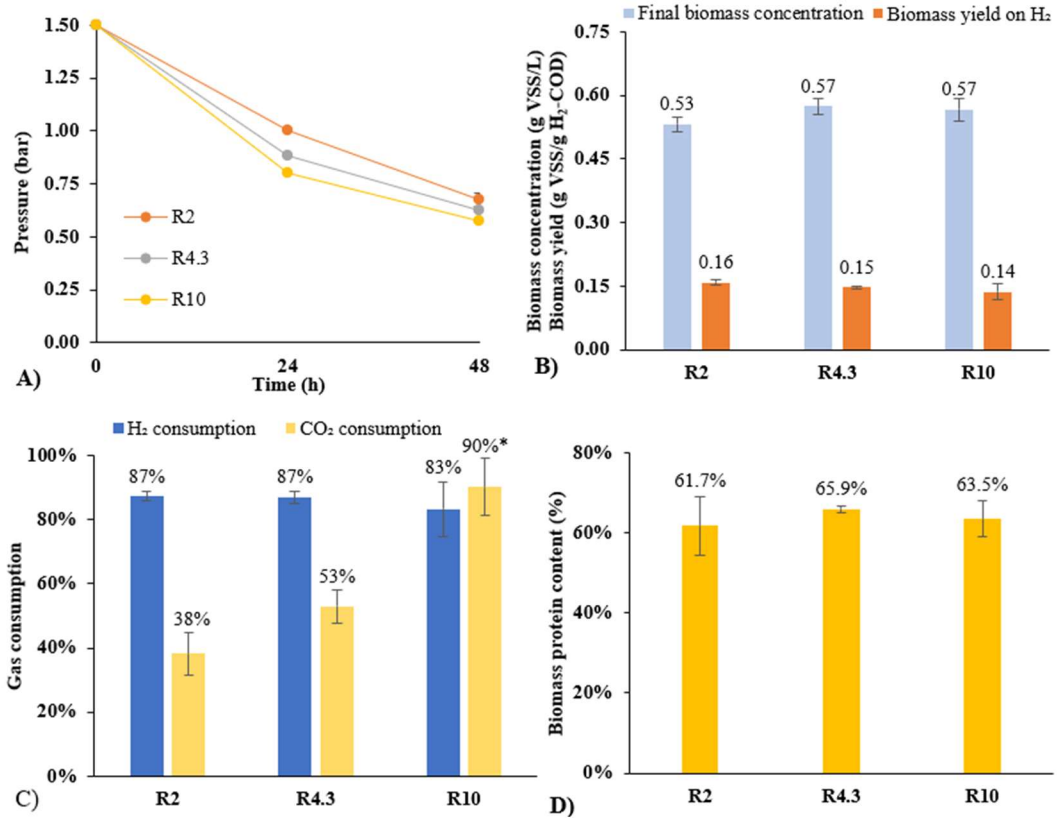


*Figure 3. 1. Results of the H_2/CO_2 ratio short-term batch tests. The influence of the variable H_2/CO_2 ratio on the growth of the HOB enrichment is expressed in terms of: A) Pressure variation over time; B) Final biomass concentration and yield on hydrogen; C) H_2 and CO_2 consumption, and D) Biomass protein content. Initial biomass concentration: 0.088 g VSS/L. *: Statistically different value (p-value <0.05). Error bars refer to the standard deviation calculated from the triplicates of each test.*

obtained for R2, R4.3 and R10 conditions, respectively (**Figure 3.1B**). These values are comparable with the average value assumed for the calculation of the balanced stoichiometric equation for HOB (0.18 g VSS/g H_2-COD), and derived from the range

of 0.07-0.28 g VSS/g H_2-COD reported in literature [255]. Furthermore, a similar protein content within the biomass was observed for each condition (**Figure 3.1D**), reaching values between 61.7 and 65.9% on a VSS basis. These values are consistent with those reported by Matassa *et al*. in similar batch conditions (average 66% crude protein content on a VSS basis) [255] with a H_2/CO_2 ratio of 4.3. Dou *et al.* also obtained a 64% crude protein content in MP produced by an axenic culture of *Paracoccus denitrificans Y5* with a H_2/CO_2 ratio of 7.0 under similar conditions (*i.e.* using NH_4Cl as source of nitrogen) [257].

Overall, the first results from the short-term batch tests indicated that the aerobic bioconversion process was not significantly influenced by varying the H_2/CO_2 ratio within typical syngas values (2.0 – 10.0). Importantly, the high values of protein content, gas consumption and biomass yield obtained in these tests also at a H_2/CO_2 ratio of 2.0, thus well below the typical 4.0 - 10.0 stoichiometric range indicated by Schink and Schlegel (1978) for HOB, and far from the optimum value of 7 indicated by Matassa *et al*. [300], suggest that HOB mixed cultures could directly valorise raw syngas characterized by a low H_2/CO_2 ratio. Furthermore, the use of syngas characterized by high H_2/CO_2 ratios could lead to an almost complete CO_2 capture and conversion into MP biomass without affecting key process parameters such as biomass yield and protein content.

3.3.1.2 The effect of H_2S

The results reported in **Figure 3.2** show how the pressure variation over time for the H_2S-2 condition (2000 ppmv) was comparable to that of the control, and also in the H_2S-3 and H_2S-4 conditions (3000 and 4000 ppmv, respectively) the same final pressure was reached, despite a lower gas consumption rate in the first 24 h. On the other hand, the H_2S-6 and H_2S-8 conditions (6000 and 8000 ppmv, respectively) showed almost no pressure decrease. Only a negligible H_2 consumption of 11% was observed for the H_2S-6 test after 48 h of incubation, and no consumption was observed

for H_2S-8 (**Figure 3.2C**). A similar H_2 and CO_2 consumption was observed for all other conditions and the control (85-97% for H_2 and 47-62% for CO_2).

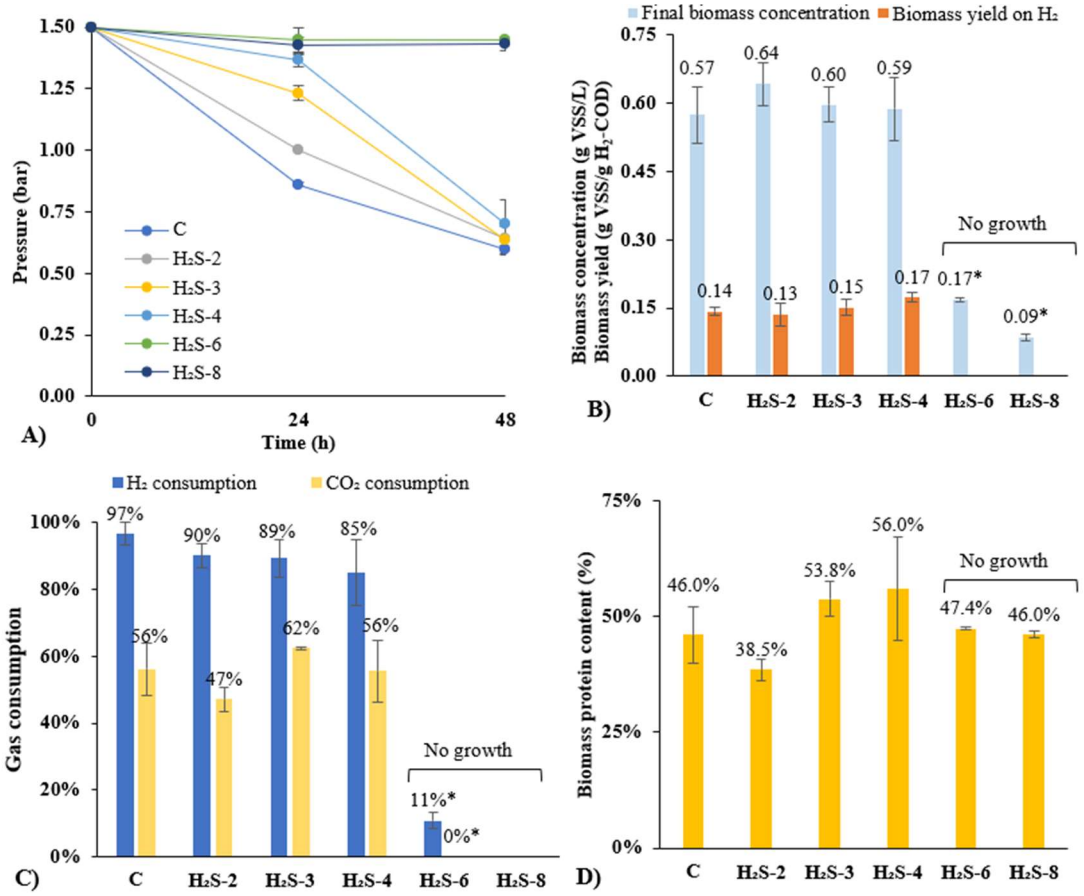


*Figure 3. 2. Results of the H_2S concentration short-term batch test. The influence of increasing H_2S concentrations on the growth of the HOB enrichment is expressed in terms of: A) Pressure variation over time; B) Final biomass concentration and yield on hydrogen; C) H_2 and CO_2 consumption, and D) Biomass protein content. Initial biomass concentration: 0.087 g VSS/L. *: Statistically different value (p-value <0.05). Error bars refer to the standard deviation calculated from the triplicates of each test.*

Starting from an initial biomass concentration of 0.09 g VSS/L, the final biomass concentration after 48 h (**Figure 3.2B**) was comparable between the control and the H_2S-2, H_2S-3 and H_2S-4 conditions, ranging between 0.57 and 0.64 g VSS/L. On the contrary, the H_2S-6 condition showed only a marginal biomass growth, reaching a final biomass concentration of 0.17 g VSS/L after 48 h of incubation, while no biomass growth was observed for H_2S-8. The biomass yield on hydrogen after 48 h (**Figure 3.2B**) was comparable between the control and the H_2S-2, H_2S-3 and H_2S-4 conditions,

ranging between 0.13 and 0.17 g VSS/g H_2-COD, and in line with the range reported in literature (0.07 – 0.28 g VSS/g H_2-COD). Due to the negligible biomass growth, the biomass yield for H_2S-6 and H_2S-8 was not taken into account.

Concerning the protein content (**Figure 3.2D**), this was not affected by the increasing equivalent H_2S concentration (38.5-56.0%), with no significant differences among the tested conditions. Similar values were observed also for H_2S-6 and H_2S-8 (47.4 and 46.0%, respectively), yet the latter were mainly linked to the initial protein content of the inoculum. It is worth noting that, in general, the protein content of the control and the test conditions was lower than that observed in the previously described tests on the effect of the H_2/CO_2 ratio (section 3.3.1.1), pointing towards an overall lower protein content in the HOB enrichment in concomitance with the tests.

Based on these results, equivalent H_2S concentrations of 6000 and 8000 ppmv were beyond the inhibition threshold for the HOB enrichment, while no inhibition was observed for equivalent H_2S concentrations as high as 4000 ppmv. It is worth stressing further that the effects of the equivalent H_2S concentrations, initially set in the headspace, on the HOB mixed were also dependent on the gas/liquid equilibrium and mass transfer phenomena. Such concentrations are nonetheless indicative of the characteristics of MSS-derived syngas mixtures simulated in the aerobic bioconversion process.

To the best of the authors' knowledge, the resistance of HOB towards H_2S was never assessed before in similar tests, although H_2S-resistant HOB species were already reported, as further discussed in section 3.3.4. H_2S uptake and sulfate formation were not monitored during the whole study, but the role of potential sulfur-oxidizing bacteria (SOB) in the HOB mixed culture could be object of further studies. Xu *et al*. studied the inhibitory effect of H_2S during MP production from biogas operated by a pure culture of *Methylocapsa acidiphila* as a methane-oxidizing bacterium (MOB) [308]. The authors observed the onset of H_2S inhibition on MOB growth and protein content for H_2S concentrations as low as 1000 ppmv. As further discussed in section 3.3.4, the higher resistance of the HOB enrichment was likely due to its more versatile metabolic potential as compared to the pure MOB strain.

Overall, the ability to withstand H_2S concentrations well above those typically found in syngas opens the possibility of direct gas-to-MP conversion processes, thus overcoming the need of preliminary treatments for H_2S removal.

3.3.1.3 The effect of CO

The final biomass concentration reached similar values for all conditions tested (**Figure 3.3B**), except for CO40 (40% v/v of CO) condition (0.43 gVSS/L), when it was significantly lower (*p-value* < 0.05). The latter result can be reasonably linked to the lower initial content of the electron donor (*i.e.* H_2) in the feed gas for the CO40 condition (see **Table 3.1**), since no differences were observed for the other key parameters. As a matter of fact, despite the lower final biomass concentration (0.43 g VSS/L), the presence of CO up to 40% v/v did not prevent HOB from completing the aerobic bioconversion process, as shown by the H_2 and CO_2 consumption (84% and 58%, respectively), biomass yield (0.16 g VSS/g H_2-COD, comparable to the average value from literature of 0.18 g VSS/g H_2-COD), and protein content (55.2%), which were comparable to those of the control and other experimental conditions with a lower CO content (**Figure 3.3**).

Additionally, no consumption of CO was revealed by the GC analysis. Interestingly, Tanaka *et al.* reported a strong reduction (85-90%) of the final OD of pure cultures of different HOB species (*Ralstonia eutropha* and *Alcaligenes latus*) already at 10% v/v of CO, while also demonstrating the capability of a more CO-tolerant HOB species (*Ideonella sp.* O-1) of growing with CO concentrations as high as 30% v/v, even though with an OD reduction of 75% [259]. A 65% reduction in biomass productivity was recently reported also by Jiang *et al.* on a pure culture of *Cupriavidus necator H16* during the bioconversion of syngas containing a CO concentration as high as 30% v/v Jiang et al. (2022). It is important to highlight that the real CO concentration to which HOB were directly exposed in the liquid phase may differ from the one initially set in the headspace due to gas/liquid equilibrium and

mass transfer phenomena. However, the initial CO concentration is representative of the characteristics of the simulated MSS-derived syngas mixture.

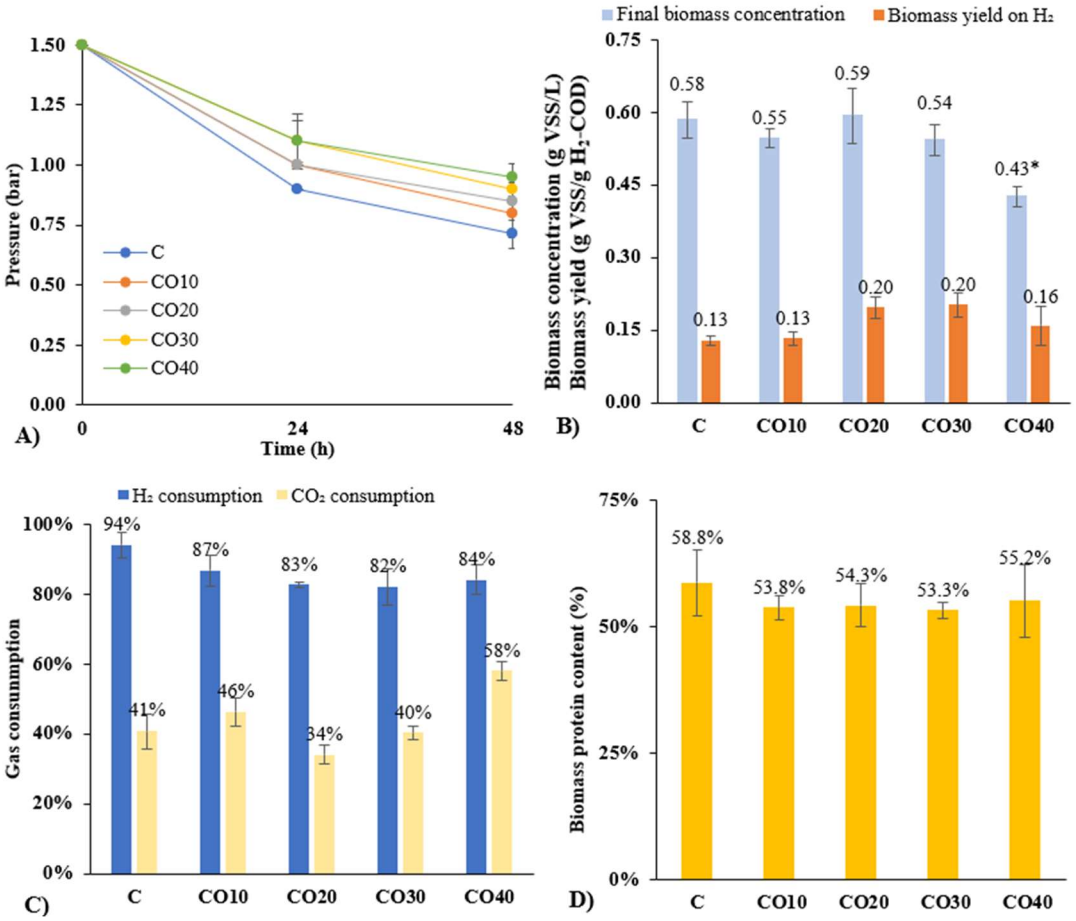


*Figure 3. 3. Results of the CO concentration short-term batch test. The influence of increasing CO concentrations on the growth of the HOB enrichment is expressed in terms of: A) Pressure variation over time; B) Final biomass concentration and yield on hydrogen; C) H_2 and CO_2 consumption, and D) Biomass protein content. Initial biomass concentration: 0.129 g VSS/L. *: Statistically different value (p-value <0.05). Error bars refer to the standard deviation calculated from the triplicates of each test.*

In terms of protein accumulation, the different levels of CO tested did not show any significant influence, since similar protein contents (53.3-58.8%) were observed across the different operating conditions (**Figure 3.3D**), consistently with what Jiang *et al.* reported for *C. necator H16* (crude protein content around 50%) [258]. As in the case of H_2S, the higher resistance to CO of the HOB enrichment might be attributed to

its mixed and more diverse nature. This aspect will be further discussed in section 3.3.4.

3.3.2 Long-term batch tests

3.3.2.1 Effect of simulated realistic syngas compositions

The high tolerance of the HOB enrichment to CO and H_2S, as observed within the short-term batch tests (section 3.3.1), was further investigated through a series of long-term batch tests over a 30 days-period (**Figure 3.4**). These tests aimed at investigating

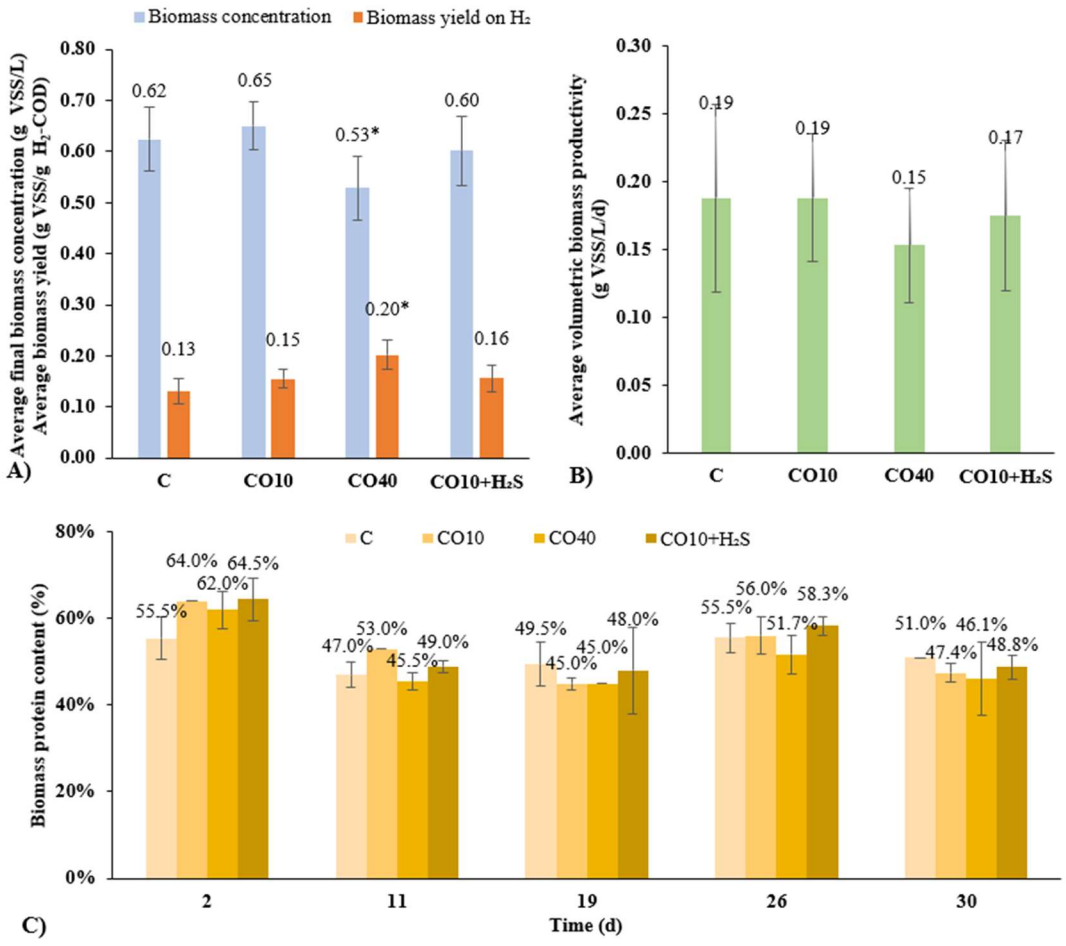


*Figure 3. 4. Results of the long-term batch test. The performance of the HOB enrichment during long-term batch test is expressed in terms of: A) Average final biomass concentration and average biomass yield on hydrogen; B) Average volumetric biomass productivity, and C) Biomass protein content. Initial biomass concentration: 0.115 g VSS/L. *: Statistically different value (p-value <0.05). Error bars refer to the standard deviation calculated from the triplicates of each test.*

the repeatability and the stability of the process performances observed in the short-term batch tests, as well as at testing for the first time the combined effect of H_2S and CO on the HOB enrichment in view of simulating realistic raw syngas.

The average biomass yield on hydrogen during the whole test was similar for C, CO10 and CO10+H_2S conditions (0.13, 0.15 and 0.16 g VSS/g H_2-COD, respectively), while a significatively higher yield (*p-value* < 0.05) was achieved in the CO40 condition (0.20 g VSS/g H_2-COD) (**Figure 3.4A**). These values were all included in the range assumed for the calculation of the balanced stoichiometric equation (Eq. 3.6) for HOB (0.07-0.28 g VSS/g H_2-COD).

Since no consumption of CO was detected, this latter result could be explained by the lower amount of H_2 available in the CO40 condition (see **Table 3.2**), pointing towards a potential improved H_2 gas utilization in the presence of H_2-limiting conditions. This lower amount of H_2 available was most likely responsible for the significantly lower average final biomass concentration observed in the CO40 condition (0.53 g VSS/L vs. 0.62, 0.63, and 0.65 g VSS/L reported for C, CO10, and CO10+H_2S, respectively) (**Figure 3.4A**), as already discussed for the short-term batch tests (section 3.3.1.3). Nevertheless, the average volumetric biomass productivity of 0.19, 0.19, and 0.18 g VSS/L/d achieved in the C, CO10, and CO10+H_2S conditions, respectively, during the 30 days of the test, were not statistically different from the value observed for CO40 (0.15 g VSS/L/d) (**Figure 3.4B**). Therefore, no significant influence of CO concentrations of 10 and 40% v/v (conditions CO10 and CO40, respectively), as well as the simultaneous presence of CO at 10% v/v and equivalent H_2S at 2000 ppmv (condition CO10+H_2S), can be individuated on the long term. Regarding the biomass protein content, the latter did not vary significantly during the whole duration of the long-term batch test (**Figure 3.4C**), with similar values in each condition (45.0-64.5%). Although the amino acidic composition of biomass was not characterized in the present study, recent studies showed how it would likely be not affected by variable CO concentrations in syngas (up to 30% v/v) [258]. This aspect may be further investigated in the future.

3.3.2.2 Potential for direct nitrogen upcycling from MSS-derived syngas

MSS is usually highly rich in nitrogen (2.4-9 % on a dry and ash-free weight basis), which is partially diverted to syngas to form mainly gaseous ammonia (NH_3) and hydrogen cyanide (HCN) [313]. Nitrogen being the main building block of MP, the potential of the envisioned process to recover resources from raw MSS-derived syngas was further evaluated in terms of the nitrogen required by the process and usually present in the MSS-derived syngas.

From the analysis of the concentration of NH_4^+-N performed during the long-term batch tests, the average NH_4^+-N consumption was calculated and related to that of H_2, indicating an average ratio of 0.014 mol NH_4^+-N/mol H_2. This average ratio is lower than the one calculated from the balanced stoichiometric equation for HOB (Eq. 3.6), equal to 0.028 mol NH_3-N/mol H_2. This suggests that, although with similar biomass yield on H_2, in the long-term batch test the average NH_4^+-N assimilation by the HOB mixed culture was lower than the stoichiometric one. Such lower NH_4^+-N/H_2 ratio could also explain the lower average protein content achieved in the long-term batch test (52.1%) with respect to the average values (around 66%) reported in literature for HOB [255].

By assuming a generic NH_3 content for MSS-derived syngas of 0.28% v/v [314] and a H_2 content variable between 10 and 40% v/v [97,217] in MSS-derived syngas, an indicative range of 0.007 to 0.027 mol NH_3-N_{syngas}/mol $H_{2\text{-}syngas}$ can be considered as generically available by syngas (calculations are reported in **Appendix C5**).

The amount of NH_3-N available for HOB during the aerobic bioconversion of raw syngas, similar to that simulated and tested in the present work could thus sustain all or at least half of the overall nitrogen requirement, potentially enabling the direct recovery and upcycling of waste nitrogen into MP. Indeed, as recently demonstrated by Matassa *et al.*, recovered gaseous ammonia can be effectively absorbed and directly converted into MP biomass, thereby avoiding the use of virgin raw chemicals (*e.g.* NH_4Cl) as source of nitrogen and leading to a more sustainable and circular nitrogen management [315].

3.3.3 Effect of CO on maximum biomass productivity, concentration and yield

The aim of this test was to evaluate the biomass volumetric productivity, concentration and yield of the HOB enrichment by increasing the rate of gas supply and by maintaining an equal H_2 content in the presence of variable CO levels, therefore avoiding potential differences linked to H_2 limitation. In this test, owing to the daily feeding of new gaseous substrate, a maximum volumetric biomass productivity of 0.37 g VSS/L/d, equal to 13 mg VSS/L/h, was achieved during the first 72 h in the CO10 condition (**Figure 3.5B**).

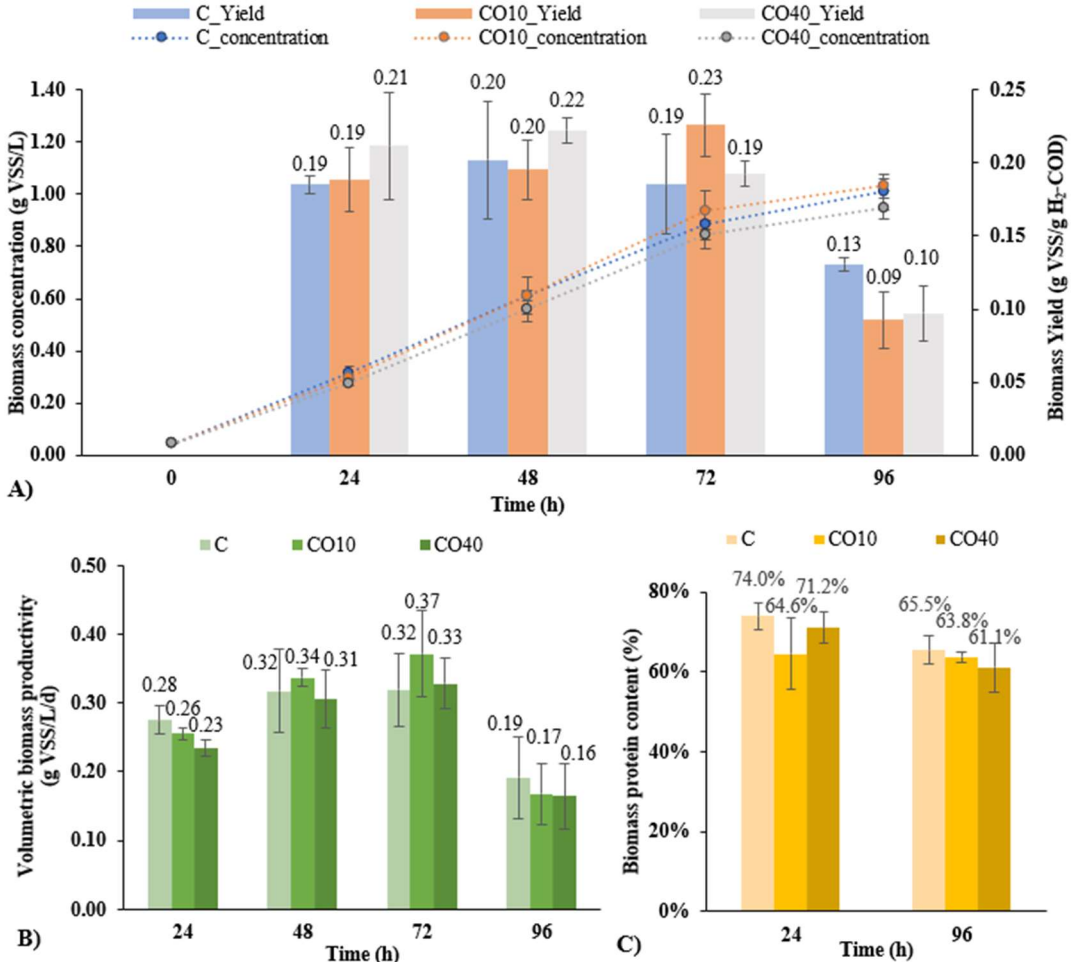


Figure 3. 5. Results on the effects of CO on maximum biomass productivity, concentration and yield. A) Biomass concentration and yield on hydrogen; B) Volumetric biomass productivity, and C) Biomass protein content. Initial biomass concentration: 0.042 g VSS/L. Error bars refer to the standard deviation calculated from the triplicates of each test.

This productivity was 34% higher than the maximum value registered during the long-term batch test (0.28 g VSS/L/d), and it was statistically similar to those obtained in both C and CO40 conditions. Dou *et al.* reported a similar biomass volumetric productivity (11 - 12 mg VSS/L/h) for the pure culture of *Paracoccus denitrificants* Y5 in similar batch conditions but without CO [257]. A similar value (11 mg VSS/L/h) was reached also by Jiang *et al.* with a pure culture of *C. necator H16* in batch conditions without CO [258], while a drop to 4 mg VSS/L/h was reported for the same culture in the presence of 30% v/v of CO.

In terms of biomass yield on hydrogen, the obtained results showed no statistically significant difference between the tests (**Figure 3.5A**), therefore confirming that the higher yield observed in the presence of 40% of CO during the long-term batch tests (section 3.3.2) was most likely due to the onset of H_2-limiting conditions. Biomass concentration constantly grew in the first 72 h (**Figure 3.5A**) and then kept increasing at a slower rate, up to the highest final concentration of 1.04 g VSS/L after 96 h, which is 1.6 times higher than the maximum average biomass concentration achieved in the long-term batch tests (0.65 g VSS/L).

The increased biomass concentration achieved after 72 h resulted in a reduction of the amount of gas substrate available per unit of biomass which, together with the low dilution rate set by daily exchanging only 7.5% of the liquid medium, induced a decrease of the volumetric biomass productivity and biomass yield between 72 and 96 h (**Figure 3.5A-B**). Concerning protein, a maximum content of 74.0% was achieved during the tests, with no statistically significant differences among the three conditions and between the start and the end of the test (**Figure 3.5C**). Such a high protein concentration is in accordance with the maximum values reported for HOB cultures (up to 75% crude protein content) [254], and higher than those reported by Jiang *et al.* (crude protein content of 50% and 54%, with and without CO, respectively) in similar batch tests [258].

3.3.4 Microbiological analysis

Microbial community analyses were performed to evaluate the composition and follow the potential evolution of the mixed HOB culture through the exposure to different syngas mixtures during the long-term batch tests. In **Figure 3.6**, the relative abundance (RA) of the different microbial species composing the HOB enrichment at the beginning and at the end of the long-term tests is reported. The initial and common HOB enrichment sample used to start the tests (T0) was mainly composed by Alphaproteobacteria of the genus *Paracoccus* (RA: 31.5%), which are known to potentially grow autotrophically at mesophilic temperatures and neutral or alkaline pH [316], thus under conditions similar to those tested in the present study.

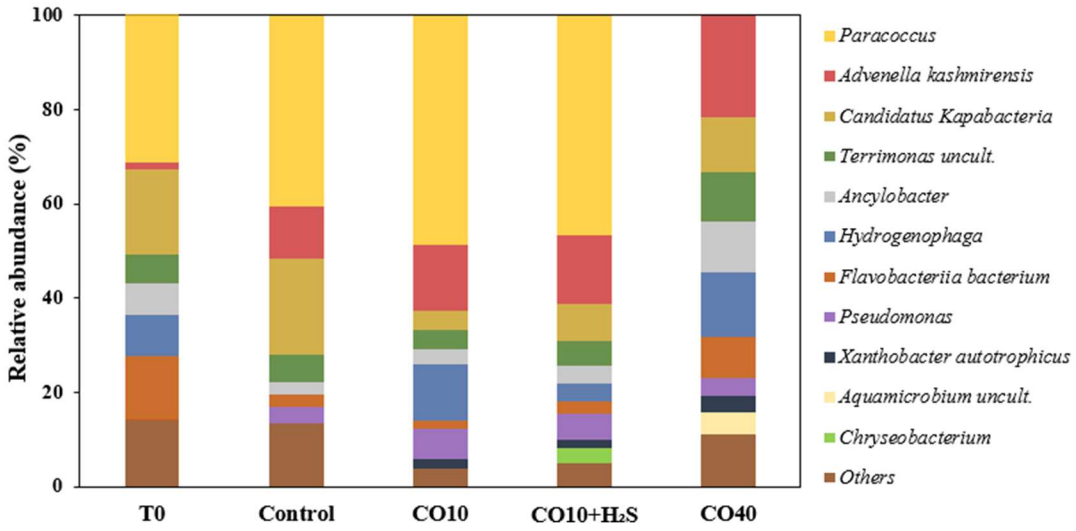


Figure 3. 6. Evolution of the mixed microbial HOB culture across the long-term batch tests. The relative abundances of the bacterial genera and species in the HOB enrichment at the start (T0) and at the end of the 30 days long-term batch test (Control, CO10, CO10+H_2S, and CO40) are reported.

The RA of the *Paracoccus* genus grew up to 40.6% in the Control condition at the end of the long-term batch test, showing its ability to grow autotrophically through H_2 oxidation. The presence of CO in the syngas at a concentration of 10% v/v in the condition CO10 did not inhibit the growth of the *Paracoccus* genus, which achieved a final RA of 48.6%. The latter value is perfectly in line with that achieved by the same genus in the condition CO10+H_2S (RA of 46.6%), thus with the same CO concentration (10% v/v) and with the addition of 2000 ppmv of equivalent H_2S. Likely, thanks to the ability to grow chemolithotrophically also through the oxidation of

reduced sulfur compounds [317], the bacteria belonging to the *Paracoccus* genus were not inhibited even under high H_2S equivalent concentrations. Further studies might focus on the role of potential SOB in the HOB mixed culture.

When the CO concentration increased, reaching up to 40% v/v in the CO40 condition, the *Paracoccus* genus disappeared from the microbial community (RA<1%), and was replaced by more CO-tolerant bacteria. *Advenella kashmirensis*, whose RA (1.3%) was negligible at the start of the long-term batch tests (T0), became the most abundant microorganism (21.5%) in condition CO40, doubling that achieved in the control condition (10.9%). Similarly, to the *Paracoccus* genus, *A. kashmirensis* showed a high resistance to H_2S since its RA in CO10 and CO10+H_2S conditions was comparable (14.0% and 14.7%, respectively). As reported by Wang *et al.*, this resistance could be attributed to the presence of an inorganic sulfur oxidation gene cluster in the *A. kashmirensis'* genome [318].

Concerning the genus *Ancylobacter,* whose RA was initially 6.7% and then decreased to 2.5, 3.3 and 3.7% in conditions C, CO10 and CO10+H_2S, respectively, a RA as high as 10.7% was achieved in condition CO40. Bacteria of the genus *Ancylobacter* are capable of growing on gaseous substrates composed by H_2, O_2 and CO_2 and were indicated as dichloromethane (DCM) degrader organisms by several authors in literature [319,320]. One of the metabolic pathways which can lead to DCM degradation involves the activation of the gene P450/MO and leads to the spontaneous formation of HCl and CO [321]. The latter could explain *Ancylobacter*'s resistance to high CO concentrations.

Concerning the other bacteria that were able to cope with CO, the starting RA of the genus *Terrimonas*, which was equal to 6.0%, was basically unaffected, as shown by the final values of 6.0, 4.1, 5.1, and 10.6% achieved in the C, CO10, CO10+H_2S, and CO40 conditions, respectively. *Flavobacteriia bacterium,* which started from an initial RA of 13.5%, decreased to a final RA of 2.5% in the Control. Similar RA values of 1.6 and 2.7% were observed in the CO10 and CO10+H_2S conditions, respectively, while a slightly higher RA of 8.7% was achieved in the CO40 condition. Finally, *Candidatus kapabacteria,* initially present at a RA of 18.2%, was stable in the Control

(20.4%), but was less abundant in the test conditions at the end of the long-term test, achieving a RA of 4.1, 7.9 and 11.8 in the CO10, CO10+H_2S, and CO40 conditions, respectively.

Uncultured bacteria of the genus *Hydrogenophaga,* initially present in the enrichment with a RA of 8.8%, reached a RA of 13.7% in the condition CO40, while RA values of 0.2 and 11.8% were achieved in the Control and CO10 conditions, respectively. The growth of this HOB seemed not to have been affected by increasing the CO concentrations, consistent with what was reported by Takors *et al*., who indicated *Hydrogenophaga pseudoflava* as a promising microorganism for biotechnological applications in aerobic gas bioconversion due to its remarkable tolerance to CO [302]. On the other hand, *Hydrogenophaga* was significantly inhibited by the presence of H_2S (3.9% in CO10+H_2S vs. 11.3% in CO10). Interestingly, *Xanthobacter autotrophicus* was present with higher RAs only when CO was contained in the syngas mixture (2.0, 1.7 and 3.5% in CO10, CO10+H_2S, and CO40, respectively), regardless of the presence of H_2S. *Pseudomonas* also seemed to be favoured by the presence of CO (6.6% in CO10 vs. 0.2 and 3.5% in the initial enrichment (T0) and the Control, respectively) and its growth was not affected by the presence of H_2S (5.6% in CO10+H_2S). Nevertheless, CO concentrations as high as 40% v/v reduced the final RA of *Pseudomonas* to 3.9%. Bacteria of the genus *Aquamicrobium* were significatively present only in CO40 (RA of 4.6%), which could be explained by the already reported high tolerance to CO [322].

3.4 Conclusions

In the present study, the aerobic bioconversion of MSS-derived syngas by a mixed HOB culture towards MP production was investigated. The effects of the variability in the syngas composition and the presence of potential inhibitory compounds (H_2S and CO) were evaluated. The main findings and implications of the study are here reported:

- The process was not negatively affected by changes in the composition of syngas in terms of H_2/CO_2 ratio. Therefore, syngas mixtures produced by

pyrolysis of different MSS feedstocks and/or through different pyrolysis conditions, and potentially resulting in widely variable H_2/CO_2 ratios, could be directly valorised into MP;

- The remarkably high H_2S and CO tolerance shown by the HOB mixed culture could enable the direct use of raw and untreated syngas, thereby avoiding the need of expensive syngas processing such as deacidification for H_2S removal and water-gas shift reactions for the conversion of CO into additional H_2;

- The adaptability to different syngas compositions and the resistance to high concentrations of inhibitory compounds, displayed by the HOB enrichment also on the long-term, suggests the possibility of upscaling this process towards continuous or semi-continuous direct aerobic bioconversion of raw syngas;

- The long-term aerobic fermentation of a realistic syngas mixture containing both CO and H_2S in concentrations of 10% v/v and equivalent to 2000 ppmv, respectively, was shown to be successful. Further tests might focus on investigating more deeply the long-term effect of higher H_2S concentrations and their combination with variable CO.

- Preliminary evaluations suggested the feasibility of a direct upcycling of the gaseous nitrogen recovered through MSS-derived syngas to guarantee the required supply of the main macronutrient needed for MP synthesis. This possibility could be further explored in future studies;

- A balanced stoichiometric equation for HOB growth was calculated from the average biomass yield on H_2 reported for HOB (0.18 g VSS/g H_2-COD), and similar to the average values achieved throughout the whole study. The balanced equation was used to compare stoichiometric H_2/CO_2 ratios and ammonium nitrogen requirements, with the values measured in this study.

Lower H_2/CO_2 supply ratios (2.0 and 4.3) guaranteed sufficient amounts of CO_2, as the measured uptake ratios were lower than the stoichiometric one, while in the presence of a supplied H_2/CO_2 ratio of 10.0, the lower amount of available CO_2 might have triggered carbon-limiting conditions. Finally, the average NH_4^+-N/H_2 uptake ratio calculated during the long-term batch test was lower than the stoichiometric one, probably resulting in a lower protein content in the biomass.

- The diverse set of metabolic options present in the enriched HOB mixed culture showed the potential to overcome the limitations of pure/axenic cultures to directly valorise recovered secondary feedstocks, *i.e.* MSS-derived syngas.

- The future application potential of the envisioned process in the feed and food domain will depend upon the possibility to completely avoid any potential contamination from the waste MSS matrix through syngas, and to further screen, identify and assemble specific microorganisms within co-cultures that are safe to use for animal and human nutrition.

CHAPTER 4. BIOMETHANATION OF PYROLYSIS GAS IN A PILOT-SCALE BIOREACTOR

4.1 Introduction

Among the numerous technologies developed for the management and treatment of municipal sewage sludge (MSS), thermochemical processes are gaining momentum. Pyrolysis, in particular, is characterized by high versatility, with the chance of converting MSS into valuable products while destroying pathogens and organic contaminants, and minimizing the enormous MSS amounts produced worldwide every year [9,323]. Pyrolysis of MSS results in the production of biochar (solid), bio-oil (liquid), and pyrolysis gas. In the context of pyrolysis products valorization, MSS-derived pyrolysis gas exploitation plays a significant role in advancing sludge management practices, promoting renewable energy and resource recovery, supporting a circular economy approach. In recent years, the research on the valorization of pyrolysis gas has received much attention as it has been considered as a key priority for the development of the pyrolysis technology.

MSS-derived pyrolysis gas represents the incondensable fraction of the vapours produced during MSS pyrolysis. It primarily contains hydrogen (H_2), carbon monoxide (CO), carbon dioxide (CO_2), methane (CH_4), and light hydrocarbons (C_2-, C_3-) (*e.g.* ethylene and propylene), and minor contaminants such as tar, S- and N-containing compounds, and other impurities (*e.g.* particulates). The influence that MSS characteristics and pyrolysis parameters can have on the composition of MSS-derived pyrolysis gas has been previously reported in **Chapter 1** of this doctoral thesis.

Different valorization pathways have been developed for the gas obtained from pyrolysis and gasification of MSS and other biomasses, such as *i*) energy production through electricity generation in gas turbines or internal combustion engines, co-heat and power (CHP) systems, and CO conversion to H_2 (*i.e.* water-gas shift (WGS) reaction) [324,325]; *ii*) chemical synthesis for methanol production, ammonia synthesis for fertilizer production, liquid hydrocarbons and biofuels production (Fischer-Tropsch process) [19]; *iii*) renewable natural gas (RNG) production through thermochemical methanation processes (*i.e.* Sabatier reaction) [326]; biotechnology applications that involve microbial conversion of the gas mixture into biofuels,

bioplastics, protein and other bioproducts through gas fermentation processes [18,327].

Among these valorization pathways, the possibility to consider the pyrolysis gas as an energy vector that can be upgraded, stored, and distributed (exported/imported) globally using the already existing infrastructures is challenging [328]. Biomethane exhibits comparable applications to synthetic natural gas (SNG) in power and heat generation, transportation, and chemical sector. Moreover, while natural gas consumption is projected to remain stable for at least a few decades, biomethane is expected to meet the growing gas demand due to its renewable nature and low CO_2 footprint [329].

Yu *et al*. investigated the purification of syngas from biomass and the capture of carbon dioxide, highlighting that the utilisation of pyrolysis gas will be significantly more efficient and valuable if carbon dioxide can be captured and synthesized [330]. More recently, a biological upgrading process through biomethanation has been proposed. The scientific literature about gas biomethanation was initially focused on the *in-situ* and *ex-situ* upgrading of biogas from anaerobic digestion plants, with high percentages of exogenous H_2 added in order to set the needed stoichiometric H_2/CO_2 ratio of 4/1 for hydrogenotrophic methanogenesis [331]. Ghofrani-Isfahani et al. (2021) reported up to 99 % v/v CH_4 in the outlet RNG when testing the *ex-situ* upgrading of biogas with the addition of 62 % exogenous H_2 [332]. Biomethanation can be successfully applied to other off-gases such as syngas/pyrolysis gas. An exogenous H_2 addition from 0 to 60 % was applied by Asimakopoulos et al. (2021) for the biomethanation of a synthetic $H_2/CO/CO_2$ mixture simulating biomass-derived syngas, obtaining an outlet RNG with a content of CH_4 up to 70% v/v [333]. In the case of MSS-derived pyrolysis gas, which is generally characterized by a lower H_2 content with respect to syngas, higher percentages of exogenous H_2 addition might be necessary to meet the stoichiometry of the biological process

According to the literature, the biomethanation of syngas-like mixtures (including pyrolysis gas) can offer several advantages when compared to the thermochemical methanation process conducted through the Sabatier reaction (Eq. 4.1) for the conversion of H_2 and CO_2 into biomethane [232,326].

$$4\,H_2 + CO_2 \rightarrow CH_4 + 2\,H_2O \quad (4.1)$$

The thermochemical process has some disadvantages linked to the process, such as strict limits for H_2/CO ratios and impurities that may induce toxicity to the employed catalysts and to the high costs related to the prohibitive temperatures and pressures needed [20,233]. Such limitations can be overcome through the biomethanation pathway conducted by different microbial species capable of converting H_2/CO/CO_2 gas mixtures via H_2/CO_2-, CO-, and acetate-based metabolic mechanisms pathways [234,235]. **Table 4.1** reports the main metabolic pathways taking place during syngas-like mixtures biomethanation, where CO_2 and CO react with H_2 and H_2O, respectively, to form CH_4.

Such pathways are differently influenced by operative conditions of the process,

Metabolic pathway	Stoichiometric reaction	Influence of temperature	References
Carboxydotrophic hydrogenogenesis (Biological water-gas shift reaction)	$CO + H_2O \rightarrow CO_2 + H_2$	Mostly thermophilic microorganisms	Alfano and Cavazza (2018); Andreides et al. (2022)
Carboxydotrophic acetogenesis	$4\,CO + 2\,H_2O \rightarrow CH_3COOH + 2\,CO_2$	Mostly mesophilic microorganisms	Figueras et al. (2023)
Carboxydotrophic methanogenesis	$4\,CO + 2\,H_2O \rightarrow CH_4 + 3\,CO_2$	Higher growing rate of microorganisms in thermophilic conditions	Andreides et al. (2022)
Homoacetogenesis/Syntrophic acetate oxidation	$4\,H_2 + 2\,CO_2 \leftrightarrow CH_3COOH + 2\,H_2O$	Favoured by mesophilic conditions	Figueras et al. (2023)
Hydrogenotrophic methanogenesis	$4\,H_2 + CO_2 \rightarrow CH_4 + 2\,H_2O$	Favoured by thermophilic conditions	Figueras et al. (2023)
Acetoclastic methanogenesis	$CH_3COOH \rightarrow CH_4 + CO_2$	Favoured by mesophilic conditions	Grimalt-Alemany et al. (2020)

Table 4. 1. Metabolic pathways involved in syngas-like mixtures biomethanation, stoichiometric reactions, and favourable temperature conditions.

especially temperature (*i.e.* mesophilic or thermophilic conditions), with

hydrogenotrophic (H_2 + CO_2 → CH_4) and carboxidotrophic (CO + H_2O→ CH_4) methanogenesis being favoured in thermophilic conditions. On the other hand, carboxydotrophic acetogenesis (CO + H_2O → CH_3COOH) and Homoacetogenesis (H_2 + CO_2 → CH_3COOH), together with acetoclastic methanogenesis (CH_3COOH → CH_4) are generally favoured in mesophilic conditions [235,238].

Issues related to CO inhibition on several methanogenic species have been highlighted [334]. CO can result in the inhibition of acetoclastic methanogens, with consequent accumulation of volatile fatty acids (VFAs). This phenomenon is generally more critical under mesophilic conditions, in which the homoacetogenic/syntrophic metabolism is usually favoured [235]. After a first inhibition effect in the adaptation phase, the continuous biomethanation of syngas with CO concentration as high as 40 % v/v conducted by Li *et al*. [236] led to a final CH_4 concentration of 43.2 – 49.7 % v/v, with the main limitation being recognized in the gas-liquid mass transfer rate.

Indeed, the involvement of syngas-like mixtures in the fermentation process is generally affected by the low solubility of CO and H_2 within the liquid medium during biomethanation. The necessity for high mixing speed in continuous-flow stirred-tank reactors (CSTRs) or up-flow bioreactors, resulting in high energy costs and low scalability, has led many authors to focus on other reactor configuration types (*e.g.* trickle-bed reactors (TBRs)) [335]. Nevertheless, besides the advantages in terms of gas-liquid mass transfer and the avoidance of energy-consuming mixing, TBRs are affected by clogging issues and biomass washout happening at higher gas loading rates [335]. Other authors have been focussing on different ways to enhance gas solubilization in bioreactors, apart from increasing mixing speed. Increasing the pressure of the gaseous substrate represents a low-effort approach to enhance H_2 and CO solubilization [242].

More sophisticated strategies for enhancing gas-liquid mass transfer in bioreactors include the employment of hydrodynamic cavitation systems [245–247]. The formation and collapse of cavitation bubbles within the gas-liquid mixture enhance the solubilization of gas components such as H_2 and/or CO, resulting in high gas-liquid mass transfer.

Although biometanation represents an interesting and innovative technology for pyrolysis gas upgrading to biomethane, there are only few studies in the literature dealing with this subject. In the present study, a pilot-scale biomethanation of a synthetic $H_2/CO/CO_2$ mixture simulating a realistic MSS-derived pyrolysis gas with the addition of exogenous H_2, conceptually produced from renewable energies, was investigated. Further, a Venturi-type ejector was employed for the maximization of gas-liquid mass transfer, testing variable inlet gas flow rates and liquid recirculation flow rates. The effect of increasing H_2/CO_2 ratios in the gas substrate was evaluated as well. The performance of the process was monitored in terms of outlet gas composition, H_2 and CO solubilization efficiency, CH_4 production rate, and CH_4 yield on H_2, while the stability of the process was assessed in terms of the evolution of VFAs concentration, pH and alkalinity.

4.2 Materials and methods

4.2.1 Set up, inlet gas, and inoculum

The experimental set-up is schematized in **Figure 4.1**, and the main operative parameters set are reported in **Table 4.2**. The biomethanation process was performed in a pilot-scale pressurized tubular stainless-steel reactor (total volume of 64 L), characterized by a height/diameter (internal) ratio equal to 8. The bioreactor was previously employed and described by Giuliano *et al*. [247]. A screw pump was used to provide the desired recirculation flow rate (Q_R) of the liquid slurry. A pressure of 2 bar was set within the bioreactor with a back-pressure valve.

A synthetic gas mixture of H_2 / CO / CO_2 = 77 ± 1 / 4 ± 1 / 19 ± 1 was used. This composition was meant to simulate the addition of exogenous H_2 in a percentage as high as 75 % to a real MSS-derived pyrolysis gas obtained in a previous work conducted by the authors (**Chapter 2** of this doctoral thesis), where pyrolysis was conducted at the temperature of 500 °C, with a solid retention time of 15 min, in a bench-scale batch pyrolyser. The addition of H_2 to the pyrolysis gas was necessary to increase the H_2/CO_2 ratio of pyrolysis gas up to 4.0 in order to meet the stoichiometry of the biomethanation process.

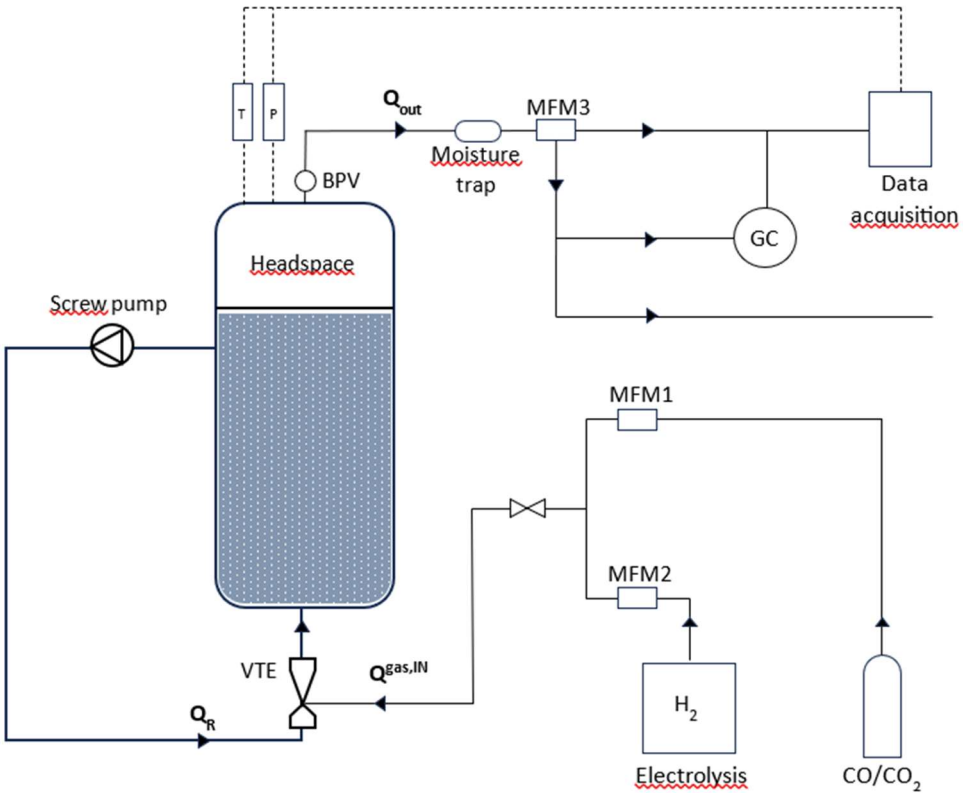


Figure 4. 1. Pilot-scale biomethanation set-up. The experimental set-up employed for the pilot-scale biomethanation of pyrolysis gas with H_2 addition is schematized. MFM: mass flow meter; VTE: Venturi-type ejector; BPV: back-pressure valve; GC: gas cromatograph; Q_{IN}: inlet gas flow rate; Q_R: liquid recirculation flow rate; Qout: outlet gas flow rate; T: temperature probe; P: pressure probe.

The synthetic gas mixture used in this study did not contain any other components or impurities typical of pyrolysis gas (*i.e.* S compounds, hydrocarbons), thus considering that the pyrolysis gas was pre-treated. H_2 was provided by an electrolyser (Cinel, Italy), while CO and CO_2 were provided by a certified gaseous $CO/CO_2 = 20/80$ v/v mixture (Sapio, Italy). Electronic flow-meters, remotely controlled by an HMI/SCADA interface, were employed to regulate the gas flow of each component of the inlet gas-flow.

In order to maximize the gas-liquid mass transfer, a 4-mm-diameter Venturi-type ejector (VTE) was employed as a gas diffusion system. The gas–liquid mixture composed by the inlet gas flow ($Q^{gas,IN}$) (1.2 – 6.1 liters per liters of reactor per day ($L/L_R/d$)) and the recirculation liquid flow (Q_R) (8 – 25 L/min) was introduced at the bottom of the reactor through the VTE.

Reactor set-up	
Reactor configuration	Tubular/up-flow
Total volume (L)	64
Working volume (L)	50
Temperature (°C)	55
Pressure (bar)	2
Q_R (L/min)	7 - 25
Gas supply	
Substrate	$H_2/CO/CO_2$
H_2/CO_2 ratio	4.0 – 4.7
Duration of gas supply (h/d)	6
$Q^{gas,IN}$ ($L/L_R/d$)	1.2 – 6.1
GRT (h)	5.1 – 25.4
Gas solubilization system	
Technology	Venturi-type ejector
Diameter (mm)	4
Inoculum	
TS (% wt)	6.7
VS (%, g VS/g TS)	54.7
pH	8.3
Total Alkalinity (mg $CaCO_3$eq/L)	2750
Partial Alkalinity (mg $CaCO_3$eq/L)	1320
VFAs (mg HAc eq/L)	220
Ammonium (mg NH_4^+/L)	663

Table 4. 2. Experimental set-up and properties of the inoculum. The characteristics of the reactor set-up, the feed-gas mixture, and the gas supply system are reported, together with the chemical characterization of the inoculum. Q_R: recirculation flow rate; Q_{IN}: inlet gas flow rate; GRT: gas retention time; TS: total solids; VS: volatile solids; VFAs: volatile fatty acids

No internal gas recirculation system was used. The continuous liquid recirculation and gas supply operations lasted 6 hours per day, 5 days per week. The bioreactor was operated at a controlled temperature of 55 °C (thermophilic conditions). This choice was made to favour hydrogenotrophic methanogenesis, biological WGS reaction, and carboxydotrophic methanogenesis, for the direct conversion of $H_2/CO/CO_2$ into CH_4 by avoiding the production and accumulation of VFAs, and acetoclastic methanogenesis.

The employed inoculum was represented by a thermophilic anaerobic digestate from a full-scale biogas plant treating mainly sewage sludge from municipal and industrial WWTPs, the same employed by Giuliano *et al*. [247]. Before the start of the process, the inoculum was maintained in a controlled temperature reactor at the operative temperature (55 °C) and atmospheric pressure for more than three months, to achieve the complete degradation of the organic matter still present [336]. The chemical characteristics of the inoculum are reported in **Table 4.2**. Prior to starting the experimental operations, the bioreactor was flushed with N_2 gas in order to remove residual gases from the headspace. A volume of 50 L of inoculum was used to fill the bioreactor. For analysis 1 L of reactor slurry was sampled every week. In order to maintain the working volume of 50 L, and to periodically provide trace elements and nutrients, avoiding the supply of a synthetic mineral medium, 1 L of fresh inoculum was added every week after sampling.

4.2.2 Experimental phases

The effects of different $Q^{gas,IN}$, Q_R, and H_2/CO_2 ratios on the performance of the pyrolysis gas biomethanation process were investigated. The different experimental phases of the study are summarized in **Table 4.3.** During the first 8 weeks, the start-up phase was performed, setting an H_2/CO_2 ratio of 4.0, a low Q_R of 8 L/min, and a $Q^{gas,IN}$ of 1.2 $L/L_R/d$. In the following Period A1, the total solids (TS) content of the reactor slurry was reduced from 6 to 4 % wt through tap water dilution to make the slurry more fluid and avoid foam-related issues. This TS content was then maintained constant during the whole experimental activity. The Q_R set by the screw pump was increased to 25 L/min in order to induce a better recirculation within the bioreactor, while the $Q^{gas,IN}$ was maintained the same (1.2 $L/L_R/d$) of the start-up phase. In Period A2, the $Q^{gas,IN}$ was progressively increased from 1.8 to 6.1 $L/L_R/d$, resulting in a reduction of the gas retention time (GRT) from 25 to 5 h. Finally, in Period B, $Q^{gas,IN}$ and Q_R were maintained constant, equal to 6.1 $L/L_R/d$ and 25 L/min, respectively,

while an increase of the H_2/CO_2 ratio (from 4.0 to 4.7) in the inlet gas flow was tested, simulating a higher exogenous H_2-supply.

Period	Week	$H_2/CO/CO_2$	H_2/CO_2	$Q^{gas,IN}$ ($L/L_R/d$)	GRT (h)	Q_R (L/min)	TS (% wt)
0	1 - 8	77 ± 1 / 4 ± 1 / 19 ± 1	4.0	1.2	25	7	6 ± 1
A1	1 – 3	77 ± 1 / 4 ± 1 / 19 ± 1	4.0	1.2	25	25	4
A2	1 – 4	77 ± 1 / 4 ± 1 / 19 ± 1	4.0	1.8 – 6.1	25 - 5	25	4
B	1 - 3	79 ± 1 / 4 ± 1 / 17 ± 1	4.7	6.1	5	25	4

Table 4. 3. Experimental periods and tested variables. The different experimental conditions tested in the dedicated experimental periods of the study are reported. Q_R: recirculation flow rate; $Q^{gas,IN}$: inlet gas flow rate; GRT: gas retention time; TS: total solids;

4.2.3 Analytical methods

The headspace pressure was monitored with an STG700 gauge pressure transmitter (Honeywell, USA), while the temperature in the reactor was measured and controlled through a PT100 probe. Inlet gas flow rate was measured and controlled through two separate mass flow meters (MFMs) (Bronkhorst®, Netherlands), one per gas line (*i.e.* H_2 and the CO/CO_2 mixture). Another MFM of the same kind was employed to continuously measure the outlet gas flow rate. The outlet gas composition was characterized by using Pollution Micro GCX gas chromatograph (Pollution, Italy) equipped with a thermal conductivity detector (TCD) employing Argon as a gas carrier, for the continuous analysis of H_2, CO, CO_2, CH_4, N_2, and O_2 concentration, with a sampling frequency of 7 min. Moisture in the outlet gas was removed through a dedicated trap.

Variations in the characteristics of the bioreactor liquid slurry were assessed twice per week in terms of pH, total solids (TS), volatile solids (VS), total (TA) and partial alkalinity (PA), according to the Standard Methods for examination of water and wastewater [309]. Volatile fatty acids (VFAs) content was analysed using a gas chromatograph (7820A, Agilent Technology, USA) equipped with a flame ionization detector (FID). The analysed samples were centrifuged and filtered with a 0.45 µm

membrane and, 2,2-Dimethylbutyric acid was employed as the internal standard [247]. Total VFAs concentration was expressed in terms of mg of acetic acid-equivalent (HAc,eq) per liter. All samples were analysed in triplicates. All data are reported as weekly mean ± standard deviation (SD).

4.2.4 Calculations

The outlet gas net composition was calculated by excluding the exogenous N_2 used for reactor inertization, and O_2 traces that might enter the reactor during sampling/maintenance operations. The net concentration of the generic component of the outlet gas (X_i^{net}) was calculated as follows (Eq. 4.2):

$$X_i^{net}(\%\ v/v) = \frac{X_i}{\sum_i X_i - (X_{N_2} + X_{O_2})} \quad (4.2)$$

where X_i represents the volumetric fraction of the generic component of the outlet gas, as measured through the continuous gas chromatographic (GC) analysis, and $X_{N_2} + X_{O_2}$ is the volumetric fraction of the exogenous N_2 + O_2 fraction, as measured through the GC analysis.

The flow rate of the generic component of the outlet gas (Q_i^{Out}) was calculated as reported in Eq. 4.3.

$$Q_i^{gas,OUT}(L/L_r/d) = \frac{X_i * Q^{gas,OUT}}{V_r} \quad (4.3)$$

Where $Q^{gas,OUT}$ is the outlet flow rate as measured by the mass flow meter (expressed in L/d), and V_r is the working volume of the bioreactor (50 L). In this study, $Q_{CH4}^{gas,OUT}$ is referred to as methane production rate (MPR).

In this study, considering the biological conversions in the bioreactor, the H_2 and CO solubilization efficiencies (η_{H_2} and η_{CO}, respectively) were calculated as reported in Eq. 4.4, where $Q_i^{gas,IN}$ represents the inlet flow rate of the gas.

$$\eta_i(\%) = \frac{Q_i^{gas,IN} - Q_i^{gas,OUT}}{Q_i^{gas,IN}} \quad (4.4)$$

CO_2 solubilization efficiency was not calculated, since it is also an intermediate product of the bioconversion of CO.

Biomethane yield on H_2 (Y_{CH_4/H_2}) was calculated as the ratio between the MPR and the used H_2 flow rate ($Q_{H_2}^{used}$), as described by Eq. 4.5.

$$Y_{\frac{CH_4}{H_2}}\left(\frac{L_{CH}}{L_{H2}}\right) = \frac{MPR}{Q_{H_2}^{used}} \quad (4.5)$$

According to Grimalt-Alemany et al. [235], in thermophilic conditions, CO conversion mainly occurs through biological WGS reaction (*i.e.* carboxydotrophic hydrogenogenesis), towards H_2 and CO_2 formation, in a 1:1 CO:H_2 molar ratio. Direct biological CO conversion to CH_4 (*i.e.* carboxydotrophic methanogenesis) could take place as well in thermophilic conditions (**Table 4.1**).

On the other hand, CO biological conversion to VFAs was reported to generally occur in mesophilic conditions. Thus, in order to allow the calculation of the biomethane yield, in this study the absence of a CO-based acetogenic pathway was assumed, consistently with previous studies reported in the literature about syngas biomethanation in thermophilic conditions [236,334].

Therefore, $Q_{H_2}^{used}$ was calculated as composed by the solubilized fraction of both H_2 and CO input flow rates (Eq. 4.6), by assuming that the whole solubilized CO fraction is converted into H_2 (WGS reaction).

$$Q_{H_2}^{used} = \eta_{H_2} * Q_{H_2}^{gas,IN} + \eta_{CO} * Q_{CO}^{gas,IN} \quad (4.6)$$

Finally, the GRT within the bioreactor was calculated as expressed in Eq. 4.7, where $V_{r,tot}$ is the total volume of the bioreactor (64 L) and $Q^{gas,IN}$ is the inlet gas flow rate ($L/L_r/d$).

$$GRT\ (h) = \frac{V_{r,tot}}{Q^{gas,IN}} \quad (4.7)$$

4.2.5 Statistical analysis

Statistically significant (p-value < 0.05) differences among the experimental results were assessed through ANOVA tests with a 95 % confidence level and Tukey's method for multiple comparisons. Each statistical analysis in this study was performed by employing Minitab Statistical Software v18.1 (Minitab Inc., State College, PA, USA).

4.3 Results and discussion

4.3.1 Start-up phase

A lack of gas solubilization efficiency was observed during the initial start-up phase. The low Q_R (8 L/min) and $Q^{gas,IN}$ (1.2 $L/L_R/d$) were not high enough to guarantee the correct pressure and functioning of the Venturi-type ejector, resulting in a remarkable variability of the concentration of the outlet gas components. The CH_4 content in the outlet gas, as well as the H_2 and CO solubilization efficiency, were substantially variable during the start-up phase, finding a pseudo-stability only at weeks 4 – 8 and assuming average values during the entire phase as high as 43 ± 15 % v/v for the CH_4 final content (**Figure 4.2A**), and 71 ± 17 % v/v and 65 ± 8 % v/v for H_2 and CO solubilization efficiency (**Figure 4.2B**), respectively.

The high variability observed for the average weekly values of these parameters can be due to the occurrence of gas accumulation during the gas supply periods (*i.e.* in the weekdays), and gas consumption during the inactivity of the bioreactor (*i.e.* at night and in the weekends). This was probably due to an overall sub-optimal functioning of the gas solubilization system in the set conditions in terms of pressure provided by $Q^{gas,IN}$ and Q_R, which did not allow hydrodynamic cavitation to occur. The inefficient activity of the bioreactor can also be noticed by observing the $Q^{gas,OUT}$, which was always similar to the $Q^{gas,IN}$. Limited gas conversion was therefore occurring. Interestingly, the CH_4 yield on H_2 ($Y_{CH4/H2}$) was beyond the maximum stoichiometric value (0.25 L_{CH4}/L_{H2}) during the whole start-up phase (**Figure 4.2C**).

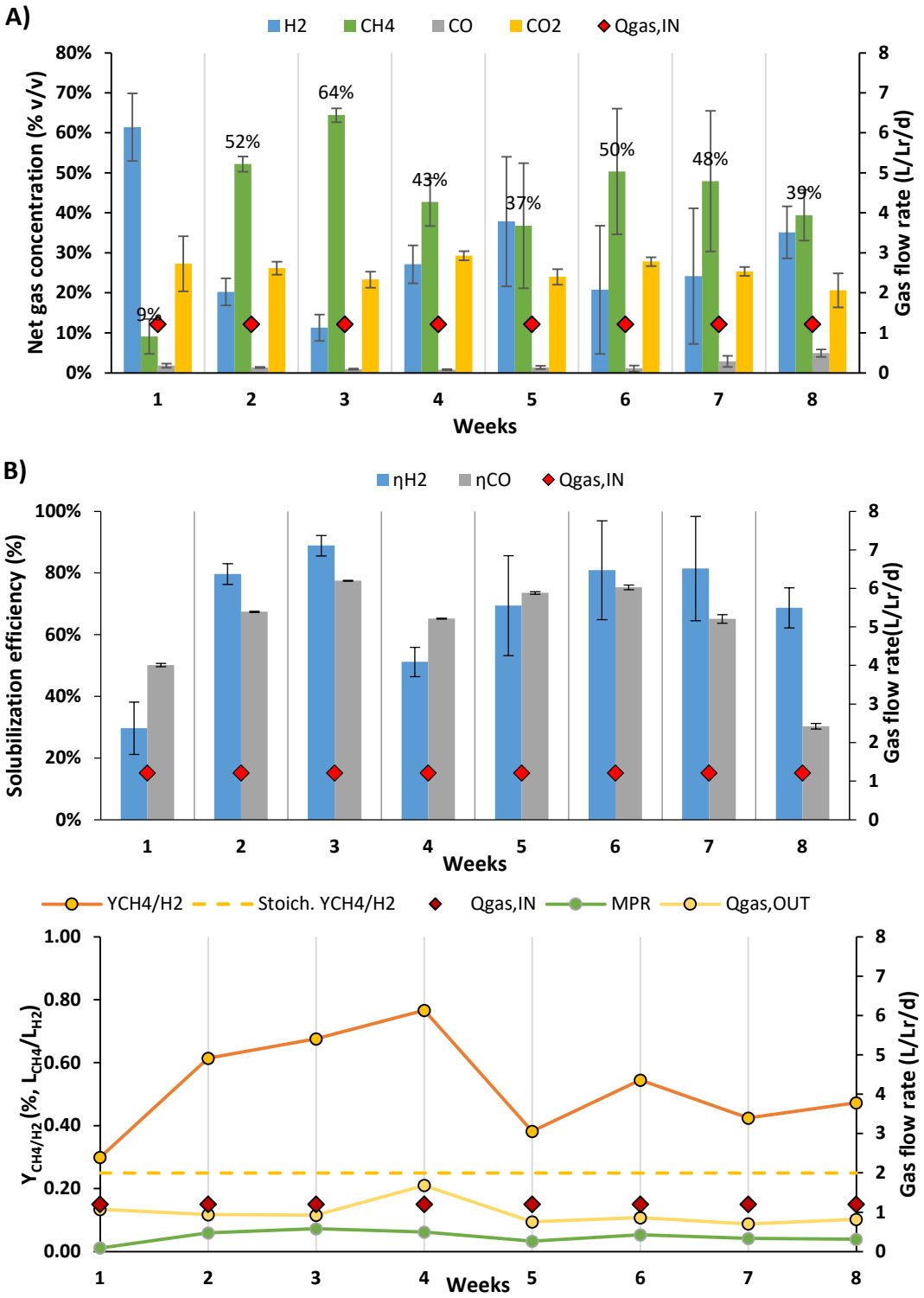


Figure 4. 2. Bioreactor performance in the start-up phase. The performance of the biomethanation process is evaluated for variable inlet gas flow rates (Qgas,in) in terms of A) outlet gas composition, B) H_2 and CO solubilization efficiency, and C) CH_4 yield on H_2, outlet gas flow rate, and methane production rate (MPR).

This can be translated in a CH_4 production coming from the conversion of other substrates apart from the inlet gas, although the MPR during this phase was limited (0.1 – 0.6 L/Lr/d). Due to the limited quantities of gas substrates available in the start-up phase, degradable substrates (*e.g.* VFAs) introduced through the periodical addition of fresh inoculum could have been preferred by the microbial biomass and converted in biogas. Additionally, the onset of microbial cannibalism induced by the scarcity of available substrates cannot be excluded. A microbial characterization of biomass within the bioreactor may help to individuate possible justifications.

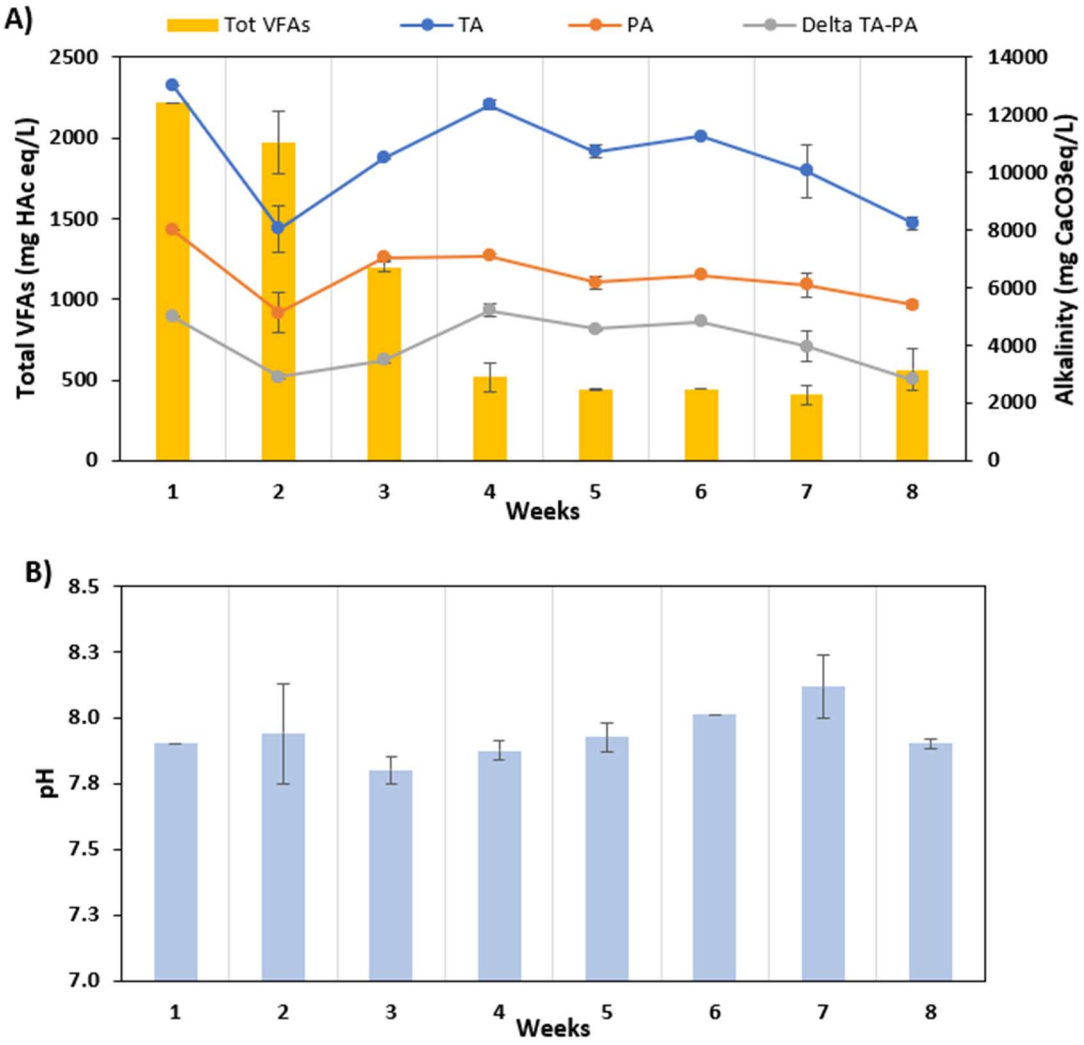


Figure 4. 3. Stability parameters in the start-up phase. The stability of the biomethanation process is evaluated in terms of A) total VFAs concentration, total alkalinity (TA), partial alkalinity (PA), and the difference between TA and PA, and B) pH.

As reported in **Figure 4.3A**, during week 1 of the start-up phase, total VFAs accumulated up to 2200 mg HAc,eq/L and then progressively decreased and remained stable in the range of 406.4 – 564.6 mg HAc,eq/L in the following weeks. TA and PA followed a similar trend, increasing up to 13,000 and 8,000 mg $CaCO_3$eq/L, respectively, in week 1, and then decreased down to 8,237 and 5,413 mg $CaCO_3$eq/L, respectively. Finally, pH remained stable between 7.8 and 8.1 during the whole start-up phase (**Figure 4.3B**).

4.3.2 The effect of inlet gas and liquid recirculation flow rates on the biomethanation performance and stability

Operative parameters such as $Q^{gas,IN}$, and Q_R were varied according to the experimental plan described in section 4.2.2. The increase of the Q_R from 8 to 25 L/min, while maintaining the minimum $Q^{gas,IN}$ of 1.2 $L/L_R/d$, determined a sudden improvement of the biomethanation performances. In the first 3 weeks of Period A, the CO_2 final content increased from 18 to 32 % v/v (**Figure 4.4a**). This result can be motivated by the enhanced CO conversion into H_2 and CO_2 through biological WGS reaction, resulted from the increase of CO solubilization efficiency after the increase of Q_R. The enhanced recirculation within the bioreactor resulted in average H_2 and CO solubilization efficiencies as high as 99 and 97 % (**Figure 4.4b**), respectively, in the weeks 1 – 3 of Period A1, with CH_4 final concentrations in the range of 68 – 74 % v/v.

The improved H_2 and CO solubilization efficiency caused an initial drop of the $Y_{CH4/H2}$ (0.05 L_{CH4}/L_{H2}) (**Figure 4.4c**) below the maximum stoichiometric value of hydrogenotrophic methanogenesis (0.25). A progressive increase was observed in the following weeks, probably due to a change in the metabolic mechanisms of methanogens, due to the sudden improvement in the availability of the gas substrates. This variation has to be attributed to the increased gas solubilization resulting from the higher Q_R.

The sudden increase of $Q^{gas,IN}$ from 1.2 to 1.8 in Period A2, caused a decrease in CO solubilization efficiency to 75 %, probably derived from the momentaneous CO accumulation in the reactor (**Figure 4.4b**).

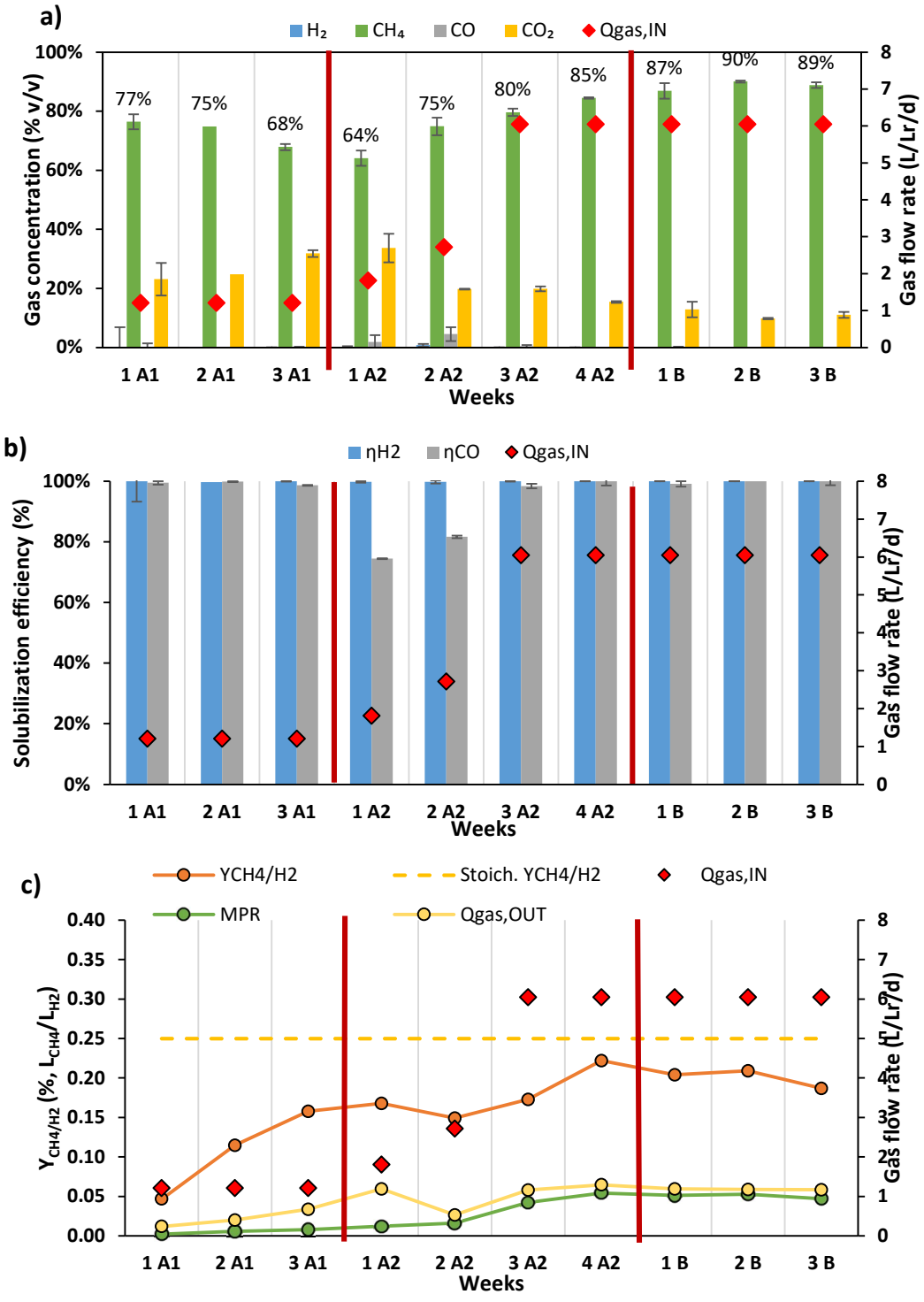


Figure 4. 4. Bioreactor performance in the experimental phases. The performance of the biomethanation process in the experimental periods A1, A2, and B, is evaluated in terms of a) outlet gas composition, b) H_2 and CO solubilization efficiency, and c) CH_4 yield on H_2, outlet gas flow rate, and methane production rate (MPR).

Further increase of $Q^{gas,IN}$ to 2.7 and 6.1 $L/L_R/d$ resulted in a progressive recovery of CO solubilization efficiency to 82 and 98 %, respectively. Therefore, after an initial CO accumulation, the effect of the sudden increase of $Q^{gas,IN}$ became less evident, resulting in a ready solubilization and consumption of the inlet gas, despite the fast $Q^{gas,IN}$ increase. CH_4 final content increased up to 75 – 80 % v/v, with the parallel decrease of CO_2 concentration in the outer gas around 20 % v/v (**Figure 4.4a**), and the increase of MPR up to 1.1 L/Lr/d (**Figure 4.4c**).

Both H_2 and CO solubilization efficiency reached 100 % (**Figure 4.4b**), with the supply of the maximum $Q^{gas,IN}$ = 6.1 $L/L_R/d$, equivalent to a GRT of 5 h. $Y_{CH4/H2}$ quickly increased up to 0.22 L_{CH4}/L_{H2}, slightly below the stoichiometric value of 0.25 L_{CH4}/L_{H2} (**Figure 4.4c**), suggesting the achievement of optimal conditions for the biomethanation process. The optimal supply of gas substrates within the bioreactor allowed the almost complete conversion of H_2, CO, and CO_2 into CH_4. Consistently, no significant variations in the VFAs concentration (around 428 mg HAc,eq/L) were observed, suggesting no further influences on the acetogenic/acetoclastic pathways (**Figure 4.5a**).

H_2 acted as the limiting factor in the biomethanation process. This can be due to the additional H_2 and CO_2 produced by CO conversion through biological WGS reaction (see **Table 4.1**), resulting in a H_2/CO_2 ratio lower than the one set in the inlet gas flow rate. Additionally, the presence of bicarbonates (*e.g.* $NaHCO_3$) in the inoculum can result in the availability of an alternative CO_2 source for CH_4 production, different from the gaseous CO_2 supplied with the inlet gas, leading to a further reduction of the real H_2/CO_2 ratio, as previously reported in the literature [335].

4.3.3 The effect of H_2/CO_2 ratio on the biomethanation performance and stability

In order to pursue the valorization of the residual 15 % v/v CO_2 and to potentially achieve a 100 % pure CH_4 outlet flow, a higher H_2/CO_2 ratio in the inlet gas (4.7) was tested in Period B as the only variable parameter. This variation did not affect the H_2 and CO solubilization efficiencies (100 % and 99 – 100 %, respectively) (**Figure 4.4b**), and an increase of the CH_4 final content to 87 – 90 % v/v was successfully obtained,

reducing CO_2 concentration down to 10 – 11 % v/v (**Figure 4.4a**). Interestingly, a slight decrease was observed for the MPR (down to 0.9 $L/L_R/d$), and $Y_{CH4/H2}$ (down to 0.19 L_{CH4}/L_{H2}) (**Figure 4.4c**).

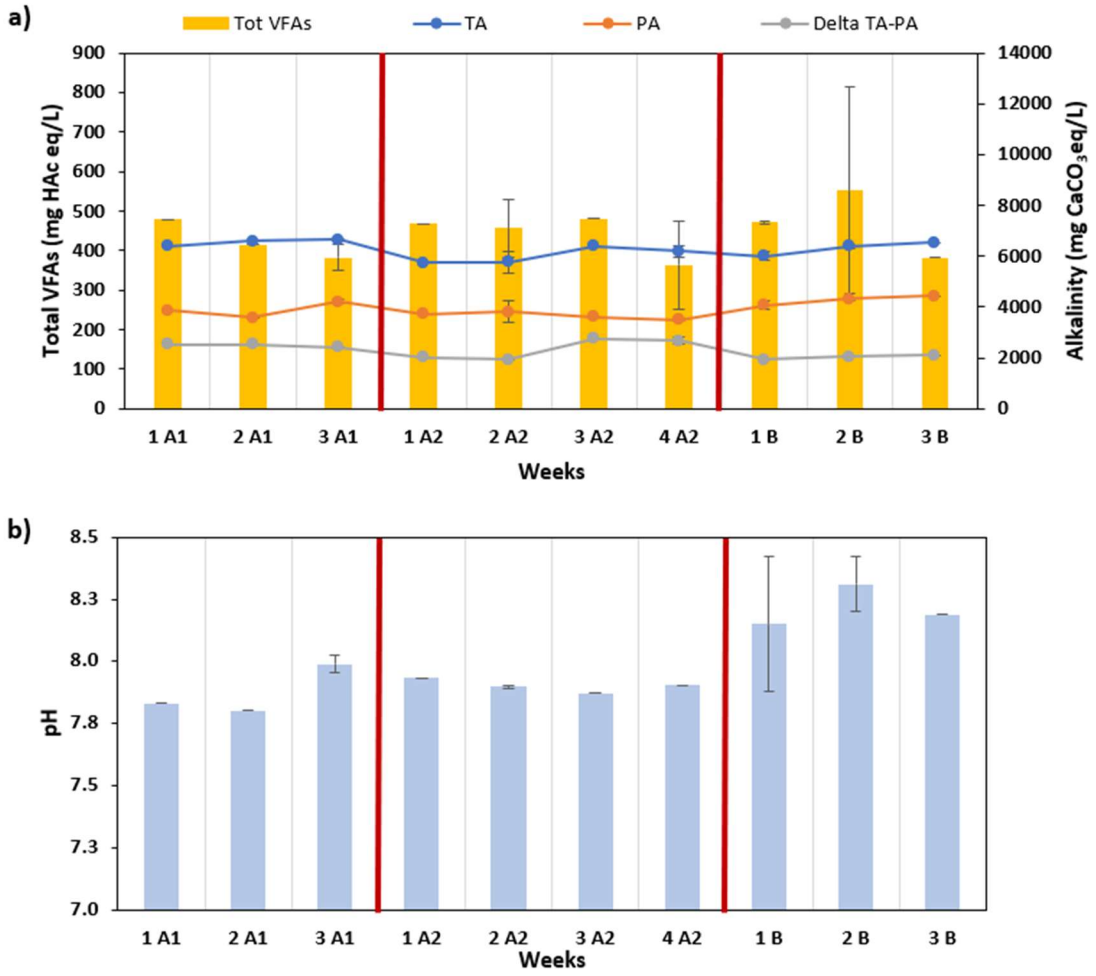


Figure 4. 5. Stability parameters in the experimental phases. The stability of the biomethanation process in the experimental periods A1, A2, and B, is evaluated in terms of a) total VFAs concentration, total alkalinity (TA), partial alkalinity (PA), and the difference between TA and PA, and b) pH.

This result could be consistent with negative effects reported in the literature due to H_2 stoichiometric excess [333]. The increase of H_2 supply, together with the enhanced gas solubilization, can favour homoacetogens and acetoclastic metabolisms [20]. Consistently, a higher variability of the total VFAs concentration was observed during week 2B around the average value of 552.6 ± 262 mg HAc,eq/L (**Figure 4.5a**), as compared to Period A. With such a high standard deviation, this increase of the average

value could suggest the onset of VFAs formation/degradation mechanisms happening differently from what was observed in the previous experimental periods. A partial VFAs accumulation might have occurred, followed by the consumption carried on by acetoclastic methanogens.

Finally, the increased H_2 supply coming from the onset of a higher H_2/CO_2 ratio could induce a loss of buffer capacity within the bioreactor [337]. This possibility is partially confirmed by the pH increase observed in Period B (**Figure 4.5b**), and at week 2B in particular (up to 8.3). However, the potential inhibition of methanogens induced by the pH increase was not reached.

It was not possible to state whether the hydrogenotrophic or the acetoclastic pathway was dominant in the production of CH_4 from $H_2/CO/CO_2$. However, no inhibition of methanogens was observed in this study, resulting in an almost complete conversion of $H_2/CO/CO_2$ into CH_4, with CH_4 yield close to the maximum stoichiometric values of hydrogenotrophic methanogenesis. Microbiological characterization of the bioreactor slurry would help to have a complete comprehension of the metabolic pathways taking place during the pyrolysis gas upgrading process, helping to individuate the main components of biomass.

4.4 Conclusions and future perspectives

In the present study, the pilot-scale biomethanation of a gas mixture simulating realistic MSS-derived pyrolysis gas with the addition of exogenous H_2 was investigated. A Venturi-type ejector for the maximization of gas-liquid mass transfer was employed, and the influence of different inlet gas flow rates and liquid recirculation flow rates entering the ejector was studied. Finally, the increase in the H_2/CO_2 ratio was tested to achieve a higher CO_2 conversion into CH_4. The main findings and implications of the study are here reported:

- A pyrolysis gas upgrading process through a biological process has been implemented in this study, achieving an almost complete conversion of $H_2/CO/CO_2$ into CH_4, with CH_4 yields close to the maximum stoichiometric values of hydrogenotrophic methanogenesis. However, both hydrogenotrophic or the acetoclastic methanogenesis pathways were supposed to be occurred.

- The employment of a Venturi-type ejector resulted in the maximization of H_2 and CO solubilization efficiencies, variable with the $Q^{gas,IN}$ and the Q_R. The optimal solubilization and conversion condition was achieved with a Q_R of 25 L/min and a $Q^{gas,IN}$ of 6.1 L/Lr/d, equivalent to a GRT of 5 h, which allowed the hydrodynamic cavitation process to be triggered. Future studies could be dedicated to the individuation of the minimum GRT applicable before the decrease of solubilization efficiency of the inlet gas. To this aim, a fluid-dynamic characterization of the bioreactor should be conducted.

- A higher H_2/CO_2 ratio of 4.7 resulted in the increase of the final CH_4 content (up to 90 % v/v), although a pure-CH_4 outlet flow was not obtained, and a slight decrease of MPR and $Y_{CH4/H2}$ was observed. A minimum CO_2 content of 10 % v/v remained unconverted. Future studies with higher $Q^{gas,IN}$ can further enhance gas conversion, towards the maximization of the CH_4 content.

- Different compositions of the inlet gas flow should be tested to simulate variable characteristics of the MSS-derived pyrolysis gas employable in the process. The presence of higher CO concentrations, as well as potential inhibitors such as H_2S could be object of future studies. Additionally, light hydrocarbons (*e.g.* C_2-, C_3-, C_4-) could be included as well.

- A microbial characterization of the inoculum should be conducted, by analysing samples collected at the start and end of the experimental activity. This will assess any switch in the composition of the mixed culture and provide a better understanding of the metabolic pathways taking place during the process.

- A techno-economic assessment of the process should be conducted. Costs and benefits derived from the employment of low-grade pyrolysis gas mixtures, with the necessary addition of exogenous H_2, should be investigated. As

already stressed by other authors in the literature, when considering the economic feasibility of the biomethanation of such gas mixtures, and the important costs for exogenous H_2 production, the effects in terms of environmental impact, reduction of GHGs emissions, and the role of biomethanation in the energetic transition phase, should be properly taken into account.

CHAPTER 5. BIOCHAR VALORIZATION IN THE ANAEROBIC DIGESTION OF MUNICIPAL SEWAGE SLUDGE

5.1 Introduction

In the context of the innovative thermochemical techniques for the management of municipal sewage sludge (MSS), pyrolysis has gained attention due to its capability to simultaneously pursue energy and nutrient recovery through the obtainment of a wide range of valuable products: biochar (solid), bio-oil (liquid), and pyrolysis gas.

Biochar (BC) is a stable carbon-rich material [103], with remarkable physical-chemical properties and a multi-application potential including, for instance, soil conditioning and nutrients supply [10,11], carbon capture and storage/utilization [12], and contaminants removal from wastewaters and soils [13]. These valorization methods are influenced by BC characteristics: specific surface area, pore density and volume, the presence of surface functional groups, pH, alkalinity, electric conductivity, and cation exchange capacity. The properties of the pyrolyzed MSS feedstock and the operative parameters of the process (especially temperature) are the main factors influencing BC properties.

Among the primary methods employed for gas capture and sequestration (including absorption, adsorption, and the use of membranes), adsorption is typically the most cost-effective and efficient option [142]. However, identifying a suitable sorbent for CO_2 separation from a gas flow can be challenging [143]. As demonstrated with BC from various feedstocks [148,149], BC derived from MSS can efficiently capture CO_2 from the atmosphere through both physical and chemical sorption mechanisms, owing to its surface chemical characteristics (such as the presence of functional groups) and pore structure [139,144]. Such properties make BC a valid material to be employed for carbon capture and storage (CCS) [12].

CO_2 adsorption capability is generally reported to increase with higher pyrolysis temperatures and to be related to the distribution of micro-, meso-, and macroporosity in BC [153]. A CO_2 adsorption capability of 28.36 mg/g was achieved at 30 °C using an MSS-derived BC produced at 800 °C [150]. This capability is often lower than that of BC produced from other feedstocks, generally characterized by lower ash content,

such as lignocellulosic materials [116,118]. However, higher CO_2 adsorption capabilities can be achieved in MSS-derived BC by conducting pre-treatments on MSS or activation post-treatments (*i.e.* air-, steam- or CO_2-activation, as well as impregnation with chemicals such as KOH) directly on the BC [13,40].

Due to its surface and pore structure characteristics, BC addition has been recently investigated as a possible solution for multiple issues affecting the anaerobic digestion (AD) process (*i.e.* acidification, presence of inhibitors, inefficiency and costs of *ex-situ* biogas upgrading to CH_4) [164]. When added to AD, BC can result in the *in-situ* CO_2 adsorption, thereby reducing the cost of the following biogas upgrading, while its buffering properties and the presence of specific functional groups can enhance CH_4 production by decreasing the formation of microbial inhibitors such as NH_3/NH_4^+ and H_2S [165,166]. Additionally, the BC capability of enhancing direct interspecies electron transfer (DIET) within the microbial community is a determinant for improving methanogenesis and VFAs degradation [178].

According to Chiappero et al. (2021), in the mesophilic AD of MSS, the addition of MSS-derived BC had no impact on biogas production but resulted in a 28 % higher final biomethane content in biogas. However, this increase was lower compared to rice husk BC due to lower specific surface area and pore volume in the MSS-derived one. Similarly, Zhang et al. (2019) reported a 77 % increase in cumulative biomethane production with MSS-derived BC addition, recommending 26 g/L as the optimal dosage to maximize yield without inhibiting the AD process. Contrarily, Wu et al. (2019) observed negligible or adverse effects from MSS-derived BC addition, attributing this to the inhibition of short-chain fatty acids production because of limited porosity. Given the contrasting results reported in the literature, a high variability in the efficiency of BC addition can be assumed, especially when considering the numerous variables playing a key role in the process. The identification of more effective indicators might be helpful in the design of BC production and application in AD.

In the present study, a possible correlation between CO_2 adsorption capability ($AdsCO_2$) of the BC and BC performance in terms of CO_2 capture and CH_4 final composition when employed in the AD process was investigated. Different types of

BC were obtained from MSS pyrolysis at variable temperatures (350 – 800 °C). Thus, after assessing BC composition and CO_2 adsorption capability, preliminary tests of the biomethanation potential of MSS were performed with and without the addition of BC, evaluating possible variations in the CH_4 production and the composition of biogas.

5.2 Materials and methods

5.2.1 Municipal sewage sludge

The MSS used for pyrolysis tests was collected at the end of the sludge line of an urban wastewater treatment plant located in Rome (Italy), after undergoing thickening, anaerobic digestion, and centrifugation treatments. The collected MSS was oven-dried at 105 °C for 24 hours and sieved to a particle size below 0.5 mm using a cutting mill (SM 2000, Retsch GmbH, Haan, Germany). Proximate and ultimate analyses of MSS were conducted using a TGA/DSC analyzer (Star^e System, Mettler Toledo, Columbus, Ohio) and an elemental analyzer (Vario Macro Cube, Elementar Italia Srl, Lomazzo, Italy), respectively.

5.2.2 Pyrolysis set-up

The employed pyrolysis set-up as was a bench-scale batch pyrolyzer constituted by a tubular quartz reactor heated in an electric furnace, as already described in **Chapter 2** (**Figure 2.1**). Pyrolysis was conducted at variable temperatures in the 350 – 800 °C range for a SRT of 15 min. The heating rate (HR) was not considered, as the reactor was inserted in the furnace only after reaching the maximum temperature. BC was retained inside the reactor at the end of the process. Vapours were allowed to exit the reactor from the bottom. Bio-oil and pyrolysis gas were separated through a dedicated condensation section, adapted according to the maximum temperature tested.

5.2.3 Characterization of biochar

After pyrolysis, BC left within the quartz tube reactor was collected, the dimension of the granules was reduced in a crucible to a particle size below 0.5 mm, and stored at room temperature. C, H, N, and S content in BC was assessed through elemental

analysis by employing an elemental analyser (Vario Macro Cube, Elementar Italia Srl, Lomazzo, Italy). The O content was determined as a difference. TGA/DSC analyses were conducted to determine BC proximate composition, and $AdsCO_2$. In order to measure the pH of BC, each type of BC was added to deionized water in a 1:5 weight ratio within a 50 mL tube and shaked for 30 min at 110 rpm, according to the method described by Tang et al. (2019) [154]. After centrifugation at 3000 rpm for 10 min, the pH of the supernatant was measured through a pH meter.

5.2.4 Determination of CO_2 adsorption capability of biochar

The $AdsCO_2$ of the different BC samples was measured by TGA/DSC. About 70 mg of BC were introduced in the TG chamber and purged with N_2 (20 mL/min) up to 150 °C (HR = 10 °C/min) to remove humidity and other impurities previously adsorbed. The initial mass loss (%, mg/mg BC) imputable to the purge phase was measured for every BC. After purging, the N_2 flow was maintained under isothermal conditions for 30 min to achieve equilibrium in mass loss. The temperature was then decreased to 70 °C (HR = - 10 °C/min), and the CO_2 inlet flow (155 mL/min) was started while reducing the temperature to 25 °C with constant HR. A last isothermal phase with CO_2 was performed at 25 °C for 40 min. $AdsCO_2$ was evaluated as the mass increase recorded from the CO_2 inlet to the end of the experiment (%, mg CO_2/mg BC). The $AdsCO_2$ was evaluated for BC produced at pyrolysis temperatures of 350, 500, 650, and 800 °C, with SRT of 15 min (BC350, BC500, BC650, and BC800, respectively).

The mass increase recorded from the N_2 isothermal phase to CO_2 inlet was measured, and it was attributed to the adsorption of N_2 on BC (%, mg N_2/mg BC), which can lead to underestimate $AdsCO_2$. Indeed, the estimation of AdsCO2 for different BCs would be affected not only by their surface characteristics, but also by the amount of N_2 already adsorbed. The role of the CO_2 inlet temperature on the N_2 adsorption was evaluated by conducting different $AdsCO_2$ analyses with variable CO_2 inlet temperatures (25 °C and 100 °C), and then by comparing the results of these tests with those obtained with CO_2 inlet at 70 °C. BCs produced at the boundaries of the temperature range (BC350 and BC800) were employed for this investigation.

5.2.5 Biomethanation potential tests

Biomethanation potential (BMP) tests were conducted in 500 mL glass bottles, with a working volume of 170 mL and a headspace of 330 mL. For these tests, primary and secondary sludge collected from a WWTP located in Cesena (Italy) were mixed together in a 1:1 weight ratio, and the mix was then employed as substrate of the test. Before its use, the secondary sludge was centrifuged and three quarters of the supernatant was discarded, in order to increase the TS content of the sludge. Anaerobically digested MSS was collected from the mesophilic anaerobic digester of the same WWTP mentioned before, and employed as inoculum in the BMP tests. Inoculum and substrate were added in each bottle with an inoculum to substrate ratio (ISR) of 2 g VS/g VS. A condition with the sole inoculum, without substrate addition, was prepared in order to assess the endogenous CH_4 production. In the latter condition, distilled water was dosed instead of the substrate, in order to maintain the same filling grade in the bottles. TS and VS content, pH, alkalinity, ammonium ion and COD concentration, were measured for the employed substrate and inoculum, according to standard methods [309]. The results of this characterization are reported in **Table 5.1**.

	Substrates (PS + SS*, 1:1 wt)		**Inoculum**
	PS	**SS***	**ADS**
TS (%, g/g)	5.84	4.96	5.22
VS (%, g/g)	3.66	3.06	2.52
VS (%, g VS/g TS)	62.67	61.69	48.28
pH	5.80	6.80	7.30
Alkalinity (mg $CaCO_3$,eq/L)	2700.0	1400.0	1975.0
tCOD (g/L)	200.53	41.01	32.56
sCOD (g/L)	4.41	1.52	1.39
NH_4^+ (mg/L)	60.0	7.2	315.0

Table 5. 1. Characterization of substrate and inoculum employed in the biomethanation potential test. PS: primary sludge; SS: concentrated secondary sludge; ADS: anaerobically digested sludge; TS: total solids; VS: volatile solids; tCOD: total COD; sCOD: soluble COD;*

Each BC produced at different pyrolysis temperatures was tested in triplicates in dedicated experimental conditions (namely, BC350, BC500, BC650, and BC800) by adding 1.69 g BC to the substrate and the inoculum in each bottle (10 g BC/L). This dosage was chosen according to previous experiments reported by Chiappero et al., (2021). Prior to being used, each biochar was washed 3 times with deionized water, and then oven-dried at 60 °C for 24 hours [154], in order to clean BC's pores and facilitate adsorption on its surface. A control condition without BC addition was prepared as well.

The tests were performed in an automatic BMP system (AMPTS II, BPC Instruments, Sweden), at a temperature of 37 °C and at 60 % of the maximum stirring speed. The gas produced in each bottle reached the automatic detection system after passing through alkaline traps consisting of glass bottles containing 80 mL of a 40 % v/v NaOH aqueous solution. The cumulative CH_4 production was expressed as mL CH_4/g VS_{added}, where g VS_{added} represents the mass of VS introduced by the substrate (1.65 g per bottle).

At the end of each test, gas samples from the headspace of the BMP bottles were collected and analysed through a GC-TCD in order to assess final CH_4 and CO_2 contents in biogas. Liquid samples were collected from each bottle. pH was determined immediately after collecting the sample.

5.3 Results and discussion

5.3.1 Municipal sewage sludge and biochar characterization

Proximate and ultimate analysis on the MSS feedstock of pyrolysis and obtained BC were conducted to assess variations in biochar composition derived from the different pyrolysis temperatures (**Table 5.2**). C content in BC350 (36.90 % wt db) was similar to that of the original MSS (35.94 % wt db), while the further organic carbon degradation obtained by increasing temperature to 500 – 800 °C resulted in a 20 – 22 % reduction of C content in BC500, BC650, and BC800, with respect to the original C content of MSS. This decrease was probably limited by the biochar FC content,

slightly variable between 17.03 and 21.67 % wt db for temperatures of 350 – 800 °C. In addition, VM in BC350 (34.86 % wt db) was significantly lower than that of the original MSS (57.31 % wt db) and progressively decreased for higher pyrolysis temperatures, down to 6.04 % wt db in BC800. This indicates a progressively enhanced degradation of the organic matter in the solid phase with increasing temperatures towards the production of volatile compounds.

	MSS	BC350	BC500	BC650	BC800
C (% wt db)	35.94	36.90	28.70	28.00	28.10
H (% wt db)	5.18	2.48	0.86	0.29	0.15
N (% wt db)	5.76	5.32	3.92	2.88	1.63
S (% wt db)	1.12	0.61	0.45	0.45	0.46
O (% wt db)	23.79	8.76	7.20	4.28	0.00
H/C (mol/mol)	0.07	0.03	0.01	0.01	0.07
O/C (mol/mol)	0.24	0.25	0.15	0.00	0.24
MC (% wt)	5.33	2.17	3.50	3.14	2.20
VM (% wt db)	57.31	34.86	18.76	13.99	6.04
FC (% wt db)	9.15	17.03	18.87	18.77	21.67
AC (% wt db)	28.21	45.93	58.87	64.10	70.09
pH	7.5	9.1	8.5	11.0	11.8

Table 5. 2. Proximate and ultimate analysis of municipal sewage sludge and biochar produced with variable pyrolysis temperature. BC350, BC500, BC650 and BC800 refer to biochar produced at 350, 500, 650, and 800 °C, respectively, with solid retention time of 15 min. [a]: calculated as difference; db: on a dry basis; MSS: municipal sewage sludge; MC: moisture content; VM: volatile matter; FC: fixed carbon; AC: ash content.

H and O contents progressively reduced from 2.48 % wt db and 8.76 % wt db down to 0.15 % wt db and 0.00 % wt db in BC350 and BC800, respectively. H/C and O/C molar ratios were calculated to assess the aromaticity/stability and polarity/hydrophilicity of BC, respectively [103,111]. Consistently with the literature,

by increasing temperature, a progressive decrease of both H/C and O/C was observed due to depolymerization and dehydration reactions [107]. BC350 and BC800 showed lower H/C and O/C ratios (0.01 – 0.07 and 0.00 – 0.25, respectively) when compared to other MSS-derived BCs produced at similar temperatures and described in the literature (0.07 – 0.10 and 0.85 – 0.95, respectively, reported by Zhang *et al.* [111] for a temperature range of 300 – 700 °C). Therefore, biochar produced in this study could show higher stability when employed as a soil conditioner or for soil remediation, although with lower polarity and, therefore, lower capacity of water retention in soils. AC in BC, increasing from 45.93 to 70.09 % wt db in the 350 – 800 °C temperature range, was also lower than what was reported in the literature for other MSS-derived BCs (up to 81.23 – 91.05 % wt reported by Zhang *et al.* [111]). This could be due to an initially low AC in the MSS feedstock (28.21 % wt db) when compared to literature ranges (up to 76.5 % wt db for dewatered MSS, according to Syed-Hassan *et al.* [23]. Future studies could include a characterization of the ashes in terms of quantity and quality of inorganic contaminants such as potentially toxic elements (PTEs).

Interestingly, N content in BC350 (5.32 % wt db) was quite similar to that of the initial MSS (5.76 % wt db). Then, it progressively reduced down to 1.63 % wt db in BC800. Therefore, up to 350 °C, the decomposition of N-containing compounds in the solid phase was limited and began to be more relevant only above 500 °C, with the obtention of higher bio-oil yields. This is consistent with what was reported by Zhang *et al.* [111] for similar temperatures and solid retention times. These values are substantially higher than those obtained by Chen *et al.* [103] (from 1.5 to 0.5 % wt db in the 400 – 800 °C temperature range) and by Zhang *et al.* [111] (1.3 – 0.5 % wt db in the 300 – 700 °C temperature range). The higher N content measured in this study could be useful for biochar application in soils.

Regarding the S content, after a 45.5 % reduction in BC350 with respect to the original MSS and a further decrease in BC500 (59.8 % lower), it remained stable (0.45 – 0.46 % wt db) in the temperature range of 500 – 800 °C. This result could be due to the degradation of different S-compounds species at 350 and 500 °C and the absence of S-compounds characterized by higher degradation temperature.

Finally, the pH of biochar was always alkaline (8.5 – 11.8), with similar values at 350 and 500 °C, and higher values at 650 and 800 °C. This progressively higher pH obtained at higher temperatures is consistent with the literature and can be due to the progressively enhanced polymerisation reactions and release of acidic surface compounds at higher temperatures [103,113].

5.3.2 Adsorption capability of biochar

5.3.2.1 Influence of pyrolysis temperature on CO_2 adsorption

Pyrolysis temperature had significant influence on the $AdsCO_2$ of the different biochars (**Figure 5.1A**). Consistently with the literature, a temperature of 350 °C could not stimulate high $AdsCO_2$ in BC350, which was characterized by the lowest value (0.98 %). Increasing temperatures led to higher $AdsCO_2$ values: BC500 and BC650 were similar and characterized by the highest $AdsCO_2$ (2.17 and 2.18 %, respectively). Finally, a temperature as high as 800 °C probably led to a partial collapse of the porous structure of biochar [111], resulting in a significantly lower $AdsCO_2$ for BC800 (1.88 %), although it was still higher than that of BC350.This trend reflects what was observed for the initial mass loss during the purge phase (**Figure 5.1A**). In fact, as with $AdsCO_2$, the initial mass loss in the purge is directly related to the porous structure of the biochar. The same relation is valid for the mass increase due to N_2 adsorption, which varied from a minimum of 0.15 % for BC350 up to 0.26 % for BC500.

Since the substances removed from BC during the purge phase can have different nature, with different affinities to biochar, the sum of N_2 physisorption and $AdsCO_2$ for every biochar was reasonably lower than the overall initial mass loss. Therefore, the adsorption capability of the different BCs did not lead to a complete saturation of the volume made available after the purge phase. By looking at the TGA curves reported for the BCs in **Figure 5.1B**, a plateau is visible after about 20 min from the CO_2 inlet. Therefore no improvements in $AdsCO_2$ can be achieved by increasing the duration of the last phase.

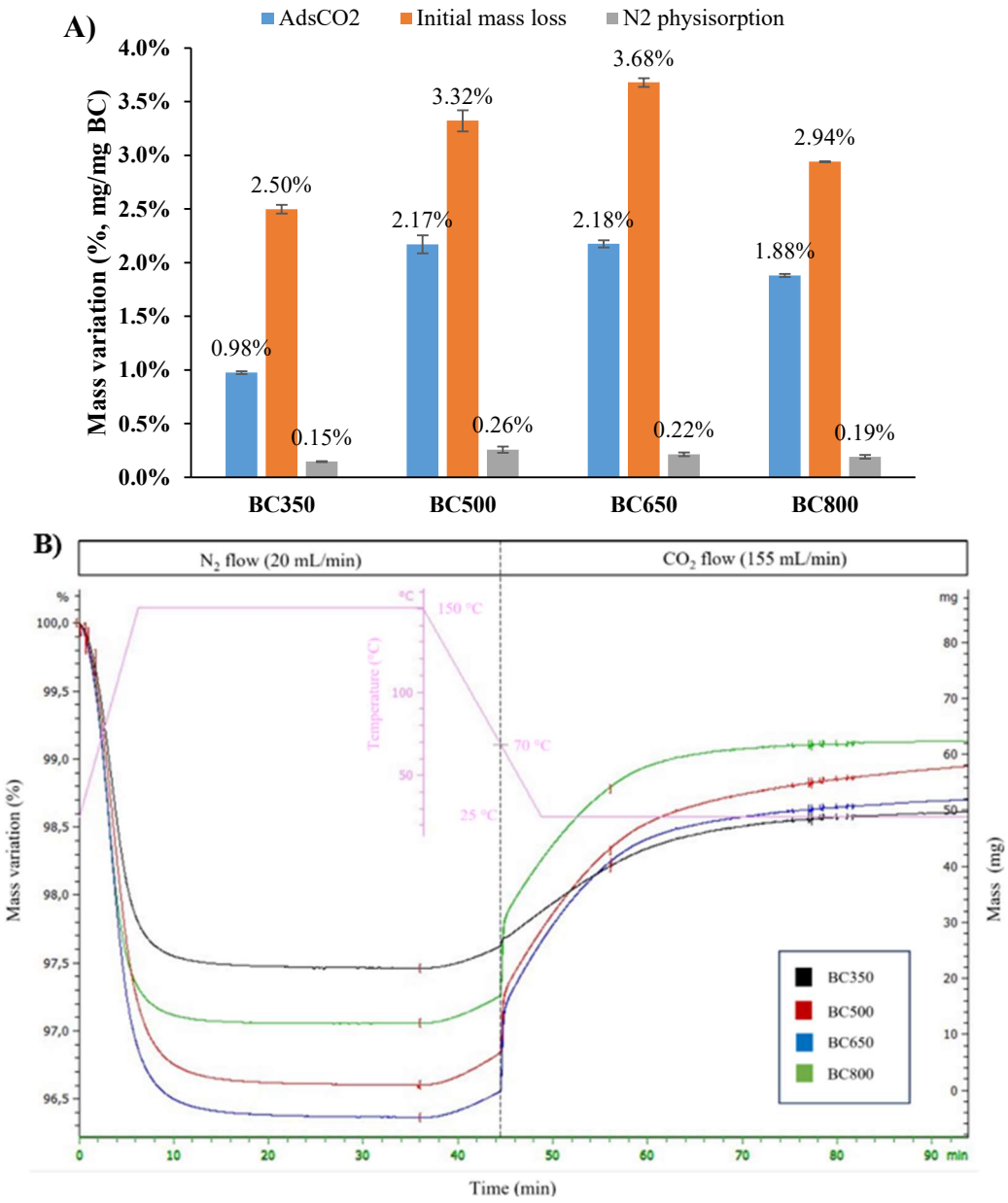


Figure 5. 1. Results of thermo-gravimetric analysis for the determination of CO_2 adsorption capability of biochar. The different biochars tested were produced through conventional pyrolysis at temperatures of 350, 500, 650 and 800 °C (namely BC350, BC500, BC650, and BC800, respectively). A) Percentages of mass variation, and B) TG curves, are reported for every biochar.

5.3.2.2 Influence of CO_2 inlet temperature on N_2 and CO_2 adsorption

By increasing the CO_2 inlet temperature, a significant reduction in the percentage of N_2 adsorbed on BC350 (**Figure 5.2A**) and BC800 (**Figure 5.2B**) was observed, with similar trends for both the biochars. This reduction can be reasonably due both to the exothermic nature of the adsorption process (N_2 flow was interrupted at progressively

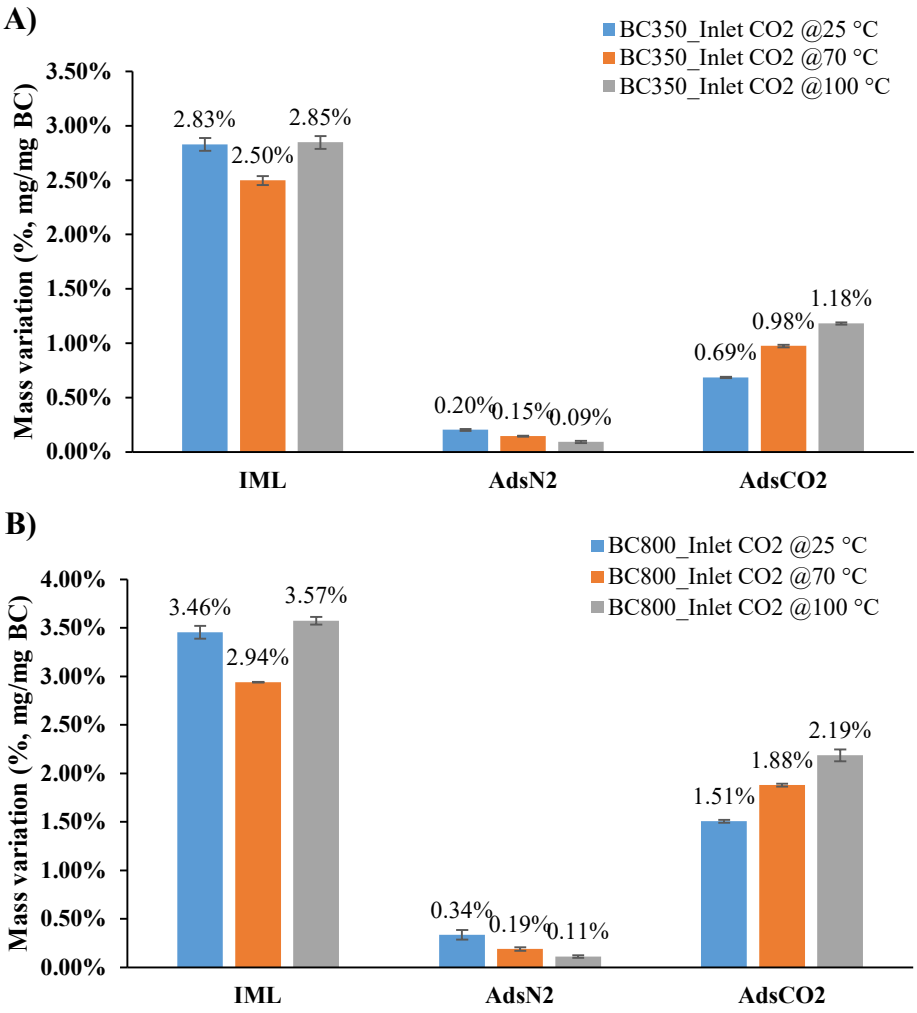


Figure 5. 2. CO_2 adsorption tests with variable CO_2 inlet temperatures. The adsorption of CO_2 on A) biochar produced at 350 °C (BC350), and B) biochar produced at 800 °C (BC800), was tested in TGA with CO_2 inlet temperature of 25, 70, and 100 °C. The influence on the initial mass loss (IML), N_2 adsorption ($AdsN_2$), and CO_2 adsorption ($AdsCO_2$), was evaluated.

higher temperatures, thus limiting its adsorption on biochar), and more simply to the shorter exposition of biochars to N_2. Interestingly, the expected increase in N_2

adsorption from BC350 to BC800, due to a higher adsorption capability, was more visible for the CO_2 inlet temperature of 25 °C (70 % higher in BC800) and became less important with the increase of CO_2 inlet temperature to 70 °C (27 % higher) and up to 100 °C (22 % higher). This behaviour could confirm the limitation in N_2 adsorption in the temperature range 100 – 150 °C.

On the other hand, a progressive increase in $AdsCO_2$ was observed when moving from CO_2 inlet temperature of 25 °C to 70 °C and up to 100 °C. As previously discussed in section 3.2.2.1, at the end of the CO_2 inlet phase, a plateau was reached by every condition in this analysis as well (TGA curves not shown). This behaviour suggests that the higher $AdsCO_2$ achieved for CO_2 inlet at 100 °C was not due to a more extendedexposition to CO_2 with respect to the condition with CO_2 inlet at 25 °C or 70 °C. A possible explanation for this higher $AdsCO_2$ can be found considering that the CO_2 flow at high temperatures (*i.e.* 70 or 100 °C) can partially oxidize BC, in a sort of CO_2-activation, resulting in a different final structure, and therefore a possible difference in $AdsCO_2$ of BC.

Although the comparison between different BCs can be conducted by referring to the same methodology, regardless of the influence of the CO_2 inlet temperature, it is still interesting to notice that the overall performance of the BC (*i.e.* in terms of CO_2 adsorpion) could be underestimated when this phenomenon is not taken into account.

5.3.3 Biochar addition in the anaerobic digestion process

Biochar produced at 350, 500, 650, and 800 °C was used as an additive in the BMP tests of MSS. After 14 days, the BMP test was considered complete (the daily CH_4 production was below 1% of the cumulative CH_4 production). Cumulative CH_4 production followed similar trends in each condition (**Figure 5.3A**), reaching similar final values in the range of 256.1 – 284.4 mL CH_4/gVS_{added}, without any statistically significant difference between the BC-additioned conditions and the control. Thus, BC was not effective in enhancing biomethanation and biogas production. Although the results of the statistical analysis have not detected any significant difference, the cumulative CH_4 production in BC-additioned conditions assumed average values

always below the one of the control condition, suggesting the onset of possible inhibition effects induced by the BC. According to Wu et al. (2019), a limitation of biomethane production could result from the inibition of short-chain fatty acids production when BC is applied. Additionally, given the capability of MSS-derived BC

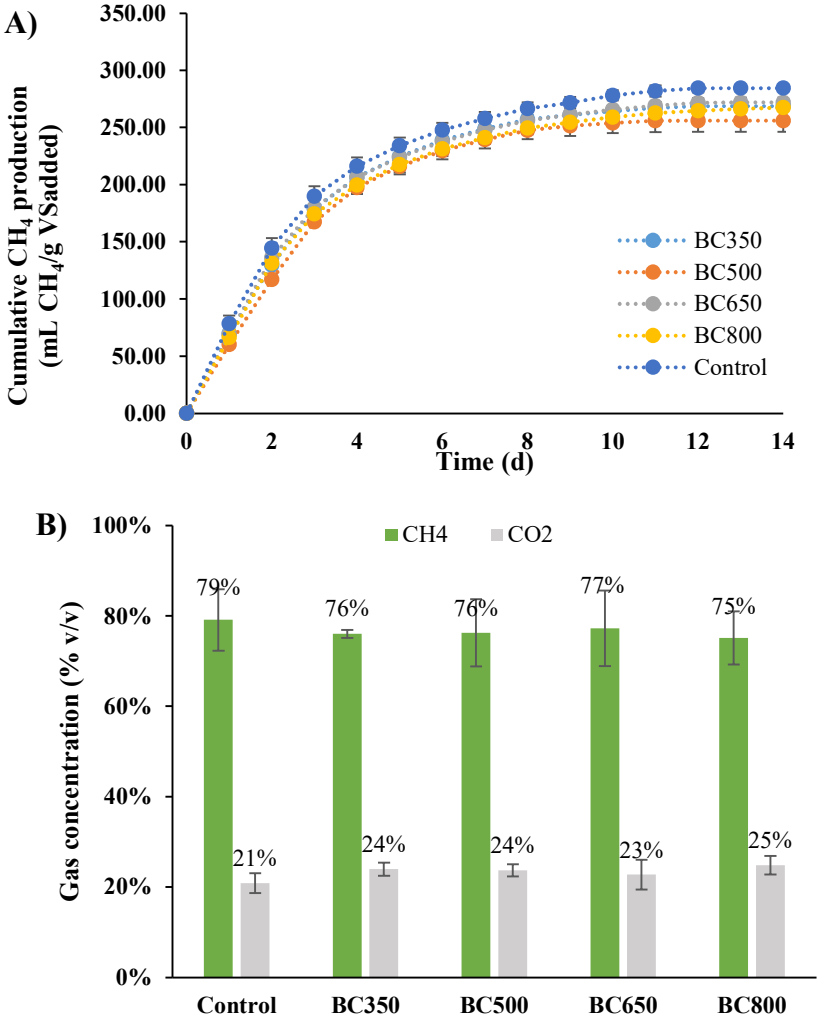


Figure 5. 3. Biochar addition in the biomethanation potential tests of municipal sewage sludge. The results of biomethanation potential test of municipal sewage sludge (MSS) with and without biochar addition were reported in terms of A) cumulative CH_4 production, and B) final composition of biogas. MSS-derived biochar produced at 350, 500, 650, and 800 °C (namely, BC350, BC500, BC650, and BC800) was employed.

to retain PTEs initially contained within MSS [132], a toxicity effect on the biomass in the BMP test cannot be excluded. Future investigation should assess these possibilities, in order to individuate a possibile correlation with the observed performance.

Concerning the quality of the produced biogas, the results of the GC analysis allowed the evaluation of the CH_4 and CO_2 content in biogas (**Figure 5.3B**). The produced biogas had a similar composition in each condition, and it was characterized by a CH_4 final content of 75 – 79 % v/v, with a remaining 21 – 25 % v/v of CO_2. In line with the results of the cumulative CH_4 production, the highest CH_4 final content was achieved in the control condition, although the observed differences in the average final values were not statistically significant.

In order to improve the possible CO_2 adsorption in the liquid phase, BC was washed and heated to obtained free pores and improve the adsorption process, as already reported in the literature [154]. Nevertheless, this treatment might be inefficient due to the necessary exposure of BC to the atmosphere between the pretreatment phase and the addition to the BMP tests, which can result in the adsorption of other molecules within BC pores, reducing its $AdsCO_2$.

Finally, it has to be considered that the absence of chemical/physical activation pre-treatments on BC can result in a poor adsorbent quality of the produced BC (0.9 – 2.8 %, mg CO_2/mg BC). Assuming that the CO_2 adsorption happened as recorded in the $AdsCO_2$ test in TGA, the difference between the CO_2 adsorbed by the different biochars would be very limited. Also, the resolution of the GC analysis could affect the estimation of the difference in the CO_2 final content with and without BC addition. In such conditions, the evaluation of BC application for the *in-situ* upgrading of biogas to biomethane via CO_2 adsorption cannot be efficently conducted based only on the effect of the pyrolysis temperature without performing important improvements of BC characteristics through physical or chemical activation treatments (*e.g.* high temperature air- or CO_2-mediated physical activation, or impregnation with chemicals such as KOH or K_2CO_3).

5.4 Conclusions

In the present study, the characterization of MSS-derived BC produced at different pyrolysis temperature in terms of composition and CO_2 adsorption capability ($AdsCO_2$), was conducted.

Decreasing trends for the content of every element in BC (C, H, N, S, and O) were observed due to a progressive degradation of the organic matter in the solid phase towards the production of volatile fractions. The high N concentration observed might allow the employment of BC in agriculture, as an alternative valorization path.

Consistent with the literature, the different pyrolysis temperatures resulted in variations of the $AdsCO_2$ due to a different influence on the development of BC porous structure and specific surface area. In particular, increasing temperatures up to 650 °C resulted in a progressively increasing $AdsCO_2$, while higher temperatures (800 °C) determined a reduction of $AdsCO_2$ in BC.

Different approaches to the determination of $AdsCO_2$ of BC through TGA were applied by investigating the influence of the CO_2 inlet temperature on the quality of the estimation. It was observed that lower temperatures cause the preliminary adsorption of N_2 on BC, thus limiting the potential CO_2 adsorption and resulting in an underestimation of the maximum CO_2 adsorbed on BC, while increasing CO_2 inlet temperature from 70 to 100 °C reduced the extent of this phenomenon.

Finally, the employment of biochar in the AD of MSS was conducted in BMP tests, in order to assess the potential of BC to adsorb CO_2 directly in the liquid phase of the AD process, aiming at an *in-situ* upgrading of biogas to biomethane. The biochar produced at 350 – 800 °C was added in BMP tests and resulted in comparable cumulative CH_4 productions and the compositions of the biogas with respect to the control condition, with lower average values achieved in the BC-amended conditions for both the parameters. Future analysis should focus on assessing the concentration of possible inhibitory compounds (*e.g.* PTEs) in BC and their potential release during AD.

According to the obtained results, it was not possible to assume $AdsCO_2$ as an indicator of the potential *in-situ* upgrading of biogas to CH_4 operated by MSS-derived BC, probably because the $AdsCO_2$ values obtained in this study were not high enough to allow a proper evaluation and comparison. After this preliminary investigation, future tests should involve the chemical-physical activation of BC in order to induce more evident variations.

CONCLUSIONS

Multiple issues affecting MSS management require innovative solutions to valorize residual organic matter and nutrients in an integrated biorefinery scheme. In order to overcome the limits of established MSS treatment/disposal methods, pyrolysis can represent a valid solution for converting MSS into a wide range of valuable products, potentially allowing the simultaneous recovery of matter and energy. The combination of MSS pyrolysis and biological valorization processes in integrated biorefinery platforms can represent a successful strategy for maximizing resource recovery from MSS. Innovative valorization routes for biochar, bio-oil and pyrolysis gas from MSS are reported in this doctoral thesis, as well as the influence of the process on the main characteristics of these products.

The variation of pyrolysis temperature and the employment of zeolitic catalysts can substantially influence product yields and composition, allowing for the proper design of the obtainable products. In particular, a significant reduction (up to 42 – 47 %) of the concentration of a potentially harmful compound such as H_2S in pyrolysis gas can be achieved using acidic zeolites such as H-Mordenite and H-ZSM5. The results reported in this thesis showed the capability of these zeolites to retain sulfur in the solid and liquid fractions partially (up to 31.8 % wt and 33.8 % wt, respectively), and/or dilute the produced H_2S thanks to the obtainment of higher gaseous yields. Different selectivity of the zeolites was observed for the adsorption-repolymerization of H_2S and other gaseous S-compounds. Further efforts should be made to understand the potential applications of these catalysts fully, and to reach lower final H_2S concentrations, which could result in the partial or complete avoidance of desulfurization processes prior to thermochemical/biological valorization of pyrolysis gas.

Indeed, the quality of the produced MSS-derived pyrolysis gas plays a key role in determining its valorization pathways. The possibility of converting MSS-derived

pyrolysis gas into value-added products such as microbial protein (MP) has been investigated, and the feasibility of this innovative process has been confirmed. The production of MP with protein content up to 74 % from an $H_2/CO/CO_2/H_2S$ gas mixture has been achieved. The HOB mixed culture employed for MP production showed high resistance to H_2S and CO concentrations up to 4000 ppmv and 40 % v/v, respectively. It was proved that the mixed nature of the microbial culture employed was fundamental for the success of the process, which was also sustainable for long-term applications (up to 30 days). This relevant result opens new perspectives in terms of syngas valorization processes aimed at the synthesis of alternative protein sources, biopolymers, and fertilizers from MSS.

Besides MP production via aerobic fermentation, syngas biomethanation could represent a valid alternative for the full exploitation of the potential of syngas. H_2, CO and CO_2 valorization into an easy-to-use and versatile biofuel such as CH_4 could facilitate the energy recovery from MSS by employing renewable H_2 produced from energy surplus. The pilot-scale syngas biomethanation process described in this thesis could fully convert H_2 and CO into CH_4, owing to the good performance of a Venturi-type ejector employed as gas solubilization system. Lowering the gas retention time (GRT) down to 5 h within the bioreactor increased final CH_4 concentration up to 85 % v/v, while a value as high as 90 % v/v was achieved by providing a higher H_2/CO_2 ratio (up to 4.7). Future studies should be conducted to maximize the CH_4 content in the obtained biogas by pursuing a complete CO_2 conversion. In the context of the ongoing energetic transition, $H_2/CO/CO_2$ mixtures conversion into CH_4 could constitute a valid strategy for the fulfilment of global energy demand by exploiting existing facilities for energy production from CH_4/natural gas.

The valorization pathways investigated for pyrolysis gas (*i.e.,* aerobic fermentation and biomethanation) might be further evaluated by testing the effects of other classic components (*e.g.* hydrocarbons and NH_3), as well as real MSS-pyrolysis gas mixtures, also in upscaled set-up.

In view of an integrated valorization platform for the products generated by MSS pyrolysis, numerous possibilities can also be evaluated for biochar. In the present doctoral thesis, the capability of biochar to adsorb CO_2 on its surface was

experimentally evaluated and correlated to the possibility of influencing biogas composition in the BMP test of MSS, acting as an *in-situ* upgrading process for the conversion of biogas to biomethane. Biochar produced at variable temperatures (350 – 800 °C) was characterized in terms of composition and CO_2 adsorption capability, and it was then dosed in BMP tests, monitoring the resulting biogas composition and biomethane concentration. In the experiment conducted in this thesis, biochar addition had no positive effect on the performance of the anaerobic digestion of MSS, and this could be due to the limited CO_2 adsorption capability of the produced biochar. Physical-chemical activation of biochar could help to better evaluate the application of various biochar types.

Finally, it can be stated that pyrolysis can deliver an innovative and comprehensive perspective on the challenges and issues related to MSS management. The study of this multidisciplinary platform developed from MSS pyrolysis can pave the way towards the full exploitation of MSS value towards carbon, nutrients, and energy recovery. Many research lines can stem from this, giving lymph to a combination of MSS pyrolysis with novel biorefinery approaches. Challenges that need to be addressed are related to the MSS drying costs, the energetic and economic sustainment of the process, the necessity of new policies to allow MSS-pyrolysis products commercialization (*i.e.* biochar-based fertilizers), innovative ways for the enhancement of bio-oil fuel properties, and a deeper comprehension of the potentials of up-scaled syngas biological valorization.

Hopefully, addressing such issues might result in the achievement of a game-changing approach to managing MSS, thereby mitigating one of the most critical challenges in the fields of wastewater management and environmental pollution, contrasting climate change, and enhancing resource recovery from waste.

APPENDIX A

European legislation on municipal sewage sludge management

To establish more sustainable municipal sewage sludge (MSS) management practices, extensive legislation was produced by the European Commission. MSS is classified as a "non-hazardous" solid waste [338]. Several directives from the European Union such as the Water Framework Directive [339] and the Waste Framework Directive [340] influence MSS management by establishing a hierarchical approach foreseeing waste prevention (*e.g.* minimization techniques), preparation for reuse (*e.g.* chemical or biological stabilization), recycling (*e.g.* material recovery), other recovery (*e.g.* energy recovery), and disposal (*e.g.* landfilling) [54].

The implementation of the Council Directive 91/271/EEC [341] concerning urban wastewater treatment, also known as "Urban Waste Water Treatment Directive" (UWWTD), has affected the increase in the amount of generated MSS. However, the Directive encourages the valorization of MSS whenever appropriate and regulates its use in order to minimize hazardous effects on the environment; thus, it was determinant for adapting to other disposal and treatment methods beyond the landfill. Subsequently, the Council Directive 91/676/EEC [342], concerning water protection against pollution caused by nitrates from agricultural sources, resulted in a reduction of areas on which MSS can be used for agricultural purposes. Council Directive 1999/31/EEC [50] introduced stringent new standards related to landfilling of biodegradable waste, while Directive 2018/850 [343] amended the former by extending such limitations to "*waste that is suitable for recycling or other recovery*", therefore including MSS.

Generally, MSS recovery methods can be categorized under two different management routes: an organic recycling route (including agricultural spreading and

composting) and a route focused on the recovery of energy and materials (including thermochemical conversion methods) [51]. In order to align the Directive with the ambitions reported in the European Green Deal and the Zero Pollution Action Plan, the European Commission opened in 2020 a public consultation for the revision of the UWWTD [344], including new circular approaches to MSS management for the recovery of nutrients, materials and energy, as well as the importance of MSS usage as fertilizer.

The most meaningful document concerning the organic recycling route is the Council Directive 1986/278/EEC [345], also known as "Sewage Sludge Directive" (SSD), which is aimed at regulating the use of MSS in agriculture. On the other hand, toxic organic and inorganic pollutants contained within MSS could be highly dangerous if dispersed in the environment because of their persistence and possible toxicity to people and wildlife [3–7]. By defining specific limits on potentially toxic elements (PTEs) concentration both in treated MSS and soils on which MSS is distributed, the SSD aimed at preventing harmful effects on soil, vegetation, animals and humans. To this end, it also prohibits the use of untreated MSS on agricultural land unless it is injected or incorporated into the soil. The SSD did not introduce limits on organic pollutants concentration nor on the presence of pathogens in soils. Therefore, to mitigate the environmental risks associated with the agricultural reuse of MSS, many EU Member States have established their own legislation to regulate these substances within MSS and/or soils, further setting more stringent limits for PTEs [346]. Lately, in light of the most recent environmental strategies and planning tools such as the New Circular Economy Action Plan [347], the European Green Deal [348], the Bioeconomy Strategy [349], the Farm to Fork Strategy [350], the EU Biodiversity Strategy for 2030 [351], and the post-Covid-19 recovery plan for Europe [352], the Directive has gained additional significance and a process of revision is currently ongoing [353], in order to exploit the potential of MSS in the context of the circular economy transition, in order to contribute to increasing resource efficiency and protect human health. A first result of this revision process has been the new Regulation 2019/1009 [131] on the market of fertilizing products, introducing for the first time organic and, in particular, bio-based and recovered fertilizers beyond

mineral/inorganic ones as fertilizing products, aiming to harmonize their production and composition. Due to their micropollutant content, “pyrolysis and gasification materials” (including biochar) derived from MSS have been excluded from the EU fertilizing products [354].

Regarding the material recycling route, many valuable raw materials can be recovered from MSS: water, compost, nutrients, agronomic additives, sulfur, phosphorous salts, fibers, proteins, biomass, up to more complex materials such as biopolymers [9,24,355–358]. However, in accordance with the Waste Framework Directive, most of these materials are classified as waste when obtained from MSS. Nevertheless, the new Fertilising Products Regulation [131], applied from July 2022, already defined conditions to obtain an “End-of-Waste” status for struvite and ash-based products from MSS. In order to develop a real market for such secondary materials, additional criteria should be proposed and discussed at the EU level in the near future.

Finally, concerning the energy recovery route, the EU aims to the following main waste-to-energy processes: incineration, AD, production of waste-derived solid, liquid or gaseous fuels, and other thermal treatments such as pyrolysis or gasification [359]. With this scope, Directive 2009/28/EC [360] (subsequently modified to the currently in-force Directive 2018/2001 [66]) promoted the use of energy from renewable sources, recognizing energy derived from biomass, landfills, and WWTP as a renewable energy source.

APPENDIX B

Elemental composition of biochar and bio-oil

The elemental composition of biochar and bio-oils produced through thermal and catalytic pyrolysis of municipal sewage sludge (MSS) are reported in Table B.1 and Table B.2, respectively. These results were employed for the determination of S migration from MSS to the pyrolysis products during thermal and catalytic pyrolysis tests.

	C (% wt db)	H (% wt db)	N (% wt db)	S (% wt db)
Thermal pyrolysis				
BC350	36.90	2.48	5.32	0.61
BC500	28.71	0.86	3.92	0.45
BC650	28.00	0.29	2.88	0.45
BC800	28.10	0.15	1.63	0.46
Catalytic pyrolysis				
BC500 (HMOR_220)	46.72	2.13	5.71	1.23
BC500 (H-ZSM5_250)	32.35	0.32	4.35	0.75
BC500 (H-ZSM5_1880)	33.07	0.94	4.21	0.59

Table B. 1. Elemental composition of biochar. The results of the elemental analysis conducted on biochar produced from thermal and catalytic pyrolysis of municipal sewage sludge (MSS) are reported. Thermal pyrolysis of MSS was conducted at 350, 500, 650, and 800 °C. The catalytic process was conducted at 500 °C, by employing different types of zeolites (H-Mordenite and HZSM-5), with variable Si/Al ratio (SAR). wt: on a weight basis; db: on a dry basis;

	C (% wt db)	H (% wt db)	N (% wt db)	S (% wt db)
Thermal pyrolysis				
BO350	20.17	10.17	5.74	0.60
BO500	15.24	9.90	6.58	0.51
BO650	14.90	9.55	5.72	0.67
BO800	12.90	9.87	6.64	0.59
Catalytic pyrolysis				
BO500 (HMOR_220)	15.40	11.31	6.72	0.80
BO500 (H-ZSM5_250)	9.81	10.13	4.05	0.50
BO500 (H-ZSM5_1880)	14.09	9.33	5.18	0.59

Table B. 2. Elemental composition of bio-oil. The results of the elemental analysis conducted on bio-oil produced from thermal and catalytic pyrolysis of municipal sewage sludge (MSS) are reported. Thermal pyrolysis of MSS was conducted at 350, 500, 650, and 800 °C. The catalytic process was conducted at 500 °C, by employing different types of zeolites (H-Mordenite and HZSM-5), with variable Si/Al ratio (SAR). wt: on a weight basis; db: on a dry basis;

APPENDIX C

C1. Hydrogen-oxidizing bacteria enrichment

Active compost sampled from a composting facility located in the Campania region (Italy) was used as source of microorganisms for the enrichment of the HOB culture. About 30 g of compost were mixed with 100 mL of mineral medium for HOB growth prepared according to Yu et al., (2013) (see **Table C1.1**), and agitated with a magnetic stirrer for 1 hour at 600 rpm.

HOB mineral medium		
NaH_2PO_4	2.029	g/L
K_2HPO_4	2.835	g/L
NH_4Cl	1.000	g/L
$MgSO_4$	0.244	g/L
$NaHCO_3$	0.500	g/L
$CaCl_2 \cdot 2H_2O$	0.010	g/L
$FeCl_3 \cdot 6H_2O$	0.009	g/L
$C_6H_8O_7 \cdot H_2O$	0.040	g/L
Trace element solution	1.000	mL/L
Trace element solution		
H_3BO_3	0.600	g/L
$CoSO_4 \cdot 7H_2O$	0.590	g/L
$ZnSO_4 \cdot 7H_2O$	0.200	g/L
$MnSO_4 \cdot H_2O$	0.071	g/L
$Na_2MoO_4 \cdot 2H_2O$	0.066	g/L
$NiCl_2 \cdot 6H_2O$	0.040	g/L
$CuSO_4 \cdot 5H_2O$	0.020	g/L

Table C1. 1.. Composition of the mineral medium used for the HOB enrichment, prepared accordingly to Yu et al., (2013).

After settling, 12 mL of supernatant were collected and diluted in mineral medium to a final volume of 120 mL, to start the enrichment. The HOB culture was enriched in three gas tight bottles with a liquid volume of 40 mL and a total volume of 306 mL, sealed with a butyl rubber stopper. The headspace of the bottles was filled with a standard feed gas mixture for HOB growth of $H_2/O_2/CO_2$, prepared with a 65/20/15 v/v/v composition according to the HOB enrichment procedure reported by Matassa et al., (2016).

During a first acclimation phase of about three weeks, the liquid phase of the culture was not exchanged, and only the gas headspace was completely refreshed every time the pressure dropped below 0.7 bar by following the same procedure described previously for the preparation of the feed gas mixture. The acclimatation phase ended when the culture started showing a high daily gas consumption (see **Figure C1.1**).

Subsequently, a series of enrichment cycles were set by exchanging 50% of the culture volume with fresh medium every 1 to 2 to days, thereby imposing a hydraulic and solid retention of about 2 to 4 days. Each cycle was started with the same initial pressure (1.5 bar) and feed gas composition (266, 82 and 61 mL of H_2, O_2 and CO_2, respectively). After 40 days, the culture was considered fully enriched as it showed reproducible and consistent growth, achieving a biomass concentration of about 0.8 to 1.2 g VSS/L (see **Figure C1.1**). Afterwards, the enriched culture was maintained under the same operating conditions throughout the whole duration of the experimentation to serve as source of fresh and active inoculum for the experimental tests.

.

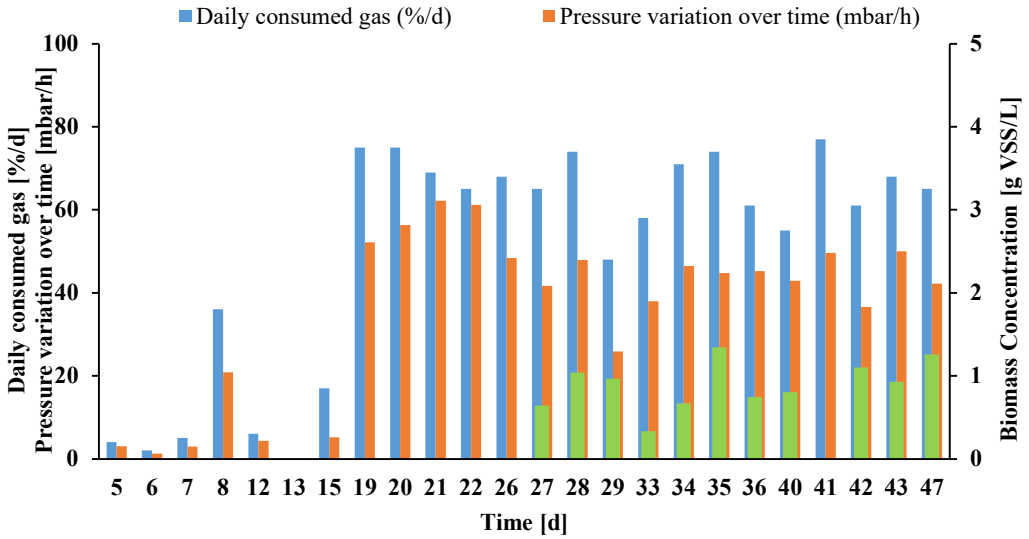


Figure C1. 1. Gas consumption, pressure variation over time and biomass concentration observed in the preliminary enrichment phase.

C2. Simulation of H_2S concentrations in syngas

The following equations describe the solubilization of $H_2S(g)$ in water (Eq. C2.1) and its dissociation to form of $S^{2-}_{(aq)}$ (Eq. C2.2 and C2.3). The same concentration of $S^{2-}_{(aq)}$ can be obtained by dissolving Na_2S in water (Eq. C2.4).

$$H_2S_{(g)} \overset{K_{H_2S}}{\Longleftrightarrow} H_2S_{(aq)} \quad \text{(C2.1)}$$

$$H_2S_{(aq)} \overset{K_{a,1}}{\Longleftrightarrow} H^+_{(aq)} + HS^-_{(aq)} \quad \text{(C2.2)}$$

$$HS^-_{(aq)} \overset{K_{a,2}}{\Longleftrightarrow} H^+_{(aq)} + S^{2-}_{(aq)} \quad \text{(C2.3)}$$

$$Na_2S_{(s)} \overset{H_2O}{\longrightarrow} 2Na^+_{(aq)} + S^{2-}_{(aq)} \quad \text{(C2.4)}$$

Where K_{H2S}, $K_{\alpha,1}$, and $K_{\alpha,2}$ were calculated according to Xu et al., (2020). The calculated concentrations of $Na_2S \cdot 9H_2O$ set towards the simulation of equivalent H_2S gaseous concentrations are reported in **Table C2.1**.

Condition	$Na_2S \cdot 9H_2O$ stock solution (g/L)	Exchanged volume (mL)	$Na_2S \cdot 9H_2O_{(aq)}$ (mg/L)	Equivalent $H_2S_{(g)}$ (ppmv)	pH	Temperature (°C)	Pressure (bar)
H_2S-2	1.916	1.0	47.9	2,000	6.3 – 6.8	30	1.5
H_2S-3		1.5	71.9	3,000			
H_2S-4		2.0	95.8	4,000			
H_2S-6	3.833	1.5	143.7	6,000			
H_2S-8		2.0	191.6	8,000			

Table C2. 1. Concentration of $Na_2S \cdot 9H_2O$ used in each tested condition and equivalent H_2S concentration in the gas headspace. The calculated H_2S concentrations were dependent upon the pH, temperature and pressure conditions set in each test.

C3: Balanced stoichiometric equation for HOB

Prior to the calculation of the balanced stoichiometric equation for HOB, a general equation (Eq. C3.1) was obtained accordingly to Yu and Lu (2019) by combining half-reactions expressing cell synthesis, hydrogen oxidation, and oxygen reduction in chemolithotrophic metabolism [362]:

$$0.1881\ f_c\ CO_2 + 0.5\ H_2 + 0.25\ f_a\ O_2 + 0.0594\ f_c\ HCO_3^- + 0.0594\ f_c\ NH_4^+ \rightarrow$$
$$\rightarrow 0.2475\ f_c\ CH_{1.68}O_{0.46}N_{0.24} + (0.5\ f_a + 0.44\ f_c)\ H_2O \quad \text{(C3.1)}$$

Where f_a represents the molar fraction of electrons (free energy) coming from the electron donor (i.e. H_2) and employed for energy purposes, while f_c represents the molar fraction of electrons employed for cell synthesis. In physiological conditions, this partitioning is balanced, therefore these two molar fractions are complementary and their sum is 1 (see Eq. C3.3). The molar fractions f_a and f_c can be calculated from the ash-free biomass yield on H_2 according to the equations (Eq. C3.2 and C3.3) reported below (Yu and Lu, 2019).

$$Y_{H_2} = \frac{f_c\ (0.2475)(MM_{CH_{1.68}O_{0.46}N_{0.24}})}{(0.5)(MM_{H_2})} = \frac{f_c\ (0.2475)(24.4)}{(0.5)(2)} \quad \text{(C3.2)}$$

$$f_a + f_c = 1 \quad \text{(C3.3)}$$

Where Y_{H_2} represents the ash-free biomass yield on H_2 (g VSS/g H_2), while 0.2475 and 0.5 are the stoichiometric coefficients of biomass ($CH_{1.68}O_{0.46}N_{0.24}$) and H_2 in Eq. C3.1, respectively, and 24.4 and 2 are their molar mass (MM) (g/mol), respectively.

By considering the generic interval for biomass yield on H_2 (0.07 - 0.28 g VSS/g H_2-COD) indicated for HOB by Matassa et al. (2016), an average biomass yield on H_2 of 0.18 g VSS/g H_2-COD (equal to 0.14 g VSS/g H_2) was assumed. With this value, partitioning of free energy would happen with f_a=0.76 and f_c=0.24, resulting in the following balanced stoichiometric equation, normalized for the synthesis of one mole of carbon into biomass [361] (Eq. C3.4):

$$CO_2 + 8.47\,H_2 + 3.22\,O_2 + 0.24\,NH_3 \rightarrow CH_{1.68}O_{0.46}N_{0.24} + 8.23\,H_2O \quad \text{(C3.4)}$$

C4: Sequence filtering and taxonomic assignation in microbiological analysis

The raw sequences were processed using qiime2 v2022.2 with DADA2 pipeline and SILVA db v138.1. The reads were trimmed to remove primer sequences; reads with ambiguous, poor-quality bases (phred quality score lower than 20) were discarded. The DADA2 algorithm was used to dereplicate and denoise the obtained reads. The paired reads were then mrged, and the chimeras identified and removed. Finally, the taxonomy was assigned to the sequence variants using the naive Bayesian classifier (scikit-learn v0.22.1) trained on V3-V4 region for 16S sequences and taxonomy data (SILVA v138.1).

C5: Direct NH_3 utilization from syngas to microbial protein

The evolution of the residual NH_4^+-N concentration during the long-term batch tests was monitored for each experimental condition (**Figure C5.1**).

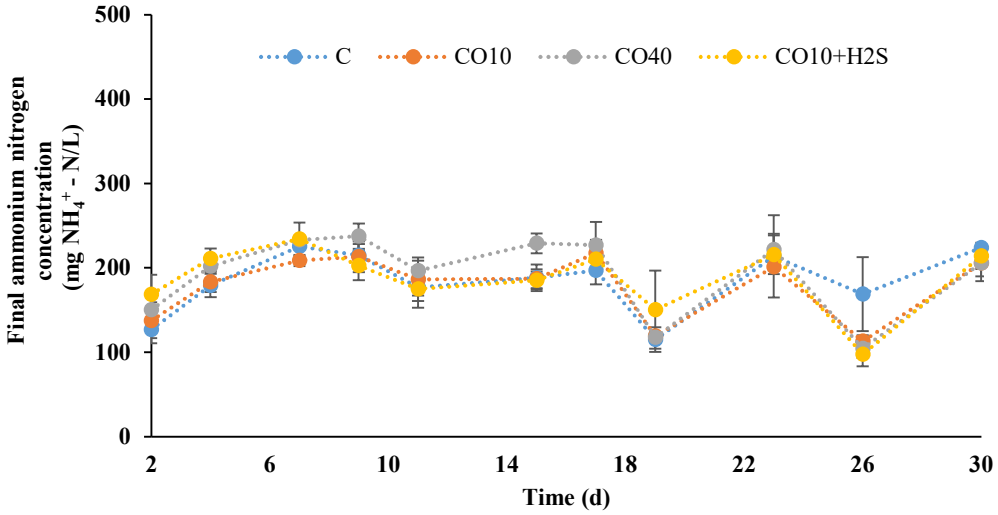


Figure C5. 1. Trend of the final NH_4^+-N concentration in each condition during the long-term batch tests.

Based on the measured NH_4^+-N and H_2 consumption within each experimental condition, a NH_4^+-N/H_2 characterizing the aerobic fermentation by means of HOB during the long-term batch test was calculated according to Eq. C5.1:

$$(NH_4^+ - N/H_2)_{HOB} = \frac{(NH_4^+ - N)_{uptake}}{(H_2)_{gas\ uptake}} \quad \text{(C5.1)}$$

Where $(NH_4^+\text{-N})_{uptake}$ and $(H_2)_{gas\ uptake}$ represent the average moles of NH_4^+-N and H_2 consumed within each experimental condition.

The NH_3-N/H_2 ratio that can generally characterize MSS-derived syngas was instead calculated according to the following Eq. C5.2:

$$(NH_3 - N/H_2)_{Syngas} = \frac{\%NH_3\text{-}N\ (v/v)}{\%H_2\ (v/v)} \quad \text{(C5.2)}$$

Where $\%NH_3$-N (v/v) and $\%H_2$ (v/v) represent generic values for NH_3-N and H_2 concentrations available in MSS-derived syngas according to the literature [71,97,217,314].

REFERENCES

[1] R. Canziani, L. Spinosa, Sludge from wastewater treatment plants, Industrial and Municipal Sludge: Emerging Concerns and Scope for Resource Recovery (2019) 3–30. https://doi.org/10.1016/B978-0-12-815907-1.00001-5.

[2] N. Gao, K. Kamran, C. Quan, P.T. Williams, Thermochemical conversion of sewage sludge: A critical review, Prog Energy Combust Sci 79 (2020) 100843. https://doi.org/10.1016/j.pecs.2020.100843.

[3] C. Li, N. Le-Minh, J.A. McDonald, A.S. Kinsela, R.M. Fisher, D. Liu, R.M. Stuetz, Occurrence and risk assessment of trace organic contaminants and metals in anaerobically co-digested sludge, Science of The Total Environment 816 (2022) 151533. https://doi.org/10.1016/J.SCITOTENV.2021.151533.

[4] M.D. Hatinoğlu, F.D. Sanin, Sewage sludge as a source of microplastics in the environment: A review of occurrence and fate during sludge treatment, J Environ Manage 295 (2021) 113028. https://doi.org/10.1016/J.JENVMAN.2021.113028.

[5] L. Lamastra, N.A. Suciu, M. Trevisan, Sewage sludge for sustainable agriculture: Contaminants' contents and potential use as fertilizer, Chemical and Biological Technologies in Agriculture 5 (2018). https://doi.org/10.1186/s40538-018-0122-3.

[6] M. Langone, G. Sabia, L. Petta, L. Zanetti, P. Leoni, D. Basso, Evaluation of the aerobic biodegradability of process water produced by hydrothermal carbonization and inhibition effects on the heterotrophic biomass of an activated sludge system, J Environ Manage 299 (2021) 113561. https://doi.org/10.1016/J.JENVMAN.2021.113561.

[7] F. Corradini, P. Meza, R. Eguiluz, F. Casado, E. Huerta-Lwanga, V. Geissen, Evidence of microplastic accumulation in agricultural soils from sewage sludge disposal, Science of The Total Environment 671 (2019) 411–420. https://doi.org/10.1016/J.SCITOTENV.2019.03.368.

[8] F.C. Jorge, M.A.P. Dinis, Sewage sludge disposal with energy recovery: a review, Proceedings of the Institution of Civil Engineers - Waste and Resource Management 166 (2013) 14–28. https://doi.org/10.1680/warm.12.00004.

[9] M. Hu, H. Hu, Z. Ye, S. Tan, K. Yin, Z. Chen, D. Guo, H. Rong, J. Wang, Z. Pan, Z.T. Hu, A review on turning sewage sludge to value-added energy and materials via thermochemical conversion towards carbon neutrality, J Clean Prod 379 (2022) 134657. https://doi.org/10.1016/J.JCLEPRO.2022.134657.

[10] A. Raj, A. Yadav, S. Arya, R. Sirohi, S. Kumar, A.P. Rawat, R.S. Thakur, D.K. Patel, L. Bahadur, A. Pandey, Preparation, characterization and agri applications of biochar produced by pyrolysis of sewage sludge at different temperatures, Science of The Total Environment 795 (2021) 148722. https://doi.org/10.1016/J.SCITOTENV.2021.148722.

[11] A. Ahmad, P. Chowdhary, N. Khan, D. Chaurasia, S. Varjani, A. Pandey, P. Chaturvedi, Effect of sewage sludge biochar on the soil nutrient, microbial abundance, and plant biomass: A sustainable approach towards mitigation of solid waste, Chemosphere 287 (2022) 132112. https://doi.org/10.1016/J.CHEMOSPHERE.2021.132112.

[12] S. Jung, Y.K. Park, E.E. Kwon, Strategic use of biochar for CO2 capture and sequestration, Journal of CO2 Utilization 32 (2019) 128–139. https://doi.org/10.1016/J.JCOU.2019.04.012.

[13] S. Jellali, B. Khiari, M. Usman, H. Hamdi, Y. Charabi, M. Jeguirim, Sludge-derived biochars: A review on the influence of synthesis conditions on pollutants removal efficiency from wastewaters, Renewable and Sustainable Energy Reviews 144 (2021) 111068. https://doi.org/10.1016/J.RSER.2021.111068.

[14] M. Haghighat, N. Majidian, A. Hallajisani, M. samipourgiri, Production of bio-oil from sewage sludge: A review on the thermal and catalytic conversion by pyrolysis, Sustainable Energy Technologies and Assessments 42 (2020) 100870. https://doi.org/10.1016/J.SETA.2020.100870.

[15] S. Xiu, A. Shahbazi, Bio-oil production and upgrading research: A review, Renewable and Sustainable Energy Reviews 16 (2012) 4406–4414. https://doi.org/10.1016/J.RSER.2012.04.028.

[16] M. Fiore, V. Magi, A. Viggiano, Internal combustion engines powered by syngas: A review, Appl Energy 276 (2020) 115415. https://doi.org/10.1016/j.apenergy.2020.115415.

[17] R.G. dos Santos, A.C. Alencar, Biomass-derived syngas production via gasification process and its catalytic conversion into fuels by Fischer Tropsch synthesis: A review, Int J Hydrogen Energy 45 (2020) 18114–18132. https://doi.org/10.1016/J.IJHYDENE.2019.07.133.

[18] V. Pelagalli, S. Matassa, M. Race, M. Langone, S. Papirio, P.N.L. Lens, M. Lazzazzara, A. Frugis, L. Petta, G. Esposito, Syngas-driven sewage sludge conversion to microbial protein through H2S- and CO-tolerant hydrogen-oxidizing bacteria, Water Res (2023) 120698. https://doi.org/10.1016/j.watres.2023.120698.

[19] X. Sun, H.K. Atiyeh, R.L. Huhnke, R.S. Tanner, Syngas fermentation process development for production of biofuels and chemicals: A review, Bioresour Technol Rep 7 (2019) 100279. https://doi.org/10.1016/J.BITEB.2019.100279.

[20] A. Grimalt-Alemany, I. V. Skiadas, H.N. Gavala, Syngas biomethanation: state-of-the-art review and perspectives, Biofuels, Bioproducts and Biorefining 12 (2018) 139–158. https://doi.org/10.1002/bbb.1826.

[21] Eurostat, Sewage Sludge Production and Disposal from Urban Wastewater, (2022). https://ec.europa.eu/eurostat/databrowser/product/page/ten00030 (accessed April 7, 2024).

[22] M. Bagheri, T. Bauer, L.E. Burgman, E. Wetterlund, Fifty years of sewage sludge management research: Mapping researchers' motivations and concerns, J Environ Manage 325 (2023) 116412. https://doi.org/10.1016/j.jenvman.2022.116412.

[23] S.S.A. Syed-Hassan, Y. Wang, S. Hu, S. Su, J. Xiang, Thermochemical processing of sewage sludge to energy and fuel: Fundamentals, challenges and considerations, Renewable and Sustainable Energy Reviews 80 (2017) 888–913. https://doi.org/10.1016/J.RSER.2017.05.262.

[24] A. Raheem, V.S. Sikarwar, J. He, W. Dastyar, D.D. Dionysiou, W. Wang, M. Zhao, Opportunities and challenges in sustainable treatment and resource reuse of sewage sludge: A review, Chemical Engineering Journal 337 (2018) 616–641. https://doi.org/10.1016/j.cej.2017.12.149.

[25] R.R. Bora, R.E. Richardson, F. You, Resource recovery and waste-to-energy from wastewater sludge via thermochemical conversion technologies in support of circular economy: a comprehensive review, BMC Chemical Engineering 2 (2020). https://doi.org/10.1186/s42480-020-00031-3.

[26] M. Langone, D. Basso, Process Waters from Hydrothermal Carbonization of Sludge: Characteristics and Possible Valorization Pathways, Int J Environ Res Public Health 17 (2020) 6618. https://doi.org/10.3390/ijerph17186618.

[27] B. Galey, M. Gautier, B. Kim, D. Blanc, V. Chatain, G. Ducom, N. Dumont, R. Gourdon, Trace metal elements vaporization and phosphorus recovery during sewage sludge thermochemical treatment – A review, J Hazard Mater 424 (2022) 127360. https://doi.org/10.1016/J.JHAZMAT.2021.127360.

[28] I. Fonts, G. Gea, M. Azuara, J. Ábrego, J. Arauzo, Sewage sludge pyrolysis for liquid production: A review, Renewable and Sustainable Energy Reviews 16 (2012) 2781–2805. https://doi.org/10.1016/j.rser.2012.02.070.

[29] Y. Cao, A. Pawłowski, Sewage sludge-to-energy approaches based on anaerobic digestion and pyrolysis: Brief overview and energy efficiency assessment, Renewable and Sustainable Energy Reviews 16 (2012) 1657–1665. https://doi.org/10.1016/J.RSER.2011.12.014.

[30] V. Frišták, M. Pipíška, G. Soja, Pyrolysis treatment of sewage sludge: A promising way to produce phosphorus fertilizer, J Clean Prod 172 (2018) 1772–1778. https://doi.org/10.1016/J.JCLEPRO.2017.12.015.

[31] H. Shahbeig, M. Nosrati, Pyrolysis of municipal sewage sludge for bioenergy production: Thermo-kinetic studies, evolved gas analysis, and techno-socio-economic assessment, Renewable and Sustainable Energy Reviews 119 (2020) 109567. https://doi.org/10.1016/J.RSER.2019.109567.

[32] W. Metcalf, C. Eddy, Wastewater Engineering: Treatment and Resource Recovery, Fifth Edition, 2014.

[33] P. Manara, A. Zabaniotou, Towards sewage sludge based biofuels via thermochemical conversion - A review, Renewable and Sustainable Energy Reviews 16 (2012) 2566–2582. https://doi.org/10.1016/j.rser.2012.01.074.

[34] M.U. Hanif, M. Zwawi, S.C. Capareda, H. Iqbal, M. Algarni, B.F. Felemban, A. Bahadar, A. Waqas, Influence of Pyrolysis Temperature on Product Distribution and Characteristics of Anaerobic Sludge, Energies (Basel) 13 (2019) 79. https://doi.org/10.3390/en13010079.

[35] M. Schnell, T. Horst, P. Quicker, Thermal treatment of sewage sludge in Germany: A review, J Environ Manage 263 (2020) 110367. https://doi.org/10.1016/j.jenvman.2020.110367.

[36] Z. Wang, T. Liu, H. Duan, Y. Song, X. Lu, S. Hu, Z. Yuan, D. Batstone, M. Zheng, Post-treatment options for anaerobically digested sludge: Current status

and future prospect, Water Res 205 (2021) 117665. https://doi.org/10.1016/J.WATRES.2021.117665.

[37] B. Wu, X. Dai, X. Chai, Critical review on dewatering of sewage sludge: Influential mechanism, conditioning technologies and implications to sludge re-utilizations, Water Res 180 (2020) 115912. https://doi.org/10.1016/J.WATRES.2020.115912.

[38] O.S. Djandja, L.-X. Yin, Z.-C. Wang, P.-G. Duan, From wastewater treatment to resources recovery through hydrothermal treatments of municipal sewage sludge: A critical review, Process Safety and Environmental Protection 151 (2021) 101–127. https://doi.org/10.1016/j.psep.2021.05.006.

[39] G. Jiang, D. Xu, B. Hao, L. Liu, S. Wang, Z. Wu, Thermochemical methods for the treatment of municipal sludge, J Clean Prod 311 (2021) 127811. https://doi.org/10.1016/J.JCLEPRO.2021.127811.

[40] Y. Xiao, A. Raheem, L. Ding, W.-H. Chen, X. Chen, F. Wang, S.-L. Lin, Pretreatment, modification and applications of sewage sludge-derived biochar for resource recovery- A review, Chemosphere 287 (2022) 131969. https://doi.org/10.1016/J.CHEMOSPHERE.2021.131969.

[41] A. Zhou, X. Wang, S. Yu, S. Deng, H. Tan, H. Mikulčić, Process design and optimization on self-sustaining pyrolysis and carbonization of municipal sewage sludge, Waste Management 159 (2023) 125–133. https://doi.org/10.1016/j.wasman.2023.01.035.

[42] W. Zhang, T. Jiang, Y. Liang, Stabilization of per- and polyfluoroalkyl substances (PFAS) in sewage sludge using different sorbents, Journal of Hazardous Materials Advances 6 (2022) 100089. https://doi.org/10.1016/j.hazadv.2022.100089.

[43] E. Gagliano, M. Sgroi, P.P. Falciglia, F.G.A. Vagliasindi, P. Roccaro, Removal of poly- and perfluoroalkyl substances (PFAS) from water by adsorption: Role of PFAS chain length, effect of organic matter and challenges in adsorbent regeneration, Water Res 171 (2020) 115381. https://doi.org/10.1016/j.watres.2019.115381.

[44] W.-J. Liu, W.-W. Li, H. Jiang, H.-Q. Yu, Fates of Chemical Elements in Biomass during Its Pyrolysis, Chem Rev 117 (2017) 6367–6398. https://doi.org/10.1021/acs.chemrev.6b00647.

[45] N. Ruiz-Gómez, V. Quispe, J. Ábrego, M. Atienza-Martínez, M.B. Murillo, G. Gea, Co-pyrolysis of sewage sludge and manure, Waste Management 59 (2017) 211–221. https://doi.org/10.1016/j.wasman.2016.11.013.

[46] J. Alvarez, G. Lopez, M. Amutio, M. Artetxe, I. Barbarias, A. Arregi, J. Bilbao, M. Olazar, Characterization of the bio-oil obtained by fast pyrolysis of sewage sludge in a conical spouted bed reactor, Fuel Processing Technology 149 (2016) 169–175. https://doi.org/10.1016/J.FUPROC.2016.04.015.

[47] P. Gururani, P. Bhatnagar, B. Bisht, K.K. Jaiswal, V. Kumar, S. Kumar, M.S. Vlaskin, A. V. Grigorenko, K.G. Rindin, Recent advances and viability in sustainable thermochemical conversion of sludge to bio-fuel production, Fuel 316 (2022) 123351. https://doi.org/10.1016/J.FUEL.2022.123351.

[48] O. Suárez-Iglesias, J.L. Urrea, P. Oulego, S. Collado, M. Díaz, Valuable compounds from sewage sludge by thermal hydrolysis and wet oxidation. A review, Science of The Total Environment 584–585 (2017) 921–934. https://doi.org/10.1016/J.SCITOTENV.2017.01.140.

[49] S. Xiong, J. Zhuo, B. Zhang, Q. Yao, Effect of moisture content on the characterization of products from the pyrolysis of sewage sludge, J Anal Appl Pyrolysis 104 (2013) 632–639. https://doi.org/10.1016/J.JAAP.2013.05.003.

[50] European Commission, COUNCIL DIRECTIVE 1999/31/EC of 26 April 1999 on the landfill of waste, (1999). http://data.europa.eu/eli/dir/1999/31/oj (accessed April 7, 2024).

[51] M. Kacprzak, E. Neczaj, K. Fijałkowski, A. Grobelak, A. Grosser, M. Worwag, A. Rorat, H. Brattebo, Å. Almås, B.R. Singh, Sewage sludge disposal strategies for sustainable development, Environ Res 156 (2017) 39–46. https://doi.org/10.1016/j.envres.2017.03.010.

[52] E. Neczaj, K. Fija, A. Grobelak, A. Grosser, Sewage sludge disposal strategies for sustainable development, 156 (2017) 39–46. https://doi.org/10.1016/j.envres.2017.03.010.

[53] R. Dhanker, S. Chaudhary, S. Goyal, V.K. Garg, Influence of urban sewage sludge amendment on agricultural soil parameters, Environ Technol Innov 23 (2021) 101642. https://doi.org/10.1016/j.eti.2021.101642.

[54] M.C. Collivignarelli, A. Abbà, A. Frattarola, M.C. Miino, S. Padovani, I. Katsoyiannis, V. Torretta, sustainability Legislation for the Reuse of Biosolids on Agricultural Land in Europe: Overview, (2019). https://doi.org/10.3390/su11216015.

[55] S. Uçaroğlu, U. Alkan, Composting of wastewater treatment sludge with different bulking agents, J Air Waste Manage Assoc 66 (2016) 288–295. https://doi.org/10.1080/10962247.2015.1131205.

[56] D. Kulikowska, Kinetics of organic matter removal and humification progress during sewage sludge composting, Waste Management 49 (2016) 196–203. https://doi.org/10.1016/J.WASMAN.2016.01.005.

[57] S.H. Joo, F. Dello Monaco, E. Antmann, P. Chorath, Sustainable approaches for minimizing biosolids production and maximizing reuse options in sludge management: A review, J Environ Manage 158 (2015) 133–145. https://doi.org/10.1016/j.jenvman.2015.05.014.

[58] Z. Liu, B.K. Mayer, K. Venkiteshwaran, S. Seyedi, A.S.K. Raju, D. Zitomer, P.J. McNamara, The state of technologies and research for energy recovery from municipal wastewater sludge and biosolids, Curr Opin Environ Sci Health 14 (2020). https://doi.org/10.1016/j.coesh.2019.12.004.

[59] V.K. Tyagi, S.-L. Lo, Energy and Resource Recovery From Sludge, Environmental Materials and Waste (2016). https://doi.org/10.1016/B978-0-12-803837-6.00010-X.

[60] S. Ducoli, A. Zacco, E. Bontempi, Incineration of sewage sludge and recovery of residue ash as building material: A valuable option as a consequence of the COVID-19 pandemic, J Environ Manage 282 (2021) 111966. https://doi.org/10.1016/J.JENVMAN.2021.111966.

[61] M. Kasina, B. Kajdas, M. Michalik, The leaching potential of sewage sludge and municipal waste incineration ashes in terms of landfill safety and potential reuse, Science of The Total Environment 791 (2021) 148313. https://doi.org/10.1016/J.SCITOTENV.2021.148313.

[62] European Commission, COMMUNICATION FROM THE COMMISSION TO THE EUROPEAN PARLIAMENT, THE COUNCIL, THE EUROPEAN ECONOMIC AND SOCIAL COMMITTEE AND THE COMMITTEE OF THE REGIONS Critical Raw Materials Resilience: Charting a Path towards greater Security and Sustainability, (2020). https://eur-lex.europa.eu/legal-content/EN/TXT/HTML/?uri=CELEX:52020DC0474 (accessed May 29, 2024).

[63] Y. Xu, L. Zhang, J. Chen, T. Liu, N. Li, J. Xu, W. Yin, D. Li, Y. Zhang, X. Zhou, Phosphorus recovery from sewage sludge ash (SSA): An integrated technical, environmental and economic assessment of wet-chemical and thermochemical methods, J Environ Manage 344 (2023) 118691. https://doi.org/10.1016/j.jenvman.2023.118691.

[64] P. Ma, C. Rosen, Land application of sewage sludge incinerator ash for phosphorus recovery: A review, Chemosphere 274 (2021) 129609. https://doi.org/10.1016/J.CHEMOSPHERE.2021.129609.

[65] Y. Liang, D. Xu, P. Feng, B. Hao, Y. Guo, S. Wang, Municipal sewage sludge incineration and its air pollution control, J Clean Prod 295 (2021) 126456. https://doi.org/10.1016/J.JCLEPRO.2021.126456.

[66] European Parliament and Council, DIRECTIVE (EU) 2018/2001 OF THE EUROPEAN PARLIAMENT AND OF THE COUNCIL of 11 December 2018 on the promotion of the use of energy from renewable sources, (2018). https://eur-lex.europa.eu/legal-content/EN/TXT/HTML/?uri=CELEX:32018L2001 (accessed June 11, 2024).

[67] European Parliament and Council, Directive (EU) 2018/851 of the European Parliament and of the Council of 30 May 2018 amending Directive 2008/98/EC on waste, (2018). http://data.europa.eu/eli/dir/2018/851/oj (accessed July 21, 2023).

[68] L. Zhang, B. Xiao, Z. Hu, S. Liu, G. Cheng, P. He, L. Sun, Tar-free fuel gas production from high temperature pyrolysis of sewage sludge, Waste Management 34 (2014) 180–184. https://doi.org/10.1016/J.WASMAN.2013.10.020.

[69] A. Magdziarz, S. Werle, Analysis of the combustion and pyrolysis of dried sewage sludge by TGA and MS, Waste Management 34 (2014). https://doi.org/10.1016/j.wasman.2013.10.033.

[70] G. Liu, H. Song, J. Wu, Thermogravimetric study and kinetic analysis of dried industrial sludge pyrolysis, Waste Management 41 (2015) 128–133. https://doi.org/10.1016/J.WASMAN.2015.03.042.

[71] P.K. Ghodke, A.K. Sharma, J.K. Pandey, W.-H. Chen, A. Patel, V. Ashokkumar, Pyrolysis of sewage sludge for sustainable biofuels and value-added biochar production, J Environ Manage 298 (2021) 113450. https://doi.org/10.1016/J.JENVMAN.2021.113450.

[72] O.S. Djandja, Z.C. Wang, F. Wang, Y.P. Xu, P.G. Duan, Pyrolysis of municipal sewage sludge for biofuel production: A review, Ind Eng Chem Res 59 (2020) 16939–16956. https://doi.org/10.1021/acs.iecr.0c01546.

[73] L. Wang, Y. Chang, A. Li, Hydrothermal carbonization for energy-efficient processing of sewage sludge: A review, Renewable and Sustainable Energy Reviews 108 (2019) 423–440. https://doi.org/10.1016/j.rser.2019.04.011.

[74] M. Pecchi, M. Baratieri, Coupling anaerobic digestion with gasification, pyrolysis or hydrothermal carbonization: A review, Renewable and Sustainable Energy Reviews 105 (2019) 462–475. https://doi.org/10.1016/J.RSER.2019.02.003.

[75] W.T. Chen, M.A. Haque, T. Lu, A. Aierzhati, G. Reimonn, A perspective on hydrothermal processing of sewage sludge, Curr Opin Environ Sci Health 14 (2020) 63–73. https://doi.org/10.1016/J.COESH.2020.02.008.

[76] J.A. Garcia-Nunez, M.R. Pelaez-Samaniego, M.E. Garcia-Perez, I. Fonts, J. Abrego, R.J.M. Westerhof, M. Garcia-Perez, Historical Developments of Pyrolysis Reactors: A Review, Energy & Fuels 31 (2017) 5751–5775. https://doi.org/10.1021/acs.energyfuels.7b00641.

[77] F.-X. Collard, M. Carrier, J.F. Görgens, Fractionation of Lignocellulosic Material With Pyrolysis Processing, in: Biomass Fractionation Technologies for a Lignocellulosic Feedstock Based Biorefinery, Elsevier, 2016: pp. 81–101. https://doi.org/10.1016/B978-0-12-802323-5.00004-9.

[78] S. Hafeez, E. Pallari, G. Manos, A. Constantinou, Catalytic Conversion and Chemical Recovery, in: Plastics to Energy, Elsevier, 2019: pp. 147–172. https://doi.org/10.1016/B978-0-12-813140-4.00006-6.

[79] V. Dhyani, T. Bhaskar, Pyrolysis of Biomass, in: Biofuels: Alternative Feedstocks and Conversion Processes for the Production of Liquid and Gaseous Biofuels, Elsevier, 2019: pp. 217–244. https://doi.org/10.1016/B978-0-12-816856-1.00009-9.

[80] V.K. Guda, P.H. Steele, V.K. Penmetsa, Q. Li, Fast Pyrolysis of Biomass, in: Recent Advances in Thermo-Chemical Conversion of Biomass, Elsevier, 2015: pp. 177–211. https://doi.org/10.1016/B978-0-444-63289-0.00007-7.

[81] N. Gao, F. Wang, C. Quan, L. Santamaria, G. Lopez, P.T. Williams, Tire pyrolysis char: Processes, properties, upgrading and applications, Prog Energy Combust Sci 93 (2022) 101022. https://doi.org/10.1016/j.pecs.2022.101022.

[82] M.A. Munawar, P. Li, Q. Ma, Md.A. Haque, W.-T. Chen, Thermochemical conversions of municipal solid waste into fuels and chemicals, (2023) 239–305. https://doi.org/10.1016/bs.aibe.2023.02.002.

[83] M.U. Babler, A. Phounglamcheik, M. Amovic, R. Ljunggren, K. Engvall, Modeling and pilot plant runs of slow biomass pyrolysis in a rotary kiln, Appl Energy 207 (2017) 123–133. https://doi.org/10.1016/j.apenergy.2017.06.034.

[84] F. Campuzano, R.C. Brown, J.D. Martínez, Auger reactors for pyrolysis of biomass and wastes, Renewable and Sustainable Energy Reviews 102 (2019) 372–409. https://doi.org/10.1016/j.rser.2018.12.014.

[85] Kore, Waste to Renewable Diesel Facility, (n.d.). https://koreinfrastructure.com/projects/ (accessed May 9, 2024).

[86] energyforskning.dk, Large scale Fluid Bed Pyrolysis - DALL ENERGY ApS, (n.d.). https://energiforskning.dk/en/node/16796 (accessed May 9, 2024).

[87] Pyrotech Energy, Converting Biomass into BioFuels & Biochemicals, (n.d.). https://pyrotechenergy.com/about/ (accessed May 9, 2024).

[88] Aquagreen, Sustainable Biomass Treatment, (n.d.). https://aquagreen.dk/technology/ (accessed May 30, 2024).

[89] H. Luo, F. Cheng, B. Yu, L. Hu, J. Zhang, X. Qu, H. Yang, Z. Luo, Full-scale municipal sludge pyrolysis in China: Design fundamentals, environmental and economic assessments, and future perspectives, Science of The Total Environment 795 (2021) 148832. https://doi.org/10.1016/j.scitotenv.2021.148832.

[90] I. Fonts, M. Azuara, G. Gea, M.B. Murillo, Study of the pyrolysis liquids obtained from different sewage sludge, J Anal Appl Pyrolysis 85 (2009) 184–191. https://doi.org/10.1016/j.jaap.2008.11.003.

[91] J.G. Speight, Assessing fuels for gasification, in: Gasification for Synthetic Fuel Production, Elsevier, 2015: pp. 175–198. https://doi.org/10.1016/B978-0-85709-802-3.00008-4.

[92] P. Basu, Biomass Characteristics, in: Biomass Gasification, Pyrolysis and Torrefaction, Elsevier, 2018: pp. 49–91. https://doi.org/10.1016/B978-0-12-812992-0.00003-0.

[93] M.K. Hossain, V. Strezov, P.F. Nelson, Thermal characterisation of the products of wastewater sludge pyrolysis, J Anal Appl Pyrolysis 85 (2009) 442–446. https://doi.org/10.1016/j.jaap.2008.09.010.

[94] J. Fan, Y. Li, H. Yu, Y. Li, Q. Yuan, H. Xiao, F. Li, B. Pan, Using sewage sludge with high ash content for biochar production and Cu(II) sorption, Science of The Total Environment 713 (2020) 136663. https://doi.org/10.1016/j.scitotenv.2020.136663.

[95] A. Jaramillo-Arango, I. Fonts, F. Chejne, J. Arauzo, Product compositions from sewage sludge pyrolysis in a fluidized bed and correlations with temperature, J Anal Appl Pyrolysis 121 (2016) 287–296. https://doi.org/10.1016/j.jaap.2016.08.008.

[96] C. Karaca, S. Sözen, D. Orhon, H. Okutan, High temperature pyrolysis of sewage sludge as a sustainable process for energy recovery, Waste Management 78 (2018) 217–226. https://doi.org/10.1016/J.WASMAN.2018.05.034.

[97] N. Gao, J. Li, B. Qi, A. Li, Y. Duan, Z. Wang, Thermal analysis and products distribution of dried sewage sludge pyrolysis, J Anal Appl Pyrolysis 105 (2014) 43–48. https://doi.org/10.1016/J.JAAP.2013.10.002.

[98] X. Huang, J.P. Cao, P. Shi, X.Y. Zhao, X.B. Feng, Y.P. Zhao, X. Fan, X.Y. Wei, T. Takarada, Influences of pyrolysis conditions in the production and chemical composition of the bio-oils from fast pyrolysis of sewage sludge, J Anal Appl Pyrolysis 110 (2014) 353–362. https://doi.org/10.1016/J.JAAP.2014.10.003.

[99] N. Gao, C. Quan, B. Liu, Z. Li, C. Wu, A. Li, Continuous Pyrolysis of Sewage Sludge in a Screw-Feeding Reactor: Products Characterization and Ecological Risk Assessment of Heavy Metals, Energy & Fuels 31 (2017) 5063–5072. https://doi.org/10.1021/acs.energyfuels.6b03112.

[100] M. Halalsheh, K. Shatanawi, R. Shawabkeh, G. Kassab, H. Mohammad, M. Adawi, S. Ababneh, A. Abdullah, N. Ghantous, N. Balah, S. Almomani, Impact of temperature and residence time on sewage sludge pyrolysis for combined carbon sequestration and energy production, Heliyon 10 (2024) e28030. https://doi.org/10.1016/j.heliyon.2024.e28030.

[101] M. Inguanzo, A. Domínguez, J.A. Menéndez, C.G. Blanco, J.J. Pis, On the pyrolysis of sewage sludge: the influence of pyrolysis conditions on solid, liquid and gas fractions, J Anal Appl Pyrolysis 63 (2002) 209–222. https://doi.org/https://doi.org/10.1016/S0165-2370(01)00155-3.

[102] O. Mašek, Biochar in thermal and thermochemical biorefineries—production of biochar as a coproduct, in: Handbook of Biofuels Production, Elsevier, 2016: pp. 655–671. https://doi.org/10.1016/B978-0-08-100455-5.00021-7.

[103] T. Chen, Y. Zhang, H. Wang, W. Lu, Z. Zhou, Y. Zhang, L. Ren, Influence of pyrolysis temperature on characteristics and heavy metal adsorptive performance of biochar derived from municipal sewage sludge, Bioresour Technol 164 (2014) 47–54. https://doi.org/10.1016/J.BIORTECH.2014.04.048.

[104] M. Ahmad, A.U. Rajapaksha, J.E. Lim, M. Zhang, N. Bolan, D. Mohan, M. Vithanage, S.S. Lee, Y.S. Ok, Biochar as a sorbent for contaminant management in soil and water: A review, Chemosphere 99 (2014) 19–33. https://doi.org/10.1016/J.CHEMOSPHERE.2013.10.071.

[105] S. Rangabhashiyam, P.V. dos S. Lins, L.M.T. de M. Oliveira, P. Sepulveda, J.O. Ighalo, A.U. Rajapaksha, L. Meili, Sewage sludge-derived biochar for the adsorptive removal of wastewater pollutants: A critical review, Environmental Pollution 293 (2022) 118581. https://doi.org/10.1016/J.ENVPOL.2021.118581.

[106] J. Jin, Y. Li, J. Zhang, S. Wu, Y. Cao, P. Liang, J. Zhang, M.H. Wong, M. Wang, S. Shan, P. Christie, Influence of pyrolysis temperature on properties and environmental safety of heavy metals in biochars derived from municipal sewage sludge, J Hazard Mater 320 (2016) 417–426. https://doi.org/10.1016/J.JHAZMAT.2016.08.050.

[107] M.L. Cayuela, S. Jeffery, L. van Zwieten, The molar H:Corg ratio of biochar is a key factor in mitigating N2O emissions from soil, Agric Ecosyst Environ 202 (2015) 135–138. https://doi.org/10.1016/J.AGEE.2014.12.015.

[108] A. Méndez, A.M. Tarquis, A. Saa-Requejo, F. Guerrero, G. Gascó, Influence of pyrolysis temperature on composted sewage sludge biochar priming effect in a loamy soil, Chemosphere 93 (2013) 668–676. https://doi.org/10.1016/J.CHEMOSPHERE.2013.06.004.

[109] H. Yuan, T. Lu, H. Huang, D. Zhao, N. Kobayashi, Y. Chen, Influence of pyrolysis temperature on physical and chemical properties of biochar made from sewage sludge, J Anal Appl Pyrolysis 112 (2015) 284–289. https://doi.org/10.1016/J.JAAP.2015.01.010.

[110] X.D. Song, X.Y. Xue, D.Z. Chen, P.J. He, X.H. Dai, Application of biochar from sewage sludge to plant cultivation: Influence of pyrolysis temperature and biochar-to-soil ratio on yield and heavy metal accumulation, Chemosphere 109 (2014) 213–220. https://doi.org/10.1016/J.CHEMOSPHERE.2014.01.070.

[111] X. Zhang, B. Zhao, H. Liu, Y. Zhao, L. Li, Effects of pyrolysis temperature on biochar's characteristics and speciation and environmental risks of heavy metals in sewage sludge biochars, Environ Technol Innov 26 (2022) 102288. https://doi.org/10.1016/J.ETI.2022.102288.

[112] H. Yuan, T. Lu, D. Zhao, H. Huang, K. Noriyuki, Y. Chen, Influence of temperature on product distribution and biochar properties by municipal sludge pyrolysis, J Mater Cycles Waste Manag 15 (2013) 357–361. https://doi.org/10.1007/s10163-013-0126-9.

[113] A. Méndez, M. Terradillos, G. Gascó, Physicochemical and agronomic properties of biochar from sewage sludge pyrolysed at different temperatures, J

Anal Appl Pyrolysis 102 (2013) 124–130. https://doi.org/10.1016/J.JAAP.2013.03.006.

[114] J. Zou, Y. Dai, X. Wang, Z. Ren, C. Tian, K. Pan, S. Li, M. Abuobeidah, H. Fu, Structure and adsorption properties of sewage sludge-derived carbon with removal of inorganic impurities and high porosity, Bioresour Technol 142 (2013) 209–217. https://doi.org/10.1016/J.BIORTECH.2013.04.064.

[115] E. Agrafioti, G. Bouras, D. Kalderis, E. Diamadopoulos, Biochar production by sewage sludge pyrolysis, J Anal Appl Pyrolysis 101 (2013) 72–78. https://doi.org/10.1016/J.JAAP.2013.02.010.

[116] R. Khan, S. Shukla, M. Kumar, A. Zuorro, A. Pandey, Sewage sludge derived biochar and its potential for sustainable environment in circular economy: Advantages and challenges, Chemical Engineering Journal 471 (2023) 144495. https://doi.org/10.1016/j.cej.2023.144495.

[117] L. Leng, Q. Xiong, L. Yang, H. Li, Y. Zhou, W. Zhang, S. Jiang, H. Li, H. Huang, An overview on engineering the surface area and porosity of biochar, Science of The Total Environment 763 (2021) 144204. https://doi.org/10.1016/J.SCITOTENV.2020.144204.

[118] L. Zhao, X. Cao, O. Mašek, A. Zimmerman, Heterogeneity of biochar properties as a function of feedstock sources and production temperatures, J Hazard Mater 256–257 (2013) 1–9. https://doi.org/10.1016/j.jhazmat.2013.04.015.

[119] A.N. Shafawi, A.R. Mohamed, P. Lahijani, M. Mohammadi, Recent advances in developing engineered biochar for CO2 capture: An insight into the biochar modification approaches, J Environ Chem Eng 9 (2021) 106869. https://doi.org/10.1016/J.JECE.2021.106869.

[120] L. Leng, S. Xu, R. Liu, T. Yu, X. Zhuo, S. Leng, Q. Xiong, H. Huang, Nitrogen containing functional groups of biochar: An overview, Bioresour Technol 298 (2020) 122286. https://doi.org/10.1016/j.biortech.2019.122286.

[121] P. Hadi, M. Xu, C. Ning, C. Sze Ki Lin, G. McKay, A critical review on preparation, characterization and utilization of sludge-derived activated carbons for wastewater treatment, Chemical Engineering Journal 260 (2015) 895–906. https://doi.org/10.1016/J.CEJ.2014.08.088.

[122] W.H. Huang, D.J. Lee, C. Huang, Modification on biochars for applications: A research update, Bioresour Technol 319 (2021) 124100. https://doi.org/10.1016/J.BIORTECH.2020.124100.

[123] A.U. Rajapaksha, S.S. Chen, D.C.W. Tsang, M. Zhang, M. Vithanage, S. Mandal, B. Gao, N.S. Bolan, Y.S. Ok, Engineered/designer biochar for contaminant removal/immobilization from soil and water: Potential and implication of biochar modification, Chemosphere 148 (2016) 276–291. https://doi.org/10.1016/J.CHEMOSPHERE.2016.01.043.

[124] T. Sizmur, T. Fresno, G. Akgül, H. Frost, E. Moreno-Jiménez, Biochar modification to enhance sorption of inorganics from water, Bioresour Technol 246 (2017) 34–47. https://doi.org/10.1016/J.BIORTECH.2017.07.082.

[125] D. Liu, W. Zhang, H. Lin, Y. Li, H. Lu, Y. Wang, A green technology for the preparation of high capacitance rice husk-based activated carbon, J Clean Prod 112 (2016) 1190–1198. https://doi.org/10.1016/j.jclepro.2015.07.005.

[126] P. Velli, I. Manolikaki, E. Diamadopoulos, Effect of biochar produced from sewage sludge on tomato (Solanum lycopersicum L.) growth, soil chemical properties and heavy metal concentrations, J Environ Manage 297 (2021) 113325. https://doi.org/10.1016/J.JENVMAN.2021.113325.

[127] D.A. Roberts, A.J. Cole, A. Whelan, R. de Nys, N.A. Paul, Slow pyrolysis enhances the recovery and reuse of phosphorus and reduces metal leaching from biosolids, Waste Management 64 (2017) 133–139. https://doi.org/10.1016/J.WASMAN.2017.03.012.

[128] C.C. de Figueiredo, A. de S.P.J. Reis, A.S. de Araujo, L.E.B. Blum, K. Shah, J. Paz-Ferreiro, Assessing the potential of sewage sludge-derived biochar as a novel phosphorus fertilizer: Influence of extractant solutions and pyrolysis temperatures, Waste Management 124 (2021) 144–153. https://doi.org/10.1016/J.WASMAN.2021.01.044.

[129] J. Liang, J. Ye, C. Shi, P. Zhang, J. Guo, M. Zubair, J. Chang, L. Zhang, Pyrolysis temperature regulates sludge-derived biochar production, phosphate adsorption and phosphate retention in soil, J Environ Chem Eng 10 (2022) 107744. https://doi.org/10.1016/J.JECE.2022.107744.

[130] M. Marcińczyk, P. Oleszczuk, Biochar and engineered biochar as slow- and controlled-release fertilizers, J Clean Prod 339 (2022) 130685. https://doi.org/10.1016/J.JCLEPRO.2022.130685.

[131] European Parliament and Council, Regulation (EU) 2019/1009 of the European Parliament and of the Council of 5 June 2019 laying down rules on the making available on the market of EU fertilising products and amending Regulations (EC) No 1069/2009 and (EC) No 1107/2009 and repealing Regulation (EC) No

2003/2003 (Text with EEA relevance), (2019). http://data.europa.eu/eli/reg/2019/1009/oj (accessed June 3, 2023).

[132] M. Alipour, H. Asadi, C. Chen, M.R. Rashti, Bioavailability and eco-toxicity of heavy metals in chars produced from municipal sewage sludge decreased during pyrolysis and hydrothermal carbonization, Ecol Eng 162 (2021) 106173. https://doi.org/10.1016/J.ECOLENG.2021.106173.

[133] J. Xing, L. Li, G. Li, G. Xu, Feasibility of sludge-based biochar for soil remediation: Characteristics and safety performance of heavy metals influenced by pyrolysis temperatures, Ecotoxicol Environ Saf 180 (2019) 457–465. https://doi.org/10.1016/J.ECOENV.2019.05.034.

[134] X. Chen, L. Yang, S.C.B. Myneni, Y. Deng, Leaching of polycyclic aromatic hydrocarbons (PAHs) from sewage sludge-derived biochar, Chemical Engineering Journal 373 (2019) 840–845. https://doi.org/10.1016/j.cej.2019.05.059.

[135] J.M. De la Rosa, Á.M. Sánchez-Martín, P. Campos, A.Z. Miller, Effect of pyrolysis conditions on the total contents of polycyclic aromatic hydrocarbons in biochars produced from organic residues: Assessment of their hazard potential, Science of The Total Environment 667 (2019) 578–585. https://doi.org/10.1016/j.scitotenv.2019.02.421.

[136] S. Khan, N. Wang, B.J. Reid, A. Freddo, C. Cai, Reduced bioaccumulation of PAHs by Lactuca satuva L. grown in contaminated soil amended with sewage sludge and sewage sludge derived biochar, Environmental Pollution 175 (2013) 64–68. https://doi.org/10.1016/J.ENVPOL.2012.12.014.

[137] F. Zhang, G. Zhang, X. Liao, Negative role of biochars in the dissipation and vegetable uptake of polycyclic aromatic hydrocarbons (PAHs) in an agricultural soil: Cautions for application of biochars to remediate PAHs-contaminated soil, Ecotoxicol Environ Saf 213 (2021) 112075. https://doi.org/10.1016/J.ECOENV.2021.112075.

[138] K.M. Krahn, G. Cornelissen, G. Castro, H.P.H. Arp, A.G. Asimakopoulos, R. Wolf, R. Holmstad, A.R. Zimmerman, E. Sørmo, Sewage sludge biochars as effective PFAS-sorbents, J Hazard Mater 445 (2023) 130449. https://doi.org/10.1016/j.jhazmat.2022.130449.

[139] L. Zhao, Z.-F. Sun, X.-W. Pan, J.-Y. Tan, S.-S. Yang, J.-T. Wu, C. Chen, Y. Yuan, N.-Q. Ren, Sewage sludge derived biochar for environmental improvement: Advances, challenges, and solutions, Water Res X 18 (2023) 100167. https://doi.org/10.1016/j.wroa.2023.100167.

[140] M. Li, X. Chen, C. Chen, L. Huang, H. Chi, N. Zhao, B. Yan, Y. Chao, Y. Tang, R. Qiu, S. Wang, The effectiveness of sewage sludge biochar amendment with Boehmeria nivea L. in improving physicochemical properties and rehabilitating microbial communities in mine tailings, J Environ Manage 345 (2023) 118552. https://doi.org/10.1016/j.jenvman.2023.118552.

[141] V.R. Celso Monteiro Zanona, C.E. Rodrigues Barquilha, M.C. Borba Braga, Removal of recalcitrant organic matter of landfill leachate by adsorption onto biochar from sewage sludge: A quali-quantitative analysis, J Environ Manage 344 (2023) 118387. https://doi.org/10.1016/j.jenvman.2023.118387.

[142] C. Song, Q. Liu, N. Ji, S. Deng, J. Zhao, Y. Li, Y. Song, H. Li, Alternative pathways for efficient CO2 capture by hybrid processes—A review, Renewable and Sustainable Energy Reviews 82 (2018) 215–231. https://doi.org/10.1016/j.rser.2017.09.040.

[143] N.S. Sifat, Y. Haseli, A Critical Review of CO2 Capture Technologies and Prospects for Clean Power Generation, Energies (Basel) 12 (2019) 4143. https://doi.org/10.3390/en12214143.

[144] X. Xu, Y. Kan, L. Zhao, X. Cao, Chemical transformation of CO2 during its capture by waste biomass derived biochars, Environmental Pollution 213 (2016) 533–540. https://doi.org/10.1016/J.ENVPOL.2016.03.013.

[145] P. Brassard, S. Godbout, J.H. Palacios, T. Jeanne, R. Hogue, P. Dubé, L. Limousy, V. Raghavan, Effect of six engineered biochars on GHG emissions from two agricultural soils: A short-term incubation study, Geoderma 327 (2018) 73–84. https://doi.org/10.1016/J.GEODERMA.2018.04.022.

[146] N. Ameloot, S. De Neve, K. Jegajeevagan, G. Yildiz, D. Buchan, Y.N. Funkuin, W. Prins, L. Bouckaert, S. Sleutel, Short-term CO2 and N2O emissions and microbial properties of biochar amended sandy loam soils, Soil Biol Biochem 57 (2013) 401–410. https://doi.org/10.1016/J.SOILBIO.2012.10.025.

[147] A. Mukherjee, V.B. Borugadda, J.J. Dynes, C. Niu, A.K. Dalai, Carbon dioxide capture from flue gas in biochar produced from spent coffee grounds: Effect of surface chemistry and porous structure, J Environ Chem Eng 9 (2021) 106049. https://doi.org/10.1016/J.JECE.2021.106049.

[148] P.D. Dissanayake, S. You, A.D. Igalavithana, Y. Xia, A. Bhatnagar, S. Gupta, H.W. Kua, S. Kim, J.H. Kwon, D.C.W. Tsang, Y.S. Ok, Biochar-based adsorbents for carbon dioxide capture: A critical review, Renewable and Sustainable Energy Reviews 119 (2020) 109582. https://doi.org/10.1016/J.RSER.2019.109582.

[149] A.D. Igalavithana, S.W. Choi, J. Shang, A. Hanif, P.D. Dissanayake, D.C.W. Tsang, J.H. Kwon, K.B. Lee, Y.S. Ok, Carbon dioxide capture in biochar produced from pine sawdust and paper mill sludge: Effect of porous structure and surface chemistry, Science of The Total Environment 739 (2020) 139845. https://doi.org/10.1016/J.SCITOTENV.2020.139845.

[150] C. Liu, Y. Wu, G. Lan, X. Ji, Y. Xia, C. Fu, J. Shen, J. Gui, Y. Liu, Y. Qu, H. Peng, CO2 capture performance of biochar prepared from sewage sludge after conditioning with different dewatering agents, J Environ Chem Eng 10 (2022) 108318. https://doi.org/10.1016/j.jece.2022.108318.

[151] H.A. Alhashimi, C.B. Aktas, Life cycle environmental and economic performance of biochar compared with activated carbon: A meta-analysis, Resour Conserv Recycl 118 (2017) 13–26. https://doi.org/10.1016/j.resconrec.2016.11.016.

[152] D. Wu, Y. Yang, J. Liu, Y. Zheng, Plasma-Modified N/O-Doped Porous Carbon for CO $_2$ Capture: An Experimental and Theoretical Study, Energy & Fuels 34 (2020) 6077–6084. https://doi.org/10.1021/acs.energyfuels.0c00415.

[153] S. Guo, Y. Li, Y. Wang, L. Wang, Y. Sun, L. Liu, Recent advances in biochar-based adsorbents for CO2 capture, Carbon Capture Science & Technology 4 (2022) 100059. https://doi.org/10.1016/j.ccst.2022.100059.

[154] Y. Tang, M.S. Alam, K.O. Konhauser, D.S. Alessi, S. Xu, W. Tian, Y. Liu, Influence of pyrolysis temperature on production of digested sludge biochar and its application for ammonium removal from municipal wastewater, J Clean Prod 209 (2019) 927–936. https://doi.org/10.1016/j.jclepro.2018.10.268.

[155] Q. Yin, M. Liu, H. Ren, Biochar produced from the co-pyrolysis of sewage sludge and walnut shell for ammonium and phosphate adsorption from water, J Environ Manage 249 (2019) 109410. https://doi.org/10.1016/j.jenvman.2019.109410.

[156] M. Jiang, Y. Yang, T. Lei, Z. Ye, S. Huang, X. Fu, P. Liu, H. Li, Removal of phosphate by a novel activated sewage sludge biochar: Equilibrium, kinetic and mechanism studies, Applications in Energy and Combustion Science 9 (2022) 100056. https://doi.org/10.1016/J.JAECS.2022.100056.

[157] J. Yang, M. Zhang, H. Wang, J. Xue, Q. Lv, G. Pang, Efficient recovery of phosphate from aqueous solution using biochar derived from co-pyrolysis of sewage sludge with eggshell, J Environ Chem Eng 9 (2021) 105354. https://doi.org/10.1016/J.JECE.2021.105354.

[158] M. Liu, R. Li, J. Wang, X. Liu, S. Li, W. Shen, Recovery of phosphate from aqueous solution by dewatered dry sludge biochar and its feasibility in fertilizer use, Science of The Total Environment 814 (2022) 152752. https://doi.org/10.1016/J.SCITOTENV.2021.152752.

[159] S. Singh, V. Kumar, D.S. Dhanjal, S. Datta, D. Bhatia, J. Dhiman, J. Samuel, R. Prasad, J. Singh, A sustainable paradigm of sewage sludge biochar: Valorization, opportunities, challenges and future prospects, J Clean Prod 269 (2020) 122259. https://doi.org/10.1016/J.JCLEPRO.2020.122259.

[160] S. Kundu, S. Patel, P. Halder, T. Patel, M. Hedayati Marzbali, B.K. Pramanik, J. Paz-Ferreiro, C.C. de Figueiredo, D. Bergmann, A. Surapaneni, M. Megharaj, K. Shah, Removal of PFASs from biosolids using a semi-pilot scale pyrolysis reactor and the application of biosolids derived biochar for the removal of PFASs from contaminated water, Environ Sci (Camb) 7 (2021) 638–649. https://doi.org/10.1039/D0EW00763C.

[161] Y. Tang, M.S. Alam, K.O. Konhauser, D.S. Alessi, S. Xu, W. Tian, Y. Liu, Influence of pyrolysis temperature on production of digested sludge biochar and its application for ammonium removal from municipal wastewater, J Clean Prod 209 (2019) 927–936. https://doi.org/10.1016/j.jclepro.2018.10.268.

[162] Q. Yin, M. Liu, H. Ren, Biochar produced from the co-pyrolysis of sewage sludge and walnut shell for ammonium and phosphate adsorption from water, J Environ Manage 249 (2019) 109410. https://doi.org/10.1016/J.JENVMAN.2019.109410.

[163] Y. Sun, B. Zeng, Y. Dai, X. Liang, L. Zhang, R. Ahmad, X. Su, Modification of sludge-based biochar using air roasting-oxidation and its performance in adsorption of uranium(VI) from aqueous solutions, J Colloid Interface Sci 614 (2022) 547–555. https://doi.org/10.1016/J.JCIS.2022.01.138.

[164] M. Kumar, S. Dutta, S. You, G. Luo, S. Zhang, P.L. Show, A.D. Sawarkar, L. Singh, D.C.W. Tsang, A critical review on biochar for enhancing biogas production from anaerobic digestion of food waste and sludge, J Clean Prod 305 (2021) 127143. https://doi.org/10.1016/J.JCLEPRO.2021.127143.

[165] Y. Cai, M. Zhu, X. Meng, J.L. Zhou, H. Zhang, X. Shen, The role of biochar on alleviating ammonia toxicity in anaerobic digestion of nitrogen-rich wastes: A review, Bioresour Technol 351 (2022) 126924. https://doi.org/10.1016/J.BIORTECH.2022.126924.

[166] M. Chiappero, O. Norouzi, M. Hu, F. Demichelis, F. Berruti, F. Di Maria, O. Mašek, S. Fiore, Review of biochar role as additive in anaerobic digestion

processes, Renewable and Sustainable Energy Reviews 131 (2020) 110037. https://doi.org/10.1016/J.RSER.2020.110037.

[167] J. Li, M. Zhang, Z. Ye, C. Yang, Effect of manganese oxide-modified biochar addition on methane production and heavy metal speciation during the anaerobic digestion of sewage sludge, Journal of Environmental Sciences 76 (2019) 267–277. https://doi.org/10.1016/J.JES.2018.05.009.

[168] M. Chiappero, F. Berruti, O. Mašek, S. Fiore, Analysis of the influence of activated biochar properties on methane production from anaerobic digestion of waste activated sludge, Biomass Bioenergy 150 (2021) 106129. https://doi.org/10.1016/J.BIOMBIOE.2021.106129.

[169] B. Wu, Q. Yang, F. Yao, S. Chen, L. He, K. Hou, Z. Pi, H. Yin, J. Fu, D. Wang, X. Li, Evaluating the effect of biochar on mesophilic anaerobic digestion of waste activated sludge and microbial diversity, Bioresour Technol 294 (2019) 122235. https://doi.org/10.1016/J.BIORTECH.2019.122235.

[170] X. Liu, Q. Meng, F. Wu, C. Zhang, X. Tan, C. Wan, Enhanced biogas production in anaerobic digestion of sludge medicated by biochar prepared from excess sludge: Role of persistent free radicals and electron mediators, Bioresour Technol 347 (2022) 126422. https://doi.org/10.1016/J.BIORTECH.2021.126422.

[171] M. Zhang, J. Li, Y. Wang, C. Yang, Impacts of different biochar types on the anaerobic digestion of sewage sludge, RSC Adv 9 (2019) 42375–42386. https://doi.org/10.1039/C9RA08700A.

[172] L. Qiu, Y.F. Deng, F. Wang, M. Davaritouchaee, Y.Q. Yao, A review on biochar-mediated anaerobic digestion with enhanced methane recovery, Renewable and Sustainable Energy Reviews 115 (2019) 109373. https://doi.org/10.1016/J.RSER.2019.109373.

[173] D. Yellezuome, X. Zhu, Z. Wang, R. Liu, Mitigation of ammonia inhibition in anaerobic digestion of nitrogen-rich substrates for biogas production by ammonia stripping: A review, Renewable and Sustainable Energy Reviews 157 (2022) 112043. https://doi.org/10.1016/J.RSER.2021.112043.

[174] W. Fuchs, X. Wang, W. Gabauer, M. Ortner, Z. Li, Tackling ammonia inhibition for efficient biogas production from chicken manure: Status and technical trends in Europe and China, Renewable and Sustainable Energy Reviews 97 (2018) 186–199. https://doi.org/10.1016/J.RSER.2018.08.038.

[175] A. Hassanein, S. Lansing, Boosting anaerobic digestion with microbial electrochemical technologies, (2022) 67–98. https://doi.org/10.1016/bs.aibe.2022.05.003.

[176] M. Li, Q. Zhang, Y. Liu, J. Zhu, F. Sun, M.-H. Cui, H. Liu, T.C. Zhang, C. Chen, Enhancing degradation of organic matter in microbial electrolytic cells coupled with anaerobic digestion (MEC-AD) systems by carbon-based materials, Science of The Total Environment 900 (2023) 165805. https://doi.org/10.1016/j.scitotenv.2023.165805.

[177] X. Ning, R. Lin, J. Mao, C. Deng, L. Ding, R. O'Shea, D.M. Wall, J.D. Murphy, Improving the efficiency of anaerobic digestion and optimising in-situ CO2 bioconversion through the enhanced local electric field at the microbe-electrode interface, Energy Convers Manag 304 (2024) 118245. https://doi.org/10.1016/j.enconman.2024.118245.

[178] J. Pan, J. Ma, L. Zhai, T. Luo, Z. Mei, H. Liu, Achievements of biochar application for enhanced anaerobic digestion: A review, Bioresour Technol 292 (2019) 122058. https://doi.org/10.1016/j.biortech.2019.122058.

[179] C. Yin, Y. Shen, R. Yuan, N. Zhu, H. Yuan, Z. Lou, Sludge-based biochar-assisted thermophilic anaerobic digestion of waste-activated sludge in microbial electrolysis cell for methane production, Bioresour Technol 284 (2019) 315–324. https://doi.org/10.1016/j.biortech.2019.03.146.

[180] M. Bertero, G. De La Puente, U. Sedran, Fuels from bio-oils: Bio-oil production from different residual sources, characterization and thermal conditioning, Fuel 95 (2012) 263–271. https://doi.org/10.1016/J.FUEL.2011.08.041.

[181] J. Lehto, A. Oasmaa, Y. Solantausta, M. Kytö, D. Chiaramonti, Review of fuel oil quality and combustion of fast pyrolysis bio-oils from lignocellulosic biomass, Appl Energy 116 (2014) 178–190. https://doi.org/10.1016/J.APENERGY.2013.11.040.

[182] R.O. Arazo, D.A.D. Genuino, M.D.G. de Luna, S.C. Capareda, Bio-oil production from dry sewage sludge by fast pyrolysis in an electrically-heated fluidized bed reactor, Sustainable Environment Research 27 (2017) 7–14. https://doi.org/10.1016/J.SERJ.2016.11.010.

[183] Y.H. Kuan, F.H. Wu, G.B. Chen, H.T. Lin, T.H. Lin, Study of the combustion characteristics of sewage sludge pyrolysis oil, heavy fuel oil, and their blends, Energy 201 (2020) 117559. https://doi.org/10.1016/J.ENERGY.2020.117559.

[184] Y. Zhou, Z. Chen, H. Gong, L. Chen, H. Yu, W. Wu, Characteristics of dehydration during rice husk pyrolysis and catalytic mechanism of dehydration

reaction with NiO/γ-Al2O3 as catalyst, Fuel 245 (2019) 131–138. https://doi.org/10.1016/j.fuel.2019.02.059.

[185] M. Asadieraghi, W.M.A. Wan Daud, In-situ catalytic upgrading of biomass pyrolysis vapor: Using a cascade system of various catalysts in a multi-zone fixed bed reactor, Energy Convers Manag 101 (2015) 151–163. https://doi.org/10.1016/j.enconman.2015.05.008.

[186] M.M. Pedroza, J.F. Sousa, G.E.G. Vieira, M.B.D. Bezerra, Characterization of the products from the pyrolysis of sewage sludge in 1 kg/h rotating cylinder reactor, J Anal Appl Pyrolysis 105 (2014) 108–115. https://doi.org/10.1016/J.JAAP.2013.10.009.

[187] M. Vuorte, S. Kuitunen, M. Sammalkorpi, Physisorption of bio oil nitrogen compounds onto montmorillonite, Physical Chemistry Chemical Physics 23 (2021) 21840–21851. https://doi.org/10.1039/D1CP01880A.

[188] S. Izhar, S. Uehara, N. Yoshida, Y. Yamamoto, T. Morioka, M. Nagai, Hydrodenitrogenation of fast pyrolysis bio-oil derived from sewage sludge on NiMo/Al2O3 sulfide catalyst, Fuel Processing Technology 101 (2012) 10–15. https://doi.org/10.1016/j.fuproc.2012.03.012.

[189] M. Sharifzadeh, M. Sadeqzadeh, M. Guo, T.N. Borhani, N.V.S.N. Murthy Konda, M.C. Garcia, L. Wang, J. Hallett, N. Shah, The multi-scale challenges of biomass fast pyrolysis and bio-oil upgrading: Review of the state of art and future research directions, Prog Energy Combust Sci 71 (2019) 1–80. https://doi.org/10.1016/J.PECS.2018.10.006.

[190] A.P. Bora, D.P. Gupta, K.S. Durbha, Sewage sludge to bio-fuel: A review on the sustainable approach of transforming sewage waste to alternative fuel, Fuel 259 (2020) 116262. https://doi.org/10.1016/J.FUEL.2019.116262.

[191] B. Zhang, Z. Zhong, P. Chen, R. Ruan, Microwave-assisted catalytic fast pyrolysis of biomass for bio-oil production using chemical vapor deposition modified HZSM-5 catalyst, Bioresour Technol 197 (2015) 79–84. https://doi.org/10.1016/J.BIORTECH.2015.08.063.

[192] S. Liu, Y. Zhang, L. Fan, N. Zhou, G. Tian, X. Zhu, Y. Cheng, Y. Wang, Y. Liu, P. Chen, R. Ruan, Bio-oil production from sequential two-step catalytic fast microwave-assisted biomass pyrolysis, Fuel 196 (2017) 261–268. https://doi.org/10.1016/J.FUEL.2017.01.116.

[193] R.O. Arazo, S.C. Capareda, B.I.G. Ofrasio, A.L. Ido, W.H. Chen, M.D.G. de Luna, Low-temperature catalytic conversion of alkaline sewage sludge bio-oil

to biodiesel: Product characteristics and reaction mechanisms, Environ Technol Innov 21 (2021) 101266. https://doi.org/10.1016/J.ETI.2020.101266.

[194] Q. Xie, P. Peng, S. Liu, M. Min, Y. Cheng, Y. Wan, Y. Li, X. Lin, Y. Liu, P. Chen, R. Ruan, Fast microwave-assisted catalytic pyrolysis of sewage sludge for bio-oil production, Bioresour Technol 172 (2014) 162–168. https://doi.org/10.1016/J.BIORTECH.2014.09.006.

[195] O.K. Choi, J.S. Song, D.K. Cha, J.W. Lee, Biodiesel production from wet municipal sludge: Evaluation of in situ transesterification using xylene as a cosolvent, Bioresour Technol 166 (2014) 51–56. https://doi.org/10.1016/J.BIORTECH.2014.05.001.

[196] O.K. Choi, J.Y. Park, J.K. Kim, J.W. Lee, Bench-scale production of sewage sludge derived-biodiesel (SSD-BD) and upgrade of its quality, Renew Energy 141 (2019) 914–921. https://doi.org/10.1016/J.RENENE.2019.04.030.

[197] Y. Liu, Y. Zhai, S. Li, X. Liu, X. Liu, B. Wang, Z. Qiu, C. Li, Production of bio-oil with low oxygen and nitrogen contents by combined hydrothermal pretreatment and pyrolysis of sewage sludge, Energy 203 (2020) 117829. https://doi.org/10.1016/J.ENERGY.2020.117829.

[198] C. Zhao, C. Hong, J. Hu, Y. Xing, W. Ling, B. Zhang, Y. Wang, L. Feng, Upgrading technologies and catalytic mechanisms for heteroatomic compounds from bio-oil – A review, Fuel 333 (2023) 126388. https://doi.org/10.1016/j.fuel.2022.126388.

[199] A. Bhatnagar, P. Khatri, M. Krzywonos, H. Tolvanen, J. Konttinen, Techno-economic and environmental assessment of decentralized pyrolysis for crop residue management: Rice and wheat cultivation system in India, J Clean Prod 367 (2022) 132998. https://doi.org/10.1016/j.jclepro.2022.132998.

[200] T.N. Trinh, P.A. Jensen, K. Dam-Johansen, N.O. Knudsen, H.R. Sørensen, Influence of the Pyrolysis Temperature on Sewage Sludge Product Distribution, Bio-Oil, and Char Properties, Energy & Fuels 27 (2013) 1419–1427. https://doi.org/10.1021/ef301944r.

[201] X. Yuan, L. Leng, H. Huang, X. Chen, H. Wang, Z. Xiao, Y. Zhai, H. Chen, G. Zeng, Speciation and environmental risk assessment of heavy metal in bio-oil from liquefaction/pyrolysis of sewage sludge, Chemosphere 120 (2015) 645–652. https://doi.org/10.1016/J.CHEMOSPHERE.2014.10.010.

[202] Y. Hu, G. Li, M. Yan, C. Ping, J. Ren, Investigation into the distribution of polycyclic aromatic hydrocarbons (PAHs) in wastewater sewage sludge and its

resulting pyrolysis bio-oils, Science of The Total Environment 473–474 (2014) 459–464. https://doi.org/10.1016/J.SCITOTENV.2013.12.051.

[203] Y. Hu, W. Yu, H. Wibowo, Y. Xia, Y. Lu, M. Yan, Effect of catalysts on distribution of polycyclic-aromatic hydrocarbon (PAHs) in bio-oils from the pyrolysis of dewatered sewage sludge at high and low temperatures, Science of The Total Environment 667 (2019) 263–270. https://doi.org/10.1016/J.SCITOTENV.2019.02.320.

[204] Y.H. Chan, S.K. Loh, B.L.F. Chin, C.L. Yiin, B.S. How, K.W. Cheah, M.K. Wong, A.C.M. Loy, Y.L. Gwee, S.L.Y. Lo, S. Yusup, S.S. Lam, Fractionation and extraction of bio-oil for production of greener fuel and value-added chemicals: Recent advances and future prospects, Chemical Engineering Journal 397 (2020) 125406. https://doi.org/10.1016/j.cej.2020.125406.

[205] D. Chen, X. Zhuang, Z. Gan, K. Cen, Y. Ba, D. Jia, Co-pyrolysis of light bio-oil leached bamboo and heavy bio-oil: Effects of mass ratio, pyrolysis temperature, and residence time on the biochar, Chemical Engineering Journal 437 (2022) 135253. https://doi.org/10.1016/J.CEJ.2022.135253.

[206] T. Hübner, J. Mumme, Integration of pyrolysis and anaerobic digestion – Use of aqueous liquor from digestate pyrolysis for biogas production, Bioresour Technol 183 (2015) 86–92. https://doi.org/10.1016/J.BIORTECH.2015.02.037.

[207] C.R. Vitasari, G.W. Meindersma, A.B. de Haan, Water extraction of pyrolysis oil: The first step for the recovery of renewable chemicals, Bioresour Technol 102 (2011) 7204–7210. https://doi.org/10.1016/j.biortech.2011.04.079.

[208] Y. Wei, H. Lei, L. Wang, L. Zhu, X. Zhang, Y. Liu, S. Chen, B. Ahring, Liquid–Liquid Extraction of Biomass Pyrolysis Bio-oil, Energy & Fuels 28 (2014) 1207–1212. https://doi.org/10.1021/ef402490s.

[209] S. Ashoor, T.U. Khang, Y.H. Lee, J.S. Hyung, S.Y. Choi, S.E. Lim, J. Lee, S.J. Park, J.-G. Na, Bioupgrading of the aqueous phase of pyrolysis oil from lignocellulosic biomass: a platform for renewable chemicals and fuels from the whole fraction of biomass, Bioresour Bioprocess 10 (2023) 34. https://doi.org/10.1186/s40643-023-00654-3.

[210] Z. Yao, W. Li, X. Kan, Y. Dai, Y.W. Tong, C.-H. Wang, Anaerobic digestion and gasification hybrid system for potential energy recovery from yard waste and woody biomass, Energy 124 (2017) 133–145. https://doi.org/10.1016/j.energy.2017.02.035.

[211] H. Zhou, R.C. Brown, Z. Wen, Anaerobic digestion of aqueous phase from pyrolysis of biomass: Reducing toxicity and improving microbial tolerance,

Bioresour Technol 292 (2019) 121976. https://doi.org/10.1016/j.biortech.2019.121976.

[212] C. Mukarakate, R.J. Evans, S. Deutch, T. Evans, A.K. Starace, J. ten Dam, M.J. Watson, K. Magrini, Reforming Biomass Derived Pyrolysis Bio-oil Aqueous Phase to Fuels, Energy & Fuels 31 (2017) 1600–1607. https://doi.org/10.1021/acs.energyfuels.6b02463.

[213] J. Justicia, J.A. Baeza, L. Calvo, F. Heras, M.A. Gilarranz, Valorization to hydrogen of bio-oil aqueous fractions from lignocellulosic biomass pyrolysis by aqueous phase reforming over Pt/C catalyst, Chemical Engineering Journal 477 (2023) 146860. https://doi.org/10.1016/j.cej.2023.146860.

[214] D. Andreides, K.O. Fliegerova, D. Pokorna, J. Zabranska, Biological conversion of carbon monoxide and hydrogen by anaerobic culture: Prospect of anaerobic digestion and thermochemical processes combination, Biotechnol Adv 58 (2022) 107886. https://doi.org/10.1016/j.biotechadv.2021.107886.

[215] O.S. Djandja, Z.-C. Wang, F. Wang, Y.-P. Xu, P.-G. Duan, Pyrolysis of Municipal Sewage Sludge for Biofuel Production: A Review, Ind Eng Chem Res 59 (2020). https://doi.org/10.1021/acs.iecr.0c01546.

[216] T. Kan, V. Strezov, T. Evans, Effect of the Heating Rate on the Thermochemical Behavior and Biofuel Properties of Sewage Sludge Pyrolysis, Energy & Fuels 30 (2016). https://doi.org/10.1021/acs.energyfuels.5b02232.

[217] R. Han, C. Zhao, J. Liu, A. Chen, H. Wang, Thermal characterization and syngas production from the pyrolysis of biophysical dried and traditional thermal dried sewage sludge, Bioresour Technol 198 (2015) 276–282. https://doi.org/10.1016/j.biortech.2015.08.071.

[218] A. Domínguez, J.A. Menéndez, J.J. Pis, Hydrogen rich fuel gas production from the pyrolysis of wet sewage sludge at high temperature, J Anal Appl Pyrolysis 77 (2006) 127–132. https://doi.org/10.1016/j.jaap.2006.02.003.

[219] D.A. Rahim, W. Fang, H. Wibowo, D. Hantoko, H. Susanto, K. Yoshikawa, Y. Zhong, M. Yan, Review of high temperature H2S removal from syngas: Perspectives on downstream process integration, Chemical Engineering and Processing - Process Intensification 183 (2023) 109258. https://doi.org/10.1016/j.cep.2022.109258.

[220] C. Frilund, P. Simell, N. Kaisalo, E. Kurkela, M.-L. Koskinen-Soivi, Desulfurization of Biomass Syngas Using ZnO-Based Adsorbents: Long-Term Hydrogen Sulfide Breakthrough Experiments, Energy & Fuels 34 (2020) 3316–3325. https://doi.org/10.1021/acs.energyfuels.9b04276.

[221] J.A. Okolie, E.I. Epelle, M.E. Tabat, U. Orivri, A.N. Amenaghawon, P.U. Okoye, B. Gunes, Waste biomass valorization for the production of biofuels and value-added products: A comprehensive review of thermochemical, biological and integrated processes, Process Safety and Environmental Protection 159 (2022) 323–344. https://doi.org/10.1016/J.PSEP.2021.12.049.

[222] F.M. Liew, M.E. Martin, R.C. Tappel, B.D. Heijstra, C. Mihalcea, M. Köpke, Gas Fermentation-A flexible platform for commercial scale production of low-carbon-fuels and chemicals from waste and renewable feedstocks, Front Microbiol 7 (2016) 694. https://doi.org/10.3389/fmicb.2016.00694.

[223] S. Esquivel-Elizondo, A.G. Delgado, B.E. Rittmann, R. Krajmalnik-Brown, The effects of CO2 and H2 on CO metabolism by pure and mixed microbial cultures, Biotechnol Biofuels 10 (2017) 220. https://doi.org/10.1186/s13068-017-0910-1.

[224] N. Shen, K. Dai, X.Y. Xia, R.J. Zeng, F. Zhang, Conversion of syngas (CO and H2) to biochemicals by mixed culture fermentation in mesophilic and thermophilic hollow-fiber membrane biofilm reactors, J Clean Prod 202 (2018) 536–542. https://doi.org/10.1016/J.JCLEPRO.2018.08.162.

[225] K. Asimakopoulos, H.N. Gavala, I. V. Skiadas, Reactor systems for syngas fermentation processes: A review, Chemical Engineering Journal 348 (2018) 732–744. https://doi.org/10.1016/J.CEJ.2018.05.003.

[226] M. Yasin, Y. Jeong, S. Park, J. Jeong, E.Y. Lee, R.W. Lovitt, B.H. Kim, J. Lee, I.S. Chang, Microbial synthesis gas utilization and ways to resolve kinetic and mass-transfer limitations, Bioresour Technol 177 (2015) 361–374. https://doi.org/10.1016/j.biortech.2014.11.022.

[227] M.U. Monir, A. Abd Aziz, A. Yousuf, M.Z. Alam, Hydrogen-rich syngas fermentation for bioethanol production using Sacharomyces cerevisiea, Int J Hydrogen Energy 45 (2020) 18241–18249. https://doi.org/10.1016/J.IJHYDENE.2019.07.246.

[228] F. Zhang, J. Ding, Y. Zhang, M. Chen, Z.W. Ding, M.C.M. van Loosdrecht, R.J. Zeng, Fatty acids production from hydrogen and carbon dioxide by mixed culture in the membrane biofilm reactor, Water Res 47 (2013) 6122–6129. https://doi.org/10.1016/J.WATRES.2013.07.033.

[229] X. Chen, B.J. Ni, Anaerobic conversion of hydrogen and carbon dioxide to fatty acids production in a membrane biofilm reactor: A modeling approach, Chemical Engineering Journal 306 (2016) 1092–1098. https://doi.org/10.1016/J.CEJ.2016.08.049.

[230] I.K. Stoll, N. Boukis, J. Sauer, Syngas Fermentation to Alcohols: Reactor Technology and Application Perspective, Chemie Ingenieur Technik 92 (2020) 125–136. https://doi.org/10.1002/cite.201900118.

[231] B. Gunes, A critical review on biofilm-based reactor systems for enhanced syngas fermentation processes, Renewable and Sustainable Energy Reviews 143 (2021) 110950. https://doi.org/10.1016/J.RSER.2021.110950.

[232] K. Müller, M. Fleige, F. Rachow, D. Schmeißer, Sabatier based CO2-methanation of Flue Gas Emitted by Conventional Power Plants, Energy Procedia 40 (2013) 240–248. https://doi.org/10.1016/j.egypro.2013.08.028.

[233] C. Li, X. Zhu, I. Angelidaki, Syngas biomethanation: effect of biomass-gas ratio, syngas composition and pH buffer, Bioresour Technol 342 (2021) 125997. https://doi.org/10.1016/J.BIORTECH.2021.125997.

[234] C. Li, X. Zhu, I. Angelidaki, Carbon monoxide conversion and syngas biomethanation mediated by different microbial consortia, Bioresour Technol 314 (2020) 123739. https://doi.org/10.1016/J.BIORTECH.2020.123739.

[235] A. Grimalt-Alemany, M. Łężyk, D.M. Kennes-Veiga, I. V. Skiadas, H.N. Gavala, Enrichment of Mesophilic and Thermophilic Mixed Microbial Consortia for Syngas Biomethanation: The Role of Kinetic and Thermodynamic Competition, Waste Biomass Valorization 11 (2020) 465–481. https://doi.org/10.1007/s12649-019-00595-z.

[236] Y. Li, Y. Liu, X. Wang, S. Luo, D. Su, H. Jiang, H. Zhou, J. Pan, L. Feng, Biomethanation of syngas at high CO concentration in a continuous mode, Bioresour Technol (2021) 126407. https://doi.org/10.1016/j.biortech.2021.126407.

[237] J. Figueras, H. Benbelkacem, C. Dumas, P. Buffiere, "Biomethanation of syngas by enriched mixed anaerobic consortium in pressurized agitated column," Bioresour Technol 338 (2021) 125548. https://doi.org/10.1016/J.BIORTECH.2021.125548.

[238] J. Figueras, H. Benbelkacem, C. Dumas, P. Buffiere, Syngas biomethanation: In a transfer limited process, is CO inhibition an issue?, Waste Management 162 (2023) 36–42. https://doi.org/10.1016/J.WASMAN.2023.03.011.

[239] S.B. Kuipers, M.V.W. Kofoed, Biomethanation of syngas in packed bed reactors: A study of adaptation and microbial pathways in a thermophilic mixed consortium, Bioresour Technol Rep 24 (2023) 101667. https://doi.org/10.1016/j.biteb.2023.101667.

[240] M. Alfano, C. Cavazza, The biologically mediated water–gas shift reaction: structure, function and biosynthesis of monofunctional [NiFe]-carbon monoxide dehydrogenases, Sustain Energy Fuels 2 (2018) 1653–1670. https://doi.org/10.1039/C8SE00085A.

[241] D. Andreides, K.O. Fliegerova, D. Pokorna, J. Zabranska, Biological conversion of carbon monoxide and hydrogen by anaerobic culture: Prospect of anaerobic digestion and thermochemical processes combination, Biotechnol Adv 58 (2022) 107886. https://doi.org/10.1016/j.biotechadv.2021.107886.

[242] M.B. Jensen, L.D.M. Ottosen, M.V.W. Kofoed, H2 gas-liquid mass transfer: A key element in biological Power-to-Gas methanation, Renewable and Sustainable Energy Reviews 147 (2021) 111209. https://doi.org/10.1016/J.RSER.2021.111209.

[243] M.U. Sieborg, B.D. Jønson, M.T. Ashraf, L. Yde, J.M. Triolo, Biomethanation in a thermophilic biotrickling filter using cattle manure as nutrient media, Bioresour Technol Rep 9 (2020) 100391. https://doi.org/10.1016/j.biteb.2020.100391.

[244] F. Ebrahimian, N. De Bernardini, P. Tsapekos, L. Treu, X. Zhu, S. Campanaro, K. Karimi, I. Angelidaki, Effect of pressure on biomethanation process and spatial stratification of microbial communities in trickle bed reactors under decreasing gas retention time, Bioresour Technol 361 (2022) 127701. https://doi.org/10.1016/j.biortech.2022.127701.

[245] D. Panda, V.K. Saharan, S. Manickam, Controlled Hydrodynamic Cavitation: A Review of Recent Advances and Perspectives for Greener Processing, Processes 8 (2020) 220. https://doi.org/10.3390/pr8020220.

[246] M.B. Jensen, M.V.W. Kofoed, K. Fischer, N.V. Voigt, L.M. Agneessens, D.J. Batstone, L.D.M. Ottosen, Venturi-type injection system as a potential H2 mass transfer technology for full-scale in situ biomethanation, Appl Energy 222 (2018) 840–846. https://doi.org/10.1016/j.apenergy.2018.04.034.

[247] A. Giuliano, C.M. Cellamare, L. Chiarini, S. Tabacchioni, L. Petta, Evaluation of the controlled hydrodynamic cavitation as gas mass transfer system for ex-situ biological hydrogen methanation, Chemical Engineering Journal 471 (2023) 144475. https://doi.org/10.1016/j.cej.2023.144475.

[248] S. Matassa, N. Boon, I. Pikaar, W. Verstraete, Microbial protein: future sustainable food supply route with low environmental footprint, Microb Biotechnol 9 (2016) 568–575. https://doi.org/10.1111/1751-7915.12369.

[249] I. Pikaar, S. Matassa, B.L. Bodirsky, I. Weindl, F. Humpenöder, K. Rabaey, N. Boon, M. Bruschi, Z. Yuan, H. van Zanten, M. Herrero, W. Verstraete, A. Popp, Decoupling Livestock from Land Use through Industrial Feed Production Pathways, Environ Sci Technol 52 (2018) 7351–7359. https://doi.org/10.1021/acs.est.8b00216.

[250] I. Pikaar, J. de Vrieze, K. Rabaey, M. Herrero, P. Smith, W. Verstraete, Carbon emission avoidance and capture by producing in-reactor microbial biomass based food, feed and slow release fertilizer: Potentials and limitations, Science of the Total Environment 644 (2018) 1525–1530. https://doi.org/10.1016/j.scitotenv.2018.07.089.

[251] L. Van Peteghem, M. Sakarika, S. Matassa, I. Pikaar, R. Ganigué, K. Rabaey, Towards new carbon–neutral food systems: Combining carbon capture and utilization with microbial protein production, Bioresour Technol 349 (2022) 126853. https://doi.org/https://doi.org/10.1016/j.biortech.2022.126853.

[252] M. Areniello, S. Matassa, G. Esposito, P.N.L. Lens, Biowaste upcycling into second-generation microbial protein through mixed-culture fermentation, Trends Biotechnol (2022). https://doi.org/10.1016/j.tibtech.2022.07.008.

[253] C. Moscariello, S. Matassa, G. Esposito, S. Papirio, From residue to resource: The multifaceted environmental and bioeconomy potential of industrial hemp (Cannabis sativa L.), Resour Conserv Recycl 175 (2021) 105864. https://doi.org/10.1016/j.resconrec.2021.105864.

[254] S. Matassa, S. Papirio, I. Pikaar, T. Hülsen, E. Leijenhorst, G. Esposito, F. Pirozzi, W. Verstraete, Upcycling of biowaste carbon and nutrients in line with consumer confidence: the “full gas” route to single cell protein, Green Chemistry 22 (2020) 4912–4929. https://doi.org/10.1039/D0GC01382J.

[255] S. Matassa, W. Verstraete, I. Pikaar, N. Boon, Autotrophic nitrogen assimilation and carbon capture for microbial protein production by a novel enrichment of hydrogen-oxidizing bacteria, Water Res 101 (2016) 137–146. https://doi.org/10.1016/J.WATRES.2016.05.077.

[256] L. Lin, H. Huang, X. Zhang, L. Dong, Y. Chen, Hydrogen-oxidizing bacteria and their applications in resource recovery and pollutant removal, Science of The Total Environment 835 (2022) 155559. https://doi.org/10.1016/j.scitotenv.2022.155559.

[257] J. Dou, Y. Huang, H. Ren, Z. Li, Q. Cao, X. Liu, D. Li, Autotrophic, Heterotrophic, and Mixotrophic Nitrogen Assimilation for Single-Cell Protein

Production by Two Hydrogen-Oxidizing Bacterial Strains, Appl Biochem Biotechnol 187 (2019) 338–351. https://doi.org/10.1007/s12010-018-2824-1.

[258] Y. Jiang, X. Yang, D. Zeng, Y. Su, Y. Zhang, Microbial conversion of syngas to single cell protein: The role of carbon monoxide, Chemical Engineering Journal 450 (2022) 138041. https://doi.org/10.1016/J.CEJ.2022.138041.

[259] K. Tanaka, K. Miyawaki, A. Yamaguchi, K. Khosravi-Darani, H. Matsusaki, Cell growth and P(3HB) accumulation from CO2 of a carbon monoxide-tolerant hydrogen-oxidizing bacterium, Ideonella sp. O-1, Appl Microbiol Biotechnol 92 (2011) 1161–1169. https://doi.org/10.1007/s00253-011-3420-2.

[260] J. Shao, R. Yan, H. Chen, H. Yang, D.H. Lee, Catalytic effect of metal oxides on pyrolysis of sewage sludge, Fuel Processing Technology 91 (2010) 1113–1118. https://doi.org/10.1016/j.fuproc.2010.03.023.

[261] Md.M. Rahman, R. Liu, J. Cai, Catalytic fast pyrolysis of biomass over zeolites for high quality bio-oil – A review, Fuel Processing Technology 180 (2018) 32–46. https://doi.org/10.1016/j.fuproc.2018.08.002.

[262] C. Santella, L. Cafiero, D. De Angelis, F. La Marca, R. Tuffi, S. Vecchio Ciprioti, Thermal and catalytic pyrolysis of a mixture of plastics from small waste electrical and electronic equipment (WEEE), Waste Management 54 (2016) 143–152. https://doi.org/10.1016/j.wasman.2016.05.005.

[263] N. Chaouati, A. Soualah, M. Chater, M. Tarighi, L. Pinard, Mechanisms of coke growth on mordenite zeolite, J Catal 344 (2016) 354–364. https://doi.org/10.1016/j.jcat.2016.10.011.

[264] R.K. Mishra, S.M. Chistie, S.U. Naika, K. Mohanty, Catalytic pyrolysis of biomass over zeolites for bio-oil and chemical production: A review on their structure, porosity and acidity co-relation, Bioresour Technol 366 (2022) 128189. https://doi.org/10.1016/j.biortech.2022.128189.

[265] H. Liu, Q. Zhang, H. Xing, H. Hu, A. Li, H. Yao, Product distribution and sulfur behavior in sewage sludge pyrolysis: Synergistic effect of Fenton peroxidation and CaO conditioning, Fuel 159 (2015) 68–75. https://doi.org/10.1016/J.FUEL.2015.06.067.

[266] H. Hu, B. Xi, W. Tan, Effects of sulfur-rich biochar amendment on microbial methylation of mercury in rhizosphere paddy soil and methylmercury accumulation in rice, Environmental Pollution 286 (2021) 117290. https://doi.org/10.1016/j.envpol.2021.117290.

[267] L. Sigot, G. Ducom, P. Germain, Adsorption of hydrogen sulfide (H2S) on zeolite (Z): Retention mechanism, Chemical Engineering Journal 287 (2016) 47–53. https://doi.org/10.1016/j.cej.2015.11.010.

[268] M. Hervy, D. Pham Minh, C. Gérente, E. Weiss-Hortala, A. Nzihou, A. Villot, L. Le Coq, H2S removal from syngas using wastes pyrolysis chars, Chemical Engineering Journal 334 (2018) 2179–2189. https://doi.org/10.1016/j.cej.2017.11.162.

[269] A. Zaker, Z. Chen, M. Zaheer-Uddin, Catalytic pyrolysis of sewage sludge with HZSM5 and sludge-derived activated char: A comparative study using TGA-MS and artificial neural networks, J Environ Chem Eng 9 (2021) 105891. https://doi.org/10.1016/j.jece.2021.105891.

[270] A.A.F. da Costa, L.H. de O. Pires, D.R. Padrón, A.M. Balu, G.N. da Rocha Filho, R. Luque, L.A.S. do Nascimento, Recent advances on catalytic deoxygenation of residues for bio-oil production: An overview, Molecular Catalysis 518 (2022) 112052. https://doi.org/10.1016/j.mcat.2021.112052.

[271] M.C. Vásquez, E.E. Silva, E.F. Castillo, Hydrotreatment of vegetable oils: A review of the technologies and its developments for jet biofuel production, Biomass Bioenergy 105 (2017) 197–206. https://doi.org/10.1016/j.biombioe.2017.07.008.

[272] M. Patel, A. Kumar, Production of renewable diesel through the hydroprocessing of lignocellulosic biomass-derived bio-oil: A review, Renewable and Sustainable Energy Reviews 58 (2016) 1293–1307. https://doi.org/10.1016/j.rser.2015.12.146.

[273] L. Spadaro, A. Palella, F. Frusteri, F. Arena, Valorization of crude bio-oil to sustainable energy vector for applications in cars powering and on-board reformers via catalytic hydrogenation, Int J Hydrogen Energy 40 (2015) 14507–14518. https://doi.org/10.1016/j.ijhydene.2015.08.010.

[274] CORDIS, PYROlysis based process to convert small WWTP sewage sludge into useful bioCHAR, 2016. https://cordis.europa.eu/project/id/603394/reporting (accessed October 19, 2023).

[275] T. Yang, Y. Xiao, X. Zhao, D. Li, Z. Ma, W. Li, T. Gong, T. Zhang, N. Huang, B. Xi., Transformation pathways of the carbon-containing group compounds during municipal sludge pyrolysis treatment, Waste Management 178 (2024) 26–34. https://doi.org/10.1016/j.wasman.2024.01.041.

[276] Y. Hu, G. Li, M. Yan, C. Ping, J. Ren, Investigation into the distribution of polycyclic aromatic hydrocarbons (PAHs) in wastewater sewage sludge and its resulting pyrolysis bio-oils, Science of The Total Environment 473–474 (2014) 459–464. https://doi.org/10.1016/j.scitotenv.2013.12.051.

[277] F. Fredriksson, U. Eriksson, A. Kärrman, L.W.Y. Yeung, Per- and polyfluoroalkyl substances (PFAS) in sludge from wastewater treatment plants in Sweden — First findings of novel fluorinated copolymers in Europe including temporal analysis, Science of The Total Environment 846 (2022) 157406. https://doi.org/10.1016/j.scitotenv.2022.157406.

[278] J. Alvarez, G. Lopez, M. Amutio, M. Artetxe, I. Barbarias, A. Arregi, J. Bilbao, M. Olazar, Characterization of the bio-oil obtained by fast pyrolysis of sewage sludge in a conical spouted bed reactor, Fuel Processing Technology 149 (2016) 169–175. https://doi.org/10.1016/j.fuproc.2016.04.015.

[279] X. Meng, W. de Jong, R. Pal, A.H.M. Verkooijen, In bed and downstream hot gas desulphurization during solid fuel gasification: A review, Fuel Processing Technology 91 (2010) 964–981. https://doi.org/10.1016/j.fuproc.2010.02.005.

[280] J.R. Phillips, R.L. Huhnke, H.K. Atiyeh, Syngas Fermentation: A Microbial Conversion Process of Gaseous Substrates to Various Products, Fermentation 3 (2017). https://doi.org/10.3390/fermentation3020028.

[281] P.J. Woolcock, R.C. Brown, A review of cleaning technologies for biomass-derived syngas, Biomass Bioenergy 52 (2013) 54–84. https://doi.org/10.1016/j.biombioe.2013.02.036.

[282] M. Boronat, A. Corma, Factors Controlling the Acidity of Zeolites, Catal Letters 145 (2015) 162–172. https://doi.org/10.1007/s10562-014-1438-7.

[283] J. Li, M. Gao, W. Yan, J. Yu, Regulation of the Si/Al ratios and Al distributions of zeolites and their impact on properties, Chem Sci 14 (2023) 1935–1959. https://doi.org/10.1039/D2SC06010H.

[284] A. Tamošiūnas, D. Gimžauskaitė, R. Uscila, M. Aikas, Thermal arc plasma gasification of waste glycerol to syngas, Appl Energy 251 (2019) 113306. https://doi.org/10.1016/j.apenergy.2019.113306.

[285] T.P. Paula, M. de F.V. Marques, M.R. da C. Marques, M.S. Oliveira, S.N. Monteiro, Thermal and Catalytic Pyrolysis of Urban Plastic Waste: Modified Mordenite and ZSM-5 Zeolites, Chemistry (Easton) 4 (2022) 297–315. https://doi.org/10.3390/chemistry4020023.

[286] D.J. Mihalcik, C.A. Mullen, A.A. Boateng, Screening acidic zeolites for catalytic fast pyrolysis of biomass and its components, J Anal Appl Pyrolysis 92 (2011) 224–232. https://doi.org/10.1016/j.jaap.2011.06.001.

[287] Y.L. Tan, A.Z. Abdullah, B.H. Hameed, Catalytic fast pyrolysis of durian rind using silica-alumina catalyst: Effects of pyrolysis parameters, Bioresour Technol 264 (2018) 198–205. https://doi.org/10.1016/j.biortech.2018.05.058.

[288] B. Csutoras, N. Miskolczi, Thermo-catalytic pyrolysis of sewage sludge and techno-economic analysis: The effect of synthetic zeolites and natural sourced catalysts, Bioresour Technol 400 (2024) 130676. https://doi.org/10.1016/j.biortech.2024.130676.

[289] Q. Li, A. Faramarzi, S. Zhang, Y. Wang, X. Hu, M. Gholizadeh, Progress in catalytic pyrolysis of municipal solid waste, Energy Convers Manag 226 (2020) 113525. https://doi.org/10.1016/j.enconman.2020.113525.

[290] X.-Y. Ren, J.-P. Cao, S.-X. Zhao, X.-Y. Zhao, X.-B. Feng, T.-L. Liu, Y. Li, J. Zhang, X.-Y. Wei, Insights into coke location of catalyst deactivation during in-situ catalytic reforming of lignite pyrolysis volatiles over cobalt-modified zeolites, Appl Catal A Gen 613 (2021) 118018. https://doi.org/10.1016/j.apcata.2021.118018.

[291] S. Du, D.P. Gamliel, M. V. Giotto, J.A. Valla, G.M. Bollas, Coke formation of model compounds relevant to pyrolysis bio-oil over ZSM-5, Appl Catal A Gen 513 (2016) 67–81. https://doi.org/10.1016/j.apcata.2015.12.022.

[292] A. Al-Shathr, B.Y. Al-Zaidi, A.K. Shehab, Z.M. Shakoor, S. Aal-Kaeb, L.Q. Gomez, H.Sh. Majdi, E.N. Al-Shafei, A.A. AbdulRazak, J. McGregor, Experimental and kinetic studies of the advantages of coke accumulation over Beta and Mordenite catalysts according to the pore mouth catalysis hypothesis, Catal Commun 181 (2023) 106718. https://doi.org/10.1016/j.catcom.2023.106718.

[293] M.G. Shelyapina, E.A. Krylova, A.S. Mazur, A.A. Tsyganenko, Y. V. Shergin, E.A. Satikova, V. Petranovskii, Active Sites in H-Mordenite Catalysts Probed by NMR and FTIR, Catalysts 13 (2023) 344. https://doi.org/10.3390/catal13020344.

[294] L. Xu, J.-H. Cheng, X.-Q. Ma, J.-Y. Shen, Z.-X. Xu, P.-G. Duan, Transformation of the Sulfur Element during Pyrolysis of Sewage Sludge at Low Temperatures, Energy & Fuels 35 (2021) 501–509. https://doi.org/10.1021/acs.energyfuels.0c02706.

[295] S. Liu, M. Wei, Y. Qiao, Z. Yang, B. Gui, Y. Yu, M. Xu, Release of organic sulfur as sulfur-containing gases during low temperature pyrolysis of sewage sludge, Proceedings of the Combustion Institute 35 (2015) 2767–2775. https://doi.org/10.1016/J.PROCI.2014.06.055.

[296] A. Pudi, M. Rezaei, V. Signorini, M.P. Andersson, M.G. Baschetti, S.S. Mansouri, Hydrogen sulfide capture and removal technologies: A comprehensive review of recent developments and emerging trends, Sep Purif Technol 298 (2022) 121448. https://doi.org/10.1016/j.seppur.2022.121448.

[297] J. Zhang, W. Zuo, Y. Tian, L. Yin, Z. Gong, J. Zhang, Release of hydrogen sulfide during microwave pyrolysis of sewage sludge: Effect of operating parameters and mechanism, J Hazard Mater 331 (2017) 117–122. https://doi.org/10.1016/J.JHAZMAT.2017.02.040.

[298] L. Song, X. Du, Y. Chen, Z. Yang, J. Ran, G. Yang, Q. Shi, Z. Xue, Screening of zeolites for H2S adsorption in mixed gases: GCMC and DFT simulations, Microporous and Mesoporous Materials 328 (2021) 111495. https://doi.org/10.1016/j.micromeso.2021.111495.

[299] A.T. Ubando, C.B. Felix, W.H. Chen, Biorefineries in circular bioeconomy: A comprehensive review, Bioresour Technol 299 (2020) 122585. https://doi.org/10.1016/J.BIORTECH.2019.122585.

[300] S. Matassa, N. Boon, W. Verstraete, Resource recovery from used water: The manufacturing abilities of hydrogen-oxidizing bacteria, Water Res 68 (2015) 467–478. https://doi.org/https://doi.org/10.1016/j.watres.2014.10.028.

[301] B. Schink, H.G. Schlegel, Hydrogen metabolism in aerobic hydrogen-oxidizing bacteria, Biochimie 60 (1978) 297–305. https://doi.org/10.1016/S0300-9084(78)80826-8.

[302] R. Takors, M. Kopf, J. Mampel, W. Bluemke, B. Blombach, B. Eikmanns, F.R. Bengelsdorf, D. Weuster-Botz, P. Dürre, Using gas mixtures of CO, CO_2 and H_2 as microbial substrates: the do's and don'ts of successful technology transfer from laboratory to production scale, Microb Biotechnol 11 (2018) 606–625. https://doi.org/10.1111/1751-7915.13270.

[303] N. Adam, M. Perner, Microbially Mediated Hydrogen Cycling in Deep-Sea Hydrothermal Vents, Front Microbiol 9 (2018). https://doi.org/10.3389/fmicb.2018.02873.

[304] J. Yu, A. Dow, S. Pingali, The energy efficiency of carbon dioxide fixation by a hydrogen-oxidizing bacterium, Int J Hydrogen Energy 38 (2013) 8683–8690. https://doi.org/10.1016/j.ijhydene.2013.04.153.

[305] E. Ehsani, C. Dumolin, J.B.A. Arends, F.-M. Kerckhof, X. Hu, P. Vandamme, N. Boon, Enriched hydrogen-oxidizing microbiomes show a high diversity of co-existing hydrogen-oxidizing bacteria, Appl Microbiol Biotechnol 103 (2019) 8241–8253. https://doi.org/10.1007/s00253-019-10082-z.

[306] F.-M. Kerckhof, M. Sakarika, M. Van Giel, M. Muys, P. Vermeir, J. De Vrieze, S.E. Vlaeminck, K. Rabaey, N. Boon, From Biogas and Hydrogen to Microbial Protein Through Co-Cultivation of Methane and Hydrogen Oxidizing Bacteria, Front Bioeng Biotechnol 9 (2021). https://doi.org/10.3389/fbioe.2021.733753.

[307] K. Agrawal, A. Roldan, N. Kishore, A.J. Logsdail, Dehydrogenation and dehydration of formic acid over orthorhombic molybdenum carbide, Catal Today 384–386 (2022) 197–208. https://doi.org/10.1016/J.CATTOD.2021.04.011.

[308] M. Xu, H. Zhou, X. Yang, I. Angelidaki, Y. Zhang, Sulfide restrains the growth of Methylocapsa acidiphila converting renewable biogas to single cell protein, Water Res 184 (2020). https://doi.org/10.1016/j.watres.2020.116138.

[309] APHA, Standard Methods for the Examination of Water and Wastewater. 22nd Edition, American Public Health Association, American Water Works Association and Water Environmental Federation, Washington DC., (2012).

[310] APAT ISRA-CNR, Analytical Methods for Water. Agenzia per la protezione dell'ambiente e per i servizi tecnici (APAT) Istituto di Ricerca sulle Acque - Consiglio Nazionale delle Ricerche (ISRA-CNR), (2003).

[311] J.H. Waterborg, H.R. Matthews, The Lowry Method for Protein Quantitation, in: Basic Protein and Peptide Protocols, Humana Press, New Jersey, 1994: pp. 1–4. https://doi.org/10.1385/0-89603-268-X:1.

[312] F. Bianco, M. Race, S. Papirio, P. Oleszczuk, G. Esposito, Coupling of desorption of phenanthrene from marine sediments and biodegradation of the sediment washing solution in a novel biochar immobilized–cell reactor, Environmental Pollution 308 (2022) 119621. https://doi.org/10.1016/J.ENVPOL.2022.119621.

[313] X. Zhuang, Y. Huang, Y. Song, H. Zhan, X. Yin, C. Wu, The transformation pathways of nitrogen in sewage sludge during hydrothermal treatment, Bioresour Technol 245 (2017) 463–470. https://doi.org/10.1016/J.BIORTECH.2017.08.195.

[314] D. Xu, D.R. Tree, R.S. Lewis, The effects of syngas impurities on syngas fermentation to liquid fuels, Biomass Bioenergy 35 (2011) 2690–2696. https://doi.org/10.1016/J.BIOMBIOE.2011.03.005.

[315] S. Matassa, V. Pelagalli, S. Papirio, C. Zamalloa, W. Verstraete, G. Esposito, F. Pirozzi, Direct nitrogen stripping and upcycling from anaerobic digestate during conversion of cheese whey into single cell protein, Bioresour Technol (2022) 127308. https://doi.org/10.1016/J.BIORTECH.2022.127308.

[316] N. Vikromvarasiri, S. Boonyawanich, N. Pisutpaisal, Optimizing Sulfur Oxidizing Performance of Paracoccus Pantotrophus Isolated from Leather Industry Wastewater, Energy Procedia 79 (2015) 629–633. https://doi.org/10.1016/J.EGYPRO.2015.11.544.

[317] A.K. Singh, P. Kohli, N.K. Mahato, R. Lal, Paracoccus sordidisoli sp. nov., isolated from an agricultural field contaminated with hexachlorocyclohexane isomers, Int J Syst Evol Microbiol 67 (2017) 4365–4371. https://doi.org/10.1099/ijsem.0.002289.

[318] X. Wang, D. Jin, L. Zhou, L. Wu, W. An, L. Zhao, Draft Genome Sequence of Advenella kashmirensis Strain W13003, a Polycyclic Aromatic Hydrocarbon-Degrading Bacterium, Genome Announc 2 (2014). https://doi.org/10.1128/genomeA.00003-14.

[319] L. Hermon, J. Denonfoux, J. Hellal, C. Joulian, S. Ferreira, S. Vuilleumier, G. Imfeld, Dichloromethane biodegradation in multi-contaminated groundwater: Insights from biomolecular and compound-specific isotope analyses, Water Res 142 (2018) 217–226. https://doi.org/10.1016/j.watres.2018.05.057.

[320] J. Firsova, N. Doronina, E. Lang, C. Spröer, S. Vuilleumier, Y. Trotsenko, Ancylobacter dichloromethanicus sp. nov. – a new aerobic facultatively methylotrophic bacterium utilizing dichloromethane, Syst Appl Microbiol 32 (2009) 227–232. https://doi.org/10.1016/j.syapm.2009.02.002.

[321] E.E.L. Muller, F. Bringel, S. Vuilleumier, Dichloromethane-degrading bacteria in the genomic age, Res Microbiol 162 (2011) 869–876. https://doi.org/10.1016/J.RESMIC.2011.01.008.

[322] K.R. Hardy, G.M. King, Enrichment of High-Affinity CO Oxidizers in Maine Forest Soil, Appl Environ Microbiol 67 (2001) 3671–3676. https://doi.org/10.1128/AEM.67.8.3671-3676.2001.

[323] M. Faragò, A. Damgaard, I. Logar, M. Rygaard, Life Cycle Assessment and Cost-Benefit Analysis of Technologies in Water Resource Recovery Facilities: The Case of Sludge Pyrolysis, Environ Sci Technol 56 (2022) 17988–17997. https://doi.org/10.1021/acs.est.2c06083.

[324] S. Di Fraia, N. Massarotti, M.R. Uddin, L. Vanoli, Conversion of Sewage Sludge to combined heat and power: Modeling and optimization, Smart Energy 5 (2022) 100061. https://doi.org/10.1016/J.SEGY.2021.100061.

[325] J. Moško, M. Pohořelý, S. Skoblia, Z. Beňo, M. Jeremiáš, Detailed Analysis of Sewage Sludge Pyrolysis Gas: Effect of Pyrolysis Temperature, Energies (Basel) 13 (2020) 4087. https://doi.org/10.3390/en13164087.

[326] Y. Rafrafi, L. Laguillaumie, C. Dumas, Biological Methanation of H2 and CO2 with Mixed Cultures: Current Advances, Hurdles and Challenges, Waste Biomass Valorization 12 (2021) 5259–5282. https://doi.org/10.1007/s12649-020-01283-z.

[327] M. Pacheco, P. Moura, C. Silva, A Systematic Review of Syngas Bioconversion to Value-Added Products from 2012 to 2022, Energies (Basel) 16 (2023) 3241. https://doi.org/10.3390/en16073241.

[328] Y. Zhang, Y. Liang, S. Li, Y. Yuan, D. Zhang, Y. Wu, H. Xie, K. Brindhadevi, A. Pugazhendhi, C. Xia, A review of biomass pyrolysis gas: Forming mechanisms, influencing parameters, and product application upgrades, Fuel 347 (2023) 128461. https://doi.org/10.1016/j.fuel.2023.128461.

[329] A. Skorek-Osikowska, M. Martín-Gamboa, D. Iribarren, D. García-Gusano, J. Dufour, Thermodynamic, economic and environmental assessment of energy systems including the use of gas from manure fermentation in the context of the Spanish potential, Energy 200 (2020) 117452. https://doi.org/10.1016/j.energy.2020.117452.

[330] M. Yu, X. Liu, Y. Chen, Z. Zhang, Y. Wang, J. Zhang, Y. Han, A 4E analysis of a novel coupling process of syngas purification and CO2 capture, transcritical CO2 power and absorption refrigeration, Chemical Engineering Journal 445 (2022) 136757. https://doi.org/10.1016/j.cej.2022.136757.

[331] T. Antukh, I. Lee, S. Joo, H. Kim, Hydrogenotrophs-Based Biological Biogas Upgrading Technologies, Front Bioeng Biotechnol 10 (2022). https://doi.org/10.3389/fbioe.2022.833482.

[332] P. Ghofrani-Isfahani, P. Tsapekos, M. Peprah, P. Kougias, X. Zhu, A. Kovalovszki, A. Zervas, X. Zha, C.S. Jacobsen, I. Angelidaki, Ex-situ biogas upgrading in thermophilic up-flow reactors: The effect of different gas diffusers and gas retention times, Bioresour Technol 340 (2021) 125694. https://doi.org/10.1016/j.biortech.2021.125694.

[333] K. Asimakopoulos, A. Grimalt-Alemany, C. Lundholm-Høffner, H.N. Gavala, I. V. Skiadas, Carbon Sequestration Through Syngas Biomethanation Coupled

with H2 Supply for a Clean Production of Natural Gas Grade Biomethane, Waste Biomass Valorization 12 (2021) 6005–6019. https://doi.org/10.1007/s12649-021-01393-2.

[334] J. Figueras, H. Benbelkacem, C. Dumas, P. Buffiere, "Biomethanation of syngas by enriched mixed anaerobic consortium in pressurized agitated column," Bioresour Technol 338 (2021) 125548. https://doi.org/10.1016/j.biortech.2021.125548.

[335] M. Sposob, R. Wahid, K. Fischer, Ex-situ biological CO2 methanation using trickle bed reactor: review and recent advances, Rev Environ Sci Biotechnol 20 (2021) 1087–1102. https://doi.org/10.1007/s11157-021-09589-7.

[336] H. Porté, P.G. Kougias, N. Alfaro, L. Treu, S. Campanaro, I. Angelidaki, Process performance and microbial community structure in thermophilic trickling biofilter reactors for biogas upgrading, Science of The Total Environment 655 (2019) 529–538. https://doi.org/10.1016/j.scitotenv.2018.11.289.

[337] G. Luo, I. Angelidaki, Integrated biogas upgrading and hydrogen utilization in an anaerobic reactor containing enriched hydrogenotrophic methanogenic culture, Biotechnol Bioeng 109 (2012) 2729–2736. https://doi.org/10.1002/bit.24557.

[338] European Commission, 2000/532/EC: Commission Decision of 3 May 2000 replacing Decision 94/3/EC establishing a list of wastes pursuant to Article 1(a) of Council Directive 75/442/EEC on waste and Council Decision 94/904/EC establishing a list of hazardous waste pursuant to Article 1(4) of Council Directive 91/689/EEC on hazardous waste (notified under document number C(2000) 1147), (2000). http://data.europa.eu/eli/dec/2000/532/oj (accessed April 7, 2024).

[339] European Commision, Directive 2000/60/EC of the European Parliament and of the Council of 23 October 2000 establishing a framework for Community action in the field of water policy, 2000. http://data.europa.eu/eli/dir/2000/60/oj (accessed April 7, 2024).

[340] European Parliament and Council, Directive 2008/98/EC of the European Parliament and of the Council of 19 November 2008 on waste and repealing certain Directives (Text with EEA relevance), (2008). http://data.europa.eu/eli/dir/2008/98/oj (accessed January 24, 2024).

[341] Council of the European Communities, COUNCIL DIRECTIVE of 21 May 1991 concerning urban waste water treatment (91/271/EEC), (1991). http://data.europa.eu/eli/dir/1991/271/oj (accessed April 7, 2024).

[342] Council of the European Communities, Council Directive 91/676/EEC of 12 December 1991 concerning the protection of waters against pollution caused by nitrates from agricultural sources, (1991). http://data.europa.eu/eli/dir/1991/676/oj (accessed June 3, 2023).

[343] European Parliament and Council, Directive (EU) 2018/850 of the European Parliament and of the Council of 30 May 2018 amending Directive 1999/31/EC on the landfill of waste (Text with EEA relevance), (2018). http://data.europa.eu/eli/dir/2018/850/oj (accessed January 24, 2024).

[344] European Commission, Proposal for a DIRECTIVE OF THE EUROPEAN PARLIAMENT AND OF THE COUNCIL concerning urban wastewater treatment (recast), (2022). https://environment.ec.europa.eu/publications/proposal-revised-urban-wastewater-treatment-directive_en (accessed June 3, 2023).

[345] Council Directive 86/278/EEC, Council Directive 86/278/EEC of 12 June 1986 on the protection of the environment, and in particular of the soil, when sewage sludge is used in agriculture, Official Journal L 181 , 04/07/1986 P. 0006 - 0012 (1986).

[346] G. Mininni, A.R. Blanch, F. Lucena, S. Berselli, EU policy on sewage sludge utilization and perspectives on new approaches of sludge management, Environmental Science and Pollution Research 22 (2015). https://doi.org/10.1007/s11356-014-3132-0.

[347] European Commission, Communication from the Commission: A new Circular Economy Action Plan For a cleaner and more competitive Europe, (2020). https://eur-lex.europa.eu/legal-content/EN/TXT/HTML/?uri=CELEX:52020DC0098 (accessed June 1, 2023).

[348] European Commission, Communication from the Commission: The European Green Deal, (2019). https://eur-lex.europa.eu/legal-content/EN/TXT/HTML/?uri=CELEX:52019DC0640 (accessed June 1, 2023).

[349] European Commission, A sustainable bioeconomy for Europe – Strengthening the connection between economy, society and the environment : updated bioeconomy strateg, 2018. https://data.europa.eu/doi/10.2777/792130 (accessed June 1, 2023).

[350] European Commission, Communication from the Commission: A Farm to Fork Strategy, (2020). https://eur-lex.europa.eu/legal-content/EN/TXT/HTML/?uri=CELEX:52020DC0381 (accessed June 1, 2023).

[351] European Commission, EU biodiversity strategy for 2030 – Bringing nature back into our lives, 2021. https://data.europa.eu/doi/10.2779/677548 (accessed June 1, 2023).

[352] European Commission, The EU's 2021-2027 long-term budget and NextGenerationEU – Facts and figures, 2021. https://data.europa.eu/doi/10.2761/808559 (accessed June 1, 2023).

[353] European Commission, Sewage sludge use in farming: evaluation, (2023). https://ec.europa.eu/info/law/better-regulation/have-your-say/initiatives/12328-Sewage-sludge-use-in-farming-evaluation_en (accessed June 1, 2023).

[354] European Commission, ANNEXES to the Commission Delegated Regulation amending Annexes II, III and IV to Regulation (EU) 2019/1009 of the European Parliament and of the Council for the purpose of adding pyrolysis or gasification materials as a component material category in EU fertilising products, (2021). https://ec.europa.eu/info/law/better-regulation/have-your-say/initiatives/12136-Fertilising-products-pyrolysis-and-gasification-materials_en (accessed February 2, 2022).

[355] L. Isern-Cazorla, A. Mineo, M.E. Suárez-Ojeda, G. Mannina, Effect of organic loading rate on the production of Polyhydroxyalkanoates from sewage sludge, J Environ Manage 343 (2023) 118272. https://doi.org/10.1016/j.jenvman.2023.118272.

[356] M. Hušek, J. Moško, M. Pohořelý, Sewage sludge treatment methods and P-recovery possibilities: Current state-of-the-art, J Environ Manage 315 (2022) 115090. https://doi.org/10.1016/j.jenvman.2022.115090.

[357] S. Vilakazi, E. Onyari, O. Nkwonta, J.K. Bwapwa, Reuse of domestic sewage sludge to achieve a zero waste strategy & improve concrete strength & durability - A review, S Afr J Chem Eng 43 (2023) 122–127. https://doi.org/10.1016/j.sajce.2022.10.012.

[358] K. Chojnacka, D. Skrzypczak, D. Szopa, G. Izydorczyk, K. Moustakas, A. Witek-Krowiak, Management of biological sewage sludge: Fertilizer nitrogen recovery as the solution to fertilizer crisis, J Environ Manage 326 (2023) 116602. https://doi.org/10.1016/j.jenvman.2022.116602.

[359] European Commission, COMMUNICATION FROM THE COMMISSION TO THE EUROPEAN PARLIAMENT, THE COUNCIL, THE EUROPEAN ECONOMIC AND SOCIAL COMMITTEE AND THE COMMITTEE OF THE REGIONS: The role of waste-to-energy in the circular economy, (2017). https://eur-lex.europa.eu/legal-content/EN/TXT/HTML/?uri=CELEX:52017DC0034 (accessed April 7, 2024).

[360] European Parliament and Council, Directive 2009/28/EC of the European Parliament and of the Council of 23 April 2009 on the promotion of the use of energy from renewable sources and amending and subsequently repealing Directives 2001/77/EC and 2003/30/EC, (2009).

[361] J. Yu, Y. Lu, Carbon dioxide fixation by a hydrogen-oxidizing bacterium: Biomass yield, reversal respiratory quotient, stoichiometric equations and bioenergetics, Biochem Eng J 152 (2019) 107369. https://doi.org/10.1016/j.bej.2019.107369.

[362] B.E. Rittmann, P.L. McCarty, Environmental Biotechnology Principles and Applications , Second, McGraw-Hill Education, 2020.

..

BIOGRAPHY



Vincenzo Pelagalli was born in 1997 in Formia (Italy). In 2020, he obtained his Master's degree in Environmental Engineering from University of Cassino and Southern Lazio (Italy). During his master thesis, he worked on microbial protein production from fermentation of agro-zootechnical wastes (*i.e.* cheese whey) and the employment of manure digestate as N-source, under the supervision of Prof. Stefano Papirio and Prof. Silvio Matassa.

In 2021, Vincenzo Pelagalli started his PhD in *Methods, models and technologies for Engineering* at the University of Cassino and Southern Lazio (Italy), with an industrial PhD project co-financed by Regione Lazio, the Italian National Agency for New Technologies, Energy and Sustainable Economic Development (ENEA), and Acea Elabori S.p.A. The PhD research activity was conducted under the supervision of Prof. Marco Race (UNICAS), Dr. Michela Langone (ENEA), and Prof. Piet N.L. Lens (NUI Galway). The project focused on the development of an integrated platform for the biological valorization of syngas and biochar produced from the pyrolysis of municipal sewage sludge (MSS). Vincenzo Pelagalli has presented the results obtained during his research at various national and international scientific conferences.

PUBLICATIONS & RELEVANT WORK

Journal articles

Matassa, S., **Pelagalli, V.**, Papirio, S., Zamalloa, C., Verstraete, W., Esposito, G., Pirozzi, F., 2022. Direct nitrogen stripping and upcycling from anaerobic digestate during conversion of cheese whey into single cell protein. Bioresour Technol 127308. https://doi.org/10.1016/J.BIORTECH.2022.127308

Pelagalli, V., Matassa, S., Race, M., Langone, M., Papirio, S., Lens, P.N.L., Lazzazzara, M., Frugis, A., Petta, L., Esposito, G., 2023. Syngas-driven sewage sludge conversion to microbial protein through H_2S- and CO-tolerant hydrogen-oxidizing bacteria. Water Res 120698. https://doi.org/10.1016/j.watres.2023.120698

Pelagalli V., Langone M., Matassa S., Race M., Tuffi R., Papirio S., Lens P.N.L., Lazzazzara M., Frugis A., Petta L., Esposito G., 2024. Pyrolysis of municipal sewage sludge: challenges, opportunities and new valorization routes for biochar, bio-oil, and pyrolysis gas. Environmental Science: Water Research & Technologies. https://doi.org/10.1039/D4EW00278D.

Pelagalli V., Tuffi R., Sabatino M.E., Langone M., De Angelis D., Matassa S., Race M., Papirio S., Lens P.N.L., Lazzazzara M., Frugis A., Petta L., Scarsella M., Esposito G., 2024. In-situ catalytic pyrolysis of municipal sewage sludge for the reduction of H_2S content in pyrolysis gas. (Submitted)

Proceeding

Pelagalli V., Matassa S., Race M., Langone M., Papirio S., Lens P.N.L., Lazzazzara M., Frugis A., Petta L., Esposito G., 2024. La fermentazione aerobica del syngas di pirolisi dei fanghi di depurazione: una soluzione innovativa per una gestione circolare di materia ed

energia. ECONOMIA VERDE, CIRCOLARE E RIGENERATIVA: RICERCA, INNOVAZIONE E NUOVE POLICIES, Atti di Ecomondo, Maggioli Editore, ISBN *9788891667670, p. 140-146.*

Journal reviewer

2021 – 2024: Reviews for *Environmental Research*

2024: Reviews for *Bioresource Technology*

2024: Reviews for *Environmental Technology & Innovation*

Invited speaker

Pelagalli V., "*The potential of H_2S- and CO-tolerant hydrogen-oxidizing bacteria to convert sewage sludge into microbial protein through aerobic syngas fermentation",* **6th IWA International Conference on eco-Technologies for Wastewater Treatment**, Girona (Spain), 26-29/06/2023.

Pelagalli V., "*From sewage sludge to microbial protein: the role of H_2S- and CO-tolerant hydrogen-oxidizing bacteria in syngas aerobic fermentation",* **1st International PhD Symposium on Engineering and Sport Science**, Cassino (Italy), 10-12/10/2023.

Pelagalli V., "*La fermentazione aerobica del syngas di pirolisi dei fanghi di depurazione: una soluzione innovativa per una gestione circolare di materia ed energia",* **ECOMONDO – The green technology expo**, 5-8/11/2023, Rimini (Italy).

Langone M., **Pelagalli V.,** "*Gestione dei fanghi di depurazione in ottica di economia circolare: valorizzazione di syngas e biochar derivanti da processo di pirolisi applicato ai fanghi",* **ECOMED – Green expo del Mediterraneo**, 17-19/04/2024, Siciliafiera, Catania (Italy).

Pelagalli V., "*Mordenite and HZSM-5 zeolites employment in the catalytic pyrolysis of municipal sewage sludge towards the in-situ H_2S removal from syngas",* **19th IWA Leading Edge Conference on Water and Wastewater Technologies**, 24-28/06/2024, Essen (Germany).